IJVP-2026

Vol.: 50(4)
December, 2026
ISSN: 0250-4758
Online ISSN: 0973-970X

INDIAN JOURNAL OF VETERINARY PATHOLOGY

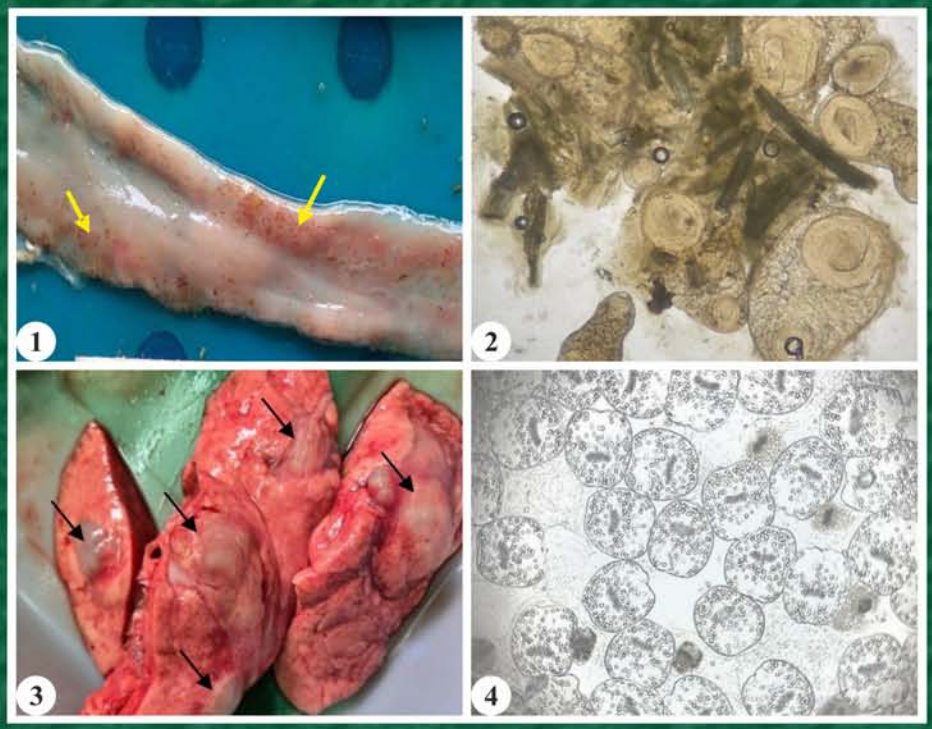

INDIAN ASSOCIATION OF VETERINARY PATHOLOGISTS
(Registered under article 21 of Societies Act 1860)

Visit us at: **www.iavp.org**
Journal available at: **www.indianjournals.com**

Vol. 50 (4)
December, 2026
ISSN: 0250-4758

INDIAN JOURNAL OF VETERINARY PATHOLOGY

Chief Editor
A. Anand Kumar

Editor
R. Madheswaran

Managing Editor
Pawan Kumar

Department of Veterinary Pathology, College of Veterinary Science,
Sri Venkateswara Veterinary University, Tirupati-517502, Andhra Pradesh
Mobile: +91-9441185383; E-mail: 7aakumar@gmail.com

INDIAN JOURNAL OF VETERINARY PATHOLOGY

Chief Editor

A. Anand Kumar

Editor

R. Madheswaran

Managing Editor

Pawan Kumar

Editorial Board

B.N. Tripathi, Jammu
A.K. Sharma, Bareilly
N. Divakaran Nair, Kerala
Amarjit Singh, Punjab
S.K. Panda, Odisha
M.K. Gupta, Jharkhand
Ajith Jacob George, Kerala
Manu Sebastian, USA
R. Somvanshi, Bareilly
Rajendra Singh, Bareilly
G.A. Balasubramaniam, Tamil Nadu
N.V. Kurkure, Maharashtra
Madhuswamy, Madhya Pradesh
Tridib Rajkhowa, Mizoram
Pankaj Goswamy, Jammu

Membership Fee and Subscription of Journal

● Individual life membership	Rs. 4,000/- (India)	US$ 600/- (Foreign)
● Individual life membership for the non-Indian citizens of the SAARC countries and other than North America, Europe and Australia	US$ 200/-	
● Individual Annual Membership (for foreign only)	US$ 60/- (with free online access; no hard copy of journal)	
● Library, Institutions, etc. (Annual)	Rs. 12,000/- (India)	US$ 400/- (Foreign)
● Individual Patron of IAVP	Rs. 1,00,000/- (Life member - paid patron for 5 years)	
● Govt./Non-Govt./Corporate/ Institution Patrons	Rs. 5,00,000/ (for 5 years)	

Advertisement Tariff

	Black and White	**Full Colour**
● Regular full page	Rs. 4,000	Rs. 6,000
● Regular half page	Rs. 2,000	Rs. 3,000
● Inside front & back cover page	–	Rs. 10,000
● Back cover page	–	Rs. 15,000

Note:

- Those submitting advertisement for two/four/six issues of the IJVP will be extended 15%/20%/25% discounts, respectively, on the above rates.
- The membership fee must be paid through Cash/Online/Crossed cheque or DD in favour of Treasurer "Indian Association of Veterinary Pathologists" payable at SBI, CARI Branch, Bareilly.
- No part of this publication should be reproduced or transmitted in any form (electronic, mechanical or otherwise including photocopy) without written permission from the Chief Editor.

Contents

Review Articles

1. Small ruminant lentiviruses: Current perspective on pathogenesis, pathology and diagnostic approaches
   Pawan Kumar, Sreelakshmi P., Monika Bhardwaj, Shweta Valecha, Hiteshwar Singh Yadav, Sonali Mishra, Kumar K., Siddharth Gautam, Vidya Singh and Rajveer Singh Pawaiya 291-299

Research Articles

2. Histopathological alterations associated with etiological determinants of chronic diarrhoea in adult Dairy Bovines
   Nuzhat Hassan, Charanjit Singh Randhawa, Kuldeep Gupta, Naresh K. Sood, Shoor Vir Singh, Kundan Chaubey and Ashiq Hussian 300-305
3. Detection of *Mycobacterium tuberculosis* complex and rifampicin resistance using Xpert MTB/RIF Ultra assay in tissue samples from cattle and buffaloes
   Anitta Thomas, Deepti Narang, Mudit Chandra, Kuldip Gupta and A.K. Arora 306-310
4. Pathomorphological and histopathological characterization of hydatid cysts in sheep: Evidence from slaughterhouses in Rayalaseema, Andhra Pradesh
   P. Lakshmisai, K. Jalajakshi, R. Venu and A. Anand Kumar 311-315
5. Pathological and molecular insights into *Toxoplasma gondii* in aborted fetuses of goat and slaughtered goats in Mymensingh district, Bangladesh
   Mahmuda Islam, Nazneen Sultana, Moutuza Mostaree, Thahsin Farjana, Munmun Pervin and Mohammad Abu Hadi Noor Ali Khan 316-323
6. First report of multidrug-resistant *Pseudomonas juntendi* from an equine suppurative lesion
   Monika Bhardwaj, Adarsh Kumar, Subhash Verma, Prasenjit Dhar, Shivani Barsain, Diksha Guleria and Rajesh Chahota 324-327
7. Pathomorphological and immunohistochemical studies on male genital tract tumors in dogs
   P. Balaram, CH. Sudha Rani Chowdary, K. Satheesh, CH. Bindu Kiranmayi and V. Rama Devi 328-334
8. Assessment of fracture healing in dogs based on the evaluation of haemato-biochemical parameters
   CH V. Surya Lakshmi, G. Vani, R.V. Suresh Kumar and P. Amaravathi 335-338
9. Mitigating effects of *Moringa oleifera* leaf extract on fipronil-induced hematobiochemical alterations in female Wistar albino rats
   J. Leela Prasad, K. Sujatha, A. Anand Kumar, Y. Muralidhar and T.V. Chaitanya Kumar 339-347
10. Pathological alterations induced by acute oral exposure to Acephate in Wistar rats
    C.S. Mishra, R.C. Ghosh, Pramod Kumar and Devesh Kumar Giri 348-352
11. PET-CT imaging, gross & microscopic features in systemic microsporidial diseases in laboratory rabbits
    Yogita Shete, Abhishek Gupta, Sutapa Rakshit and Sandip Basu 353-360
12. Integrated anti-oxidant and anti-inflammatory actions of *Saussurea costus* root attenuate severe hepatic pathophysiology in poultry *(Gallus gallus domesticus)* experimentally challenged with *Salmonella enterica* Serovar Typhimurium
    Mridul Soni, Rakesh Kumar, R.K. Asrani, Sahil Choudhary and R.D. Patil 361-369
13. Molecular epidemiology and pathobiology of Newcastle disease virus in chickens in and around Hyderabad
    Pavan Kumar Sangamoni, Swathi Bora, Ravi Kumar Yadala, L. Gopala, B. Raju and D. Madhuri 370-377

Case Reports

14. Pathological effects of immature amphistomosis in a goat – A case report
    K. Thilagavathi and J. Selvaraj 378-380
15. Pathomorphology of ulcerated cutaneous eosinophilic granuloma in a horse
    M. Karthick, M. Thangapandiyan, K. Gopal, D.C. Monisha, P. Srinivasan and K. Balamurugan 381-383
16. Fibrosarcoma in a labrador retriever dog
    K. Kalai, B. Debroy and S.W. Monsang 384-385
17. An unusual case of fibroma in a Japanese quail
    D.C. Monisha, K. Gopal, P. Srinivasan, M. Karthick and P. Thirunavukkarasu 386-387

Thesis Abstracts

18. Pathology of porcine parvovirus infection in pig and expression of recombinant NS1 protein to evaluate the immunodiagnostic potential
    Deepti Singh 388

IAVP News i-iii

Reviewers List

INDIAN JOURNAL OF VETERINARY PATHOLOGY

INDIAN ASSOCIATION OF VETERINARY PATHOLOGISTS
(Estd. 1974)

PATRONS : D.D. Heranjal
N.C. Jain
D.L. Paikne
U.K. Sharma

EXECUTIVE COMMITTEE (w.e.f. 2026)

President	:	Dr K.P. Singh, Izatnagar
Vice-Presidents	:	Prof T.V. Anilkumar, Trivendrum Prof S.K. Mukhopadhyay, West Bengal
Secretary General	:	Dr R.V.S. Pawaiya, Izatnagar
Joint Secretary	:	Dr Chandrakanta Jana, Izatnagar
Treasurer	:	Dr Vidya Singh, Izatnagar
Chief Editor	:	Dr A. Anand Kumar, Tirupati
Editor	:	Dr R. Madheswaran, Namakkal
Managing Editor	:	Dr Pawan Kumar, Izatnagar
Web Manager	:	Dr Asok Kumar M., Izatnagar
Zonal Secretary	:	Dr Gaya Prasad Jatav, Jabalpur (Central) Dr Kanika Kalai, Tripura (North-East) Dr Rajeev Ranjan, Bhubaneswar (East) Dr M. Saminathan, Mukteswar (North) Dr P. Srinivasan, Namakkal (South) Dr Chandrashekhar S. Mote, Maharashtra (West)
Executive Members	:	Dr M. Karikalan Dr Siddharth Gautam Dr S.S. Manjunatha Dr Rabindra Nath Hansda Dr Nittin Dev Singh Dr H. Srinivasa Naik

Cover Page Photo: Fig. 1. Intestinal mucosa showing multiple grey fleshy spots of 1-2 mm in diameter (arrow) attached to the mucosa; **Fig. 2.** Intestinal scraping showing immature amphistomes with oral and ventral sucker; **Fig. 3.** Goat lung with multiple hydatid cysts (arrows) embedded in the parenchyma and **Fig. 4.** Clusters of protoscoleces on glass slide (100X).

Indian J. Vet. Pathol., 50(4) : 291-299, 2026: DOI: https://doi.org/10.56093/b928xd65

REVIEW ARTICLE

Small ruminant lentiviruses: Current perspective on pathogenesis, pathology and diagnostic approaches

Pawan Kumar[1*], Sreelakshmi P.[1], Monika Bhardwaj[2], Shweta Valecha[1], Hiteshwar Singh Yadav[1], Sonali Mishra[3], Kumar K. [1], Siddharth Gautam[1], Vidya Singh[1] and Rajveer Singh Pawaiya[1]

[1]Division of Pathology, ICAR- Indian Veterinary Research Institute, Izatnagar, Bareilly, Uttar Pradesh-243122 (INDIA)
[2]Department of Veterinary Microbiology, COVAS, CSKHPKV, Palampur, Himachal Pradesh-176062 (INDIA)
[3]Department of Veterinary Pathology, COVAS, CSKHPKV, Palampur, Himachal Pradesh-176062 (INDIA)

***Address of correspondence**
Dr. Pawan Kumar, Senior Scientist, E-mail: chauhan2k1@gmail.com
ORCID ID: 0000-0002-0024-8925, 0009-0002-9002-6695

Received: 25-6-26; Accepted: 10-8-26

ABSTRACT

Small ruminant lentiviruses (SRLVs) are important retroviral pathogens of sheep and goats belonging to the genus Lentivirus within the family *Retroviridae*. These viruses are responsible for two major chronic diseases in small ruminants viz. maedi-visna (MV) and caprine arthritis encephalitis (CAE). SRLV infections are characterized by prolonged incubation periods, lifelong persistence, and progressive multisystemic inflammatory lesions affecting the respiratory, nervous, mammary, and musculoskeletal systems. Transmission occurs primarily through respiratory secretions and ingestion of infected colostrum or milk, while transplacental and semen-mediated transmission have also been documented. SRLVs establish persistent infection through integration of proviral DNA into host cells of the monocyte–macrophage lineage, leading to chronic immune-mediated pathology. Viral genetic diversity, antigenic variation, and the ability to infect multiple domestic and wild ruminant species complicate disease control and raise concerns regarding animal health and wildlife conservation. Diagnosis relies on a combination of serological, molecular, pathological, and immunohistochemical approaches, each contributing to improved detection and characterization of infection. Despite advances in diagnostic technologies, effective control remains challenging because of viral persistence, latent infections, and the absence of effective antiviral therapies or commercially successful vaccines. This review summarizes the current understanding of SRLV pathogenesis, pathology, and diagnostic strategies, while highlighting existing challenges for its control.

Keyword: Caprine arthritis encephalitis, Diagnosis, Maedi, Visna, Pathology, Small ruminant lentiviruses (SRLV)

INTRODUCTION

Small ruminant lentiviruses (SRLVs) belong to the genus Lentivirus within the family *Retroviridae* and causes important disease of sheep and goats viz. maedi-visna (MV) and caprine arthritis encephalitis (CAE). Besides lentiviral diseases, retroviruses also caused neoplastic diseases such as ovine pulmonary adenocarcinoma (OPA) and enzootic nasal adenocarcinoma in sheep[1,2,3]. Usually MV is more commonly observed in sheep, and CAE in goats but both species are susceptible to SRLVs infection and show varied range of pathological lesions. These lentiviral diseases are chronic and progressive in nature and produce multi-systemic pathologies. Spread of the infection to the susceptible population usually occurs through aerosol and milk or colostrum, but transmission through placenta and semen is also reported[4]. The prevalence is substantially higher in farms following practice of feeding lambs or kids from pooled colostrum or milk from the tank[5].

SRLVs refers to two distinct viruses viz. MV virus (MVV) and CAE virus (CAEV). Both are put together as SRLVs due to their extensive genetic relatedness[6]. Natural infections involving sheep and goats, as well as mixed infections with multiple viral subtypes, have been reported in several countries[7]. Furthermore, SRLV infections have been documented in wild ruminant species including ibex, mouflon, and chamois[8,9,10]. Isolated reports of mixed pathological lesions of Maedi and OPA/ Mycoplasmosis are also reported[11-13]. SRLVs replicate in the cells of the monocyte-macrophage lineage and establish lifelong persistence through integration of proviral DNA into the host genome. Disease development is primarily mediated by chronic inflammatory responses induced by infected macrophages and lymphocytes in the lungs, mammary glands, central nervous system, and joints[14].

The diagnosis of SRLV infection relies on a combination of serological, molecular, and pathological techniques, while histopathology and immunohistochemistry (IHC) provide valuable support in confirming infection and characterizing tissue lesions[12,14,15].

How to cite this article : Kumar, P., Sreelakshmi, P., Bhardwaj, M., Valecha, S., Yadav, H.S., Mishra, S., Kumar, K., Gautam, S., Singh, V. and Pawaiya, R.S. 2026. Small ruminant lentiviruses: Current perspective on pathogenesis, pathology and diagnostic approaches. Indian J. Vet. Pathol., 50(4) : 291-299.

Despite significant advances in diagnostic methodologies, effective control of SRLV infections remains challenging because of viral persistence, prolonged latent infection, antigenic variation, and the existence of genetically diverse viral strains. Currently, no effective antiviral therapy or commercially successful vaccine is available for the prevention or treatment of SRLV infections.

Etiological agent: SRLVs

The genome of SRLVs consists of a single-stranded, positive-sense RNA molecule approximately 8.4–9.2 kb in length. SRLVs genome contain three major structural genes, viz. *gag*, *pol*, and *env*, flanked by long terminal repeat (LTR) at both the 5′ and 3′ ends[7] (Fig. 1). The *gag* gene encodes the structural proteins of the viral core (matrix, capsid, nucleocapsid proteins); *pol* gene encodes viral enzymes (reverse transcriptase, integrase, protease); and *env* gene encodes the envelope glycoproteins responsible for receptor recognition, host-cell attachment, and membrane fusion. In addition, SRLVs also possess accessory genes, such as *rev*, *vif*, and *vpr-like* gene. The *rev* gene facilitates the nuclear export of incompletely spliced viral transcripts and is essential for efficient viral replication[16,17]; *vif* gene counteract host antiviral restriction factors belonging to the APOBEC3 family and enhance the viral survival and replication[18]; and *vpr-like* gene have role in intracellular trafficking and nuclear localization of pre-integration complex[19]. LTRs present at both 5′ and 3′ ends play a critical role in viral replication by regulating transcription, integration, and polyadenylation of viral transcripts.

Mature SRLV virions are enveloped particles composed of an outer lipid bilayer derived from the host cell membrane and embedded viral surface glycoprotein and transmembrane glycoprotein. SRLVs are reported to have extensive genetic diversity and exhibit high mutation rates. The genetic diversity of SRLVs arises primarily from the error-prone nature of reverse transcription as reverse transcriptase enzyme lacks proofreading activity and leads to frequent nucleotide substitutions and the accumulation of mutations, which ultimately leads to production of heterogeneous population of closely related SRLV variants, referred as viral quasispecies[20,21].

SRLVs: Genotypes and subtypes

Phylogenetic analysis of SRLVs sequences reported from various countries classified SRLVs into five groups (A, B, C, D, and E) based on two long segments, the *gag-pol* (1.8 kb) and the *pol* segment (1.2 kb)[22]. According to HIV classification standards, the nucleotide sequences among these genotypes and subtypes vary by 25-35% and 15-27%, respectively[23]. Genotype A comprises classical MVV strains and several related variants, whereas Genotype B includes the classical CAEV strains. The remaining genotypes (C, D, and E) are less common and are primarily restricted to specific geographical regions within Europe[24,25,26,27,28]. Genotype A is reported to be most heterogenous group comprising of 27 subtypes (A1-A27), whereas Genotype B (subtypes B1-B5) is genetically less diverse as compared to Genotype A[29,30]. The genetic variants circulating among Indian sheep and goat population hitherto remains unknown as only partial sequences targeting the LTR region had been amplified and showed homology with sequences generated from European countries[15].

Epidemiology and transmission of SRLV diseases

Worldwide scenario: A comprehensive analysis of worldwide serological studies demonstrated that SRLV infections are most prevalent in Europe (40.9%) followed by North America (21.8%), Asia (20.4%), Africa (16.7%), and Central and South America (1.7%)[31]. At the flock level, prevalence is generally much higher than individual animal prevalence because infected animals often remain asymptomatic for prolonged periods while continuing to transmit the virus to susceptible population. Among Asian countries, China, Iran, Turkey, Jordan, and Lebanon have reported substantial levels of infection in sheep and goat populations. Similarly, serological surveys conducted in Taiwan, Bangladesh, and Malaysia have demonstrated varying levels of CAEV exposure, reflecting the widespread distribution of SRLV

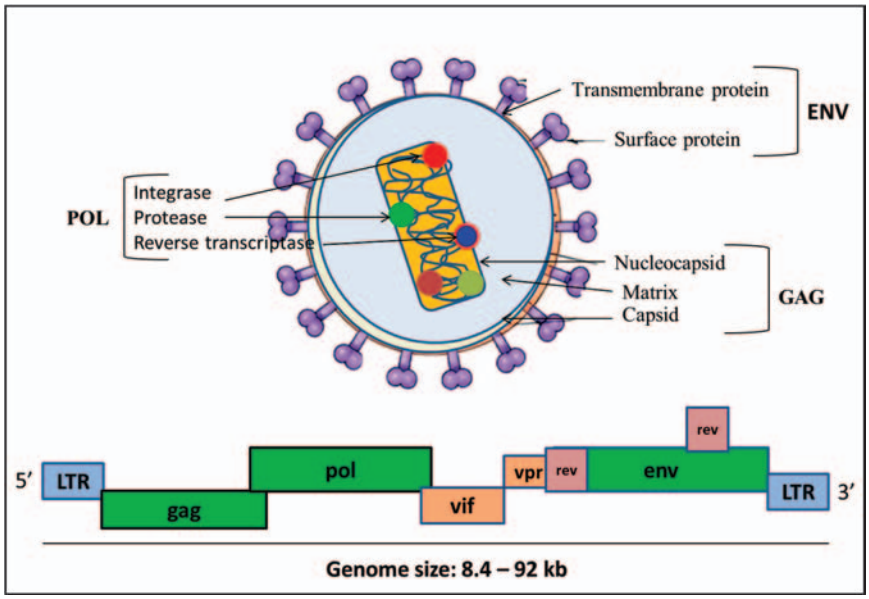

Fig. 1. SRLV genome organization and protein composition (gag, pol, env).

infections throughout the region[32,33]. Australia and New Zealand, have successfully maintained free status from these infections through rigorous surveillance and control programmes. In Iceland outbreak of MV resulted in death of 1 lakh sheep and more than half a million animals culling in order to eradicate MVV[6].

Indian scenario: The history of SRLV infection in India dates back to the 1960s, when maedi-like pulmonary lesions were reported in sheep and goats, although the etiological agent could not be conclusively identified[34]. First report of CAEV antibodies in sera of small ruminant in India reported by Singh et al.[35], where they detected 18 % sero-positivity by AGID and ELISA. Other serological studies conducted in different regions of northern India have reported prevalence rates ranging from 12.17% to 29.16% in sheep and goats[14,15]. Lower prevalence rates have also been reported from Mathura and Andhra Pradesh[36.37]. Molecular detection of proviral DNA of MVV using PCR-based assays has yielded positivity rates ranging from 6.85% to 10.65%, confirming active viral circulation within these populations. Recent investigations have also highlighted the occurrence of mixed infections involving SRLVs and other respiratory pathogens such as jaagsiekte sheep retrovirus (JSRV) and *Mycoplasma* spp.[11] (Table 1).

Transmission: Transmission of SRLVs occurs through both horizontal and vertical routes. Horizontal transmission occurs primarily through prolonged close contact and inhalation of respiratory secretions containing infected monocytes and macrophages, particularly in intensive production systems[40]. Consequently, flock density, ventilation, housing conditions, and management practices substantially influence transmission dynamics[40]. Vertical transmission primarily occurs through the ingestion of infected colostrum and milk. The lactogenic route is considered the most important mechanism for maintaining infection within affected flocks as infected macrophages and monocytes with proviral DNA present in the mammary glands and serve as major sources of virus for newborn lambs and kids[5,41]. In addition, intrauterine transmission has also been reported, however, the epidemiological importance of prenatal transmission remains controversial and appears to be less significant than colostral and milk-borne transmission[42]. SRLV nucleic acids have been detected in semen, indicating the possibility of venereal transmission[43]. Similarly, contaminated instruments and management procedures involving blood transfer may contribute to mechanical transmission under field conditions.

Pathogenesis of SRLVs

The cellular receptor for the SRLVs remains incompletely understood as studies suggested that different SRLV strains may employ distinct cellular receptors, explaining differences in host range, tissue tropism, and pathogenicity[44]. Viral entry in the cell is initiated by interaction between envelope glycoproteins and host-cell receptors, followed by membrane fusion and release of the viral core into the cytoplasm. MHC II, CD4 and CXCR4 proteins suggested as possible receptors for the SRLVs, but none of these have been reported to be the main receptor. It is reported that C type lectins part of the mannose receptor family may act as alternative SRLV receptor as MVV gains entry into the cell via mannosylated residues on its envelope proteins[45].

SRLVs are reported to replicate in the monocyte-macrophage lineage cells and infection to T lymphocytes does not lead to productive infection[46]. Macrophages and dendritic cells are considered the principal target cells for viral replication and dissemination[47,48]. Following entry, the viral RNA genome undergoes reverse transcription to form proviral DNA, which subsequently integrates into the host genome. This integrated provirus establishes a lifelong infection and serves as a template for future viral replication. Although circulating monocytes are readily infected and may harbour integrated proviral DNA, viral replication remains largely restricted until these cells

Table 1. Occurrence/prevalence of SRLVs in Indian sheep and goat population.

S. No.	SRLV infection	Occurrence/ prevalence	Sample type	Methodology	References
1.	CAEV	18 %	Serum	AGID & ELISA	Singh *et al.*[35]
2.	CAEV	3.3 %	Serum	ELISA	Waseem *et al.*[36]
3.	MVV	4.28 %	Serum	ELISA	Didugu *et al.*[37]
4.	CAEV	4.5 %	Serum	ELISA	Didugu *et al.*[37]
5.	SRLVs	12.17 %	Serum	ELISA	Mishra *et al.*[38]
6.	MVV	6.85 %	Lung	Nested PCR	Mishra *et al.*[38]
7.	SRLVs	19.58 %	Serum	ELISA	Kumar *et al.*[14]
8.	MVV	10.41 %	Blood, lung, nasal swabs, mammary gland	Nested PCR	Kumar *et al.*[14]
9.	SRLVs	29.16	Serum	ELISA	Valecha *et al.*[15]
10.	MVV	10.65 %	Blood, lung, mammary gland, joints, brain	Nested PCR	Valecha *et al.*[15]
11.	MVV	2.66 %	Milk	Nested PCR	Yadav *et al.*[39]

differentiate into mature macrophages. This phenomenon has led to the description of infected monocytes as "Trojan horses" that disseminate the virus throughout the host organs while avoiding immune elimination[49].

Viral integration is followed by viral transcription by promoter elements located within the LTR, resulting in the synthesis of viral RNA and proteins that assemble into progeny virions. Newly formed virions bud from the host-cell membrane and mature through proteolytic processing of viral proteins[4,19]. The pathological lesions produced by SRLV infection are largely immune-mediated rather than the direct result of viral cytopathic effects. The infected macrophages within target organs cause continuous antigenic stimulation and recruit mononuclear inflammatory cells to affected tissues through the production of cytokines, chemokines, and other inflammatory mediators. The lungs, mammary glands, joints, and central nervous system represent the principal target organs. Persistent accumulation of lymphocytes, macrophages, and plasma cells within these tissues leads to chronic inflammation, tissue remodeling, and progressive loss of organ function. The resulting chronic inflammatory microenvironment contributes to the development of interstitial pneumonia, non-suppurative mastitis, proliferative arthritis, and encephalomyelitis that are characteristic of SRLV infections[12,14].

Pathology of SRLVs associated diseases

Maedi (ovine progressive pneumonia): Maedi represents the respiratory form of MVV infection, and is the most common clinical manifestation in sheep. The disease is characterized by chronic, progressive, non-febrile interstitial pneumonia that primarily affects adult sheep older than two years of age. Although goats may also develop respiratory disease but the pulmonary lesions are generally more severe and more frequently reported in sheep[5,50]. Clinical signs of maedi often become apparent only after years of subclinical infection and early manifestations include exercise intolerance and reduced physical performance, which progresses to dyspnoea, tachypnoea, abdominal breathing, nostril dilatation, neck extension, and open-mouth breathing. The affected animals show marked weight loss and cachexia despite normal appetite[5].

The lungs of the maedi affected sheep are enlarged, heavy, and fail to collapse upon opening of the thoracic cavity. Affected lungs appear pale grey to pink, firm, rubbery, and diffusely consolidated along with rib impressions on the pleural surface. Mediastinal and tracheobronchial lymph nodes are reported to be enlarged due to chronic lymphoid hyperplasia[51]. Histological hallmark lesion of maedi include chronic lymphocytic interstitial pneumonia, prominent lymphoid follicle formation around bronchioles and blood vessels, and marked thickening of alveolar septa due to infiltration of lymphocytes, plasma cells and macrophages (Fig. 2). Progressive interstitial fibrosis and smooth muscle hyperplasia also reported as consistent finding in many studies. Occurrence of the maedi on basis of histological lesions in the pulmonary affection contributes around 5-6.5%[14,52,53]. The lymphoid follicles in lungs are composed predominantly of CD4+ and CD8+ T lymphocytes[44].

Visna (Neurological Form): Visna represents the neurological manifestation of MVV infection and neurological signs include progressive hind-limb weakness, ataxia, incoordination, paresis, and eventual paralysis. As the disease progress, affected animals may become recumbent and lose weight progressively. Grossly, the pathological lesions are usually absent, however, some cases may exhibit meningeal thickening, granular changes within the choroid plexus, grey discoloration of the brainstem and cerebellum, or focal areas of softening and discoloration within periventricular regions of the brain and spinal cord[54]. Development of chronic non-suppurative encephalomyelitis is main histological lesion observed in visna[55]. Based upon histology, three patterns of lesion have been described *viz*. vascular pattern (perivascular cuffing with lymphocytes and macrophages), infiltrative pattern (diffuse infiltration of MNCs within neural tissues), and malacic pattern (demyelination, tissue degeneration, focal necrosis)[56].

MVV associated lesions also develop in mammary gland and joint tissues. Involvement of mammary gland is considered important manifestations of SRLV infection after the respiratory form[57]. It occurs in both sheep and goats, and characterized by chronic, bilateral and non-painful indurative mastitis often accompanied by enlargement of the supramammary lymph nodes (Fig.2). Histological lesions are characterized by chronic non-suppurative interstitial mastitis with extensive infiltration of lymphocytes, plasma cells, and macrophages around mammary gland acini and lactiferous ducts[54,58]. MVV nucleic acid have been detected in the milk samples of the Indian goats indicating mammary gland involvement[39]. Arthritic form is not commonly reported in MVV infection of sheep, but lesions in carpal and tarsal joints reported in some cases. Microscopically, the joint tissue showed infiltration of MNCs in the synovial membrane and villous hypertrophy[4,5,59].

Caprine arthritis encephalitis (CAE): CAE is characterized by the presence of neurological and arthritic form. Neurological form usually seen in kids between 2-4 months of age and initial clinical signs include ataxia, weakness, lameness, and incoordination, which may progress further to paresis, paralysis, recumbency, and occasional paddling movements[60]. Focal areas of discoloration within the white matter of the brain and spinal cord are frequently observed gross lesion (Fig.2).

Histopathological lesions characterized by chronic non-suppurative leukoencephalomyelitis with perivascular cuffing, demyelination, gliosis, astrocytosis, and infiltration of macrophages and lymphocytes. The lesions are largely confined to white matter tracts and resemble those observed in visna.

Arthritic form of CAE is usually seen in adult goats (older than 1 year) and affected animals exhibit progressive lameness, stiffness, reluctance to move, weight loss, poor body condition, and reduced productivity. Carpal joints in particular show swelling/enlargement due to thickening of the synovial membrane, distension of the joint capsule, accumulation of synovial fluid, and hypertrophy of periarticular tissues[61]. Microscopic lesions include chronic proliferative synovitis characterized by synovial cell hyperplasia, villous hypertrophy, fibrosis, and infiltration of lymphocytes, macrophages, and plasma cells[62]. Progressive destruction of joint structures contributes to chronic pain and lameness. Besides arthritis and encephalitis, CAEV affected animals also show lesions in respiratory and mammary gland similar to those observed in MVV. Pulmonary lesions include chronic lymphocytic interstitial pneumonia, whereas mammary lesions are characterized by chronic indurative mastitis[61]. Few reports also indicated that renal tissues are also affected in CAE, showing glomerulonephritis, amyloid deposition, interstitial nephritis, fibrosis, and lymphocytic fibrino-necrotizing arteritis[63].

Diagnosis of SRLVs

Different diagnostic tests (serological, nucleic acid based, protein based) are available for detection of SRLVs for surveillance and control programmes but a single gold test to confirm the disease at early stage is lacking due to absence of overt clinical signs. So, a combination of molecular and serological techniques is usually employed to diagnose the disease at early stage[64] (Fig. 3).

Clinical and pathological diagnosis: Affected animals with characteristics clinical signs and symptoms can be suspected for SRLV infections. Clinical signs and symptoms viz. chronic progressive pneumonia, indurative mastitis, proliferative arthritis, and non-suppurative encephalomyelitis are most common. As the clinical incubation period is very long for these diseases and clinical disease develops only in few infected animals, the clinical findings alone are insufficient for definitive diagnosis. Necropsy and histopathological findings with characteristic gross and microscopic lesions may provide valuable diagnostic information.

Serological tests: The immune response against the SRLVs is non-protective but by detecting the antibodies in the serum, it is possible to diagnose the disease at flock level. Different serological tests viz. AGID, ELISA, Western blotting (WB), radioimmunoprecipitation assay (RIPA), and radioimmunoassay (RIA), etc. are available for the SRLV diagnosis[26,65,66]. AGID was the World Organization of Animal Health (WOAH) for recommended test for routine disease screening at early stage, however, after the development of ELISA assays, AGID is used for confirmatory diagnosis only[67]. Commonly used antigens for the development of the serological assays include envelope glycoprotein gp135, p28 capsid antigen of MVV and p35 capsid antigen of CAEV[66,68]. Serological tests are rapidly used in the SRLV surveillance and control programmes because they are relatively inexpensive, practical, and suitable for large-scale screening of small ruminant populations. Sometimes ELISAs provide unsatisfactory results due difference between the viral antigen in the kit/test, and the antigens expression at different stages of the infection, as antibody response against capsid and matrix protein (p16, p28, p25) prevails during the early stages and antibody responses are mounted against the envelope glycoproteins (gp135 and gp46) at later stage[67,69]. Similarly, difference between the strains circulating

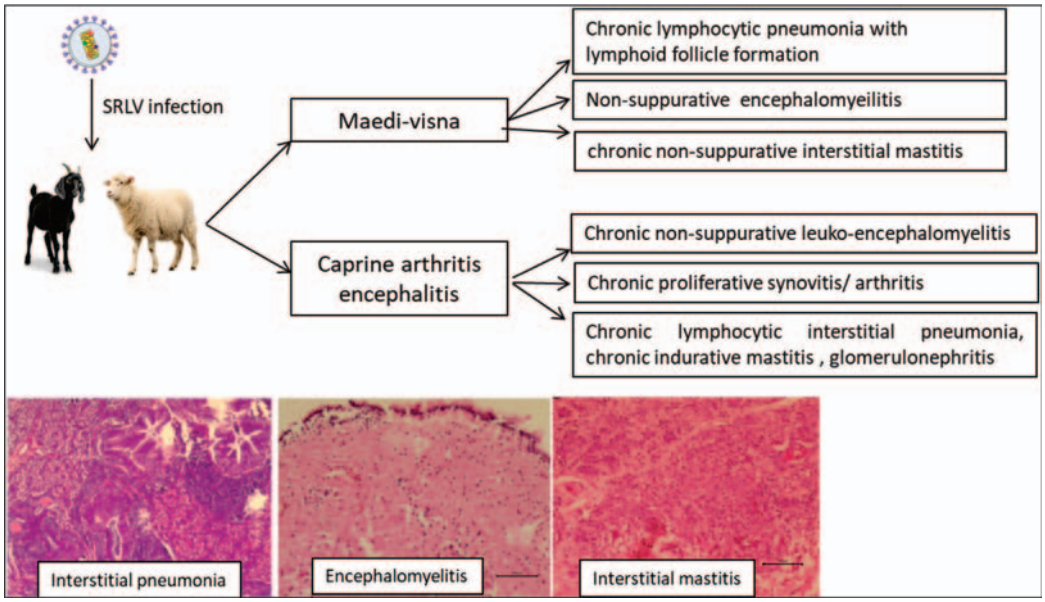

Fig. 2. Pathology of SRLV associated diseases in small ruminants.

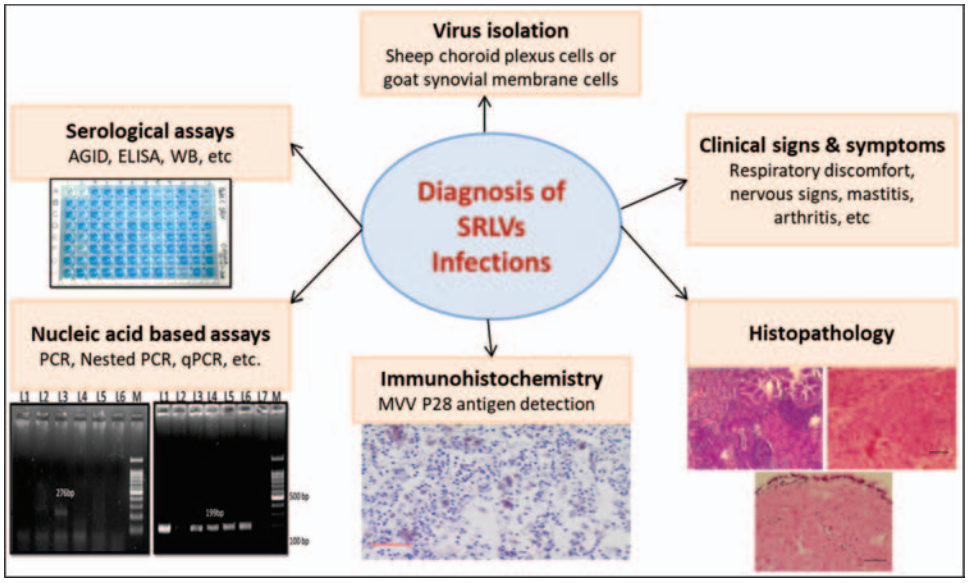

Fig. 3. Diagnostic approaches for the SRLV associated diseases

developed for SRLV diagnosis targeted the *gag* and *pol* genes of MVV and CAEV[72] (Zanoni et al., 1990). Subsequently, numerous assays targeting the *LTR*, *gag*, *pol*, and *env* regions have been described[64]. A major advantage of PCR is its ability to detect infection prior to antibody development. However, diagnostic sensitivity may be compromised by low viral loads, latent infection, and extensive genetic variability among circulating strains. Nested PCR developed for MVV detection showed enhanced sensitivity and specificity, and has been widely applied in epidemiological investigations[73,74]. Real time PCR assays have also been developed to detect low copy numbers of the proviral DNA and it offers improved analytical sensitivity and reduced contamination risk. Despite various advantages of the PCR based assays, detection of the SRLV strains with high mutation is challenging and lead to false-negative results. In addition, the low number of infected circulating cells and uneven distribution of proviral DNA among tissues may reduce diagnostic sensitivity. Combining molecular and serological approaches generally provides the highest diagnostic accuracy. Additionally, techniques such as loop-mediated isothermal amplification (LAMP) and recombinase polymerase amplification lateral flow dipstick (RPA-LFD) have recently been successfully used for CAEV diagnosis[75,76].

IHC: IHC serves as a valuable adjunctive diagnostic tool by enabling the direct demonstration of viral antigens within tissue lesions. Antibodies directed against viral capsid proteins, particularly p28, have been successfully employed to identify infected cells in lungs, mammary glands, lymph nodes, joints, and central nervous system tissues[14,15,58,74]. It is suggested that anti-inflammatory and down regulatory alveolar macrophage retain MVV capsid antigen and may be harbouring a prolonged MVV infection[66]. The technique not only confirms infection but also provides important information regarding viral distribution and lesion pathogenesis.

Virus Isolation: Isolation process of SRLVs in the cell culture is definitive method to demonstrate the virus presence, but it requires presence of living cells in tissue samples. SRLVs may remain in latency, so the development of clear CPE may not always be obtained[77,78]. MVV and CAEV can be isolated by cell culture by using blood leukocytes and milk samples from the seropositive live animal and positive tissues from the necropsied animals (lungs, brain, joint, spleen, udder etc.). For MVV, sheep choroid plexus (SCP) cells can be used for isolation and usually prepared as primary explant cultures from fetal or new-born MVV free lambs. For CAEV, goat synovial membrane (GSM) cell culture can be used. Foetal lamb lung (FLL) and foetal goat lung (FGL) can also be used for the culturing of SRLVs[79] (Oguma *et al.*, 2013). Successful isolation is confirmed through observation of cytopathic effects, detection of reverse transcriptase activity, or positive molecular assays like PCR and FAT[51,79].

Nucleic acid based assays: PCR is widely employed for the detection of proviral DNA in various sample types (blood mononuclear cells, plasma, milk, bronchoalveolar lavage fluid, lungs, brain, mammary gland, synovial tissues, lymph nodes, spleen, liver, kidneys, reproductive tissues, bone marrow) of the SRLV infected animals[64]. The first PCR assays at particular region leads to misdiagnosis[26,70]. Milk is reported to impede reliable diagnosis of the SRLVs due to the false positive results and suppressed immune response during lactation[51,71].

CONCLUSION

SRLVs are worldwide in distribution and cause slow progressive diseases in small ruminants with their ability to establish lifelong infections. Unlike many acute viral infections, SRLVs infections have prolonged incubation periods, latent infection, extensive genetic diversity, and persistent viral replication within host macrophages, which makes them difficult to control and

eradicate from an infected population. So, the success of a control programme can be achieved by employing a multifaceted approach integrating regular surveillance, proper biosecurity measures, restricted flock movement and molecular epidemiological monitoring.

ACKNOWLEDGEMENTS

The authors are thankful to the SERB-DST, Govt. of India and Director, ICAR-Indian Veterinary Research Institute, Izatnagar for providing the necessary facilities for carrying research work on retrovirus associated diseases of small ruminants.

Financial support and sponsorship: No

Conflict of interest: None

Use of artificial intelligence for manuscript preparation: The author confirms that there was no use of AI-assisted technology for assisting in the writing of the manuscript and no images were manipulated using AI.

REFERENCES

1. Palmarini M, Cousens C, Dalziel RG, Bai J, Stedman K. 1996. The exogenous form of Jaagsiekte retrovirus is specifically associated with a contagious lung cancer of sheep. *J Virol* **70:** 1618-1623
2. Pawaiya RVS, Kumar P. 2011. Occurrence of neoplastic diseases in small ruminants in India: an overview. *Indian J Small Ruminants* **17(2):** 151-165.
3. Mishra S, Kumar P, Dar JA, George N, Singh V, Singh R. 2021. Differential immunohistochemical expression of JSRV capsid antigen and tumour biomarkers in classical and atypical OPA: A comparative study. *Biol Rhythm Res* **52(6):** 946-956.
4. Blacklaws BA, Berriatua E, Torsteinsdottir S, Watt NJ, de Andres D, Klein D, Harkiss GD. 2004. Transmission of small ruminant lentiviruses. *Vet Microbiol* **101(3):**199-208..
5. Gomez-Lucia E, Barquero N, Domenech A. 2018. Maedi-visna: current perspectives. *Vet Med* **9:** 11-21.
6. Leroux C, Cruz JCM, Mornex JF. 2010. SRLVs: A genetic continuum of lentiviral species in sheep and goats with cumulative evidence of cross species transmission. *Curr HIV Res* **8:** 94-100.
7. Pisoni G, Bertoni G, Puricelli M, Maccalli M, Moroni P. 2007. Demonstration of coinfection with and recombination by caprine arthritis-encephalitis virus and maedi-visna virus in naturally infected goats. *J Virol* **81:** 4948-4955.
8. Minardi da Cruz JC, Singh DK, Lamara A, Chebloune Y. 2013. Small ruminant lentiviruses (SRLVs) break the species barrier to acquire new host range. *Viruses* **5:** 1867-1884.
9. Olech M, Osinski Z, Kuzmak J. 2020. Seroprevalence of small ruminant lentivirus (SRLV) infection in wild cervids in Poland. *Prev Vet Med* **176:** 104905.
10. Kuhar U, Vengust DZ, Vengust G. 2022. Serological survey of small ruminant lentivirus infections in free-ranging mouflon and chamois in Slovenia. *Animals* **12(8):** 1032.
11. Valecha S, Roopa N, Yadav HS, Singh R, Singh V, Kumar P. 2023. Co-infection of maedi visna virus (MVV) with jaagsiekte sheep retrovirus (JSRV) and mycoplasma in Indian sheep and goats. *Indian J Vet Pathol* **47(1):** 13-17.
12. Rosato G, Abril C, Hilbe M, Seehusen F. 2023. A combined approach for detection of ovine small ruminant retrovirus co-infections. *Viruses* **15(2):** 376.
13. Yadav HS, Neha, Kumar SDV, Singh CP, Jana C, Singh V, Kumar P. 2024. Mixed infection of ovine pulmonary adenocarcinoma and maedi in sheep: A case study. *Indian J Vet Pathol* **48(2):** 196-198.
14. Kumar K, Kumar P, Sindhoora K, Valecha S, Kumar R, Singh V, Singh R. 2022. Detection and immune cell response of natural maedi visna virus (MVV) infection in Indian sheep and goats. *Microb Pathog* **165:** 105467.
15. Valecha S, Yadav HS, Roopa N, Vinaykumar SD, Bhardwaj M, Singh V, Kumar P. 2024. Distribution of maedi-visna virus in different organs of the spontaneously affected small ruminants in India. *Iranian J Vet Res* **25(1):** 41-47.
16. Tiley LS, Brown PH, Le SY, Maizel JV, Clements JE, Cullen BR. 1990. Visna virus encodes a post-transcriptional regulator of viral structural gene expression. *Proc Natl Acad Sci USA* **87(19):** 7497-7501.
17. Toohey KL, Haase AT. 1994. The rev gene of visna virus is required for productive infection. *Virology* **200(1):** 276-280.
18. Harmache A, Russo P, Guiguen F, Vitu C, Vignoni M, Bouyac M, Hieblot C, Pepin M, Vigne R, Suzan M. 1996. Requirement of caprine arthritis encephalitis virus *vif* gene for *in vivo* replication. *Virology* **224(1):** 246-255.
19. Villet S, Bouzar BA, Morin T, Verdier G, Legras C, Chebloune Y. 2003. Maedi-visna virus and caprine arthritis encephalitis virus genomes encode a Vpr-like but no Tat protein. *J Virol* **77(17):** 9632-9638.
20. Haflidadottir BS, Matthiasdottir S, Agnarsdottir G, Torsteinsdottir S, Petursson G, Andresson OS, Andresdottir V. 2008. Mutational analysis of a principal neutralization domain of visna/maedi virus envelope glycoprotein. *J Gen Virol* **89(3):** 716-721.
21. Olech M. 2023. The genetic variability of small-ruminant lentiviruses and its impact on tropism, the development of diagnostic tests and vaccines and the effectiveness of control programmes. *J Vet Res* **67(4):** 479-502.
22. Shah C, Böni J, Huder JB, Vogt HR, Mühlherr J, Zanoni R, Miserez R, Lutz H, Schüpbach J. 2004. Phylogenetic analysis and reclassification of caprine and ovine lentiviruses based on 104 new isolates: evidence for regular sheep-to-goat transmission and worldwide propagation through livestock trade. *Virology* **319(1):** 12-26.
23. Peeters M, Esu-Williams E, Vergne L, Montavon C, Mulanga-Kabeya C, Harry T, Ibironke A, Lesage D, Patrel D, Delaporte E. 2000. Predominance of subtype A and G HIV type 1 in Nigeria, with geographical differences in their distribution. *AIDS Res Hum Retroviruses* **16(4):** 315-325.
24. Gjerset B, Storset AK, Rimstad E. 2006. Genetic diversity of small-ruminant lentiviruses: Characterization of Norwegian isolates of caprine arthritis encephalitis virus. *J Gen Virol* **87(3):** 573-580.
25. Grego E, Bertolotti L, Quasso A, Profiti M, Lacerenza D, Muz D, Rosati S. 2007. Genetic characterization of small ruminant lentivirus in Italian mixed flocks: evidence for a novel genotype circulating in a local goat population. *J Gen Virol* **88:** 3423-3427.
26. Reina R, Grego E, Profiti M, Glaria I, Robino P, Quasso A, Amorena B, Rosati S. 2009. Development of specific diagnostic test for small ruminant lentivirus genotype E. *Vet Microbiol* **138:** 251-257.
27. Giammarioli M, Bazzucchi M, Puggioni G, Brajon G, Dei Giudici S, Taccori F, Feliziani F, De Mia GM. 2011. Phylogenetic analysis of small ruminant lentivirus (SRLV) in Italian flocks reveals the existence of novel genetic subtypes. *Virus Genes* **43:** 380-384.

28. Kuhar U, Barlič-Maganja D, Grom J. 2013. Development and validation of TaqMan probe based real time PCR assays for the specific detection of genotype A and B small ruminant lentivirus strains. *BMC Vet Res* **9(1):** 1-11.
29. Michiels R, Adjadj NR, De Regge N. 2020. Phylogenetic analysis of Belgian small ruminant lentiviruses supports cross species virus transmission and identifies new subtype B5 strains. *Pathogens* **9(3):** 183.
30. Arcangeli C, Torricelli M, Sebastiani C, Lucarelli D, Ciullo M, Passamonti F, Giammarioli M, Biagetti M. 2022. Genetic characterization of small ruminant lentiviruses (SRLVs) circulating in naturally infected sheep in Central Italy. *Viruses* **14(4):** 686.
31. Miguel R, Arrieta M, Rodriguez-Largo A, Echeverria I, Resendiz R, Perez E, Ruiz H, Pérez M, de Andres D, Reina R. 2021. Worldwide prevalence of small ruminant lentiviruses in sheep: A systematic review and meta-analysis. *Animals* **11(3):**784
32. Yang WC, Chen HY, Wang CY, Pan HY, Wu CW, Hsu YH, Su JC, Chan KW. 2017. High prevalence of caprine arthritis encephalitis virus (CAEV) in Taiwan revealed by large-scale serological survey. *J Vet Med Sci* **79(2):** 273-276.
33. Rahman MH, Akther S, Alam MS, Ali MZ, Ahmed S. 2023. Caprine arthritis and encephalitis virus infection in goats of Bangladesh: Serological detection and its associated risk factors. *Vet World* **16(11):** 2256-2263.
34. Rajya BS, Singh CM. 1964. The pathology of pneumonia and associated respiratory disease of sheep and goats. Occurrence of jaagsiekte and maedi in sheep and goats in India. *Am J Vet Res* **25:** 61-71.
35. Singh DK, Paliwal OP, Dubey SC. 1997. Caprine arthritis encephalitis in Indian goats. *Curr Sci* **72:** 702-702
36. Waseem A, Pawaiya RVS, Singh R, Gupta VK, Rajukumar K, Mir MS, Aamir S. 2015. Seroprevalence of caprine arthritis encephalitis virus infection (CAEV) in Indian goats. *Indian J Vet Pathol* **39(1):** 15-19.
37. Didugu H, Sagi S, Reddy CEN, Kishore KN, Reddy MV, Vishnu PG. 2016. First report of Maedi-Visna and Caprine Arthritis-Encephalitis viruses in Krishna district, Andhra Pradesh, *India. J Anim Res* **6(1):** 177-179.
38. Mishra S, Kumar P, Dar JA, George N, Singh R, Singh V, Singh R. 2020. Detection and prevalence of small ruminant lentiviral (SRLV) infections in Indian sheep and goats. *Indian J Vet Path* **44(4):** 207-211.
39. Yadav HS, Neha, Kumar SDV, Singh V, Kumar P. 2024. Detection of maedi visna virus (MVV) in milk samples of Indian goats. *Int J Adv Biochem Res* **SP-8(1):** 143-145.
40. Blacklaws BA, Berriatua E, Torsteinsdottir S, Watt NJ, De Andres D, Klein D, Harkiss GD. 2004. Transmission of small ruminant lentiviruses. *Vet Microbiol* **101(3):** 199-208.
41. Peterhans E, Greenland T, Badiola J, Harkiss G, Bertoni G, Amorena B, Eliaszewicz M, Juste R, Krassnig R, Lafont JP, Lenihan P. 2004. Routes of transmission and consequences of small ruminant lentiviruses (SRLVs) infection and eradication schemes. *Vet Res* **35(3):** 257-274.
42. Araujo JF, Andrioli A, Pinheiro RR, Sider LH, de Sousa ALM, de Azevedo DAA, Peixoto RM, Lima AMC, Damasceno EM, Souza SCR, Teixeira MFDS. 2020. Vertical transmissibility of small ruminant lentivirus. *PLoS One* **15(11):** e0239916.
43. Reina R, Glaria I, Cianca S, Crespo H, de Andres X, Goni C, Lasarte JM, Lujan L, Amorena B, de Andres DF. 2011. Use of small ruminant lentivirus-infected rams for artificial insemination. *Vet J* **189(1):** 106-107.
44. Minguijon E, Gonzalez L, De Las Heras M, Gomez N, Marcia GM, Juste RA, Moreno B. 2013. Pathological and aetiological studies in sheep exhibiting extrathoracic metastasis of ovine pulmonary adenocarcinoma. *J Comp Pathol* **148:** 71-78.
45. Crespo H, Reina R, Glaria I, Ramírez H, de Andrés X, Jáuregui P, Luján L, Martínez-Pomares L, Amorena B, de Andrés DF. 2011. Identification of the ovine mannose receptor and its possible role in Visna/Maedi virus infection. *Vet Res* **42:** 1-10.
46. Gorrell MD, Brandon MR, Sheffer D, Adams RJ, Narayan O. 1992. Ovine lentivirus is macrophagetropic and does not replicate productively in T lymphocytes. *J Virol* **66:** 2679-2688.
47. Ryan S, Tiley L, McConnell I, Blacklaws B. 2000. Infection of dendritic cells by the Maedi-Visna lentivirus. *J Virol* **74(21):** 10096-10103.
48. Crespo H, Bertolotti L, Juganaru M, Glaria I, de Andres D, Amorena B, Rosati S, Reina R. 2013. Small ruminant macrophage polarization may play a pivotal role on lentiviral infection. *Vet Res* **44:** 1-13.
49. Peluso R, Haase A, Stowring L, Edwards M, Ventura P. 1985. A Trojan Horse mechanism for the spread of visna virus in monocytes. *Virology* **147(1):** 231-236.
50. Callado AKC, Castro RSD, Teixeira MFDS. 2001. Small ruminant lentiviruses (CAEV and Maedi-Visna): review and perspectives. *Braz J Vet Res Anim Sci* **21:** 87-97.
51. Barquero N, Gomez-Lucia E, Arjona A, Toural C, Las Heras A, Fernández-Garayzábal JF, Ruiz-Santa Quiteria JA, Doménech A. 2013. Investigation of risk factors associated with infections caused by small ruminant lentiviruses. *J Vet Res* **57(4):** 473-478.
52. Singh R, Kumar P, Singh R, Dhama K, Kumari S, Yadav JP, Kashyap G, Singh KP, Singh V, Sahoo M. 2017. Pathology and polymerase chain reaction detection of ovine progressive pneumonia (maedi) cases in slaughtered sheep in India. *Vet World* **10(11):** 1401-1406.
53. Mishra S, Kumar P, George N, Singh R, Singh V, Singh R. 2018. Survey of lung affections in sheep and goats: a slaughterhouse study. *J Entomol Zool Stud* **6(4):** 118-120.
54. Cecco BS, Henker LC, Lorenzett MP, Molossi FA, Schwertz CI, Baumbach LF, Weber MN, Canal CW, Driemeier D, Pavarini SP, Langohr IM. 2022. An outbreak of visna-maedi in a flock of sheep in Southern Brazil. *Braz J Microbiol* **53(3):** 1723-1730.
55. Benavides J, Fuertes M, Garcia-Pariente C, Ferreras MC, Marín JG, Perez V. 2006. Natural cases of visna in sheep with myelitis as the sole lesion in the central nervous system. *J Comp Pathol* **134:** 219-230.
56. Sigurdsson B, Palsson PA. 1954. Visna of sheep. A slow demyelinating infection. *Brit Exp Path* **39**: 519-528.
57. Lujan L, Garcia Marin JF, Fernandez de Luco D, Vargas A, Badiola JJ. 1991. Pathological changes in the lungs and mammary glands of sheep and their relationship with maedi-visna infection. *Vet Rec* **129(3):** 51-54.
58. Bolea R, Monleón E, Carrasco L, Vargas A, de Andrés D, Amorena B, Badiola JJ, Luján L. 2006. Maedi-visna virus infection of ovine mammary epithelial cells. *Vet Res* **37:** 133-144.
59. Christodoulopoulos G. 2006. Maedi-Visna: Clinical review and short reference on the disease status in Mediterranean countries. *Small Rumin Res* **62:** 47-53.
60. Cork LC, Hadlow WJ, Gorham JR, Piper RC, Crawford TB. 1974. Pathology of viral leukoencephalomyelitis of goats. *Acta Neuropathol* **29:** 281-292.
61. Son GI, Hong EJ, Shin HJ. 2021. Case report: A case of caprine arthritis encephalitis in dairy goat farms in South Korea. *Front Vet Sci* **8:** 773039.
62. von Bodungen U, Lechner F, Pfister H, Vogt HR, Cheevers WP, Bertoni G, Jungi TW, Peterhans E. 1998. Immunohistology of the early course of lentivirus-induced arthritis. *Clin Exp Immunol* **111(2):** 384-390.
63. Murphy BG, Castillo D, Mete A, Vogel H, Goldsmith D, Barro M, Gonzales-Viera O. 2021. Caprine arthritis encephalitis virus is associated with renal lesions. *Viruses* **13:** 1051.

64. Kalogianni AI, Stavropoulos I, Chaintoutis SC, Bossis I, Gelasakis AI. 2021. Serological, molecular and culture-based diagnosis of lentiviral infections in small ruminants. *Viruses* **13(9):** 1711.
65. Ramirez H, Reina R, Amorena B, Andres D, Martinez H. 2013. Small ruminant lentiviruses: genetic variability, tropism and diagnosis. *Viruses* **5(4):** 1175-1207.
66. Herrmann-Hoesing LM. 2010. Diagnostic assays used to control small ruminant lentiviruses. *J Vet Diagn Invest* **22(6):** 843-855.
67. Michiels R, Van Mael E, Quinet C, Adjadj NR, Cay AB, De Regge N. 2018. Comparative analysis of different serological and molecular tests for the detection of small ruminant lentiviruses (SRLVs) in Belgian sheep and goats. *Viruses* **10(12):** 696.
68. de Andres D, Klein D, Watt NJ, Berriatua E, Torsteinsdottir S, Blacklaws BA, Harkiss GD. 2005. Diagnostic tests for small ruminant lentiviruses. *Vet Microbiol* **107:** 49-62.
69. Brinkhof J, Van Maanen C. 2007. Evaluation of five enzyme-linked immunosorbent assays and an agar gel immunodiffusion test for detection of antibodies to small ruminant lentiviruses. *Clin Vaccine Immunol* **14(9):** 1210-1214.
70. Nogarol C, Bertolotti L, Klevar S, Profiti M, Gjerset B, Rosati S. 2019. Serological characterization of small ruminant lentiviruses: A complete tool for serotyping lentivirus infection in goats. *Small Rumin Res* **176:** 42-46.
71. Adjadj NR, Vicca J, Michiels R, De Regge N. 2019. Non-sense of milk testing in small ruminant lentivirus control programs in goats: Comparative analysis of antibody detection and molecular diagnosis in blood and milk. *Viruses* **12(1):** 3.
72. Zanoni R, Pauli U, Peterhans E. 1990. Detection of caprine arthritis encephalitis and maedi-visna viruses using the polymerase chain reaction. *Experientia* **46:** 316-319.
73. Extramiana AB, González L, Cortabarría N, Garcia M, Juste RA. 2002. Evaluation of a PCR technique for the detection of Maedi-Visna proviral DNA in blood, milk and tissue samples of naturally infected sheep. *Small Rumin Res* **44:** 109-118.
74. Preziuso S, Taccini E, Rossi G, Renzoni G, Braca G. 2003. Experimental maedi visna virus infection in sheep: a morphological, immunohistochemical and PCR study after three years of infection. *Eur J Histochem* **47:** 373-378.
75. Huang J, Sun Y, Liu Y, Xiao H, Zhuang S. 2012. Development of a loop-mediated isothermal amplification method for rapid detection of caprine arthritis-encephalitis virus proviral DNA. *Arch Virol* **157:** 1463-1469.
76. Tu PA, Shiu JS, Lee SH, Pang VF, Wang DC, Wang PH. 2017. Development of a recombinase polymerase amplification lateral flow dipstick (RPA-LFD) for the field diagnosis of caprine arthritis-encephalitis virus (CAEV) infection. *J Virol Methods* **243:** 98-104.
77. Johnson GC, Adams DS, McGuire TC. 1983. Pronounced production of polyclonal immunoglobulin G1 in the synovial fluid of goats with caprine arthritis-encephalitis virus infection. *Infect Immun* **41:** 805-815.
78. Pepin M, Vitu C, Russo P, Mornex J, Peterhans E. 1998. Maedi-visna virus infection in sheep: a review. *Vet Res* **29:** 341-367.
79. Oguma K, Tanaka C, Harasawa R, Kimura A, Sasaki J, Goryo M, Sentsui H. 2014. Isolation of maedi/visna virus from a sheep in Japan. *J Vet Med Sci* **76(2):** 211-218.

Indian J. Vet. Pathol., 50(4) : 300-305, 2026: DOI: https://doi.org/10.56093/vjp1xe76

RESEARCH ARTICLE

Histopathological alterations associated with etiological determinants of chronic diarrhoea in adult Dairy Bovines

Nuzhat Hassan[1*], Charanjit Singh Randhawa[1], Kuldeep Gupta[2], Naresh K. Sood[2], Shoor Vir Singh[3], Kundan Chaubey[3] and Ashiq Hussian[1]

Guru Angad Dev Veterinary and Animal Sciences University, Ludhiana-1410 04, Punjab, India

[1]Department of Veterinary Medicine;

[2]Department of Veterinary Pathology;

[3]Department of Microbiology, Central Institute for Research on Goats, India

***Address of correspondence**

Dr Nuzhat Hassan, E-mail: drnuzhatzargar@gmail.com

ORCID ID: 0000-0002-8871-9655, 0000-0002-2946-8585

Received: 2.1.26; Accepted: 18.8.26

ABSTRACT

The study investigated the histopathological markers of various etiologies of chronic diarrhoea in adult dairy cattle and buffaloes, thereby identifying the tissue structural changes and associated cellular abnormalities. Various diagnostic methods, including microscopy and PCR-based molecular techniques, were employed to identify the underlying etiologies associated with histopathological changes. The key finding revealed that chronic diarrhoea in affected bovines is attributed to both non-infectious/infectious factors, as well as dietary complications. Consequent to the specific etiologies, histopathology of intestinal tissue biopsies and postmortem samples revealed mild to chronic enteritis, superficial to chronic inflammation and mucosal shedding. Furthermore, lymph node examination revealed the presence of multinucleated giant cells, lymphoid hyperplasia, chronic inflammation and granulomatous infiltration. The findings underscore the significance of histopathological markers as diagnostic indicators, enabling more precise and targeted management strategies for chronic diarrhoea in dairy animals.

Keywords: Biopsy, Bovines, Chronic diarrhoea, Etiologies, Histopathology

INTRODUCTION

Diarrhoea is the hallmark prodrome of intestinal dysfunction and may or may not be accompanied by additional or secondary clinical symptoms[1]. When diarrhoea persists for over two weeks (>2 weeks), it is categorised as chronic[2]. The clinical manifestation of chronic diarrhoea not only adversely affects the animal's general health but also carries substantial economic consequences[1,3]. These include losses through culling, weight reduction, diminished milk production, increased treatment expenses and an increased risk of transmitting infections to healthy herd mates[4]. The aetiology of chronic diarrhoea can be difficult to identify and requires an expensive diagnostic and therapeutic approach[5]. However, further laboratory testing, particularly histopathological findings, can be explored to enhance diagnostic accuracy.

Recognising the intricate nature of chronic diarrhoea underscores the importance of a comprehensive approach to diagnosis and treatment within the field of animal health[6]. Understanding the diverse factors triggering gastrointestinal dysfunction is crucial. Inflammatory causes, often from infections or irregular physiological processes, significantly affect gut health[7]. Infectious agents like bacteria and parasites play a critical role, particularly in tropical regions, posing challenges to dairy industries due to persistent diarrhoea and diminished body condition among livestock[8]. Despite these challenges, a gap remains in understanding the frequency and distribution of primary and secondary causes of chronic diarrheal diseases in adult cattle and buffalo, particularly in tropical conditions. This study highlights the importance of examining histopathological changes associated with various enteropathies of chronic diarrheal diseases in bovines. The objective is to explore and refine diagnostic protocols, thereby enhancing clinical management strategies for bovines with recurrent or persistent chronic diarrhoea.

How to cite this article: Hassan, N., Randhawa, C.S., Gupta, K., Sood, N.K., Singh, S.V., Chaubey, K. and Hussian, A. 2026. Histopathological alterations associated with etiological determinants of chronic diarrhoea in adult Dairy Bovines. Indian J. Vet. Pathol., 50(4) : 300-305.

MATERIALS AND METHODS

Study population:

The adult dairy cattle and buffaloes (n=101) exhibiting clinical signs of persisting diarrhoea for over a week were selected for the study. These animals were presented to the large animal clinics of the Guru Angad Dev Veterinary and Animal Sciences University (GADVASU), College of Veterinary Science (COVS), in Ludhiana. The study population

include female cross-bred adult dairy bovines (>2 years old) with varying lactation status.

Clinical examination and sampling:

Detailed clinical examinations were performed after a thorough anamnesis of each case. Based on that, a provisional diagnosis was constructed. Appropriate samples (rectal biopsies, ileum and mesenteric lymph node biopsies; necropsy samples) and rectal scrapings were taken from the clinically affected animals, immediately transferred to the clinical diagnostic laboratory and examined for microscopic, molecular and histopathological diagnosis.

Various diagnostic techniques were employed, including parasitic identification techniques for parasite eggs[9], which revealed amphistomes and strongyles in many cases. Diagnosis based on microscopic examination of the cyst morphology predominantly identified *Balantidium coli* cysts[10]. Acid-fast bacilli were identified through Ziehl-Neelsen staining[11]. Molecular diagnosis involved DNA extraction[12] followed by PCR for *Mycobacterium paratuberculosis* using IS900 primers[13] and *Salmonella enterica* subsp. *enterica* detection was confirmed using genus-specific primers[14], as both agents are commonly responsible for chronic diarrhoea in adult animals. Details of these methods have been published[15].

Histopathology:

The rectal biopsies were obtained from a total of forty animals (n=40) using a modified mare uterine biopsy punch. Additionally, postmortem samples (n=40), surgical biopsies of the ileum and mesenteric lymph nodes were performed on adult dairy animals (n=4). The collected intestinal tissue fragments, biopsies and mesenteric lymph nodes were preserved in 10% buffered formalin. After fixation in 10% neutral buffered formalin, the tissue samples were washed overnight with tap water to remove residual fixative. The tissues were embedded in paraffin wax for the subsequent processing steps, utilising Leica Microsystems' Paraplast tissue embedding medium at 56°C. Slices of 4 or 5 microns were cut from the paraffin-embedded tissues. To examine the cellular and tissue structures in detail, the paraffin sections were stained using the standard hematoxylin and eosin method, following the established protocol[16].

The data were analysed using the Statistical Package for the Social Sciences (SPSS), applying one-way analysis of variance (ANOVA) wherever needed. A significance level of $P<0.05$ was set, with results below this threshold considered statistically significant.

RESULTS AND DISCUSSION

The study revealed that affected adult dairy animals (n = 101) experienced recurrent or persistent diarrhoea of varying durations (more than 2 weeks). The investigation identified distinct inflammatory and non-inflammatory etiologies contributing to chronic diarrhoea in affected adult bovines (Fig. 1). Histopathological analysis of rectal biopsy samples from animals with *Balantidium coli*-associated diarrhoea revealed a range of changes, from moderate enteritis to superficial inflammation with mucosal shedding. In some *Balantidium coli*-infected cases, inflammation was accompanied by deep ulceration, presenting a characteristic wedge-shaped pattern (Figs. 2, 3). In animals infected with salmonellosis, distinct histopathological changes in the intestine were observed, including chronic enteritis with plasma cell infiltration, hyperplasia, epithelial sloughing and crypt loss (Figs. 4, 5). Cases of chronic peritonitis exhibited polyp-like projections with widespread chronic enteritis along the intestinal lining, highlighting the distinctive pathological features of this condition (Fig.6). In cases of amphistomiasis, the primary histopathological findings included chronic inflammation, enteritis, granulomatous responses and mucosal hyperplasia, reflecting the diverse pathological effects of amphistome infections (Fig.7).

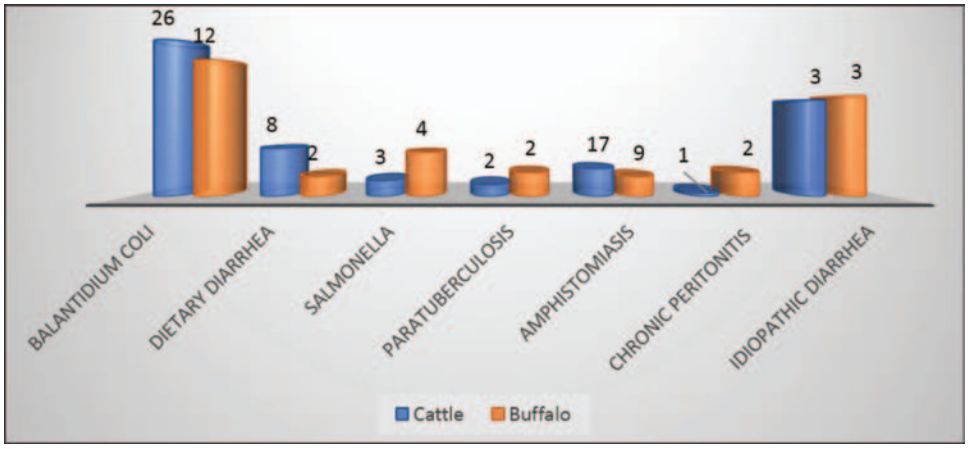

Fig. 1. Identified aetiologies associated with chronic diarrhoea in adult dairy bovines

Rectal biopsies from animals with parasitic or protozoal infections consistently showed goblet cell hyperplasia accompanied by localised inflammation (Figs. 8,9). In contrast, animals with clinical paratuberculosis (Johne's disease) exhibited enteritis, mononuclear cell infiltration and significant granulomatous reactions, highlighting the severity and complexity of the disease. Idiopathic lesions exhibited

chronic enteritis with pronounced infiltration between crypts and inflammation extending beneath the lamina muscularis (Fig. 10). Lymph node lesions in paratuberculosis cases showed characteristic features, including giant cells with lymphoid hyperplasia, marked inflammation, granulomatous infiltration and early-stage cellular hyperplasia (Figs. 11-13). Acid-fast bacilli were detected within large cells and macrophages, confirming mycobacterial infection (Figs. 14, 15).

The findings highlighted the significant histopathological changes in animals with chronic diarrhoea. However, in large animals, comprehensive studies on the underlying causes and associated pathophysiological features of chronic diarrhoea remain limited[3,15]. Our study identified multiple etiologies[16], with *Balantidium coli* infection notably prevalent, confirming its common role in causing chronic diarrhoea in adult bovines in this region[17,18]. Additionally, large amounts of rumen-degradable protein have been implicated in the development of diarrhoea[19,20]. Salmonella infection was confirmed as a bacterial cause of diarrhoea in buffalo and dairy cattle across all age groups[21,22]. Chronic diarrhoea due to amphistomiasis was previously overlooked but has recently been recognised as a significant cause of productivity loss[23]. Bovine paratuberculosis typically presents with intermittent diarrhoea and chronic weight loss[24], while peritonitis has been shown to cause persistent diarrhoea and weight loss in cattle and buffalo[25].

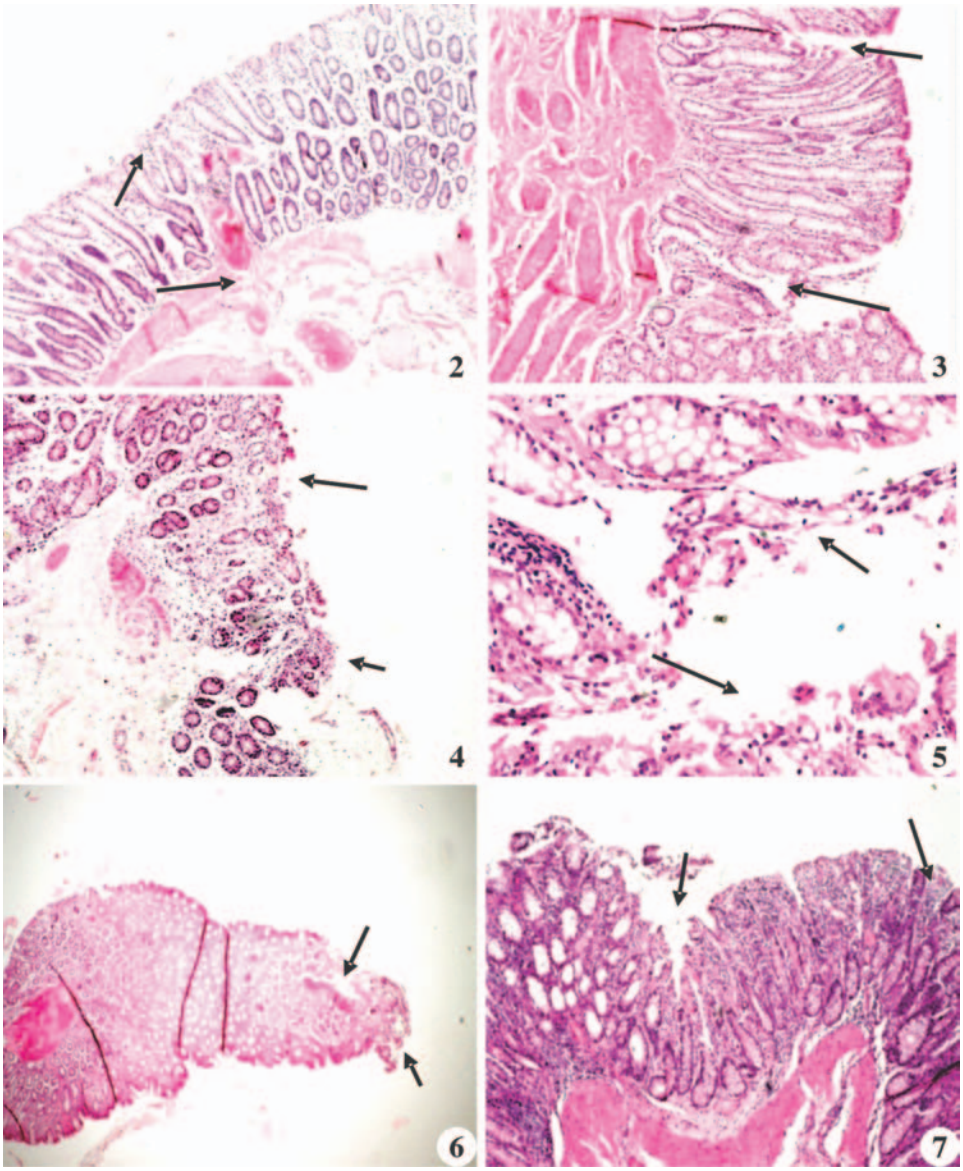

Fig. 2. Section of rectal biopsy shows mild enteritis changes (arrow), H&Ex20X; **Fig. 3.** Section of intestine shows chronic enteritis with marked mucosal hyperplasia, crypt elongation and inflammatory cell infiltration of the lamina propria (arrow), H&Ex40X; **Fig. 4.** Rectal biopsy section shows sloughing of epithelium (arrow), H&Ex10X; **Fig. 5.** Section of intestine shows inflammation associated with deep ulcer and deep wedge H&Ex100X; **Fig. 6.** Section of intestine shows chronic enteritis with mucosal thickening, prominent goblet cell hyperplasia and inflammatory cell infiltration of the lamina propria, H&Ex20X; **Fig. 7.** Section of ileum shows chronic enteritis with mucosal hyperplasia, crypt distortion, epithelial sloughing and dense inflammatory cell infiltration of the lamina propria (arrows), H&Ex20X

Consistent with these observations, our study identified significant histopathological changes in animals affected by chronic diarrhoea. In a concurrent study, animals with diarrhoea associated with amphistomiasis (a parasitic disease of domestic ruminants caused by trematodes) exhibited mucosal hyperplasia and progressive inflammatory cell infiltration in affected intestinal regions, indicating mild, moderate and severe degrees of intestinal damage[26]. Several studies have reported that *Balantidium coli* infections are associated with inflammation, intestinal haemorrhage, and necrosis, attributed to the production of proteolytic enzymes by the parasite[27,28]. Salmonella organisms

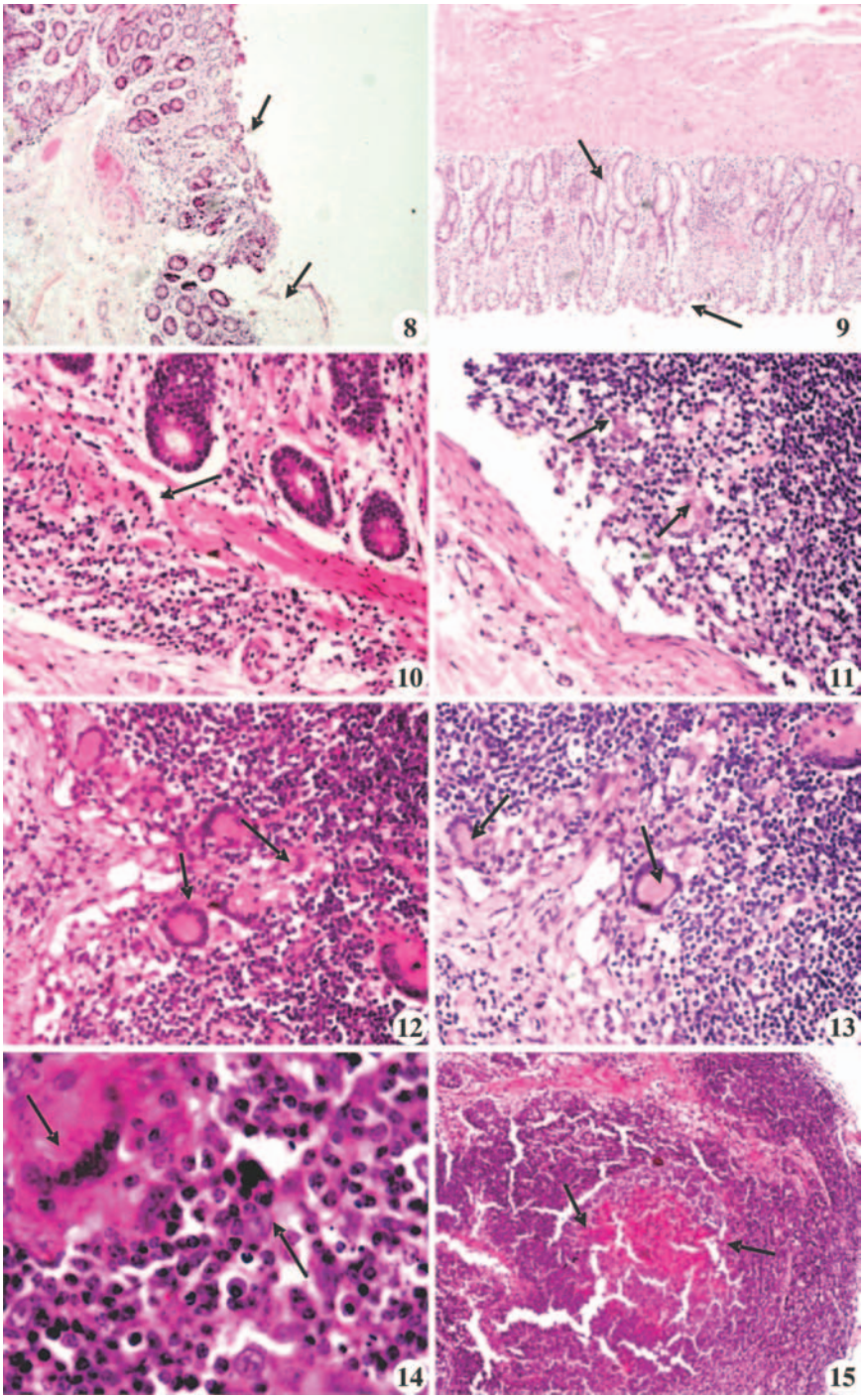

Fig. 8. Section of rectal biopsy shows severe inflammatory changes with the destruction of crypts (arrows) H&Ex10X; **Fig. 9.** Section of rectal biopsy shows chronic inflammatory changes with plasma cells infiltration (arrow), H&Ex10X; **Fig. 10.** Section of ileum shows inflammation below lamina muscularis (black arrow), H&Ex40X; **Fig. 11.** Mesenteric lymph nodes section shows giant cells infiltration (arrow), H&Ex100X; **Fig. 12.** Section of Ileocecal lymph node shows giant cells and hyperplasia (arrow), H&Ex40X; **Fig. 13.** Mesenteric lymph node section shows granulomatous inflammation with dense mononuclear cell infiltration with multinucleated giant cells, suggestive of paratuberculous involvement (arrow), H&Ex40X The section; **Fig. 14.** Section of lymph node shows macrophages and epithelioid cells with foamy plasm (arrow), H&Ex100X; **Fig. 15.** Section of lymph node shows reactive hyperplasia with haemorrhage (arrow) with no primary follicles, H&Ex10X

proliferate and invade the intestinal lamina propria, resulting in fibrin exudation and increased infiltration of macrophages and lymphocytes[29], a pathological pattern consistent with clinical cases of salmonellosis observed in farm settings[30]. Paratuberculosis cases demonstrate histopathological alterations in the submucosal glands, characterised by diffuse inflammatory responses, mononuclear cell infiltration, and degenerative or necrotic changes[31]. Animals affected by Johne's disease exhibit intestinal wall thickening and corrugation, along with enlargement of mesenteric lymph nodes, resulting from extensive mononuclear cell infiltration[32,33]. In a study consistent with our findings, early histological lesions of Johne's disease, including multinucleated Langhans-type giant cells in lymph node sinuses and at the tips of intestinal villi, were observed. These features are considered valuable indicators for disease surveillance in control programs[34]. Histopathological examination of mesenteric lymph nodes is a valuable diagnostic tool for identifying moderate subclinical infections in ruminants from herds with uncertain infection status. Additionally, idiopathic cases showed an increased crypt-to-interstitium ratio, highlighting the complexity and multifactorial nature of these diagnostic challenges[32]. Due to a limited understanding of the causes and mechanisms of chronic diarrhoea, a definitive diagnosis is achieved in only 60-70% of cases, often requiring postmortem histopathological evaluation. The observed severity of clinical symptoms aligns closely with the histologic lesions identified in this investigation, supporting the importance of histopathological examinations in elucidating the underlying aetiology of diarrhoea in these animals.

CONCLUSION

Integrating histopathological findings with other diagnostic methods

may provide a deeper understanding of the causes of chronic enteritis in affected dairy animals. The findings emphasise the importance of a thorough diagnostic approach addressing immediate signs and predisposing etiologies in affected animals with chronic diarrhoea, aiming to reduce severe economic losses associated with this condition.

ACKNOWLEDGEMENT

The authors sincerely acknowledge the Department of Science and Technology (DST) for supporting this research program. We also acknowledge the cooperation and technical support of the Departments of Veterinary Medicine, Microbiology and Pathology at GADVASU, Ludhiana.

Conflict of interest : None

Financial sponsorship: None

Use of artificial intelligence (AI)-assisted technology for manuscript preparation: The authors confirm that there was no use of AI-assisted technology for assisting in the writing of the manuscript and no images were manipulated using AI.

REFERENCES

1. Du W, Wang X, Xu L, Zhou X, Song D and Xu Q. 2023. Editorial: Research Du W, Wang X, Xu L, Zhou X, Song D and Xu Q. 2023. Editorial: Research advances in intestinal diseases and related diarrhoea in animal production. Front. *Vet. Sci* **10**:1201231.
2. Radostits OM, Gay CC, Hinchcliff KW, Constable PD. 2010. Veterinary Medicine. A Textbook of the Diseases of Cattle, Horses, Sheep, Pigs, and Goats, 10th edn. Saunders Elsevier, Philadelphia, pp. 337–342, 349.
3. Osterstock JB, Mansell JL, Roussel AJ.2005. Protothecal enteritis as a cause of protein-losing enteropathy in a bull. *J Am Vet Med Assoc* **227**:1476–1479. doi: 10.2460/javma.2005.227.1476.
4. Raizman EA, Fetrow J, Wells SJ, Godden SM, Oakes MJ, Vazquez J. 2007. The association between *Mycobacterium avium* subsp. paratuberculosis fecal shedding or clinical Johne's disease and lactation performance on two Minnesota, USA dairy farms. *Prev Vet Med* **78**: 179-195 DOI: 10.1016/j prevetmed.2006.10.006.
5. Hassan N, Randhawa CS, Narang D, Singh SV, Sharma S, Singh. S. 2019. Bio-incidence and Bio-type of Mycobacterium avium subspecies paratuberculosis in diarrheic dairy cattle and buffaloes of Punjab area in India. *Indian J Anim Res* DOI: 10.18805/ijar. B-3694.
6. Hassan N, Randhawa CS, Randhawa SS, Narang D. 2018. Chronic diarrhoea due to lymphosarcoma in an adult cow: A sporadic clinical report. *Turkish J Vet Anim Sci* **42**: 669–671DOI: 10.3906/vet-1804-71.
7. Jiminez JA, Uwiera TC, Douglas Inglis G, Uwiera RR. 2015. Animal models to study acute and chronic intestinal inflammation in mammals. *Gut Pathogens* **7**: 29 DOI: 10.1186/s13099-015-0076-y.
8. Peek SF, Mcguirk SM, Sweeney RW, Cummings KJ. 2018. Infectious diseases of the gastrointestinal tract. Rebhun's Diseases of Dairy Cattle, 249–356.
9. Paras KL, George MM, Vidyashankar AN, Kaplan RM. 2018. Comparison of fecal egg counting methods in four livestock species. *Vet Parasitology* **257**:21–27. DOI: 10.1016/j.vetpar.2018.05.015.
10. Samad MA. Balantidiasis. Pashu palon O Chikitsavidya. 1996. (Animal Husbandry and Medicine). Lyric- Epic Prokasoni. Mymensingh, Bangladesh, pp. 765–767.
11. Van Deun A, Hossain M, Gumusboga M, Rieder HL. 2008. Ziehl-Neelsen staining: Theory and practice. *International J Tuberculosis Lung Dis* **12**: 108–110.
12. Van Embden JDA, Cave D, Crawford JT, Dale JW, Eisenach KD, Gicquel B, Hermans P, Martin C, McAdam R, Shinnick TM, Small PM. 1993. Strain Identification of Mycobacterium tuberculosis by DNA Fingerprinting: Recommendations for a Standardised Methodology. *J Clin Microbiol* **31***:* 406.
13. Millar D, Ford J, Sanderson J, Withey S, Tizard M, Doran T, Hermon-Taylor J. 1995. IS900 PCR to detect *Mycobacterium paratuberculosis* in retail supplies of whole pasteurized cow's milk in England and Wales. *Appl Environ Microbiology*, **62**:3446–3452.
14. Cohen ND, Neibergs HL, Mcgruder ED, Whitford HW, Behle RW, Ray PM, Hargis BM. 1993. Genus-specific detection of salmonellae using the polymerase chain reaction (PCR). *J Vet Diagn Investig* **5:** 368–371 DOI: 10.1177/104063879300500311.
15. Hassan, N., Randhawa, C.S. and Zargar, U.R. 2022. Evaluating the hemato-biochemical indices in relation to the different etiologies of chronic diarrhoea in dairy cattle and buffalo. *Comp Clin Pathol* **31**; 585–595. https://doi.org/10.1007/s00580-022-03357-x.
16. Bancroft JD, Stevens A. 1990. Theory and Practice of Histological Techniques. Churchill Livingstone: Edinburgh, pp. 21–119.
17. Randhawa SNS, Singla LD, Randhawa CS. 2010. Chronic cattle diarrhoea due to *Balantidium coli* infection: a clinical report. *J Vet Parasitology* **24**: 197–198.
18. Hassan N, Randhawa C, Randhawa S, Narang D. 2017. Chronic diarrhoea and therapeutic trial with metronidazole in *Balantidium coli-infected* cattle and buffaloes. *International J Livestock Res* **7:**74–81 DOI: 10.5455/ijlr.20170423031718.
19. Davidson S, Hopkins BA, Diaz DE, Bolt SM, Brownie C, Fellner V, Whitlow LW. 2003. Effects of amounts and degradability of dietary protein on lactation, nitrogen utilisation, and excretion in early lactation Holstein cows. *J Dairy Sci* **86**: 1681–1689 DOI: 10.3168/jds. S0022-0302(03)73754–0.
20. Radostits OM, Blood DC,Gay CC. 2007. Doenças Causadas por Bacterias IV, Rio de Janeiro, cap. In: Guanabara K (ed) *Clínica Vet*, IV.19 (597–622).
21. Warnick LD, Kanistanon K, McDonough P, Power L. 2003. Effect of previous antimicrobial treatment on fecal shedding of *Salmonella enterica* subsp. *enterica* serogroup B in New York dairy herds with recent clinical salmonellosis. *Prev Vet Med* **56**: 285–297 DOI: 10.1016/s0167-5877(02)00210-6.
22. Wray C, Davies R. 2004. Salmonella in cattle: Update. *Cattle Practitioner* **12**:313–316.
23. Anuracpreeda P, Wanichanon C, Sobhon P. 2008. *Paramphistomum cervi* antigenic profile adults as recognised by infected cattle sera. *Exp Parasitology* **118**: 203–207 DOI: 10.1016/j.exppara.2007.08.005.
24. Abdullah FFJ, Adamu L, Yin YJ, Osman AY, Haron AW, Saharee A. 2013. Suspected Johne's disease in a herd of dairy cattle: A case report. *IOSR J Agri Vet Sci* **4**: 58–62 DOI: 10.9790/2380-0415862.
25. Tharwat M, Ahmed AF, El-Tookhy OS. 2012. Chronic peritonitis in buffaloes and cattle: Clinical, haematological, ultrasonographic findings and treatment. *J Anim Vet Adv* **11**: 2775–2781 DOI: 10.3923/javaa.2012.2775.2781.

26. Tehrani A, Javanbakht J, Khani F, Hassan MA, Khadivar F, Dadashi F, Alimohammadi S, Amani A. 2015. Prevalence and pathological study of paramphistomum infection in the small intestine of slaughtered ovine. *J Parasitic Dis* **39**: 100–106 DOI: 10.1007/s12639-013-0287-4.
27. Anargyrou K, Petrikkos G, Suller MTE, Skiada A, Siakantaris MP, Osuntoyinbo RT, Pangalis G, Vaiopoulos G. Pulmonary. 2003. B. coli infection in a leukemic patient. *American J Haemat* **73**: 180–183 DOI: 10.1002/ajh.10336.
28. Paul TR, Begum N, Shahiduzzaman M, Hossain MS, Labony SS, Anisuzzaman A, Dey AR. 2019. Balantidiasis, a zoonotic protozoan infection, in cattle and domestic pigs. *Bangladesh J Vet Med* **1** DOI: 10.33109/bjvmjj19fam1.
29. Frizzo LS, Zbrun MV, Soto LP, Bertozzi E, Sequeira GJ, Marti LE, Signorini ML, Armesto RR, Rosmini MR. 2012. Pathogen translocation and histopathological lesions in an experimental model of Salmonella Dublin infection in calves receiving lactic acid bacteria and lactose supplements. *J Vet Sci* **13**: 261–270DOI: 10.4142/jvs.2012.13.3.261.
30. Gelberg HB. 2001. Alimentary system. In: Thomson's Special Veterinary Pathology, 3rd edn (edited by M. D. McGavin, W. W. Carlton & J. F. Zachary). Mosby: St Louis, USA, pp. 1–79.
31. Chaturvedi S, Singh SV, Srivastava AK, Gangwar NK, Kumar N, Rawat KD, Gupta S, Chaubey KK, Singh R, Singh R, Dhama K.2017. Comparative evaluation of FAT, IS900 PCR and microscopy vis-a-vis histopathology for detection of *Mycobacterium avium* subsp. *paratuberculosis* infection in tissues of goats naturally died in herds endemic for Johne's disease. *Indian J Anim Sci* **87**: 685–693DOI: 10.56093/ijans.v 87i6.71061.
32. Maxie MG, Jubb KVF, Kennedy PC, Palmer NC. 2007. Pathology of Domestic Animals, 5th edn, Vol. 2. Saunders Elsevier: London, pp. 222–225.
33. Koets AP, Eda S, Sreevatsan S. 2015. The within-host dynamics of Mycobacterium avium ssp. Paratuberculosis infection in cattle: Where time and place matter. *Vet Res* **46**: 61 DOI: 10.1186/s13567-015-0185-0.
34. Sikandar A, Cheema AH, Adil M, Younus M, Zaneb H, Zaman MA, Tipu MY, Masood S. 2013.Ovine paratuberculosis: A histopathological study from Pakistan. *Journal of Animal and Plant Sciences* **23**: 749–753.hological study from Pakistan. *J Anim Plant Sci* **23**: 749–753.

Indian J. Vet. Pathol., 50(4) : 306-310, 2026: DOI: https://doi.org/10.56093/1jdm4b26

RESEARCH ARTICLE

Detection of *Mycobacterium tuberculosis* complex and rifampicin resistance using Xpert MTB/RIF Ultra assay in tissue samples from cattle and buffaloes

Anitta Thomas[1], Deepti Narang[*], Mudit Chandra[2], Kuldip Gupta[3] and A.K. Arora[4]
Department of Veterinary Microbiology, College of Veterinary Science, Guru Angad Dev Veterinary and Animal Sciences University, Ludhiana-141004, Punjab, India.
[1]M.V.Sc Student; [2]Principal Scientist cum Head; [3]Professor cum Head, Department of Veterinary Pathology; [4]Professor

***Address of correspondence**
Dr. Deepti Narang, Principal Scientist, E-mail: deeptivet@rediffmail.com
ORCID ID: 0009-0002-9289-8112, 0000-0002-8960-6388, 0000-0003-1513-2340, 0000-0002-2496-8585, 0000-0002-2175-2960

Received: 29.5.26; Accepted: 10.7.26

ABSTRACT

Mycobacterium bovis belonging to *Mycobacterium tuberculosis* complex (MTBC) is the major causative agent of bovine tuberculosis in cattle and buffaloes. Inhalation and ingestion of bacilli remains the major route of transmission. Thus, to interrupt the transmission cycle, rapid and accurate detection of the infected animals is necessary. This study, evaluated the role of Xpert MTB/RIF Ultra assay in detecting bovine tuberculosis causing MTBC in postmortem tissue samples and its resistance to rifampicin. A total of 25 tissue samples were collected from cattle and buffaloes died of respiratory ailments and were used in the study. Conventional PCR was employed to confirm the presence of mycobacterial DNA. Xpert MTB/RIF Ultra assay detected the presence of MTBC in 5 out of 25 lung tissue samples, of which none of the samples positive displayed rifampicin resistance. Out of the 5 samples tested positive by Xpert MTB/RIF Ultra assay 2 samples gave positive *IS6100* PCR results. Thus, Xpert MTB/RIF Ultra assay could potentially serve as a valuable and easy to perform technique for diagnosing tuberculosis in postmortem tissue samples.

Keywords: MTBC, PCR, Tissue samples, Xpert MTB/RIF Ultra assay

INTRODUCTION

Tuberculosis (TB) continues to be a major contributor to illness and death, particularly in low and middle-income nations. According to the World Health Organization (WHO), approximately one-third of all TB cases are either undiagnosed or not reported[1]. Globally, India being endemic for tuberculosis, accounts for 26% of TB prevalence and 34% of tuberculosis deaths. The "End TB Strategy" by government of India (WHO & NTEP) will only be successful if all means of disease transmission like zoonosis and reverse zoonosis are properly addressed[2]

Mammalian tuberculosis is a persistent condition characterized by the formation of granulomas arising as a result of the infection with harmful bacteria within the *Mycobacterium tuberculosis* complex (MTBC). A significant contribution of disease in cattle comes from infection with *M. bovis.* The other members of MTBC includes *M. tuberculosis*, *M. caprae*, *M. africanum*, *M. microti*, *M. canettii* and *M. pinnipedii.* The disease reduces the productivity of livestock intended for both local consumption and export markets[3].

Although inhaling infected respiratory droplets is regarded as the primary means of transmitting MTBC in livestock, infection can also occur through other routes. These include ingesting contaminated milk, consuming meat taken from wild as well as domesticated animals which may not undergo veterinary examination, poses a potential risk of infection to humans[4].

Most prevalently used antibiotics in treatment of tuberculosis are rifampicin (RIF), isoniazid (INH), pyrazinamide (PZA), ethambutol (EMB) etc. Organisms belonging to *Mycobacterium tuberculosis* complex had developed resistance towards multiple antibiotics leading to multi-drug resistant (MDR) and extensively drug resistant (XDR) strains of *Mycobacterium* in both humans and animals[5]. The rise of multidrug resistance in animals has garnered global concern, primarily because of the potential for pathogen transmission to humans[6].

How to cite this article: Thomas, A., Narang, D., Chandra, M., Gupta, K. and Arora, A.K. 2026. Detection of *Mycobacterium tuberculosis* complex and rifampicin resistance using Xpert MTB/RIF Ultra assay in tissue samples from cattle and buffaloes. Indian J. Vet. Pathol., 50(4) : 306-310.

The Xpert MTB/RIF Ultra assay is a semi-quantitative, nested real-time PCR assay that has revolutionized the management of *Mycobacterium tuberculosis* in humans. It offers a faster and more accurate diagnosis of tuberculosis by simultaneously detecting *M. tuberculosis* and rifampicin resistance. According to the World Health Organization (2015), the implementation of

the Xpert MTB/RIF Ultra assay has led to significant improvements in human TB programs in more than 130 countries[7].

The assay focuses on multicopy sequences, specifically *IS6110* and *IS1081*, significantly enhancing DNA detection in samples with low bacterial load. *IS1081* and *IS6110* are unique to members of the *Mycobacterium tuberculosis* complex (MTBC), making them well-suited for samples collected from animals potentially infected with MTBC members. While the GeneXpert is primarily employed for detecting MTBC DNA in human samples, studies have demonstrated its accurate detection of *M. bovis* in wildlife specimens[8].

In this current study, we evaluated the application of Xpert MTB/RIF Ultra assay for detecting both *M. bovis* in animal lung tissue samples, collected from cattle and buffaloes died of respiratory ailments in comparison to results obtained from *IS6100* PCR.

MATERIALS AND METHODS

Study design and sample collection

The study was conducted in Department of Veterinary Microbiology, College of Veterinary Science, Guru Angad Dev Veterinary and Animal Sciences University, Ludhiana, Punjab. All animal carcasses analysed in this study underwent examination for visible bTB lesions (Fig. 1). Lung tissue samples and lymph nodes from cattle and buffaloes died of respiratory ailments, with or without tubercle lesions were collected from Veterinary Pathology postmortem hall. All the samples collected were stored at -20°C till further processing.

All authors appreciate the ethical committee for permitting the use of animals and the IAEC/CPCSEA clearance may be accessed under reference number IAEC/2023/68/07.

Sample processing for Xpert ® MTB/RIF Ultra assay analysis

2-5 grams of tissue specimens was homogenized in a sterile mortar in a biosafety cabinet. Approximately 2 ml of sterile phosphate buffered saline was added into it. Approximately 0.7 ml of homogenised tissue without clumps was transferred into a conical screw-capped tube using a transfer pipette. Double the volume i.e 1.3ml of sample reagent was added to the tube using transfer pipette. The tube was vortexed for 10 seconds and incubated for 15 min at room temperature. 2ml of sample reagent treated specimen was added to Xpert® MTB/RIF Ultra cartridge and was loaded on to the instrument using a fresh transfer pipette to obtain results after 1 hr (Fig. 2).

Result interpretation of Xpert® MTB/RIF Ultra assay.

The results were interpreted by the GeneXpert DX System from measured fluorescent signals and embedded calculation algorithms and will be displayed in the laptop. Lowest Ct values represents a higher concentration of DNA template. The MTB result will be displayed as High, Medium, Low, Very low or Trace depending on the Ct value of the MTB target present in the sample.

- MTB DETECTED HIGH- MTB target is detected in the sample with a Ct range <16
- MTB DETECTED MEDIUM- MTB target is detected in the sample with a Ct range 16-22
- MTB DETECTED LOW- MTB target is detected in the sample with a Ct range 22-28
- MTB DETECTED VERY LOW- MTB target is detected in the sample with a Ct range >28
- MTB TRACE DETECTED- MTB target is detected in the sample with a Ct range One or both probes for multi-copy targets are positive with Ct <37 and no more than one *rpoB* probes have a Ct<40

RIF Resistance DETECTED, RIF Resistance NOT DETECTED, RIF Resistance INDETERMINATE will be displayed only in MTB DETECTED results.

- RIF Resistance DETECTED: a mutation in *rpoB* gene has been detected that falls within the valid Ct setting.
- RIF Resistance INDETERMINATE: the MTB concentration was very low and resistance could not be detected due to insufficient signal production.
- RIF Resistance NOT DETECTED: no mutation in *rpoB* gene is detected

DNA isolation and *IS6100* polymerase chain reaction

Sample DNA (n=25) was extracted using the DNeasy Blood and Tissue Kit (Qiagen, Germany), following the manufacturers' instructions along with appropriate adjustments and subsequently were accurately labelled and stored at -20°C until further analysis.

IS6100 PCR

The PCR technique utilized INS1 and INS1 primers designed to aim at the *IS6100* insertion sequences. These genetic markers are frequently utilized for identifying MTBC strains in samples, as described[9]. The amplified products were verified to be of the expected size by electrophoresis on a 1.5% (w/v) agarose gel (Thermo Scientific, USA) in 1X Tris Acetate EDTA buffer.

RESULTS

Results obtained from this study are shown in Table 1. A total of 25 tissue samples were subjected to molecular detection using Xpert MTB/RIF Ultra assay. 5 out of 25 samples were identified as MTC positive, of which 3 samples belonged to the category of "MTB detected very low (Fig. 3) and 2 samples under "MTB trace detected" (Fig. 4) category. Resistance to rifampicin was not

Table 1. Xpert MTB/RIF Ultra assay results from tissue samples in comparison to PCR results.

S.No.	Lab No.	Species	Age (yrs)	Smear Results	GeneXpert Ultra result	RIF results	IS6100 PCR
1.	TS1	Cattle	4.5Y	Negative	MTB detected very low	ND	Positive
2.	TS2	Buffalo	5Y	Negative	MTB trace detected	I	Negative
3.	TS5	Buffalo	7Y	Negative	MTB detected very low	ND	Positive
4.	TS8	Cattle	6Y	Negative	MTB detected very low	ND	Negative
5.	TS14	Cattle	5.5Y	Negative	MTB trace detected	I	Negative

detected in any of the collected samples that gave positive GeneXpert results. In samples under "MTB trace detected" category, RIF resistance detection is labelled "indeterminate" as it cannot be determined due to insufficient signal detection. Out of the 5 samples tested positive by Xpert MTB/RIF Ultra assay, only 2 samples were confirmed to be positive by *IS6110* PCR (Fig. 5). Out of 25 samples that were subjected to ZN staining, none of samples showed presence of acid-fast bacilli.

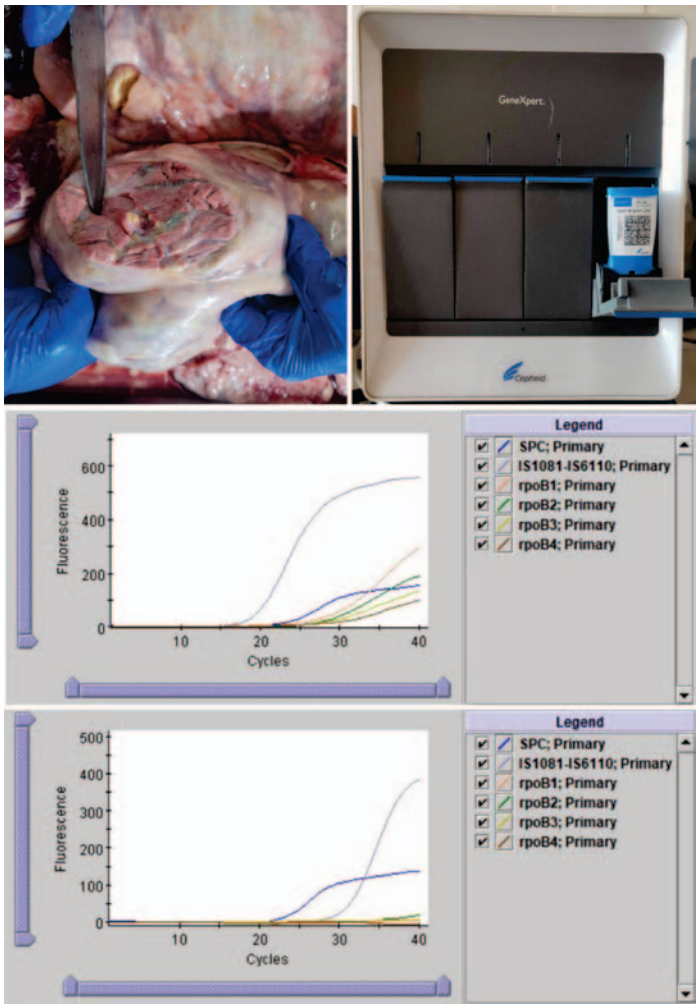

Fig. 1. Gross lesions showing tuberculous lesions in lung tissue; **Fig. 2.** Xpert® MTB/RIF Ultra machine along with its cartridge; **Fig. 3.** Amplification plot of Tissue samples using Xpert MTB/RIF Ultra assay in category, "MTB DETECTED VERY LOW", "RIF RESISTANCE NOT DETECTED"; **Fig. 4.** Amplification plot of Tissue samples using Xpert MTB/RIF Ultra assay in category, "MTB TRACE DETECTED", "RIF RESISTANCE INDETERMINATE".

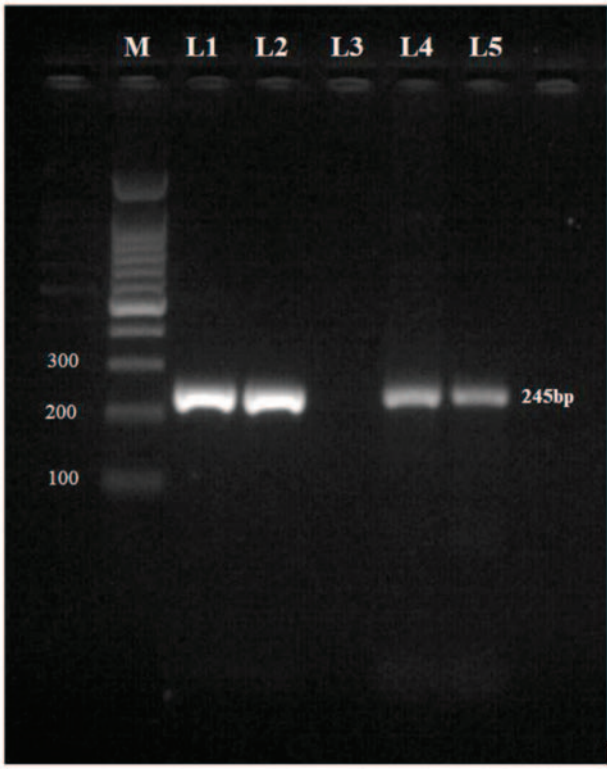

Fig. 5. Agarose gel electrophoresis of amplified IS6100 gene of MTC at 245 bp using INS1/INS2 primers for tissue samples. Lane M: 100 bp ladder. Lane 1,2: Positive control of M. bovis, Lane 3: Negative control, Lane 4,5: Positive samples for IS6100 PCR

DISCUSSION

The objective of this pilot study was to assess the feasibility of detecting MTBC DNA in *M. bovis*-infected cattle and buffaloes using post-mortem tissue samples with the rapid Xpert MTB/RIF Ultra assay. The original Xpert MTB/RIF assay was among the most commonly utilized tests for tuberculosis and drug resistance in humans. However, since its endorsement by the World Health Organization (WHO) in 2010, the manufacturers have consistently improved its diagnostic capabilities. Unintentionally,

these enhancements have also transformed it into a potential diagnostic tool for detecting *M. bovis* in animals[10].

Research conducted using human sputum samples has proved that GeneXpert results offer an indication of the bacterial load in a specimen. There is a direct relationship between the semi-quantitative GeneXpert results and the detection of acid-fast bacilli through smear microscopy. GeneXpert results indicating "MTB trace detected" or "MTB not detected" have been linked with the absence of acid-fast bacilli, while results indicating "MTB detected high" and "medium" typically correspond to positive results in smear microscopy [11]. In the current study, none of the samples gave positive smear results may be because GeneXpert results of all 5 positive samples belonged to "MTB detected very low" (n=3) and "MTB trace detected" (n=2) category.

Out of 5 samples giving positive GeneXpert results, surprisingly only 2 were found to be positive by PCR. *IS6110* PCR did not identify 3 of the positive samples. In a previous study[12], utilizing GeneXpert to identify MTBC DNA with tissue samples, similar results were observed and the reason for this phenomenon remains unidentified.

While mycobacterial culture of post-mortem tissues and the identification of bacterial isolates continue to be regarded as the gold standard method for confirming *M. bovis* infection in animals, this approach is constrained by challenges in obtaining tissue samples without contamination and the suboptimal sensitivity of culture techniques[13]. In many previous studies, the utilization of GeneXpert with tissue samples gathered from cattle buffaloes and wildlife to identify MTBC DNA was evaluated[14-17]. This method was determined to be a secure, straightforward, and efficient approach to screen animals for the existence of *M. bovis*.

Limitations of this study includes a limited sample size and the occurrence of multiple freeze-thaw cycles on samples before testing. Another limitation of the study is the inability of Xpert MTB/RIF Ultra assay to conclusively determine whether the detection of MTBC DNA was from the animals or environmental contamination. In conclusion, the Xpert MTB/RIF Ultra assay emerges as a rapid diagnostic test capable of detecting MTBC DNA in tissue samples obtained from cattle and buffaloes.

ACKNOWLEDGEMENT

The authors are thankful to the Director of Research, Guru Angad Dev Veterinary and Animal Sciences University (GADVASU), Ludhiana for providing the necessary facilities and RKVY for providing the necessary support.

Financial support and sponsorship: Yes

Conflict of interest: None

Use of artificial intelligence for manuscript preparation: The author confirms that there was no use of AI-assisted technology for assisting in the writing of the manuscript and no images were manipulated using AI.

REFERENCES

1. World Health Organization. Global Tuberculosis Report 2014. (WHO/HTM/TB/2014.08, 2014).
2. Ramanujam H, Palaniyandi K. 2023. Bovine tuberculosis in India: The need for One Health approach and the way forward. One Health *16*(September 2022), 100495.
3. Ramos DF, Silva PEA, Dellagostin OA. 2015. Diagnosis of bovine tuberculosis: review of main techniques. *Braz J of Biol* **75(4):**830-837.
4. Pokam BT, Guemdjom P, Yeboah-Manu D, Weledji E, Enoh J, Tebid P, Asuquo A. 2019. Challenges of bovine tuberculosis control and genetic distribution in Africa. *Biomed and Biotechnol Res J* **3(4)**: 217.
5. Gedawy E, Abdelghafar AE, Shazly YAE, Elkady A, Abdelrahman MA, Shalaby M. 2024. Highlighting on *Mycobacterium bovis* in cattle, focusing on its antimicrobial resistance. *Egy J Anim Health* **4(1):**134-140.
6. Borham M, Oreiby A, El-Gedawy A, Hegazy Y, Khalifa HO, Al-Gaabary M, Matsumoto T. 2022. Review on bovine tuberculosis: An emerging disease associated with multidrug-resistant *Mycobacterium* species. *Pathog* **11(7):** 1-25.
7. Hlokwe TM, Mogano RM. 2020. Utility of Xpert® MTB/RIF Ultra assay in the rapid diagnosis of bovine tuberculosis in wildlife and livestock animals from South Africa. Prev Vet Med 177.
8. Clarke C, Smith K, Goldswain SJ, Helm C, Cooper DV, Kerr TJ, Kleynhans L, van Helden PD, Warren RM, Miller MA, Goosen WJ. 2021. Novel molecular transport medium used in combination with Xpert MTB/RIF ultra provides rapid detection *of Mycobacterium bovis* in African buffaloes. *Sci Rep* **11(1).**
9. Figueiredo EES, Silvestre FG, Campos WN, Furlanetto LV, Medeiros L, Lilenbaum W, Fonseca LS, Silva JT, Paschoalin VMF. 2009. Identification of *Mycobacterium bovis* isolates by a multiplex PCR. *Braz J Microbiol* **40(2)**:231-233.
10. Goosen WJ, Kerr TJ, Kleynhans L, Warren RM, van Helden PD, Persing DH, Parsons SDC, Buss P, Miller MA. 2020. The Xpert MTB/RIF Ultra assay detects *Mycobacterium tuberculosis* complex DNA in white rhinoceros (*Ceratotherium simum*) and African elephants (*Loxodonta africana*). *Sci Rep* **10(1)**.
11. Opota O, Mazza-Stalder J, Greub G, Jaton K. 2019. The rapid molecular test Xpert MTB/RIF ultra: towards improved tuberculosis diagnosis and rifampicin resistance detection. *Clin Microbiol Infect* **25**: 1370-1376.
12. Alves da Silva D, Rêgo AM, Ferreira NV, de Andrade MAS, Campelo AR, Caldas PCS, Pereira MAS, Redner P, de Pina LC, Resende FC, Pissinatti TA, Lopes CAA, Kugelmeier T, Perea JAS, de Souza IV, da Silva FA, Campos CF, Fandinho Montes FCO, Antunes LCM. 2017. Detection of mycobacterial infection in non-human primates using the Xpert MTB/RIF molecular assay. *Tuberculosis* **107**: 59-62.
13. de la Rua-Domenech R, Goodchild AT, Vordermeier HM, Hewinson RG, Christiansen KH, Clifton-Hadley RS. 2006. Ante mortem diagnosis of tuberculosis in cattle: A review of

the tuberculin tests, γ-interferon assay and other ancillary diagnostic techniques. *Res J Vet Sci* **81(2):**190-210.

14. García-Basteiro AL, Ismail MR, Carrilho C, Ussene E, Castillo P, Chitsungo D, Rodríguez C, Lovane L, Vergara A, López-Varela E, Mandomando I, Lorenzoni C, Ordi J, Menéndez C, Bassat Q, Martínez MJ. 2016. The role of Xpert MTB/RIF in diagnosing pulmonary tuberculosis in post-mortem tissues. *Sci Rep* **6**: 1-6.
15. Clarke C, Cooper DV, Miller MA, Goosen WJ. 2022. Detection of *Mycobacterium tuberculosis* complex DNA in oronasal swabs from infected African buffaloes (*Syncerus caffer*). *Sci Rep* 12(1).
16. Kerr T, Goosen W, Gumbo R, Deklerk-Lorist LM, Pretorius O, Buss P, Kleynhans L, Lyashchenko K, Warren R, Van Helden P, Miller M, Kerr TJ, Goosen WJ, De Klerk-Lorist LM, Buss PE, Lyashchenko KP, Warren RM, Van Helden PD, Miller MA. 2020. Title: Implications of interspecies transmission and diagnosis of *Mycobacterium bovis* infection in free-ranging common hippopotamus (*Hippopotamus amphibius*) Running Title: *Mycobacterium bovis* infection in common hippopotamus.
17. Kerr TJ, Goosen WJ, Gumbo R, de Klerk-Lorist LM, Pretorius O, Buss PE, Kleynhans L, Lyashchenko KP, Warren RM, van Helden PD, Miller MA. 2022. Diagnosis of *Mycobacterium bovis* infection in free-ranging common hippopotamus (*Hippopotamus amphibius*). *Transbound Emerg Dis* **69(2)**: 378-384.

Indian J. Vet. Pathol., 50(4) : 311-315, 2026: DOI: https://doi.org/10.56093/rvnqmx07

RESEARCH ARTICLE

Pathomorphological and histopathological characterization of hydatid cysts in sheep: Evidence from slaughterhouses in Rayalaseema, Andhra Pradesh

P. Lakshmisai*, K. Jalajakshi, R. Venu and A. Anand Kumar[1]
Department of Veterinary Parasitology, College of Veterinary Science, Sri Venkateswara Veterinary University, Tirupati
[1]Professor & Head, Department of Veterinary Pathology

***Address for correpondence**
Dr. P. Lakshmisai, MVSc Scholar, E-mail: lakshmisaipalluru@gmail.com
ORCID ID: 0009-0001-3859-652X

Received: 13.4.26; Accepted: 13.5.26

ABSTRACT

Hydatidosis is primarily caused by the metacestode stages of *Echinococcus granulosus* also known as cystic echinococcosis (CE), which causes a significant zoonotic parasitic disease. The disease is considered one of the most significant helminthic infections of livestock and humans worldwide and poses major veterinary, public health, and economic concerns. A slaughterhouse study was conducted to determine the histopathological changes in liver and lungs of the sheep infected with hydatid disease across various districts of the Rayalaseema region of Andhra Pradesh, India for a period of 9 months from July 2025 to March 2026. All the infected liver and lungs were processed further for histopathological examination using haematoxylin and eosin (H&E) and iodine staining techniques. To record the pathomorphological changes in organs affected by hydatidosis in slaughtered sheep. Out of 3,683 sheep examined during slaughter, 87 (2.36%) sheep were found to be infected with hydatid cysts. Microscopic examination of cystic fluid revealed the presence of protoscoleces with rostellum, and hook lets in the hydatid sand. Out of 87 collected cyst samples (41 livers and 46 lungs) 39 samples found to be fertile due to the presence of protoscoleces, 28 cysts were found sterile because of absence of protoscoleces and remaining 20 cysts were found to be calcified because of its hard consistency. The study concludes that histopathological examination demonstrated significant and consistent tissue reaction in both lungs and liver, characterized by a trilaminar cyst wall, pericystic fibrosis, inflammatory cell infiltration, hepatocellular degeneration, pulmonary alveolar compression with granuloma formation.

Keywords: Brood capsules, Histopathological changes, Hydatid cysts, Lungs, Liver, Microscopy, Protoscoleces, Slaughtered sheep

INTRODUCTION

Hydatidosis/Cystic echinococcosis (CE) is a meat-borne cyclo-zoonotic disease caused by the larval stage of Echinococcus spp., the smallest dog tapeworm of the family *Taeniidae*, with sheep serving as important intermediate hosts[1,2]. The disease poses major public health and economic concerns due to zoonotic transmission and organ condemnation at slaughter[3]. CE is endemic in regions where livestock rearing and close animal contact are common, and its spread is further influenced by migration of humans and animals[4]. In sheep, the liver and lungs are the most affected organs because larvae reach these organs through the hepatopulmonary circulation[5,6]. Although hydatidosis is prevalent in many parts of India, information on its histopathological changes in sheep from southern regions, particularly Rayalaseema of Andhra Pradesh, is limited. Therefore, the present study was undertaken to investigate the histopathological alterations in the liver and lungs affected by hydatidosis.

How to cite this article: Lakshmisai, P., Jalajakshi, K., Venu, R. and Kumar A.A. 2026. Pathomorphological and histopathological characterization of hydatid cysts in sheep: Evidence from slaughterhouses in Rayalaseema, Andhra Pradesh. Indian J. Vet. Pathol., 50(4) : 311-315.

MATERIALS AND METHODS

Samples collection

A total of 3,683 slaughtered sheep including both males and females were systematically examined during routine post-mortem meat inspection for the presence/absence of hydatid cysts from various abattoirs present in the Rayalaseema region which included Anantapur, Sri Satya Sai, Chittoor, Tirupati, YSR Kadapa, Annamayya, Kurnool and Nandhyal districts. Data collected was analysed for the organ-wise prevalence of cysts.

Gross examination

The livers and lungs specimens affected with hydatidosis were grossly examined for any alterations resulted due to the infection.

Microscopic examination of hydatid cyst fluid

The hydatid cystic fluid was aspirated using 18G needle and a drop of fluid was placed on a

glass slide for the detection of protoscoleces. The viability of cysts were assessed microscopically using 0.1% eosin and 1% iodine stains.

Processing of tissues for histopathology

Tissue samples of hydatid cysts were gathered and preserved in 10% neutral formal saline. Using a standard paraffin embedding procedure, the fixed tissues were cut into 3-5mm thickness and washed thoroughly under water over night prior to dehydration with ascending grades of alcohol, followed by clearing with xylene. The blocks were sectioned 4-5 µm thickness using microtome and stained with routine haematoxylin and eosin (H&E) stain[9]. The DPX mounted slides were examined for lesions and captured using light microscope.

RESULTS

In this period of study, out of 3,683 slaughtered sheep examined 87 sheep were found to be infected with hydatid cysts among all the districts. Of which 41 livers cysts (1.11%) and 46 lung cysts (1.25%) were identified. Among all districts, Tirupati exhibited the highest prevalence of hydatidosis with 1.85% prevalence of hepatic involvement and 2.35% prevalence of pulmonary tissue involvement showing a comparatively higher burden of infection in this region. Whereas, in Nandyal district showed the lowest liver infection 0.31%, while lung infection was relatively higher 1.23% suggesting organ-specific variation. The organ wise prevalence of hydatidosis infection during this study was shown in Table 1 and Fig 1.

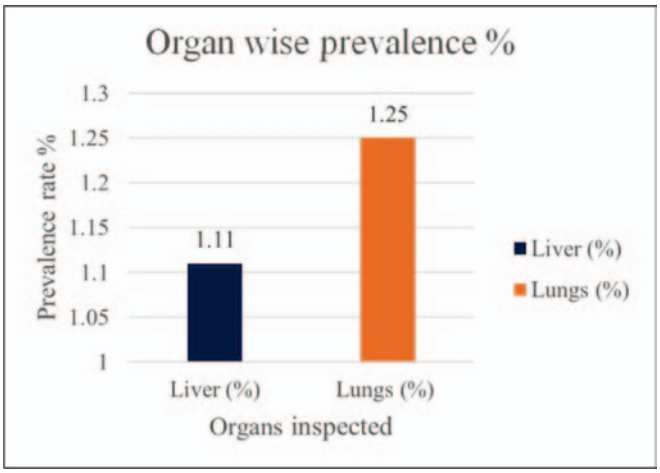

Fig. 1. Graph showing the organ wise prevalence of hydatidosis in the Rayalaseema region

Table 1. Organ wise prevalence of hydatidosis in sheep of Rayalaseema region of Andhra Pradesh.

District	No. examined	Liver, n (%)	Lungs, n (%)
Anantapur	563	4 (0.71)	7 (1.24)
Sri Sathya Sai	424	2 (0.47)	3 (0.70)
Chittoor	392	5 (1.27)	6 (1.53)
Tirupati	595	11 (1.85)	14 (2.35)
YSR Kadapa	546	9 (1.64)	4 (0.73)
Annamayya	412	4 (0.97)	5 (1.21)
Kurnool	427	5 (1.17)	3 (0.70)
Nandyal	324	1 (0.31)	4 (1.23)
Total	3683	41 (1.11)	46 (1.25)

Gross examination of organs

On gross examination, affected organs revealed single to multiple hydatid cysts ranged from small to larger sized cysts 2-6 cms containing white fluid filled cavities, fully or partially embedded inside the liver and lungs (Fig. 2 and Fig. 3). These cysts were soft to touch on palpation, and some were calcified and hard to cut. The hepatic regions surrounding the cyst showed clearly marked diffuse pale-coloured areas of necrosis with some dark congested regions showing petechial haemorrhages and hepatomegaly. The pulmonary regions infected with CE showed marked congestion with large sized cysts than the liver.

Microscopic examination

Microscopic examination of cystic fluid derived the flame cell activity of the protoscoleces in clusters and brood capsules with protoscoleces (Fig. 4). Viability evaluation was done on staining with 0.1% eosin stain and results revealed that live ones were unstained whereas, the dead ones had taken up the stain and marked in pink colour (Fig. 5). The iodine-stained sections showed with clear refractile nature of the protoscoleces (Fig. 6).

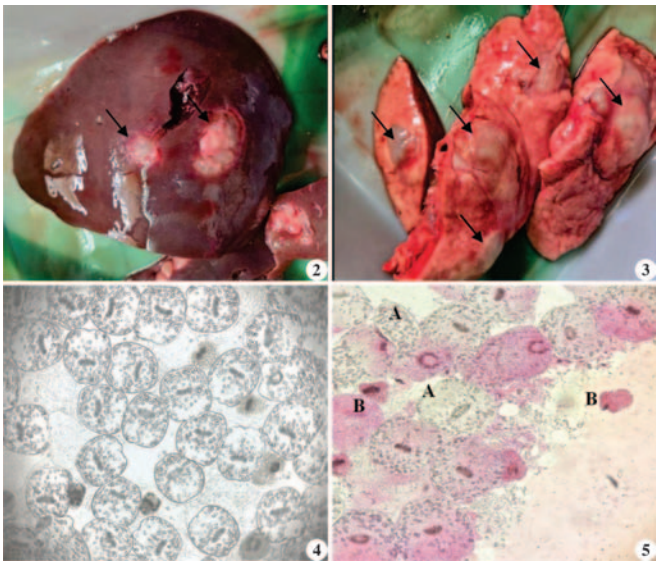

Fig. 2. Liver showing hydatid cysts (arrows) with pathological lesions; **Fig. 3.** Lung sections with multiple cysts (arrows); **Fig. 4.** Depicting clusters of protoscoleces (100X); **Fig. 5.** Eosin stain test for the protoscoleces viability A. Note unstained live protoscolices. B. Note pink stained dead protoscoleces (100X)

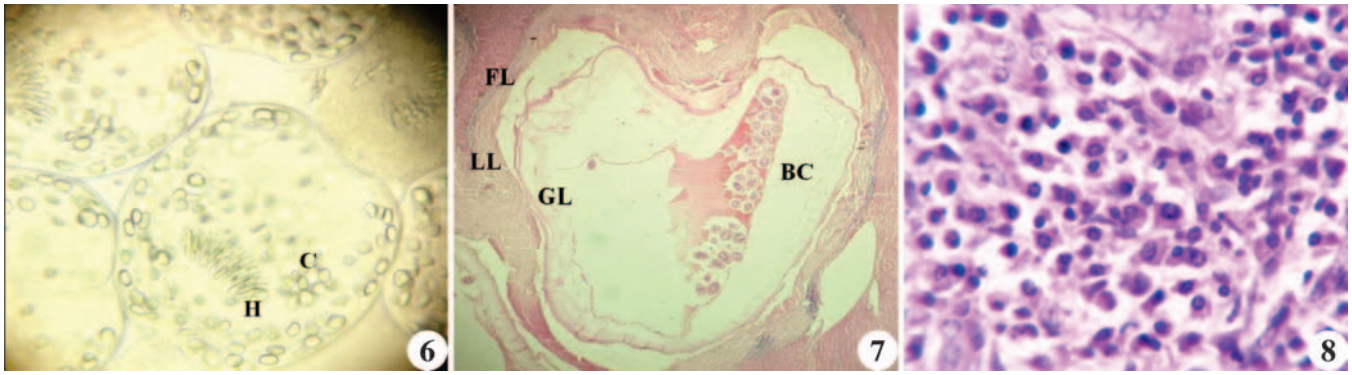

Fig. 6. Iodine stained mature invaginated protoscoleces with hooklets (H) and calcareous bodies (C) (400X); **Fig. 7.** Liver sections showing three layers of the cyst (Germinal layer [GL], acellular laminated membrane [AL] and fibrous layer [FL], Broode capsule [BC]wall with infiltration of inflammatory cells (H&E, 40X); **Fig. 8.** Liver section showing multifocal microscopic infiltration of lymphoplasmacytic inflammatory reaction (H&E, 1000X).

Histopathological sections

The resulted histopathological sections from the liver, showed a clear demarcation of three layers of the cyst with inner germinal layer/endocyst with attached protoscoleces and brood capsules, middle acellular laminated membrane/exocyst and outer fibrous layer/pericyst (Fig. 7). The pericyst provides protection to the cyst and the other two layers supplement nutrition to the hydatid cyst. A zone of inflammatory reaction observed with infiltration of monocytes, lymphocytes, plasma cells with moderate to dense fibrous tissue formation (Fig. 8). Necrosis (chronic venous congestion) was observed in the tissues present adjacent to the hydatid cyst (Fig. 9). Some of the liver microscopic sections revealed calcified tissue adjacent to the cyst wall (Fig. 10).

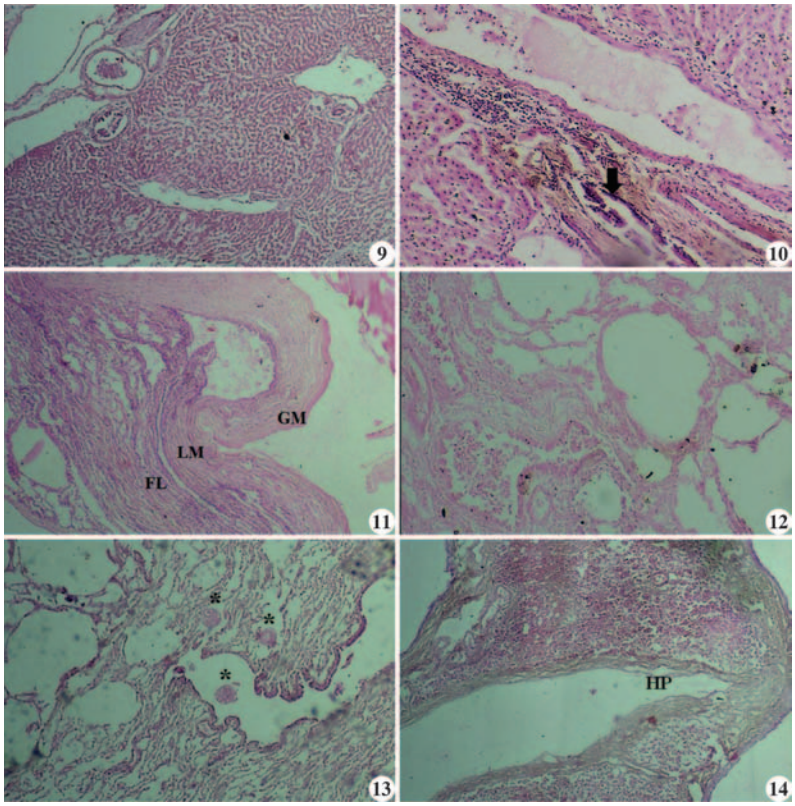

Fig. 9. Liver section showing congestion and necrosis of tissue adjacent to the cyst formation (H&E, 100X); **Fig. 10.** Liver section showing infiltration of inflammatory cells and calcification (arrow) surrounding the cyst wall development (H&E, 100X); **Fig. 11.** Lung section showing three layers of the hydatid cyst; germinal layer (GM), laminated membrane (LM) and fibrous layer (FM) (H&E, 40X); **Fig.12.** Lung section showing atelectasis, congestion due to the cyst development in the alveoli (H&E, 100X); **Fig. 13.** Lung section with migrating protoscoleces (*) with inflammatory cells surrounding (H&E, 40X); **Fig. 14.** Lung section showing hemosiderin pigment deposition (HP) surrounding the cyst wall (H&E, 40X)

Lung sections showed similar structure as of liver with trilaminar layers of the cyst (Fig. 11). In addition to this, lungs showed collapsed alveolar tissues with congestion of blood vessels due to the pressure created during the cyst development (Fig. 12). In some lung sections free migrating protoscoleces were observed with inflammatory cells infiltration around the surrounding tissue with multifocal microscopic lympho-plasmocytic infiltration (Fig. 13). Other lung sections showed deposition of hemosiderin pigment all over the cyst wall (Fig. 14).

DISCUSSION

Cystic echinococcosis is recorded as one of the neglected tropical diseases reported by WHO, 2021[10]. Of the 3,683 slaughtered sheep examined, 87 (2.36%) sheep of which 41 livers (1.11%) 46 lungs (1.25%) were found infected with hydatid cysts, across various districts of Rayalaseema region of Andhra Pradesh**.** Since liver and lungs were the first organs to receive the circulating blood during which protoscoleces enters these organs and development of cyst takes place[6,11].

Higher prevalence of CE was recorded in the lungs compared to liver in sheep could be associated with the immune competence of the host and rigid consistency of the organ (liver) resist the cyst development to larger sizes[13]. In contrast the pulmonary tissue contains greater capillary bed and the consistency of the organ makes the cysts to wider distribution, gives more space to develop[11]. The results indicated that there was no significant difference among districts and the organ-wise prevalence of hydatidosis. Indicating that hydatid cysts were uniformly distributed across all the districts[12,13]. Grossly, hydatid cysts in liver ranged from single to multiple cysts of varying sizes on visceral surfaces. Most of the cysts were smaller in size and some were large cricket ball sized. Some cysts were partially embedded protruding from the liver parenchyma and others were fully embedded with only a part of visible cyst wall. These observations on distribution of cysts were similar with the research findings of above authors[8,12]. Gross examination of the infected lungs revealed variable-sized, greyish white, unilocular to multilocular fluid-filled cysts embedded within the lung parenchyma ranging from small nodules to large space-occupying cysts[14]. The lung cysts were predominantly located in the diaphragmatic lobes, either as solitary or multiple lesions involving one or more pulmonary lobes[15]. The liver cysts were firm on palpation, often surrounded by a zone of hardened hepatic parenchyma[16]. In addition to that, liver surrounding tissues showed severe congestion, hepatomegaly, haemorrhages and pale areas of necrosis. These findings were corelated with the author [17] who recorded the similar details. Microscopic examination of cystic fluid confirmed the presence of protoscoleces with a characteristic two rows of hooks[18]. Viability of protoscoleces was confirmed with eosin stain was accordance with the author [19]. In iodine staining the refractile appearance of protoscoleces was related with the findings of earlier scientist[20].

Histopathological examination of the sections of the liver and lungs associated with hydatid cyst revealed a characteristically trilaminar structure, consisting of an innermost germinal (nucleated) layer, a middle acellular laminated layer composed of concentrically arranged collagen fibres, and an outer host-derived adventitial layer of fibrous connective tissue[12]. The adventitial layer was composed of densely packed fibroblasts, inflammatory cells, and granulation tissue, representing the host's protective response to the expanding parasitic cyst[21]. The protoscoleces structural details were clearly perceptible[15]in the histology sections. The liver sections also showed histopathological changes like congestion, infiltration of inflammatory cells and mononuclear cells mainly eosinophils and lymphocytes, chronic venous condition (Nutmeg appearance of the liver). Hepatocytes exhibited degeneration, with cytoplasmic vacuolation and nuclear pyknosis at the periphery of the cysts, with severity inversely proportional to the distance from the cyst wall[11,12]. Focal to extensive fibrosis and cirrhotic changes were observed in the hepatic parenchyma surrounding the cysts[22]. Increased numbers of Kupffer cells with sinusoidal congestion, bile duct proliferation, and areas of hepatic necrosis were also recorded in heavily infected livers[23]. Mononuclear inflammatory cell infiltration, predominantly lymphocytes and plasma cells, was distributed throughout the pericystic zones, with occasional eosinophils, reflecting both innate and adaptive immune responses of the host[24]. Focal calcification was also observed in some hepatic cysts, associated with degenerative changes in the cyst wall[12].

Histopathological changes observed in the lung cyst sections were similar as the liver cyst sections showing three layers i.e., inner germinal layer, middle lamellated/ laminated and outer fibrous layer. The germinal layer consists of brood capsules which were distinct in the cyst wall with free floating protoscoleces[22]. Lung sections adjacent to the hydatid cyst showed alveolar rupture, atelectatic or emphysematic areas with congestion, haemorrhages, mega alveoli formation, hyperplasia of bronchiolar epithelium. Infected lungs on rupture of the cyst showed collapsed condition with distortion of the laminated layer and adventitial layer present in the alveoli. Some of the sections revealed developing protoscoleces attached to the cyst wall. In few sections calcification was observed surrounding the cyst wall. In the lungs, significant histopathological changes were observed in the adjacent parenchyma, including dilatation and compression of pulmonary alveoli, extensive inflammatory cell infiltration comprising lymphocytes, eosinophils, neutrophils, and macrophages around the peri-cystic zone with necrotic areas[23]. Compact granuloma formation with a fibrous capsule was noted surrounding the cysts, along with fibrin-rich exudate leading to hyaline deposition in the alveolar walls. Bronchiolar epithelial proliferation was evident in sections adjacent to expanding cysts[24].

Previous studies have reported that simultaneous liver and lung involvement is comparatively less common than single-organ localization. Some scientist[26] reported that synchronous pulmonary and hepatic hydatid disease occurs only in about 4–25% of hydatid cases. Similarly[24] described concurrent liver and lung hydatid cysts as a relatively rare presentation despite both organs being the principal predilection sites. Studies on sheep hydatidosis have also demonstrated predominance of either hepatic or pulmonary localization independently[25]. Therefore, the absence of concurrent liver and lung infection in the present investigation does not contradict the established pathogenesis of hydatidosis but rather reflects variations

in host–parasite interaction, infection dynamics, and local epidemiological conditions.

CONCLUSION

In the current study overall prevalence of 2.37% hydatidosis was recorded in sheep slaughtered across the Rayalaseema region of Andhra Pradesh, confirming the occurrence of cystic echinococcosis in this part of southern India. Histopathological examination demonstrated significant and consistent tissue reaction in both lungs and liver, characterized by a trilaminar cyst wall, pericystic fibrosis, inflammatory cell infiltration, hepatocellular degeneration, pulmonary alveolar compression, and granuloma formation. These findings underscore the pathological impact of hydatidosis on ovine health, with implications for meat hygiene, organ condemnation, and zoonotic public health risk. Strengthening slaughterhouse surveillance, implementing targeted deworming programs in dogs, and public health awareness campaigns are warranted to curtail the transmission and spread of echinococcosis in the Rayalaseema region of Andhra Pradesh.

ACKNOWLEDGEMENT

The authors extend their sincere thanks to the Sri Venkateswara Veterinary University, Tirupati for providing the facilities necessary to conduct this study.

Financial support & sponsorship*:* None

Conflict of interest : None

Use of artificial intelligence (AI)-assisted technology for manuscript preparation: The authors confirm that there was no use of AI-assisted technology for assisting in the writing of the manuscript and no images were manipulated using AI.

REFERENCES

1. Haftu B, Kebede T. 2014. Study on prevalence and economic significance of bovine hydatidosis in Bako municipal abattoir, West Shoa zone, Oromiya regional state. *J Vet Sci Technol* **5**:197.
2. Vaidya VM, Zende RJ, Paturkar AM, Gatne ML, Dighe DG, Waghmare RN, Moon SL, Bhave SS, Bengale KG, Nikale NV. 2018. Cystic echinococcosis in animals and humans of Maharashtra State, India. *Acta Parasitol* **63(2)**:232–243.
3. Soulsby EJL. 1982. *Helminths, Arthropods and Protozoa of Domesticated Animals*. 7th edn. Bailliere Tindall, London, pp. 119–122.
4. Shahnazi, M., Jafari, A., Javadi, M. and Saraei, M. (2013). Fertility of hydatid cysts and viability of protoscoleces in slaughtered animals in Qazvin, Iran. Journal of Agricultural Sciences, **5(1)**:141.
5. Mandal S, Mandal MD. 2012. Human cystic echinococcosis: epidemiologic, zoonotic, clinical, diagnostic and therapeutic aspects. *Asian Pac J Trop Med* **5(4)**:253–260.
6. Godara R, Katoch R, Yadav A. 2012. Hydatidosis in goats in Jammu, India. *J Parasit Dis* **38(1)**:73–76.
7. Ibrahim SEA, Gameel AA. 2014. Pathological, histochemical and immunohistochemical studies of lungs and livers of cattle and sheep infected with hydatid disease. In: *Proceedings of 5th Annual Conference-Agricultural and Veterinary Research*, Khartoum, Sudan, **2(1)**:1–17.
8. Bancroft JD, Cook HC. 1994. *Manual of Histological Techniques and Their Diagnostic Application*. Churchill Livingstone, Edinburgh.
9. WHO. 2021. Echinococcosis. Available at: World Health Organization.
10. Beigh AB, Darzi MM, Bashir S, Shah A, Shah SA. 2018. The pathology of cystic echinococcosis and structural details of hydatid cyst and protoscolex. *Indian J Vet Pathol* **42(1)**:8–14.
11. Beigh AB, Darzi MM, Bashir S, Kashani B, Shah A. 2017. Gross and histopathological alterations associated with cystic echinococcosis in small ruminants. *J Parasit Dis* **41(4)**:1028–1033.
12. Moudgil A, Moudgil P, Asrani RK, Agnihotri RK. 2020. Hydatidosis in slaughtered sheep and goats in India: prevalence, genotypic characterization and pathological studies. *J Helminthol* **93(6)**:768–775.
13. Kumari S, Singh R, Kumar A, Singh S, Yadav J. 2017. Pathomorphological diagnosis of hydatidosis in slaughtered sheep. *Int J Livest Res* **7(9)**:246–251.
14. Rashid A, Darzi MM, Mir MS, Dar LM. 2019. Pathological and histochemical studies on cystic echinococcosis in sheep. *SKUAST J Res* **21(1)**:50–58.
15. Hansh WJ. 2019. The study of histopathological changes in some of intermediate hosts infected with cystic echinococcosis. *Univ Thi-Qar J Sci* **7(1)**:249.
16. Jogdand BM, Gangane GR, Moregaonkar SD, Rathod PR, Chigure GM, Ghorpade BP, Zende RJ, Patil AA, Bhagwat PN, Kadam ST. 2024. Pathomorphological alterations in goats afflicted with cystic echinococcosis. *Int J Vet Sci Anim Husb* **9(5)**:692–698.
17. Fallah M, Kavand A, Mashouf RY. 2014. Infected hydatid cyst bacteria in slaughtered livestock and their effects on protoscoleces degeneration. *Jundishapur J Microbiol* 7(6):e10135.
18. Mahmoudvand H, Harandi MF, Shakibaie M, Aflatoonian MR, ZiaAli N, Makki MS, Jahanbakhsh S. 2014. Scolicidal effects of biogenic selenium nanoparticles against protoscolices of hydatid cysts. *Int J Surg* **12(5)**:399–403.
19. Siddartha PV, Babu AJ, Rao TM, Rayulu VC, Swetha CS. 2022. A comparative evaluation of four different immunoassays in the diagnosis of cystic echinococcosis using crude and purified hydatid cyst fluid antigen. *Acta Parasitol* **67(4)**:1667–1679.
20. Barnes TS, Hinds LA, Jenkins DJ, Bielefeldt-Ohmann H, Lightowlers MW. 2011. Comparative pathology of pulmonary hydatid cysts in macropods and sheep. *J Comp Pathol* **144(4)**:333–342.
21. Al Malki J, Ahmed N. 2022. Epidemiological and histomorphic studies in sheep infected with hydatid cyst in Taif area. *Saudi J Biol Sci* **29(2)**:886–893.
22. Al-Aubaidi IK, Yaseen AN, Gathwan MA. 2019. Histopathological study of hepatic and pulmonary sheep hydatidosis. *Ann Trop Med Publ Health* **22(4)**: SPe155.
23. Usman M, Rizwan HM, Sajid MS, Kausar R, Tahir UB, Abbas H, Ateeq MK, Raza M, Maqbool M, Fouad D, Ataya FS. 2024. Prevalence and histopathological analysis of cystic echinococcosis in ruminants of District Narowal, Pakistan: focus on pulmonary involvement. *Braz J Vet Parasitol* **33(4):**e016824.
24. Iqbal N, Hussain M, Idress R. 2017. Disseminated hydatid cyst of liver and lung. *BMJ Case Rep*. **bcr-2017**-222808.
25. Dalal U, Dalal AK, Singal R. 2017. Concomitant lung and liver hydatid cyst managed as one-stage surgery. *Maedica (Bucur)* **12(1):**19–22.
26. Amarir FE, Rhalem A, Marcotty T, Dorney P, Sadak A, Azrib R, Kirschvink N. 2022. Epidemiological aspects of cystic echinococcosis in small ruminants. *Small Rum Res* **210**:106671.

Indian J. Vet. Pathol., 50(4) : 316-323, 2026: DOI: https://doi.org/10.56093/v1rm4f03

RESEARCH ARTICLE

Pathological and molecular insights into *Toxoplasma gondii* in aborted fetuses of goat and slaughtered goats in Mymensingh district, Bangladesh

Mahmuda Islam, Nazneen Sultana, Moutuza Mostaree, Thahsin Farjana[1], Munmun Pervin and Mohammad Abu Hadi Noor Ali Khan[*]

Department of Pathology, Faculty of Veterinary Science, Bangladesh Agricultural University (BAU), Mymensingh-2202
[1]Department of Parasitology

[*]**Address for correspondence**
Dr Mohammad Abu Hadi Noor Ali Khan, E-mail: hadi.khan@bau.edu.bd, nazneen41151@bau.edu.bd
ORCID ID: 0000-0002-3612-2443, 0000-0001-8060-4805, 0000-0003-1380-908X, 0000-0001-6033-5505, 0000-0002-5514-5798, 0000-0002-8409-4571

Received: 26.8.26; Accepted: 25.9.26

ABSTRACT

The study attempted to investigate *Toxoplasma gondii* infection in aborted goat fetuses and slaughtered goats. A total of 29 aborted fetuses and 50 slaughtered goats were examined. The liver, spleen, kidney, stomach, and placenta from the aborted fetuses and the liver, spleen, and kidney from the slaughtered goats were collected from Mymensingh district, Bangladesh. The organs were fixed in 10% neutral buffered formalin and processed for H&E staining to visualize specific lesions. Gross examination revealed hepatomegaly with fragile, pale livers and kidneys, while placentas showed necrosis, swelling, and whitish foci. Histopathological examination revealed banana-shaped tachyzoites of *T. gondii* in three fetuses. In addition, placentitis with congestion, haemorrhage, and mononuclear cell infiltration, as well as hepatic granulomas, were observed in suspected *T. gondii*-infected cases. Tissue samples were collected aseptically in falcon tubes and cryovials and preserved at -20ºC for DNA extraction and PCR detection. PCR analysis of fetal DNA detected *T. gondii* (B1 gene, 512 bp) in five cases (17.24%), and DNA extracted from slaughtered goats (N = 50) detected *T. gondii* in one case (2%). The partial sequence of the B1 gene of *T. gondii* was sequenced and deposited in GenBank (accession number: OP627282). Bangladeshi isolates of *T. gondii* showed the highest similarity with the isolates from Mexico but also revealed genetic relatedness with other global isolates.

Keywords: Abortion, Black Bengal goats, Histopathology, PCR, phylogeny, *T. gondii*

How to cite this article: Islam, M., Sultana, N., Mostaree, M., Farjana, F., Pervin, M. and Khan, M.A.H.N.A. 2026. Pathological and molecular insights into *Toxoplasma gondii* in aborted fetuses of goat and slaughtered goats in Mymensingh district, Bangladesh. Indian J. Vet. Pathol., 50(4) : 316-323.

INTRODUCTION

Toxoplasmosis is an important intracellular apicomplexan protozoan disease of humans and animals caused by the parasite *Toxoplasma gondii*. Globally, approximately 500 million people are infected yearly by these protozoa[1]. Throughout the world, *T. gondii* is a significant medical and veterinary issue[2] causing financial losses due to congenital disease and abortions, [3,4]. Among animals, Toxoplasmosis is an economically significant disease of small ruminants and is recognized as one of the focal causes of infective abortions as it can result in early embryonic death and resorption, foetal death and mummification, abortion, stillbirth, and neonatal death[5]. The main methods of transmission for humans are eating raw or undercooked meat contaminated with *T. gondii* cysts, drinking contaminated food or water, or accidentally ingesting the oocysts[6]. Infection from raw goat and sheep milk consumption has recently reported[7,8].

Numerous serological tests conducted throughout the world, including Bangladesh, served as the basis for most of the epidemiological studies on *T. gondii*[9]. In Bangladesh, sheep, goats, and cattle are frequently used as food sources. Earlier studies in Bangladesh have reported that the seroprevalence of toxoplasmosis in cattle varied from 12 to 27%, 12 to 61% in goats 18 to 69% in sheep[10-13].

Histopathological analysis, serological tests, isolation of the parasite in mouse inoculation[14-17], and the amplification of parasite DNA by various molecular techniques, such as polymerase chain reaction (PCR), quantitative polymerase chain reaction (qPCR), and loop-mediated isothermal amplification (LAMP), have been used for the diagnosis of toxoplasmosis. Although the LAMP procedure is simple, quick, and requires the least amount of time, LAMP reagents are expensive[18]. Molecular methods based on polymerase chain reaction (PCR) are simple, sensitive, and reproducible and can be applied to all clinical samples[19,20,21]. The B1 gene of *T. gondii* is extremely conserved, and PCR amplification of this gene has been effectively used to detect a minute amount of

parasite DNA[22]. In this study, B1 gene fragment of *T. gondii* were amplified using a uniplex conventional PCR. Due to its frequent use in the detection of *T. gondii*, this gene was chosen [9,23,24]. In Bangladesh, there are few investigations on the molecular detection of caprine abortion[9,13]. This study aimed to investigate gross and histopathological alterations in visceral organs and to molecularly characterize *T. gondii* infection in aborted goat fetuses and slaughtered goats in Mymensingh, Bangladesh.

MATERIALS AND METHODS

Collection of samples

A total of 29 aborted fetuses and 50 slaughtered female goats were collected from Mymensingh during the period from January 2018 to December 2019. Aborted fetuses were collected from veterinary clinics and Upazilla Livestock Hospital in Mymensingh district. Slaughtered goat samples were collected from different slaughterhouses in Mymensingh District, Bangladesh. The liver, spleen, kidney, stomach, and placenta from the aborted fetus and the liver, spleen, and kidney from the slaughtered goats were collected. The organs were fixed in 10% neutral buffered formalin, and the formalin-fixed tissues were processed, sectioned, and stained with hematoxylin and eosin (H&E) stain[25]. Parts of the organs were collected in falcon tubes and cryovials and preserved at -20°C for DNA extraction and PCR detection of *T. gondii*.

Histopathology

Formalin-fixed tissues were processed and embedded in paraffin. Paraffin-embedded tissues were then sectioned and stained with hematoxylin and eosin (H&E) stain[25]. The stained sections were observed under a light microscope (Carl-Zeiss), and images were captured

DNA extraction from tissue samples

DNA was extracted from the liver, spleen, kidney, stomach, and placenta of the aborted fetus and from the liver, spleen, and kidney of the slaughtered goats. The Wizard® Genomic DNA Extraction Kit (Promega, Inc., USA) was used to extract the DNA using manufacturer instructions. The quality and quantity of the extracted DNA were measured by spectrophotometry (A^{260}/A^{280}) (Nanodrop 2000 machine, Shimadzu, Japan) and agarose gel (1.5%) electrophoresis, respectively. A260/A280ratio of 1.75 -2.0 was considered a reasonable purity of DNA and was used in this study. Approximately 200–300 ng/µL was dissolved in RNase-free water and stored at -20°C until used in PCR amplification. Table. 1 contains the list of primers used in this study to detect *T. gondii*[26].

Polymerase chain reaction (PCR)

PCR reactions were performed on each DNA sample in a 25 µl reaction mix containing 12.5 µl of One *Taq*® Quick-Load® 2X Master Mix with standard buffer (New England Biolabs, USA), 1 µl (20 pmol) of each primer, 9.5 µl nuclease-free water, and 1 µl template DNA/water (for the water control tube). The following thermal profile was used for DNA amplification in a thermal cycler (Thermal Cycler PCR systems with Gradient Thermo Fisher Scientific, USA): Initial denaturation step at 94°C for 30 s in the first cycle, followed by 35 cycles on 30 sec at 94°C for denaturation, 58.5°C for 30 sec for annealing, and 30 sec at 68°C for extension. This was followed by a final extension of 5 minutes at 68 °C. After completion of the PCR reaction, the tubes were held at 4°C.

Electrophoresis

The amplified PCR products were electrophoresed in 1.5% agarose gel, stained with ethidium bromide, and examined using a UV transilluminator documentation system (Cell Biosciences, Alphalmager HP, USA).

RESULTS

Age distribution

In this study, the gestational age of the aborted fetuses ranged from 1.5 to 5 months (Fig. 1). The ages of goats with abortion cases ranged from 10 months to 4 years.

Gross pathological observations

The majority of fetuses were collected fresh, but a few showed evidence of autolysis. Obvious lesions were not seen on the fetuses (Fig. 1). Although no significant gross lesions were seen, hepatomegaly, fragile and pale liver and kidney were recorded (Fig. 2). The placental changes recorded were necrosis, swelling, and freckling with whitish foci in the cotyledons (Fig. 3). No significant gross changes could be ascertained in the visceral organs examined of the slaughtered goats.

Histopathological observations

Histopathological changes demonstrated banana-shaped tachyzoites of *T. gondii* in the fetal spleen. The spleen showed atrophic changes, thickened trabeculi, lymphocytic depletion and haemorrhages (Fig. 4). Tachyzoites of *T. gondii* were also in the hepatic

Table 1. Oligonucleotide primers used for the detection of ***Toxoplasma gondii***

Primers	Sequences (5′-3′)	Gene/Amplicon size	References
ToxoplsF1	gaattcgttcgacagaaaggg	B1/ 512bp	Ahmad *et al.*[26]
ToxoplsR1	catttcacctgtatttgccagc		



Fig. 1. Gross findings of aborted goat fetuses (a–c) delivered at 2.5, 3, and 3.5 months of gestation, respectively.



Fig. 2. Visceral organs of aborted fetus (a) pale liver and kidney, fragile liver, (b) fragile liver, (c) hepatomegaly.



Fig. 3. Placenta from goat (a) necrosed, swollen and whitish cotyledon; (b) whitish necrotic foci in the cotyledon; (c) autolyzed placenta.

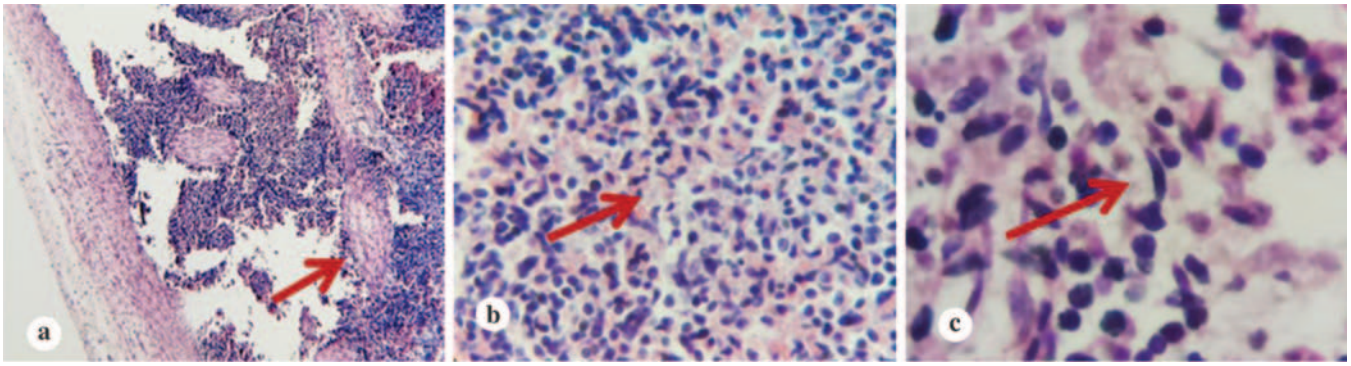

Fig. 4. Histopathology of the spleen of *Toxoplasma gondii* infected aborted goat fetus. a: atrophy of the spleen with thicker trabeculi and lymphocytic depletion(arrow), b: lymphocytic depletion and haemorrhages(arrow), c: higher magnification of (b) showing banana shaped tachyzoites of *Toxoplasma* (arrow). H&E; a = 10×, b = 40×, c = 100×.

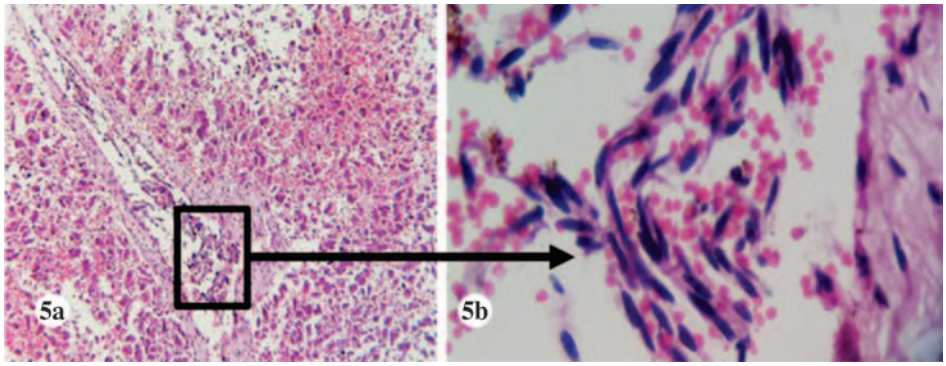

Fig. 5. Histopathology of the liver of *Toxoplasma gondii* infected aborted goat fetus. **(a-b)** banana-shaped tachyzoites of *Toxoplasma* in the central vein (arrow). H&E; a = 40x, b = 100x

Fig. 6. Histopathology of the placenta of *Toxoplasma gondii* infected aborted goat fetus; **(a)** placentitis; **(b)** congestion and haemorrhages (arrow); **(c)** infiltration of mononuclear cells (arrow) into the trophoblastic epithelium. H&E; a=10x, b=40x, c=100x.

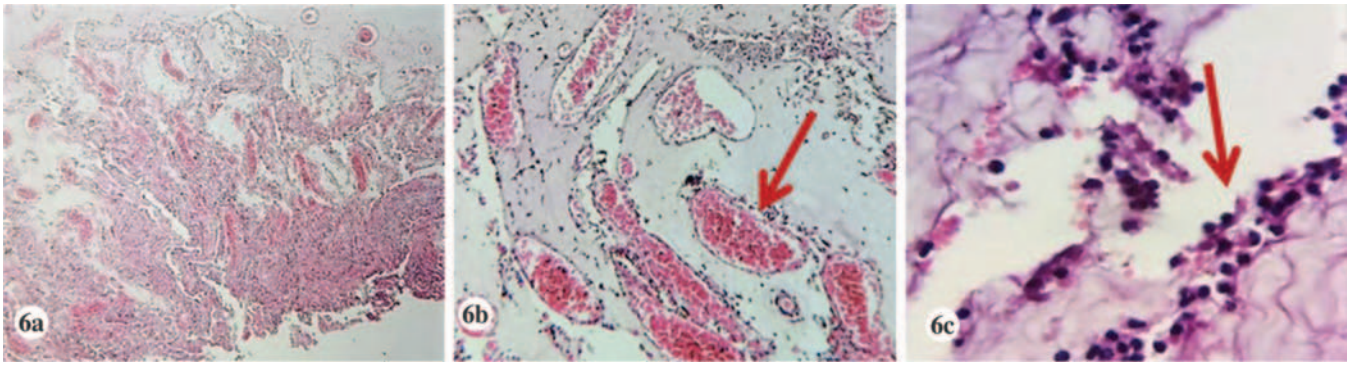

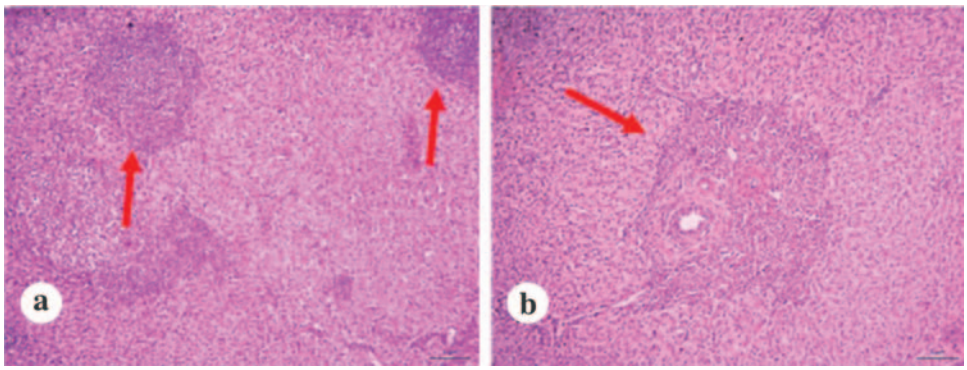

Fig. 7. Histopathology of the liver of slaughtered goat; **(a)** hepatic granuloma; **(b)** hepatic granuloma in the portal area (arrow) were seen in cases infected with *Toxoplasma gondii*. H&E; a-b = 10x.

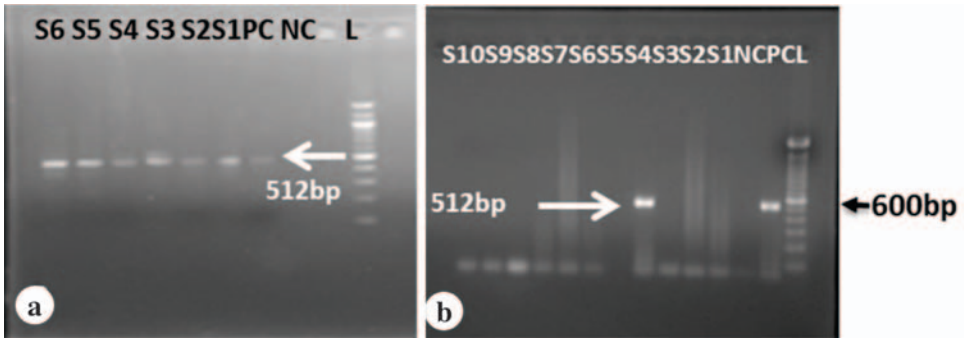

Fig. 8. PCR detection of the **B1 gene of *T. gondii*** from **(a)** the aborted fetus and **(b)**slaughtered goat, respectively. The lane L stands for 100bp DNA ladder, PC is for positive control, and NC is for negative control. Amplification of 512bp fragment specific for *T. gondii* was seen on agarose gel electrophoresis in **(a)** aborted fetus Lane S1 to S6: positive samples and **(b)** slaughtered goat Lane S4: positive sample.

central vein (Fig. 5). Placental examination of two aborted fetuses suspected of *T. gondii* infection and revealed placentitis, congestion and haemorrhages, and infiltration of mononuclear cells (Fig. 6). The histopathological examination of the liver of a slaughtered goat suspected to be infected with *T. gondii* showed a hepatic granuloma (Fig. 7).

Results of PCR

PCR analysis of DNA extracted (N=29) showed *T. gondii* PCR amplicons (B1 gene, 512bp) (Figure 8a) in five cases (17.24%). DNA (N=50) extracted from the slaughtered goats showed *T. gondi* (B1 gene, 512bp) (Figure 8b) in a case (2%).

Phylogenetic analyses of *T. gondii*

The partial sequence of the B1 gene (512 bp length) of *T. gondii was* carried out, and the sequence information was used in phylogenetic

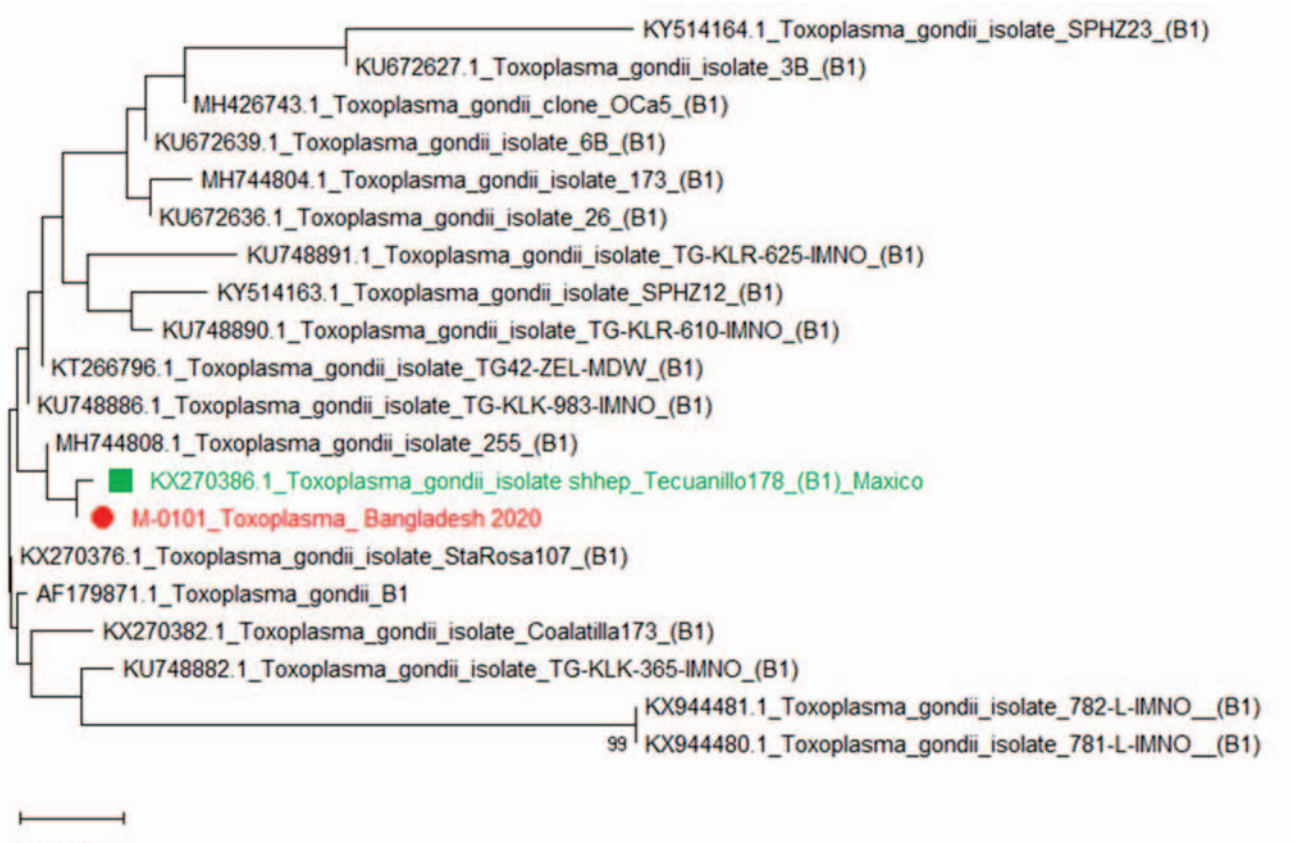

Fig. 9. Bangladeshi isolate showed highest similarity with a Mexican isolate but also revealed genetic relatedness with other global isolates

analysis. The B1 gene of *T. gondii* sequences obtained in the current study were submitted to GenBank database and the accession number (OP627282) was obtained. Results of phylogenetic analysis of B1 gene showed that the *T. gondii* of the Bangladeshi isolate showed the highest similarity to isolates from Mexico and North India but also revealed genetic relatedness with other global isolates. The current study successfully analyzed the sequences of the B1 gene of *Toxoplasm*a, and its phylogenetic position was identified (Fig. 9).

DISCUSSION

In this study, the gestation age of aborted fetuses ranged from 1.5 to 5 months. Abortion cases in goats were observed in the age group of 10 months to 4 years. Infections that occur between 40 and 120 days of gestation may cause fetal mummification and maceration or abortion. Infection after 120 days causes stillbirth and or the birth of weak offspring[5]. Most abortions associated with *T. gondii* infection occurred in ewes aged 1–3 years during the late stages of pregnancy, consistent with the previous[27] and current study.

At necropsy, the majority of the aborted fetuses had hepatomegaly, along with fragile and pale livers and kidneys. Grossly, the placenta was enlarged, reddish, and friable in aborted ewe fetuses, and its cotyledons were covered in white foci or necrotic nodules, which is consistent with previous findings[27]. The cotyledons of aborted sheep fetuses showed necrotizing placentitis with several white foci[28]. Grossly, the placenta was enlarged, reddish, and friable in aborted ewe fetuses, and its cotyledons were covered with white foci or necrotic nodules[27]. The cotyledons of aborted sheep fetuses showed necrotizing placentitis with several white foci[28]. Grossly, numerous focal areas of necrosis and grayish white calcification were present in the placenta of goat[29]. Ahmed *et al*[30]. reported reported that most of the aborted caprine fetuses infected by *Toxoplasma* displayed a rounded-bordered, friable, congested liver[30]. In this study, in addition to the histopathological changes in tissues banana-shaped tachyzoites of Toxoplasma were seen in the fetal spleen. Atrophy of the spleen with thicker trabeculi, lymphocytic depletion and hemorrhages were present. The liver of an aborted goat fetus showed banana-shaped tachyzoites of toxoplasma in the central vein. According to previous study, the liver, brain, heart, and lungs of the aborted fetuses /species showed the most frequent histopathological changes, including severe congestion, necrosis, and infiltration of multinucleated cells, as well as tissue cysts, tachyzoites, and bradyzoites, and the brain and heart showed the

most clusters of dark purple, banana-shaped *T. gondii* tachyzoites[27]. There were intracellular protozoa in the heart, lung, and liver tissues[31]. Histological investigation revealed many parasite cysts of varied sizes embedded and dispersed between cardiac muscle fibers in sheep hearts[32]. Mild multifocal necrotizing pneumonia with intralesional protozoan tachyzoites was discovered in the lungs of sows and aborted fetuses. Histopathologic analysis of lungs, livers, lymph nodes, and brains revealed multifocal necrotic lesions connected to nearby protozoan tachyzoites[33]. Large clusters of *T. gondii* with the appearance of dark purple bananas were seen in the cardiac tissue of most of the individuals examined [30]. In the present study, the placenta of an aborted goat infected by *T. gondii* shows placentitis, haemorrhage and congestion, and infiltration of mononuclear cells. In the placental sections of some aborted goats, the placenta was bloated, crimson, and friable, and its cotyledons were covered in whitish foci or nodules of necrosis, as well as intracellular *T. gondii* tachyzoites[27]. The most frequent lesion caused by *T. gondii* during abortion is necrotizing placentitis, which almost exclusively affects cotyledonary regions [34]. In this study, histopathological examination of the liver of a slaughtered goat infected with *T. gondii* revealed a hepatic granuloma. The liver also displayed multifocal necrosis with mononuclear cell infiltration, primarily comprising lymphocytes and macrophages[35]. Multifocal portal granuloma with macrophage and mononuclear cell infiltration was also noted[36].

In the present study, *T. gondii* DNA was detected in five cases (17.24%) in aborted fetuses and DNA extracted from the slaughtered goats showed *T. gondii* in one case (2%) by PCR. Results obtained from the aborted fetus were almost identical to those reported by Sah *et al*.[9] who were also the first to report on molecular detection of *T. gondii* in sheep and goat aborted fetuses in Bangladesh, with a rate of 15.52%[9]. Similar findings were reported by[37] from Chennai, South India. In Iran, the presence of *T. gondii* DNA was detected by PCR in liver samples from 17.3% and 16% of sheep and goats, respectively [38]. *Toxoplasma* DNA was found in 12.0% of aborted sheep fetuses in Iran's North Khorasan Province[39] and 8.3% of aborted caprine and ovine fetuses in Iran's Kordestan Province[40]. The result of the slaughter sample analysis was identical to that reported by[2] from North India, where *T. gondii* infection was found in 1.35% and 1.69% of slaughter goats and sheep, respectively. The prevalence of *T. gondii* infection in aborted fetuses of sheep and goats was estimated to be 5.4% and 3.8%, respectively, in Spain[41]. The prevalence of *T. gondii* DNA in goats was reported as 5.2% in China [42]. However, many studies showed higher prevalence values for *T. gondii* infection. The infection rate of *T. gondii* was found to be 27% and 31% in goats and sheep, respectively, in Iran [43]. *T. gondii* PCR positivity was detected as 29.8% in Jordan [44]. In Bangladesh, a higher prevalence of *T. gondii* as detected by PCR was reported as 35% in aborted goat fetuses [45]. Literature available indicates the prevalence of toxoplasmosis ranges from 2 to 35%. The study observed the prevalence of toxoplasmosis of around 17%, which appeared similar to the previous observation. The BLAST comparison of the partial sequences of the B1 gene (512 bp length) of *T. gondii* Bangladeshi isolate (accession no. OP627282) was found to be more closely related to those reported from other geographical locations, and include: Mexico (accession no. KX270376, KX270382), USA (accession no. AF179871, MH426743, MH744808), Iran (accession no. KU672636, KU672627, KU672639), Poland (accession no. KX270376, KU748891, KU748886), and India (accession no. KY514164, KY514163). The isolate of *T. gondii* revealed 97–99% identity with sequences from other strains present in the GenBank. The Bangladeshi isolate of *T. gondii* showed the highest similarity with the isolates from Mexico (99.4%), North India (98.5%), and Poland (98.89%) but also revealed genetic relatedness with other global isolates. B1 gene of *T. gondii* coding sequences obtained by[2] and found (94–98%) homology with *T. gondii* type I RH strain, USA (AF179871). 99% similarity in sequence of *T. gondii* with the sequence from Brazil (FJ176233) was reported by[46].

CONCLUSIONS

The present study has provided evidence of the involvement of *T. gondii* in the aborted fetuses and placentas of goats. *T. gondii* may be one of the potential agents responsible for causing a significant rate of goat abortions in Bangladesh. The presence of the organism in the tissue demonstrates a health hazard for the human inhabitants who ordinarily consume goat meat. The possibility of *T. gondii* infection in goats poses a threat to public health. We need more research to better understand the different genotypes of *T. gondii* that cause abortion in goat populations in Bangladesh.

ACKNOWLEDGEMENT

The authors extend their gratitude to the Department of Veterinary Pathology, Faculty of Veterinary Science, Bangladesh Agricultural University for providing the facilities necessary to conduct this study.

Financial support & sponsorship: The authors are grateful to the Ministry of Education (MOE), Bangladesh for funding the research (Project ID.:2017/189/MoE) and thanked the Bangladesh Agricultural University Research System (BAURES).

Conflicts of Interest: None

Use of Artificial Intelligence (AI)-Assisted Technology for manuscript preparation: The authors confirm that

there was no use of AI-assisted technology for assisting in the writing of the manuscript and no images were manipulated using AI.

REFERENCES

1. Bob. 2011. Dr. Bob's all creatures site. WWW.Petdoc.ws, Zoonotic Diseases. pp 1-169 file:///F:/zoonotic_ diseases1.htm.
2. Kalambhe D, Gill JP, Singh BB.2017. Molecular detection of *Toxoplasma gondii* in the slaughter sheep and goats from North India. *Vet Parasitol.* **241:**35-38.
3. Dubey JP, Beattie CP.1988. Toxoplasmosis of Animals and Man. CRC Press, Florida, U.S.A, Boca Raton. pp. 1–220.
4. Remington JS, Desmonts G.1990. Toxoplasmosis: Infectious Diseases of the Fetus and Newborn Infant. vol. *30. W. B. Saunders, Philadelphia, Santa Maria* pp. 123–127.
5. Dubey J. 2009. Toxoplasmosis in sheep—the last 20 years. *Vet Parasitol.* **163**(1–2): 1–14.
6. Dubey JP, Schares G. 2011. Neosporosis in animals – the last five years. *Vet Parasitol* **180(1-2)**:90-108.
7. de Santana Rocha D, de Sousa Moura RL, Maciel BM, Guimarães LA, O'dwyer HN, Munhoz AD, Albuquerque GR. 2015. Detection of *Toxoplasma gondii* DNA in naturally infected sheep's milk. *Genet Mol Res.* **14(3)**:8658-8662.
8. Amairia S, Rouatbi M, Rjeibi MR, Nouasri H, Sassi L, Mhadhbi M and Gharbi M .2016. Molecular prevalence of *Toxoplasma gondii* DNA in goats' milk and seroprevalence in Northwest Tunisia. *Vet Med Sci.***2(3):**154–160.
9. Sah RP, Dey AR, Rahman AA, Alam MZ, Talukder MH.2019. Molecular detection of *Toxoplasma gondii* from aborted fetuses of sheep, goats and cattle in Bangladesh. *Vet Parasitol Reg Stud Reports.* **18:**100347.
10. Samad MA, Rahman KB and Halder AK. 1993. Seroprevalence of *Toxoplasma gondii* in domestic ruminants in Bangladesh. *Vet Parasitol* **47**(1-2):157-159.
11. Shahiduzzaman M, Islam MR, Khatun MM, Batanova TA, Kitoh K, Takashima Y. 2011. *Toxoplasma gondii* seroprevalence in domestic animals and humans in Mymensingh District, Bangladesh. *J Vet Med Sci.***73:**1375– 1376
12. Rahman M, Azad MT, Nahar L, Rouf SM, Ohya K, Chiou SP, Baba M, Kitoh K, Takashima Y.2014. Age-specificity of *Toxoplasma gondii* seroprevalence in sheep, goats and cattle on subsistence farms in Bangladesh. *Bangladesh. J Vet Med Sci.***76**(9):1257-1259.
13. Sah RP, Talukder MH, Rahman AA, Alam MZ, Ward MP.2018. Seroprevalence of *Toxoplasma gondii* infection in ruminants in selected districts in Bangladesh. *Vet Parasitol Reg Stud Reports.* **11**:1-5.
14. da Silva AV, Langoni H.2001.The detection of *Toxoplasma gondii* by comparing cytology, histopathology, bioassay in mice, and the polymerase chain reaction (PCR). *Vet Parasitol* **97**(3):193-200.
15. Masala G, Porcu R, Madau L, Tanda A, Ibba B, Satta G, Tola S.2003. Survey of ovine and caprine toxoplasmosis by IFAT and PCR assays in Sardinia, Italy. *Vet Parasitol* **117**(1-2):15-21.
16. Remington JS, Thulliez P, Montoya JG.2004. Recent developments for diagnosis of toxoplasmosis. *J Clin Microbiol.* **42**:941–945.
17. Garcia JL, Gennari SM, Machado RZ, Navarro IT .2006. *Toxoplasma gondii*: detection by mouse bioassay, histopathology, and polymerase chain reaction in tissues from experimentally infected pigs. *Exp Parasitol.* **113**(4):267-271.
18. Wang Y, Wang G, Zhang D, Yin H, Wang M.2013. Detection of acute toxoplasmosis in pigs using loop mediated isothermal amplification and quantitative PCR. *Korean J Parasitol.* **51:**573–577.
15. Contini C and Picot S. 2005. Evaluation of a Real-time PCR based assay using the light cycler system for detection of *Toxoplasma gondii* bradyzoite genes in blood 23 specimens from patients with toxoplasmic retinochoroiditis. *Int J Parasitol.* **35**(3):275-283.
16. Tlamçani Z, Lemkhenete Z and Lmimouni BE. 2013.Toxoplasmosis: The value of molecular methods in diagnosis compared to conventional methods. *J. Microbiol. Infect. Dis.* **3**(2):93-99.
17. Gashou A, Amro A, Erhuma M, Al-Dwibe H, Elmaihub E, Babba H, Nattah N, Abudher A. 2016. Molecular diagnosis of *Toxoplasma gondii* infection in Libya. *BMC Infect Dis*.**16**(1):1-8.
18. Dubey JP, Morales JA, Villalobos P, Lindsay DS, Blagburn BL, Topper MJ.1996. Neosporosis-associated abortion in a dairy goat. *J Am Vet Med Assoc.* **208**:263–265.
19. Thakur R, Sharma R, Aulakh RS, Gill JP, Singh BB.2019. Prevalence, molecular detection and risk factors investigation for the occurrence of *Toxoplasma gondii* in slaughter pigs in North India. *BMC Vet Res.***15**(1):1-7.
20. Sroka J, Karamon J, Wójcik-Fatla A, Piotrowska W, Dutkiewicz J, Bilska-Zając E, Zając V, Kochanowski M, Dąbrowska J, Cencek T.2020. *Toxoplasma gondii* infection in slaughtered pigs and cattle in Poland: seroprevalence, molecular detection and characterization of parasites in meat. *Parasit Vectors.***13**(1):223.
21. Luna LG.1968. Manual of Histologic Staining Methods of the Armed Forces Institute of Pathology; McGraw Hill Book Co., New York, USA
22. Jahan AA, Ruba T, Mumu TT, Rana MS, Islam M, Belal SM, Khan MA and Bari AM. 2018.Pathological and molecular detection of diseases of cattle at slaughter. *Bangl. j. vet. med.* **16**:213-222.
23. Khanamir RA, Naqid IA, Zangana IQ.2020. Histopathological and Serological Analysis of Aborted Ewes and Neonatal Death with *Toxoplasma gondii* in Duhok City, Kurdistan-Iraq. *Arch Razi Inst.* **75**(2):241-248.
24. Dorsch MA, Francia ME, Tana LR, González FC, Cabrera A, Calleros L, Sanguinetti M, Barcellos M, Zarantonelli L, Ciuffo C, Maya L, Castells M, Mirazo S, da Silva Silveira C, Rabaza A, Caffarena RD, Doncel Díaz B, Aráoz V, Matto C, Armendano JI, Salada S, Fraga M, Fierro S, Giannitti F.2022. Diagnostic Investigation of 100 Cases of Abortion in Sheep in Uruguay: 2015-2021. *Front Vet Sci.* 9:904786.
25. AbouZeid NZ, Amer HA, Barakat TM, Selim A, El-Balkemey F.2010. Toxoplasmosis is naturally and experimentally infected goats. *Am. J. Sci.* **6**(11):122-9.
26. Ahmed YF, Sokkar SM, Desouky HM, Soror AH.2008. Abortion is due to toxoplasmosis in small ruminants. *Glob. Vet.* **2**(6):337-342.
27. Tokiwa T, Yoshimura H, Hiruma S, Akahori Y, Suzuki A, Ito K, Yamamoto M, Ike K.2019. *Toxoplasma gondii* infection in Amami spiny rat on Amami Oshima Island, Japan. *Int J Parasitol Parasites Wildl.* **9**:244-247.
28. Al-Khafagi AM, Zainab RZ.2016. Histopathological and diagnostic study of Toxoplasmosis in human and sheep by using ELISA in Kut city. *Iraqi J. Vet. Med.* **40**(2):94-9.
29. Kim JH, Kang KI, Kang WC, Sohn HJ, Jean YH, Park BK, Kim Y, Kim DY.2009. Porcine abortion outbreak associated with *Toxoplasma gondii* in Jeju Island, Korea. *J Vet Sci.***10**(2):147-151.
30. Dubey JP, Kirkbride CA.1990. Toxoplasmosis and other causes of abortions in sheep from north central United States. *J Am Vet Med Assoc.* **196**:287-290.
31. El-Gawady HM, Abdel-Aal AA, Sallam NH, Youssif EM.2018. Molecular studies on *Toxoplasma gondii* in sheep and goats in

Ismailia Province. *Archives of Infectious Diseases and Therapy* **2**:1-4.
32. Mahmood NA, Dawood MN. 2012. Liver function tests in toxoplasmosis. *Ann. Coll. Med. Mosul.* **38**(2).
33. Satbige AS, Sreekumar C, Rajendran C, Vijaya BM.2017. Isolation and characterization of *Toxoplasma gondii* from small ruminants (sheep and goats) in Chennai City, South India. *J Parasit Dis.***41**:869-873.
34. Yousefvand A, Mirhosseini SA, Ghorbani M, Mohammadzadeh T, Moghaddam MM, Mohammadyari S.2021. Molecular and serological detection and of *Toxoplasma gondii* in small ruminants of southwest Iran and the potential risks for consumers. *J Verbrauch Lebensm.***16(2)**:117-127.
35. Salehi M, Nezami H, Niazkar HR.2020. Investigation of *Toxoplasma gondii* infection in aborted fetuses of sheep using PCR: a study in north Khorasan province, Iran. *Vet Med Int.* **2020**:7913912.
36. Partoandazanpoor A, Sadeghi-Dehkordi Z, Ekradi L, Khordadmehr M, Rassouli M, Sazmand A.2020. Molecular diagnosis and pathological study of *Toxoplasma gondii* in aborted caprine and ovine fetuses in borderline of Iran–Iraq. *Acta Parasitol.* **65**(1):187-192.
37. Moreno B, Collantes-Fernández A,Villa A, Navarro A, Regidor-Cerrillo J, Ortega-Mora LM.2012. Occurrence of *Neospora caninum* and *Toxoplasma gondii* infections in ovine and caprine abortions. *Vet Parasitol.***187**:312–318.
38. Qian W, Yan W, Lv C, Bai R, Wang T, Wei Z, Zhang M.2020. Molecular detection and genotyping of *Toxoplasma gondii* and *Neospora caninum* in slaughtered goats in Central China. *Foodborne Pathog Dis.***17**(5):348–356.
39. Sharif M, Sarvi S, Shokri A, Hosseini Teshnizi S, Rahimi MT, Mizani A, Daryani A.2015. *Toxoplasma gondii* infection among sheep and goats in Iran: a systematic review and meta-analysis. *Parasitol Res.***114**:1–16.
40. Abu-Dalbouh MA, Ababneh MM, Giadinis ND, Lafi SQ.2012. Ovine and caprine toxoplasmosis (Toxoplasma gondii) in aborted animals in Jordanian goat and sheep flocks. *Trop Anim Health Prod.***44**(1):49-54.
41. Hasan T, Mannan A, Hossain D, Rekha A, Hossan MM, Alim MA, Uddin AHMM.2021. Molecular detection of *Toxoplasma gondii* in aborted fetuses of goats in Chattogram, Bangladesh. *Vet World.* **14**(9): 2386-2391.
42. Rouatbi M, Amdouni Y, Amairia S, Rjeibi MR, Sammoudi S, Rekik M, Gharbi M. 2016.Molecular detection and phylogenetic analyses of *Toxoplasma gondii* from naturally infected sheep in Northern and Central Tunisia. *Vet Med Sci.* **3(1)**:22-31

Indian J. Vet. Pathol., 50(4) : 324-327, 2026: DOI: https://doi.org/10.56093/ywjd9977

RESEARCH ARTICLE

First report of multidrug-resistant *Pseudomonas juntendi* from an equine suppurative lesion

Monika Bhardwaj, Adarsh Kumar[1], Subhash Verma, Prasenjit Dhar, Shivani Barsain, Diksha Guleria and Rajesh Chahota*

Department of Veterinary Microbiology, Dr. G.C. Negi College of Veterinary and Animal Sciences, CSKHPKV, Palampur –176062 (Himachal Pradesh)

[1]Department of Veterinary Surgery and Radiology

***Address for correspondence**

Dr. Rajesh Chahota, E-mail: rchahota@yahoo.com

ORCID ID: 0000-0001-8075-730X

Received: 19.5.26; Accepted: 24.6.26

ABSTRACT

Pseudomonas juntendi is a recently identified opportunistic pathogen belonging to the *Pseudomonas putida* group. Strains of *P. juntendi* are frequently associated with multidrug resistance, posing significant challenges in the clinical management of associated disease condition. To the best of our knowledge, this is the first report describing the isolation and identification of *P. juntendi* from a horse. In the present study, a horse presented with swelling in the neck region accompanied by purulent discharge was investigated. A pus sample was aseptically collected and subjected to bacteriological isolation and biochemical characterization. Bacteriological examination revealed the presence of an aerobic, Gram-negative, non-spore-forming, non-motile, rod-shaped bacterium. Biochemically, the isolate tested positive for catalase, cytochrome oxidase, and citrate utilization, while negative reactions were observed for urease, methyl red, Voges–Proskauer, indole production, motility, and triple sugar iron tests. Based on the phenotypic and biochemical characteristics, the organism was preliminarily identified as a Pseudomonas species. For molecular confirmation, 16S rRNA gene sequencing was performed. Sequence analysis confirmed that the isolate belonged to the *Pseudomonas putida* group and was identified as *Pseudomonas juntendi*. Antimicrobial susceptibility testing against 17 antibiotics was carried out using the disc diffusion method. The isolate exhibited resistance to eight antibiotics, thereby demonstrating a multidrug-resistant phenotype. In this study, we report the first isolation of *Pseudomonas juntendi* from a suppurative lesion on the neck of a horse.

Keywords: *Pseudomonas juntendi*, Horse, Pus, 16S rRNA sequencing

INTRODUCTION

Pseudomonas juntendi is an opportunistic bacterial pathogen notable for its resilience across diverse environments, versatile metabolic capabilities, rapid growth, and high tolerance to oxidative stress and toxic compounds[1]. Recently, *P. juntendi* has been recognized as a novel member of the *Pseudomonas putida* group, which includes species such as *P. alloputida, P. anuradhapurensis, P. asiatica, P. fulva, P. inefficax, P. kurunegalensis, P. monteilii, P. oryzicola, P. parafulva, P. putida, P. pyomelaninifaciens, P. persica*, and *P. shirazica*[2].

P. juntendi is an aerobic, Gram-negative, non-spore-forming, motile, rod-shaped bacterium measuring approximately 1.0–2.0 μm in length and 0.5–0.8 μm in width[3]. It can grow within a temperature range of 4–40 °C and tolerate NaCl concentrations of 1.0–7.0%. The organism was initially identified as a potential human pathogen[4]. Although it has been isolated from various clinical specimens in Japan and Myanmar[5], its role as an animal pathogen remains unclear and warrants further investigation.

Previous studies have established *P. aeruginosa* as a significant pathogen causing urinary tract infections and exhibiting antimicrobial resistance, highlighting the pathogenic potential of other *Pseudomonas* species[6]. However, *P. juntendi* remains an understudied member of the *P. putida* group, particularly with respect to antimicrobial resistance[7]. Therefore, the present study aimed to detect the presence of *P. juntendi* in a pus sample from a horse and to evaluate its antimicrobial susceptibility profile.

How to cite this article: Bhardwaj, M., Kumar, A., Verma, S., Dhar, P., Barsain,S., Guleria, D. and Chahota, R. 2026. First report of multidrug-resistant *Pseudomonas juntendi* from an equine suppurative lesion. Indian J. Vet. Pathol., 50(4) : 324-327.

MATERIALS AND METHODS

Sample collection

Pus sample was collected aseptically from the neck swelling in a horse using a sterile swab at the Veterinary Clinical Complex, DGCN COVAS, CSKHPKV, Palampur. The swab was transported in phosphate-buffered saline (PBS) on ice to the Bacteriology Laboratory, Department of Veterinary Microbiology, and processed immediately for bacterial isolation.

Isolation and identification of *P. juntendi*

The pus sample was inoculated onto blood agar and incubated at 37 °C for 24 hours. Representative colonies were subjected to Gram staining and standard biochemical tests for identification, following the methodology described by Wulandari *et al*. (2019)[8]. Biochemical characterization included catalase, oxidase, nitrate reduction, Triple Sugar Iron (TSI), sulfide indole motility (SIM), methyl red (MR), Voges–Proskauer (VP), indole, and oxidative-fermentative (O/F) tests.

DNA extraction and 16S rRNA sequencing

Genomic DNA was extracted from purified bacterial colonies using the DNeasy blood and tissue kit (Qiagen). The extracted DNA was sent to Eurofins Genomics India Pvt. Ltd., Bangalore, for 16S rRNA gene amplification and sequencing. Universal primers 27F (5′-AGAGTTTGATCMTGGCTCAG-3′) and 1492R (5′-GGTTACCTTGTTACGACTT-3′) were used[9]. The obtained sequences were analyzed using BLASTn against the NCBI nucleotide database for species identification based on sequence homology.

Antimicrobial susceptibility testing

Antimicrobial susceptibility testing was performed using the Kirby–Bauer disk diffusion method[10] against 17 antibiotics: amikacin (AK) (10 µg), ampicillin (AMP) (10 µg), amoxicillin (AMX) (30 µg), amoxicillin/clavulanic acid (AMC) (30 µg), cefepime (CPM) (30 µg), ceftriaxone (CTR) (30 µg), chloramphenicol (C) (30 µg), cloxacillin (COX) (5 µg), cotrimoxazole (COT) (25 µg), imipenem (IPM) (10 µg), meropenem (MRP) (10 µg), penicillin-G (P) (2 units), piperacillin/tazobactam (PIT) (100/10 µg), polymyxin B (50 units), gentamicin (GEN) (30 µg), neomycin (N) (30 µg), and streptomycin (S) 10 µg), following CLSI guidelines[11].

RESULTS

Clinical signs and symptoms

A prominent swelling (appx. 4-5 cm in diameter) on the ventral aspect of the neck and mandibular region (persisting for 15 days) of a horse was present with a fistula in the center. The yellowish purulent discharge was coming out of the fistula (Fig. 1A). The animal was lethargic, showed inappetence and exhibited severe pain at the wound site.

Isolation of *P. juntendi*

Pure cream colored bacterial cultures with non-hemolytic, circular, and convex colonies were obtained on blood agar after 24 hours of incubation at 37 °C (Fig. 1B). On brain heart infusion (BHI) agar, colonies were characteristic cream color, circular, medium-sized, with entire margins, raised elevation, and smooth consistency (Fig. 1C). Gram's staining revealed presence of gram-negative bacilli with solitary arrangement (Fig. 1D).

Biochemical characterization of *P. juntendi*

Biochemical tests showed that the *P. juntendi* isolate was positive for catalase, cytochrome oxidase, and citrate utilization, while it tested negative for urease, MR, VP, indole and TSI tests (Fig. 2). The isolate exhibited an oxidative metabolism in Hugh–Leifson's oxidative/fermentative (O/F) medium, indicating an aerobic nature.

Sequencing

The sequence of 16S rRNA gene of the *P. juntendi* was received and edited by using DNA Star Bioinformatics tool. The sequence was analyzed for their similarity with previously published sequences in NCBI by BLASTn module available on the NCBI and it was observed that the sequence showed 100% similarity with the *P. juntendi* isolates sequences reported from other countries. The 16S rRNA sequence of *P. juntendi* has been submitted in the NCBI database (Accession no. PX453077).

Antimicrobial susceptibility testing

The results suggest that the *P. juntendi* bacterial strain exhibited resistant to amoxicillin, amoxicillin/clavulanic acid, ampicillin, co-trimoxazole, chloramphenicol, cloxacillin, penicillin, polymyxin B, and meropenem. However, the isolate was found sensitive to gentamicin,

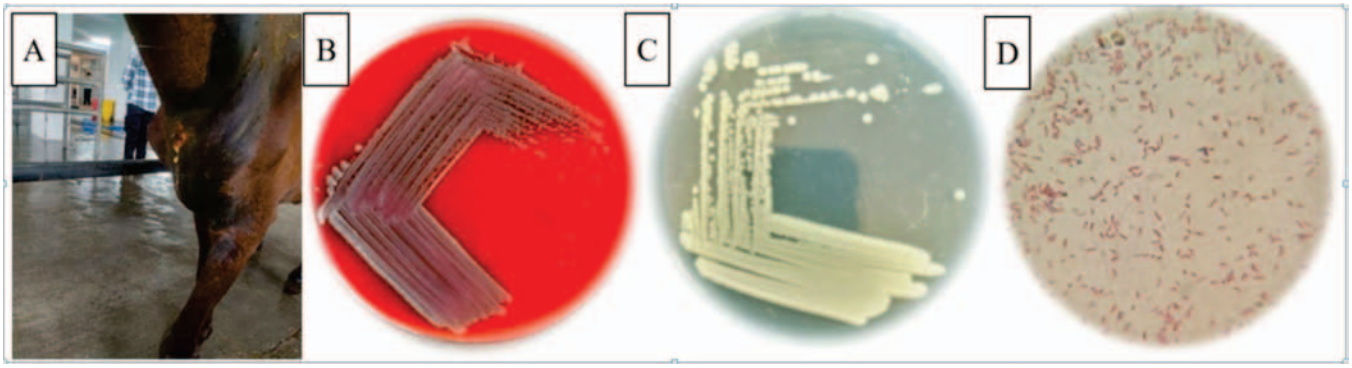

Fig. 1. (A) Purulent discharge from fistular track in the swelling at base of neck of horse; **(B)** Non-hemolytic colonies of *P. juntendi* on 5% sheep blood agar; **(C)** *P. juntendi* colony morphology on Brain Heart Infusion (BHI) agar; **(D)** Gram's stained *P. juntendi* organisms.

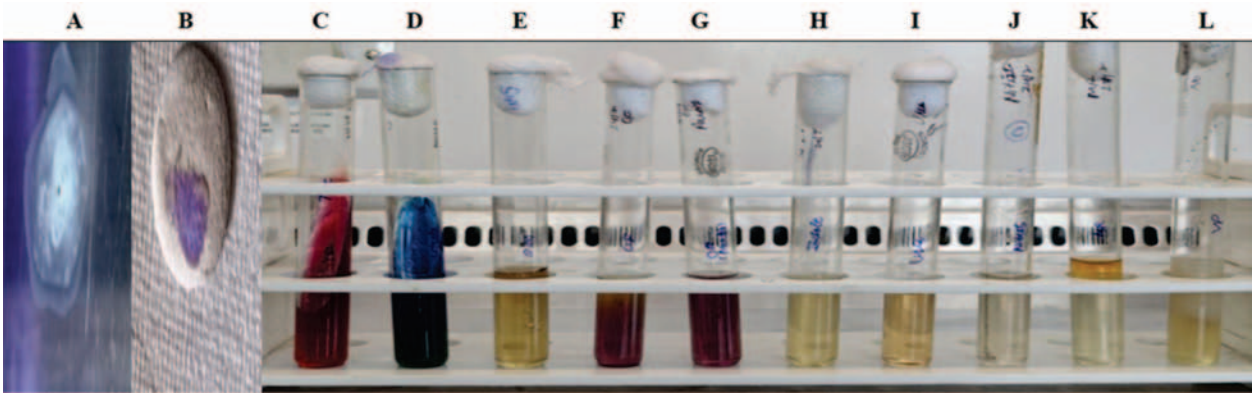

Fig.2. Biochemical characterization of *P. juntendi* **(A)** Catalase positive, **(B)** Oxidase Positive; **(C)** Triple Sugar Iron agar Negative, **(D)** Citrate Positive; **(E)** SIM: Non-motile **(E,F,G)** O/F Test: Oxidative, **(H)** Indole Negative; **(I)** Urea Negative; **(J)** Nitrate Negative; **(K)** MR Negative; **(L)** VP Negative)

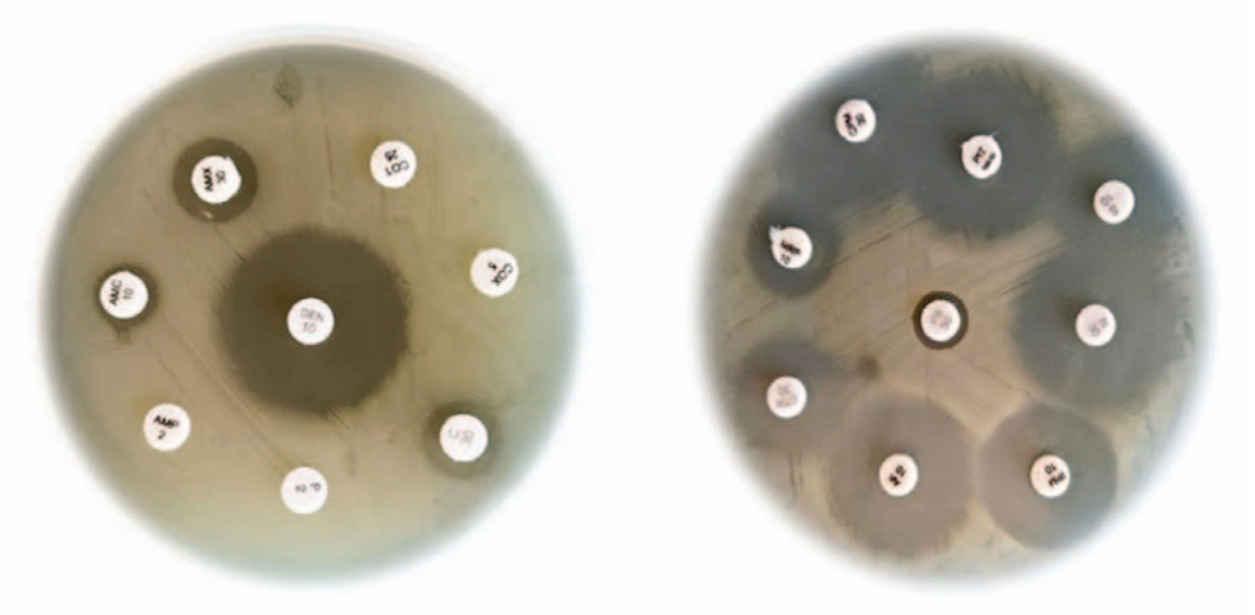

Fig. 3. Antimicrobial susceptibility testing of *P. juntendi* showing resistance to ampicillin, amoxicillin, amoxicillin/clavulanic acid, co-trimoxazole, cloxacillin, chloramphenicol, meropenem, penicillin and polymyxin B.

ceftriaxone, cefepime, streptomycin, imipenem, amikacin, piperacillin/tazobactam and neomycin.

DISCUSSION

P. juntendi is an opportunistic pathogen capable of harboring multiple antimicrobial resistance genes, contributing to persistent infections and reduced therapeutic efficacy. In the present study, pure colonies of *P. juntendi* were obtained from a suppurative lesion on the neck of a horse. The isolate showed no pigment production on BHI agar, which aligns with the previous reports indicating *P. juntendi* forms protruding colonies with smooth and regular edges, non-confluent growth and lacks pyocyanin production after overnight incubation at 37°C [5]. Gram's staining confirmed the presence of Gram-negative bacilli, consistent with in agreement with earlier findings for *Pseudomonas group*[12].

Biochemical characterization results were also consistent with previous reports[13]. Although *P. juntendi* is generally reported as motile[3], the isolate in this study was non-motile, suggesting possible phenotypic variation. Phylogenetic analysis based on 16S rRNA sequencing showed that *Pseudomonas* species comprise 13 distinct groups, including *P. putida*, *P. aeruginosa*, *P. fluorescens*, and *P. syringae*[14]. The 16S rRNA gene is widely used for bacterial identification due to the presence of conserved and variable regions[15]. BLASTn analysis revealed, 100% sequence similarity of the isolate with *P. juntendi* strain Sample 9-9 (CP125214.1) and *P. putida* strain IMV B-7289 (MZ373330.1), confirming its taxonomic affiliation.

The *P. putida* group is considered a potential reservoir for antimicrobial resistance (AMR) genes[16] and may facilitate horizontal gene transfer[17]. The isolate exhibited resistance to co-trimoxazole, cloxacillin, penicillin, amoxicillin, polymyxin B, ampicillin, amoxicillin/clavulanic acid and meropenem. It was sensitive to gentamicin, ceftriaxone, cefepime, streptomycin, imipenem, amikacin, piperacillin/tazobactam and neomycin. Based on resistance to multiple antibiotics, the isolate can be classified as multidrug-resistant[18]. The widespread antimicrobial resistance observed in *P. juntendi* may enhance its persistence and dissemination in both animal and human populations. However, this study has limitations, as the animal was not followed up for treatment outcomes. Recent reports of clinical isolates suggest that *P. juntendi* may be an emerging pathogen rather than a rare laboratory isolate.

CONCLUSION

This study identifies *P. juntendi* as a multidrug-resistant pathogen associated with pus forming abcess in horses. Further research focusing on genomic characterization and surveillance is essential to monitor its spread in animal and human populations.

ACKNOWLEDGEMENTS

The authors are thankful to the Head, Department of Veterinary Microbiology, DGCN COVAS, Palampur for providing the necessary facilities for carrying out this work.

Financial support and sponsorship: Yes

Conflict of interest: None

Use of artificial intelligence for manuscript preparation: The author confirms that there was no use of AI-assisted technology for assisting in the writing of the manuscript and no images were manipulated using AI.

REFERENCES

1. Weimer A, Kohlstedt M, Volke DC, Nikel PI, Wittmann C. 2020. Industrial biotechnology of *Pseudomonas putida*: Advances and prospects. *Appl Microbiol Biotechnol* **104:** 7745–7766.
2. Girard L, Lood C, Höfte M, Vandamme P, Rokni-Zadeh H, van Noort V, Lavigne R, De Mot R. 2021. The ever-expanding *Pseudomonas* genus: description of 43 new species and partition of the *Pseudomonas putida* group. *Microorganisms* **9:** 1766.
3. Tohya M, Watanabe S, Teramoto K, Shimojima M, Tada T, Kuwahara-Arai K, War MW, Mya S, Tin HH, Kirikae T. 2019. *Pseudomonas juntendi* sp. nov, isolated from patients in Japan and Myanmar. *Int J Syst Evol Microbiol* **69:** 3377–3384.
4. Bartlett A, Padfield D, Lear L, Bendall R, Vos M. 2022. A comprehensive list of bacterial pathogens infecting humans. *Microbiology* **168:** 001269.
5. Zheng L, Zhang X, Zhu L, Lu G, Guan J, Liu M, Jing J, Sun S, Wang Y, Sun Y, Ji X, Jiang B, Chen J, Liu J, Chen P, Guo X. 2022. A clinical *Pseudomonas juntendi* strain with blaIMP-1 carried by an integrative and conjugative element in China. *Front Microbiol* **13:** 929800.
6. Newman J N, Floyd R V, Fothergill J L. 2022. Invasion and diversity in *Pseudomonas aeruginosa* urinary tract infections. *J Med Microbiol* **71:** 001458.
7. Jiang S, Li Y, Bi K, Yang S, Xia H, Li S, Chen H, Li L. 2024. Characterization of a novel multi-resistant *Pseudomonas juntendi* strain from China with chromosomal blaVIM-2 and a mega plasmid co harboring blaIMP-1-like and blaOXA-1. *BMC Genom* **25:** 774.
8. Wulandari D, Purwaningsih D. 2019. Morphological, biochemical, and molecular identification and characterization of amylolytic bacteria in tubers of Colocasia esculenta. *JBBI* **6:** 247–258.
9. Kirby WM, Bauer AW. 1966. Antibiotic susceptibility testing by a standardized single disc method. *Am J Clin Pathol* **45:** 493–496.
10. CLSI. 2020. Performance standards for antimicrobial susceptibility testing. Clinical and Laboratory Standards Institute, Wayne, PA.
11. Miller CS, Handley KM, Wrighton KC, Frischkorn KR, Thomas BC, Banfield JF. 2013. Short-read assembly of full-length 16S amplicons reveals bacterial diversity in subsurface sediments. *PLoS One* **8(2):** e56018.
12. Thairu Y, Nasir IA, Usman Y. 2014. Laboratory perspective of gram staining and its significance in investigations of infectious diseases. *Sub Saharan Afr J Med* **1:** 168–174.
13. Mulamattathil SG, Bezuidenhout C, Mbewe M, Ateba CN. 2014. Isolation of environmental bacteria from surface and drinking water in Mafikeng, South Africa, and characterization using their antibiotic resistance profiles. *J Pathog* **2014**: 371208.
14. Peix A, Ramírez-Bahena MH, Velázquez E. 2018. The current status on the taxonomy of *Pseudomonas* revisited: an update. *Infect Genet Evol* **57:** 106–116.
15. De Souza PA, Ramos JN, Vasconcellos L, Costa LV, Forsythe SJ, Brandão MLL. 2025. Application and limitations of 16S rRNA gene sequencing for identifying WHO priority pathogenic gram-negative bacilli. *Infect Drug Resist* **18:** 6353–6375.
16. Brovedan MA, Marchiaro PM, Diaz MS, Faccone D, Corso A, Pasteran F, Viale AM, Limansky AS. 2021. *Pseudomonas putida* group species as reservoirs of mobilizable Tn402-like class 1 integrons carrying blaVIM-2 genes. *Infect Genet Evol* **96:** 105131.
17. Molina L, Udaondo Z, Duque E, Fernández M, Molina-Santiago C, Roca A, Porcel M, de la Torre J, Segura A, Plesiat P, Jeannot K, Ramos JL. 2014. Antibiotic resistance determinants in a *Pseudomonas putida* strain isolated from a hospital. *PLoS One* **9:** e81604.
18. Magiorakos AP, Srinivasan A, Carey RB. 2012. Multidrug-resistant, extensively drug-resistant and pandrug-resistant bacteria: interim standard definitions for acquired resistance. *Clin Microbiol Infect* **18:** 268–281.

Indian J. Vet. Pathol., 50(4) : 328-334, 2026: DOI: https://doi.org/10.56093/n9dm6440

RESEARCH ARTICLE

Pathomorphological and immunohistochemical studies on male genital tract tumors in dogs

P. Balaram[1], CH. Sudha Rani Chowdary[*], K. Satheesh[2], CH. Bindu Kiranmayi[3] and V. Rama Devi[4]
Department of Veterinary Pathology, NTR College of Veterinary Science, Sri Venkateswara Veterinary University, Gannavaram, Andhra Pradesh, India- 521102.
[1]M.V.Sc. Scholar; [2]Professor and Head, Department of Veterinary Pathology, C.V.Sc, Garividi; [3]Associate Professor, Department of Veterinary Public Health, [4]Professor & Head, Dept. of Veterinary Pathology, NTR CVSc, Gannavarm

***Address for correspondence**
CH. Sudha Rani Chowdary, Assistant Professor, E-mail: drsudha84@gmail.com
ORCID ID: 0000-0002-4714-5149

Received: 13.4.26; Accepted: 3.6.26

ABSTRACT

The present study was undertaken to know the occurrence of tumors in canine male reproductive tract and to study the cytology, gross and histopathology and to diagnose the origin of different neoplasms by immunohistochemistry. Tumors of the male genitalia in the present study were observed in the testes and penis. Testicular tumors included germ cell tumors, represented exclusively by seminomas (26.9%), and sex cord-stromal tumors, including Sertoli cell (19.2%) and Leydig cell tumors (7.7%). Seminomas were cytologically characterized by highly cellular smears of pleomorphic round-to-polygonal cells with prominent nucleoli and mitotic figures, while histologically presenting as either intratubular or diffuse patterns. Sertoli cell tumors exhibited moderate to highly cellular, pleomorphic cytology with vacuolated cytoplasm and prominent nucleoli, while histologically presenting as intratubular and diffuse patterns. Leydig cell tumors were characterized cytologically as clusters of polyhedral cells with vacuolated cytoplasm, eccentric nuclei, and prominent nucleoli; histologically, they displayed angiomatoid and sarcomatoid patterns with the presence of lipochrome pigment. Penile tumors exclusively comprised transmissible venereal tumors (46.2%) that were characterized by sheets of round cells with vacuolated cytoplasm and high mitotic index. IHC revealed that all tumors were negative for pancytokeratin and S100. Diffuse immunopositivity for both calretinin and vimentin was observed in seminomas, whereas Leydig cell tumors and TVTs expressed vimentin exclusively. Sertoli cell tumors demonstrated no immunoreactivity to any of the tested antibodies.

Keywords: Canine, Male reproductive tract, Leydig cell tumor, Seminoma, Sertoli cell tumor

INTRODUCTION

Shifting lifestyles and increased pet ownership have rendered dogs more susceptible to various metabolic and infectious diseases, as well as a rising incidence of neoplasms. Although robust vaccination programs have successfully mitigated many infectious threats, the lack of preventive measures for cancer has seen tumors particularly those of cutaneous and reproductive origin become a leading health concern in the canine population[1]. Indeed, genital tract tumors now rank among the most frequently diagnosed malignancies in dogs, surpassed only by skin and mammary tumors[2].

In veterinary clinical practice, tumors of the male genital tract are particularly prevalent among aging, intact populations[3]. These neoplasms primarily target the testes, prostate, and penis or prepuce, each presenting with distinct biological behaviors. For instance, testicular tumors such as Sertoli cell tumors (SCTs), seminomas, and Leydig cell tumors (LCTs) are usually benign, yet they can trigger severe paraneoplastic syndromes like hyperestrogenism. In contrast, prostatic neoplasia, most notably adenocarcinoma, is typically highly aggressive and often diagnosed at an advanced stage, carrying a guarded prognosis regardless of castration status. Furthermore, the canine transmissible venereal tumor (CTVT) represents a unique oncological entity: a physically transmissible clonal cell line affecting the external genitalia[1]. Consequently, a thorough understanding of the histopathological diversity and clinical progression of these various tumors is essential for effective diagnosis and management.

How to cite this article: Balaram, P., Chowdary, S.R., Satheesh, K., Kiranmayi, B. and Rama Devi, V. 2026. Pathomorphological and immunohistochemical studies on male genital tract tumors in dogs. . Indian J. Vet. Pathol., 50(4) : 328-334.

Given the clinical significance and histopathological diversity of these conditions, the present study was conducted to provide a comprehensive analysis of the occurrence of different male genital tract tumors in dogs in and around the Vijayawada region.

MATERIALS AND METHODS

A total of 26 male genital tract tumors were included in the study that were sourced from the Veterinary Clinical Complex

(VCC), NTR College of Veterinary Science, Gannavaram, Super Speciality Veterinary Hospital (SSVH), Animal Birth Control centre and various local private clinics in and around Vijayawada.

Diagnostic samples were obtained by fine-needle aspiration (FNA) and touch impression for cytological evaluation. For histopathological and immunohistochemical analysis, representative excisional biopsies were preserved in 10% neutral buffered formalin. Tissue samples fixed in 10% neutral buffered formalin were processed using standard paraffin embedding techniques. Sections of 4 micron thickness were then cut and stained with Hematoxylin and Eosin (H&E) according to the methods described by Bancroft and Cook[4].

Immunohistochemical staining was performed on 4 micron thick sections mounted on positively charged slides (BioGenex, USA) using a Super Sensitive Polymer-HRP detection system. Following deparaffinization in xylene and rehydration through graded ethanol, antigen retrieval was conducted in 0.01M citrate buffer (pH 6.0) using a pressure cooker for 20 minutes. Endogenous peroxidase activity was quenched with 3% hydrogen peroxide (Peroxide Block™, BioGenex) for 20 minutes, followed by a 10 - minute incubation with Power Block™ (BioGenex) to minimize non-specific binding. Sections were incubated with primary antibodies (Biogenex, USA) including pancytokeratin, vimentin, calretinin and S100 for 60 minutes at room temperature. Signal amplification was achieved using Super Enhancer™ (20 min) and Polymer-HRP reagent (30 min). Immunoreactivity was visualized using 3,3'-Diaminobenzidine (DAB) chromogen. Finally, sections were counterstained with Harris Hematoxylin and mounted with DPX. Negative controls were maintained by omitting the primary antibody.

RESULTS

In this study, 26 out of 411 canine tumor biopsies (6.5%) were identified as male reproductive tract neoplasms involving testes and penis (Table 1). The study did not record any tumors in the prostate gland. The testicular tumors consisted of germ cell tumors (seminoma) and sex-cord stromal tumors (Sertoli and Leydig cell tumors), whereas the penile tumors were exclusively TVTs. Among all the histological types of male reproductive tract tumors, the highest occurrence was observed in the penis, consisting entirely of TVTs at 46.2% followed by seminomas at 26.9% and SCTs at 19.2%. The least frequent histological type recorded was the LCT, which accounted for 7.7% of the total male reproductive tract neoplasms. On immunohistochemistry, none of the tumors revealed positive staining to cytokeratin and S100 antibodies (Table 2).

The pathological features of different histological types of male canine reproductive tract tumors identified in the present study are detailed in separate sections.

Seminoma

In the present study, seminomas were unilateral in a few cases and bilateral in majority of the cases. In all the cases, they were associated with cryptorchidism. On gross examination, the affected testes were irregular in shape, markedly enlarged and measured approximately 4-7 cm in diameter. Cut sections revealed bulging, homogeneous masses that were grayish white to pale cream in colour. The tumor masses exhibited a soft to firm, fleshy consistency and a lobulated appearance (Fig. 1). Cytological smears were highly cellular, featuring discrete round-to-polygonal cells arranged individually or in loose clusters. These cells exhibited indistinct borders, pale-to-basophilic cytoplasm, and large, central nuclei with prominent nucleoli. Significant anisokaryosis and moderate pleomorphism were also observed. On histopathological examination, two different types of seminomas were observed in the present study *viz.* intratubular and diffuse forms. In intratubular seminoma, the seminiferous tubules were filled with proliferating neoplastic germ cells replacing the normal spermatogenic and Sertoli cells. In the diffuse type, the neoplastic cells were arranged in large sheets that infiltrated into the testicular parenchyma. The stroma often showed large infiltrates of lymphocytes. The neoplastic cells were large, round to polyhedral with distinct cell borders and clear to granular eosinophilic to amphophilic cytoplasm. The nuclei were single to multiple, centrally located, round and vesicular with prominent nucleoli. The tumor occasionally exhibited giant cells with abundant cytoplasm

Table 1. Histological classification of male reproductive tract tumors (n=26).

Anatomical Site	Histological Type	Number of cases	Occurrence (%)
Testis	Seminoma (SEM)	7	26.9
	Sertoli cell tumor (SCT)	5	19.2
	Leydig cell tumor (LCT)	2	7.7
Penis	Transmissible Venereal Tumor (TVT)	12	46.2

Table 2. Immunohistochemical characterization of male reproductive tract tumors.

Antibody	SEM	SCT	LCT	TVT
Cytokeratin	-	-	-	-
Vimentin	+	-	+	+
Calretinin	+	-	-	-
S100	-	-	-	-

and mitotic figures. In a few foci atypical mitotic figures appeared as filamentous chromatin, the spiremes. The neoplastic sheets often showed individual necrosis of cells giving the "starry - sky" appearance (Fig.2). In a few cases, tumor emboli were noticed in the vascular spaces.

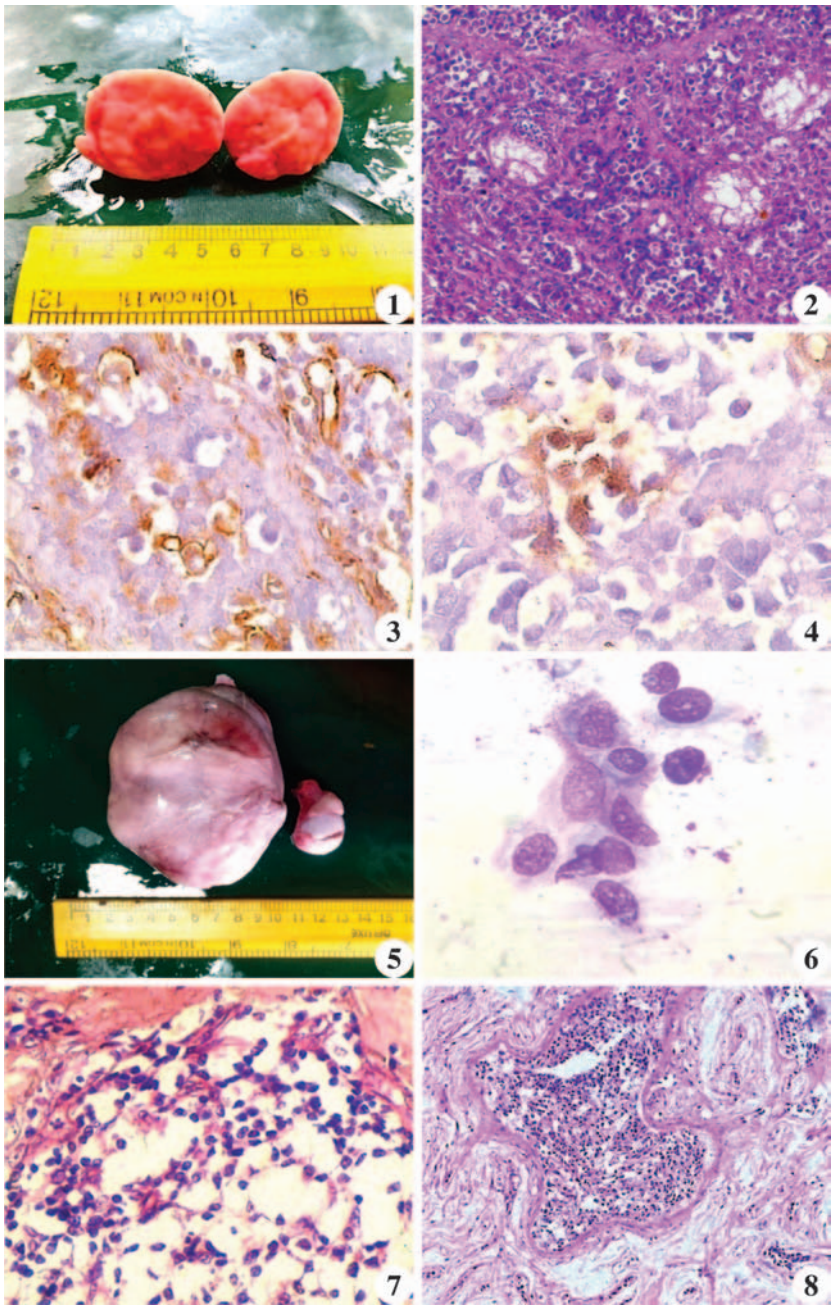

Fig.1. Seminoma - Lobulated, grayish white cut surfaces; **Fig.2.** Diffuse seminoma - Section showing "starry sky appearance" with sheets of neoplastic germ cells. H&E x100; **Fig.3.** Seminoma: IHC, vimentin - Note a moderate to intense cytoplasmic expression in the neoplastic germ cells x400; **Fig.4.** Seminoma: IHC, calretinin - Section showing a focal area of intense cytoplasmic and nuclear expression in the neoplastic cells x400; **Fig.5.** Sertoli cell tumor - Affected testes showing severe enlargement compared to the normal testes; **Fig.6.** Sertoli cell tumor - Cytology showing a cluster of pleomorphic cells with prominent nucleoli. Leishman's stain x1000; **Fig.7.** Intratubular Sertoli cell tumor - Section showing neoplastic cells forming microcystic pattern. H&E x400; **Fig.8.** Intratubular Sertoli cell tumor - Section showing sclerosing pattern with severe hyalinising stroma. H&E x100

On IHC, seminomas revealed moderate cytoplasmic positivity for vimentin (Fig. 3) and multifocal intense cytoplasmic and nuclear positivity for calretinin (Fig. 4).

Sertoli cell tumor

In the present study, SCTs were majorly observed in cryptorchid testes. The tumors were unilateral and the affected testes were enlarged and distorted in shape while the contralateral testes showed severe atrophy (Fig. 5). The tumors measured about 5 - 9 cm in diameter and were firm in consistency. On cut sections, the tumors were lobulated, solid, gray to tan in colour with foci of haemorrhages. Cytological smears of SCTs revealed moderate to high cellularity with moderate pleomorphism, predominantly large and arranged as clusters. The cells were irregular to elongated and polygonal in shape, with indistinct cell borders and a moderate amount of pale to slightly basophilic cytoplasm containing fine vacuoles (Fig. 6). The nuclei were round to oval and generally centrally placed. Nuclear chromatin was finely granular with one or more prominent nucleoli. Histologically, two forms *viz.* intratubular and diffuse patterns were recorded. The intratubular Sertoli cell tumors displayed different architectures that included microcystic, palisading, whorling and sclerosing patterns. In the microcystic pattern, the neoplastic cells formed back to back, small cystic spaces (Fig. 7), while in the palisading pattern, the neoplastic cells were parallel to each other and perpendicular to the seminiferous tubules. In the whorling pattern, the neoplastic cells formed whorls, while in the sclerosing pattern, the neoplastic cells were arranged within the tubules as nests with a huge intertubular hyalinising fibrous connective tissue (Fig.8). The Sertoli cells exhibited moderate degree of pleomorphism and were slender, round to elongated and triangular in shape with pale, eosinophilic to vacuolated cytoplasm and indistinct cell borders. A few cells contained lipochrome granules in the cytoplasm. The nuclei were hyperchromatic, oval to elongated and central to eccentrically located with

finely stippled chromatin. The diffuse form of Sertoli cell tumor was characterized by sheets of small to large, slender to oval and triangular shaped cells with eccentric nuclei and eosinophilic cytoplasm. In a few foci, the tumor cells formed multicellular spheres (Fig. 9), whorls and microcystic structures. The stroma was minimal to moderate and often appeared hyalinised with infiltration of lymphocytes. In a few foci, the tumor parenchyma exhibited necrosis, infiltration of neutrophils and vascular invasion. On IHC, the neoplastic Sertoli cells did not exhibit positivity for any of the antibodies used.

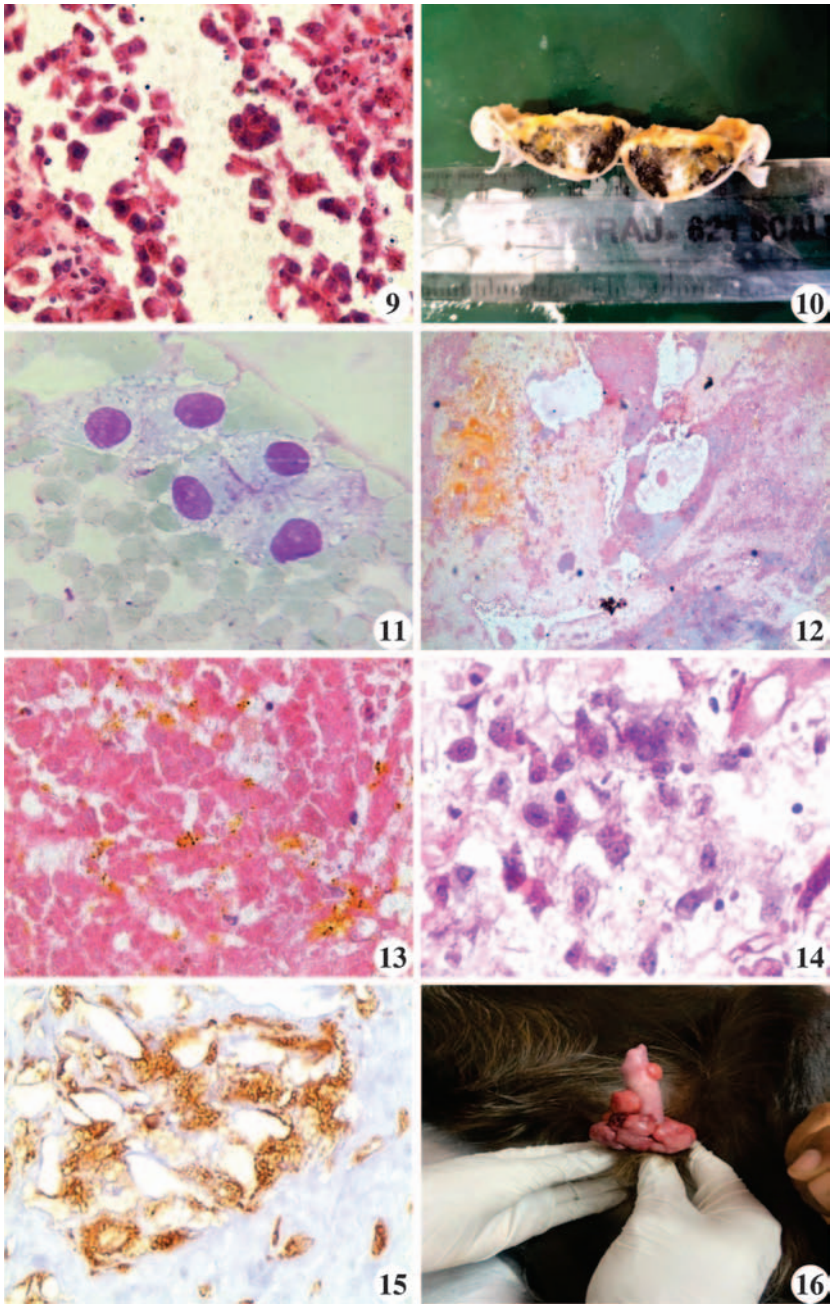

Fig. 9. Diffuse Sertoli cell tumor - Section showing neoplastic multicellular spheres. H&E x400; **Fig. 10.** Leydig cell tumor - Yellowish brown, fleshy cut surfaces showing foci of hemorrhage and necrosis; **Fig. 11.** Leydig cell tumor - An impression smear showing polyhedral cells with eccentric nuclei and vacuolated cytoplasm. Leishman's stain x1000; **Fig. 12.** Angiomatoid Leydig cell tumor - Section showing vascular spaces filled with proteinaceous fluid amidst solid areas of neoplasm. H&E x100; **Fig. 13.** Angiomatoid Leydig cell tumor - Section showing multifocal deposition of golden yellow lipochrome pigment amidst neoplastic Leydig cells. H&E x400; **Fig. 14.** Diffuse Leydig cell tumor - Section showing loose clusters of pleomorphic Leydig cells within a hyalinised stroma. H&E x400; **Fig. 15.** Leydig cell tumor: IHC, vimentin - Note intense cytoplasmic positivity in the neoplastic Leydig cells x400; **Fig. 16.** TVT: Nodular to cauliflower like masses on the entire length of penis.

Leydig cell tumor

LCTs were unilateral and occurred in the scrotal testes. Grossly, the tumors distorted the shape and size of the affected testes. The tumors measured about 3 - 5 cm in diameter and were irregular in shape. On sectioning, the tumors were solid and firm, golden brown to dark in colour. The cut surfaces were fleshy with focal areas of necrosis, hemorrhage and displayed multiple cystic spaces (Fig. 10). Cytological smears revealed presence of loose clusters of polyhedral cells with finely vacuolated to granular cytoplasm. The nuclei were eccentrically placed exhibiting coarse chromatin and prominent nucleoli (Fig. 11). Histologically, two types of LCTs were observed in the present study that included an angiomatoid and a diffuse type. The angiomatoid LCT was characterized by the presence of large vascular spaces filled with erythrocytes and proteinaceous fluid amidst nests and cords of neoplastic cells (Fig. 12). The neoplastic Leydig cells were large, round to polyhedral in shape with an abundant eosinophilic cytoplasm and central to eccentrically placed nuclei. The tumor also displayed abundant sclerosing stroma and multifocal deposition of golden yellow lipochrome pigment (Fig. 13) that was negative for Perl's stain. In the diffuse type of LCT, the neoplastic cells were arranged in loose clusters separated by abundant hyalinised matrix (Fig. 14), while in a few foci, they assumed sarcomatoid architecture. In those foci with clusters, the cells were large, pleomorphic, oval to polyhedral in shape with vacuolated to granular cytoplasm. The nuclei were large, vesicular, central to eccentric with a single, small, basophilic nucleolus. In those foci with sarcomatoid

architecture, the cells were elongated to fusiform and arranged in bundles, with an abundant eosinophilic cytoplasm, vesicular nuclei containing multiple nucleoli and indistinct cell borders. Occasionally, the cells contained lipochrome pigment. On immunohistochemistry, LCTs demonstrated intense cytoplasmic positivity to vimentin (Fig. 15).

Transmissible venereal tumor (TVT)

TVTs were recorded on the external genitalia of males. Grossly, tumors were multiple, nodular and fleshy. They occurred on the entire length of the penis in male dogs (Fig.16) and at the base of the penis, the tumors were larger and multinodular to cauliflower in shape.

Impression smears exhibited two cell types: lymphocytoid cells (Fig. 17), which were round to polyhedral with a high nuclear-to-cytoplasmic ratio, scant vacuolated cytoplasm, and prominent nucleoli, and plasmacytoid cells (Fig. 18), which were oval with abundant vacuolated cytoplasm and an eccentrically placed hyperchromatic nucleus. Mitotic figures are frequently seen in both patterns. Histopathologically, the tumor showed densely packed round to polyhedral cells in sheets with delicate fibrovascular stroma. Cells exhibited eccentric nuclei with prominent nucleoli, frequent mitoses (Fig. 19), vacuolated cytoplasm, and focal hemorrhage and necrosis. IHC showed diffuse mild to moderate cytoplasmic vimentin positivity in the tumor cells (Fig. 20).

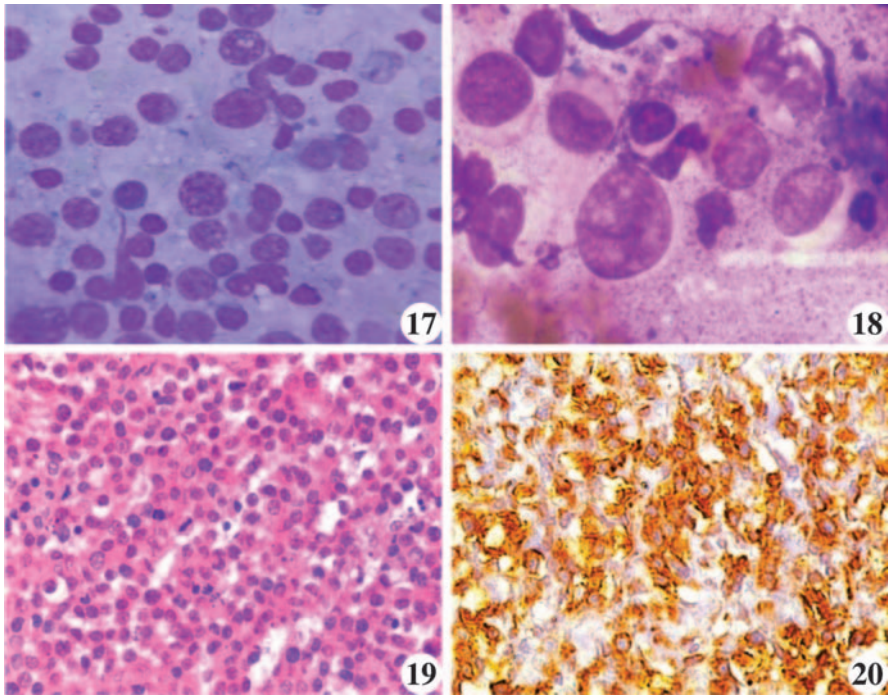

Fig. 17. TVT: An impression smear showing pleomorphic, round to oval cells with coarse chromatin and cytoplasmic vacuolation. Leishman's stain x1000; **Fig. 18.** TVT: an impression smear showing anisocytic plasmacytoid cells with eccentric nuclei. Leishman's stain x1000; **Fig.19.** TVT: Section showing sheets of round cells with mitotic figures. H&E x400; **Fig. 20.** TVT: IHC, vimentin - Section showing strong cytoplasmic immunostaining x400

DISCUSSION

In the present study, tumors were observed affecting the testes and penis of the male genital tract in dogs. The susceptibility of testes to tumors in geriatric, intact dogs, is exacerbated by conditions such as cryptorchidism, which increases the likelihood of tumor development by 9 to 14-fold[5]. The present study did not record prostatic tumors, although earlier reports[6,7] have documented prostatic tumors, that typically represented less than 1% of all canine neoplasms and roughly 5% of all prostatic diseases. In the present study, the sample size was smaller and could be one of the reasons for absence of prostatic tumors. Furthermore, because prostatic tumors are often internal and present with non-specific clinical signs, they may be unnoticed by the owners and may not be presented for diagnosis.

In the present study, testicular neoplasms consisted of seminomas (26.9%), followed by SCTs and LCTs. While the findings in the present study are in accordance with that of earlier reports[8,9] in identifying seminoma as the most frequent type, they contrast with that of a few studies[10,11,12] that reported a higher prevalence of Leydig cell tumors. Additionally, rare types like mixed germ cell-sex cord stromal tumors and hemangiosarcomas, noted by earlier authors[8,13], were not observed in this study.

The gross and microscopic morphology of seminomas in the present study aligns with the findings of previous reports. Key microscopic features, such as lymphocytic infiltration, "starry sky" patterns, and high mitotic indices, were consistent with established literature[14]. Although canine seminomas typically exhibit low metastatic potential, the vascular invasion observed in diffuse seminoma in the present study serves as a significant prognostic indicator of malignancy.

The majority of SCTs in this study were found in cryptorchid testes consistent with earlier reports[15, 16]. Cytologically, the tall columnar to polygonal cells with vacuolated cytoplasm mirrored features described by earlier finding[17]. Histologically, both intratubular and diffuse forms exhibited severe desmoplasia and stromal

hyalinization, highlighting the dynamic interaction between tumor cells and connective tissue[18]. In the present study, an interesting finding in diffuse SCTs was the presence of multicellular spheres. Because the diffuse type also demonstrated vascular invasion, these spheres may play a critical role in vascular invasion and metastasis.

LCTs in this study presented as solid, golden-brown scrotal masses, consistent with the earlier findings[19]. Cytological analysis showed dyscohesive, vacuolated cells, while histology revealed angiomatoid and diffuse sarcomatoid patterns. Angiomatoid type of Leydig cell tumor has been rarely reported in the literature. The characteristic golden-yellow lipochrome pigment observed in the neoplastic Leydig cells reflects intense steroidogenesis and lipid peroxidation[20].

TVTs represented the most common male canine genital neoplasm in this study. This high occurrence is likely attributed to the sample source, an Animal Birth Control centre handling free-roaming street dogs. The unrestricted sexual behaviour of these free-range dogs facilitates the transmission of TVTs, thereby elevating their occurrence in the study. The gross, cytological and histopathological findings of canine TVTs in the present study are consistent with previous reports[21,22,23].

Despite existing studies on canine testicular tumor markers, the relatively sparse data available presently hinders their implementation as diagnostic tools[24]. In the present study, to characterize the tumors, a panel of antibodies including pancytokeratin, vimentin, S100 and calretinin were utilized for immunohistochemical analysis. All evaluated tumors in this study lacked pancytokeratin and S100 expression, ruling out an epithelial or neuroectodermal origin. Regarding calretinin, seminomas in the present study demonstrated multifocal positivity, whereas Leydig and Sertoli cell tumors showed no expression. As calretinin expression is typically observed in steroid-hormone-producing cells, this protein has been postulated as a marker for the secretory activity of testicular tumors[25]. Radi and Miller[26] documented variable calretinin expression across all canine testicular tumor types, which contrasts sharply with human studies, where LCTs are the sole testicular neoplasms expressing this protein[25]. However, the usefulness of calretinin for diagnosis is limited because its expression is not consistent in all cases[27].

In this study, vimentin expression was recorded in seminomas, LCTs and TVTs. Although traditionally a marker of mesenchymal origin, as confirmed by the intense immunolabeling in our LCT and TVT cases, vimentin is also a hallmark of epithelial-mesenchymal transition (EMT), which promotes tumor invasion and metastasis. Our findings partially align with an earlier study[28] that observed vimentin expression across all three tumor types and noted that its overexpression contributes to localized canine testicular tumor invasion

In conclusion, the present study revealed gross, cytological, histopathological and immunohistochemical features of canine male reproductive tract tumors in the study area.

Financial support & sponsorship*:* None

Conflict of interest : None

Use of artificial intelligence (AI)-assisted technology for manuscript preparation: The authors confirm that there was no use of AI-assisted technology for assisting in the writing of the manuscript and no images were manipulated using AI.

REFERENCES

1. Brodzki P, Wolniaczyk K, Głodkowska K and Brodzki N. 2023. Tumors of the reproductive system of bitches based on the description of selected own clinical cases and literature data. *Med Weter 79***(7)**: 334–344.
2. Baioni E, Scanziani E, Vincenti M C, Leschiera M, Bozzetta E, Pezzolato M and Ru G. 2017. Estimating canine cancer incidence: findings from a population-based tumour registry in northwestern Italy. *BMC Veterinary Research* **13(1)**: 203.
3. Valli VE, Bienzle D and Meuten DJ. 2017. Tumors of the hemolayphatic system. In: Meuten DJ, eds. Tumors in domestic animals, NC, USA: John Wiley & Sons, Inc. 203-295.
4. Bancroft DJ and Cook CH. 1994. Fundamentals of normal histology and histopathology. In: Manual of histopathological techniques and their diagnostic application, Edinburgh: Churchill Livingstone: 1-17.
5. Ciaputa R, Nowak M, Kiełbowicz M, Antończyk A, Błasiak K and Madej J A. 2012. Seminoma, sertolioma, and leydigoma in dogs: clinical and morphological correlations. *Bull Vet Inst Pulawy* **56(3)**: 361-367.
6. Leroy B E and Northrup N. 2009. Prostate cancer in dogs: comparative and clinical aspects. *Vet J* **180(2)**: 149-162.
7. Vasilatis D M and Ghosh P M. 2024. Clinicopathologic characterization of prostatic cancer in dogs. *Animals* **14(4)**: 588.
8. Catoi C, Moussa R, Bolfa P, Taulescu M and Negrea O 2008. Morphological study of testicular tumors in dogs. *Lucr Şt Med Vet* **41**:100-105.
9. Svara T, Gombac M, Pogorevc E, Plavec T, Zrimsek P and Pogačnik, M. 2014. A retrospective study of canine testicular tumours in Slovenia. *Slov Vet Res* **51(2)**: 81-88.
10. Nielsen S W and Lein D H. 1974. Tumours of the testis. *Bull World Health Organ* **50(1-2)**: 71-78.
11. Manuali E, Forte C, Porcellato I, Brachelente C, Sforna M, Pavone S and Mechelli L. 2020. A five-year cohort study on testicular tumors from a population-based canine cancer registry in central Italy (Umbria). *Prev Vet Med* **185:** 105201.
12. Gazin A A, Vatnikov Y A, Sturov N V, Kulikov E V, Grishin V, Krotova E A and Lisitskaya K V. 2022. Canine testicular tumors: An 11-year retrospective study of 358 cases in Moscow Region, Russia. *Vet World* **15(2)**: 483.
13. Liao A T, Chu P Y, Yeh L S, Lin C T and Liu C H. 2009. A 12-year retrospective study of canine testicular tumors. *J Vet Med Sci* **71(7)**: 919-923.
14. Ramesh S, Vijayendran V, Balakumar A and Kumar V. 2025. Cytological diagnosis of seminoma in dog. *Indian J Vet*

Pathol **49(3)**: 250-253.
15. Masserdotti C, Bonfanti U, De Lorenzi D, Tranquillo M and Zanetti O. 2005. Cytologic features of testicular tumours in dog. *J Vet Med A* **52(7)**: 339-346.
16. Chang A, Lee P, Smith J and Yang K 2022. Cytologic and histopathologic features of an extratesticular Sertoli cell tumor with Call-Exner-like bodies in a castrated dog. *J. Vet Diagn Invest 34***(3)**: 123–129.
17. Silva G M, De Oliveira IC, De Toledo RS, Bezerril J E, Vasques G M B, Gasser B and Romani I. 2021. Seminoma and sertolioma in non-cryptorchid dog–case report. *Acta Vet Bras* **15(4)**: 296-300.
18. Finazzi M and Cammarata G. 1981. Histopathologic observations on Sertoli cell tumors in dog. *Tumori*, **67(5)**: 391–398.
19. Kudo T, Kamiie J, Aihara N, Doi M, Sumi A, Omachi T, and Shirota K. 2019. Malignant Leydig cell tumor in dogs: two cases and a review of the literature. *J Vet Diagn Invest* **31(4)**: 557-561.
20. Handa U, Sood T, Punia R S. 2010.Testicular Leydig cell tumor diagnosed on fine needle aspiration. *Diagn Cytopathol* **38(9)**: 682–684.
21. Ajayi O L, Oluwabi M, Ajadi R A, Antia R E, Omotainse S O, Jubril A J, and Makinde A F. 2018. Cytomorphological, histopathological and immunohistochemical observations on the histiocytic origin of canine transmissible venereal tumour. *Sokoto J Vet Sci* **16(2)**: 10-20.
22. Thangathurai R, Balasubramaniam G A, Dharmaceelan S, Balachandran P, Srinivasan P, Sivaseelan S and Manohar B M. 2008. Cytological diagnosis and its histological correlation in canine transmissible venereal tumour. *Vet Arh* **78(5):** 369–376.
23. Ucar M. 2016. Transmissible venereal tumor: a review. *Kocatepe Vet J* **9(3):** 230-235.
24. Yu C H, Hwang D N, Yhee JY, Kim JH, Im K S, Nho W G and Sur J H. 2009. Comparative immunohistochemical characterization of canine seminomas and Sertoli cell tumors. *J Vet Sci* **10(1):** 1-7
25. Ciaputa R, Nowak M, Madej JA, Poradowski D, Janus I, Dziegiel P and Kandefer-Gol, M. 2014. Inhibin-α, E-cadherin, calretinin and Ki-67 antigen in the immunohistochemical evaluation of canine and human testicular neoplasms. *Folia Histochemica et Ccytobiologica* **52(4):** 326-334.
26. Radi ZA and Miller D L.2005. Immunohistochemical expression of calretinin in canine testicular tumours and normal canine testicular tissue. *Res Vet Sci* **79(2):** 125-129.
27. OwstonMA, and Ramos-Vara JA 2007. Histologic and immunohistochemical characterization of a testicular mixed germ cell sex cord-stromal tumor and a leydig cell tumor in a dog. *Vet Pathol*, **44(6)**: 936-943.
28. de BarrosM D, Dos Santos Batista B P, Amaral C B, da Silva Leite J and Ferreira A M R. 2025. Vimentin expression in canine testicular tumors: a local invasion predictive biomarker. *Biotechnic & Histochemistry* **100(4):** 208-215.

Indian J. Vet. Pathol., 50(4) : 335-338, 2026: DOI: https://doi.org/10.56093/6m5yzy72

RESEARCH ARTICLE

Assessment of fracture healing in dogs based on the evaluation of haemato-biochemical parameters

CH V. Surya Lakshmi, G. Vani*, R.V. Suresh Kumar and P. Amaravathi[1]
Department of Veterinary Surgery and Radiology, College of Veterinary Science, Sri Venkateswara Veterinary University, Tirupati, Andhra Pradesh, India
[1]Assistant Professor, Department of Veterinary Pathology

***Author for correspondence**
Dr. G. Vani, E-mail: vanigaddam.vet@gmail.com
ORCID ID: 0000-0002-2164-189X

Received: 24.5.26; Accepted: 25.6.26

ABSTRACT

The purpose of this research is to assess the fracture healing in long bones in dogs based on the haemato-biochemical parameters. All the 18 dogs with long bone fractures were stabilized with intramedullary pinning. Six dogs (Group I) received no grafting material., whereas in Group II and Group III, platelet rich fibrin and CAD-MSCs were inspissated at the fracture site after stabilization. Haematological parameters like haemoglobin (Hb), packed cell volume (PCV), leukocyte, neutrophil, platelets, differential leukocyte count and serum biochemical parameters like calcium, phosphorous and alkaline phosphatase was evaluated in all the animals on 0, 15th, 30th, 45th, and 60th post-operatively. The mean haemoglobin and PCV values in dogs were statistically significant within the groups and also between the groups I & II and I & III. Group III animals showed a significant gradual reduction in leukocyte and neutrophil counts post-operatively compared to groups I, indicating effective immunomodulation and favourable healing dynamics in mesenchymal cell treated group. A significant increase in serum calcium levels was observed in all the groups from 0 day to 30th day, followed by significant decrease on 45th day in group III. However, the calcium values differed significantly within the groups and between the groups I & II and I & III. A significant difference of alkaline phosphatase values was recorded within the groups and between the groups I & II and I &III. Alterations in serum calcium and alkaline phosphatase levels corresponded with osteoblastic activity and mineralization at the fracture site.

Keywords: Dogs, Fracture, Intramedullary pinning, Mesenchymal stem cells, Platelet rich fibrin

INTRODUCTION

Fracture healing in dogs is a complex biological process influenced by fracture characteristics, stabilization method, local biological factors, and postoperative care. Early identification of complications such as infection, inflammation, and delayed bone healing is essential for optimal clinical outcomes. Haematological parameters, including haemoglobin (Hb) concentration, total leucocyte count (TLC), and neutrophil percentage, are routinely assessed as indicators of systemic inflammation and postoperative recovery following fracture stabilization. While fracture union is commonly evaluated through clinical and radiographic methods, biochemical markers allow more sensitive assessment of bone resorption and formation over shorter time intervals.

Serum biochemical markers of bone metabolism particularly alkaline phosphatase, calcium, and phosphorus, provide important insights into osteoblastic activity, mineralization, and the progression of bone healing. Evaluation of these parameters enables objective monitoring of biological events during different phases of fracture repair.

MATERIALS AND METHODS

The study was conducted on dogs presented with long-bone fractures to the Teaching Veterinary Clinical Complex and Department of Veterinary Surgery & Radiology, over a period of 18 months (May 2023 to October 2024). A total of 18 dogs of varying age, sex, and breed were included based on clinical and radiographic confirmation of fractures and divided into three groups of six animals in each group.

How to cite this article: Surya Lakshmi, CH V., Vani, G., Suresh Kumar, R.V. and Amaravathi, P. 2026. Assessment of fracture healing in dogs based on the evaluation of haemato-biochemical parameters. Indian J. Vet. Pathol., 50(4) : 335-338.

GROUP I:

Animals were subjected to open reduction and the fractured bone was stabilized with stainless steel intramedullary plain pin or positive profile end threaded pinning technique.

GROUP II:

Animals were subjected to open reduction and the fractured bone was stabilized with stainless steel intramedullary plain pin or positive profile end threaded pin and autogenous Platelet Rich Fibrin (PRF) was deposited into the fracture site intra operatively.

GROUP III:

Animals were subjected to open reduction and the fractured bone was stabilized with stainless steel intramedullary plain pin or positive profile end threaded pin and allogenic canine adipose tissue derived mesenchymal stem cells (CAD-MSc) was deposited into the fracture site intra operatively.

All dogs were subjected to detailed pre-operative clinical and orthopaedic examination, which included recording of temperature, pulse, and respiration, assessment of lameness, pain, weight bearing, fracture location and type, presence of crepitus, limb deformity, soft tissue involvement, neurovascular status, and evidence of inflammation or infection at the fracture site.

Pre-operative haematological and biochemical investigations were performed on the day of presentation. Blood samples were collected aseptically for estimation of haemoglobin, packed cell volume, total and differential leukocyte counts, and platelet count, while serum samples were analysed for calcium, phosphorus, and alkaline phosphatase.

The treatment in three groups was evaluated clinically and biochemically on 0, 15th, 30th,45th and 60th post-operative days. Data obtained from clinical, haematological and biochemical evaluations were analysed using appropriate statistical tests (ANOVA). Differences were considered statistically significant at $p < 0.05$.

RESULTS & DISCUSSION

In this study, blood samples were collected on 0, 15th, 30th, 45th, and 60th post-operative days to measure haemoglobin, packed cell volume, total leukocyte count, differential leukocyte count, platelet count and serum levels of calcium, phosphorus, and alkaline phosphatase.

The mean haemoglobin and PCV values in dogs were statistically significant within the groups and also between the groups I & II and I & III. All the values were within the normal physiological range. The progressive rise in haemoglobin values may be attributed to erythropoiesis[1,2,3].

The total leucocyte count in the present study was decreased significantly within the groups and non-significantly between the groups, and the values were within the normal physiological range. This was due to significant reduction of inflammation. Post-operative leukocytopenia may be due to gradual decrease in inflammatory reaction and stress resolution[1]. In this study, higher leukocyte counts on the pre-operative day could be attributed to systemic inflammatory changes following the fracture[3,4,5,6.]

In the present study, the neutrophil count decreased significantly within the groups and also between the groups I & III and non-significant decrease in group I & II, indicating reduced inflammation and infection. The reduced neutrophil count in group II and III compared to group I may be attributed to fact that biomaterials used at the fracture site reduces inflammatory response[1,6].

In our study, group III animals showed a significant gradual reduction in leukocyte and neutrophil counts post-operatively compared to groups I. This can be attributed to the anti-inflammatory effects of mesenchymal stem cells, which shifted the tissue environment from a pro- inflammatory to an anti-inflammatory state[7,8,9], ultimately promoting bone regeneration by reducing the inflammatory phase and thus suppressing the inflammatory response[10,11].

Leucocytosis with neutrophilia is generally observed during the initial stage of inflammation, likely due to fracture-related stress, muscle damage, hematoma, or infection[1,6,12,13]. In our current investigation, all the

Table 1. Biochemical parameters (mean + SE) in the pre- and post-operative period in group I, II & III

S. No.	Parameters	Groups	Time Intervals					
			0th Day	15th Day	30th Day	45th Day	60th Day	Overall mean
1.	Calcium (mg%)	Group I	$8.18^{a}\pm0.19$	$8.55^{ab}\pm0.042$	$9.06^{c}\pm0.07$	$8.70^{bc}\pm0.06$	$8.43^{ab}\pm0.07$	$8.59^{A}\pm0.06$
		Group II	$8.15^{a}\pm0.25$	$9.03^{b}\pm0.08$	$10.05^{c}\pm0.18$	$9.56^{bc}\pm0.12$	$9.25^{b}\pm0.09$	$9.21^{B}\pm0.13$
		Group III	$8.03^{a}\pm0.16$	$9.15^{b}\pm0.08$	$10.53^{d}\pm0.16$	$9.81^{c}\pm0.07$	$9.45^{bc}\pm0.04$	$9.40^{B}\pm0.16$
2.	Phosphorus (mg%)	Group I	$5.15^{a}\pm0.02$	$5.23^{a}\pm0.04$	$5.25^{a}\pm0.02$	$5.21^{a}\pm0.04$	$5.16^{a}\pm0.05$	$5.20^{A}\pm0.01$
		Group II	$5.18^{a}\pm0.03$	$5.26^{a}\pm0.03$	$5.33^{a}\pm0.03$	$5.26^{a}\pm0.04$	$5.20^{a}\pm0.03$	$5.25^{A}\pm0.01$
		Group III	$5.15^{a}\pm0.03$	$5.26^{a}\pm0.03$	$5.36^{a}\pm0.04$	$5.30^{a}\pm0.05$	$5.23^{a}\pm0.04$	$5.26^{A}\pm0.02$
3.	Alkaline phosphatase (U/L)	Group I	$97.50^{ab}\pm1.47$	$101.50^{c}\pm0.22$	$99.33^{bc}\pm0.55$	$98.83^{bc}\pm0.47$	$95.33^{a}\pm0.61$	$98.50^{A}\pm0.50$
		Group II	$97.00^{a}\pm1.15$	$110.50^{b}\pm1.72$	$108.50^{b}\pm1.72$	$106.58^{b}\pm1.24$	$96.00^{a}\pm0.68$	$103.77^{B}\pm1.25$
		Group III	$97.33^{a}\pm1.08$	$115.50^{c}\pm2.04$	$109.16^{b}\pm1.79$	$106.83^{b}\pm0.47$	$96.16^{a}\pm0.47$	$105.00^{B}\pm1.46$

Means bearing different superscript (a, b, c, d) within a row differ significantly $P<0.05$; Means bearing different subscripts (A, B, C, D) within a column differ significantly $P<0.05$

Table 2. Hematological parameters (mean + SE) in the pre and post-operative period in group I, II & III

S. No.	Parameters	Groups	Time Intervals					Overall mean
			0th Day	15th Day	30th Day	45th Day	60th Day	
1.	Haemoglobin (g%)	Group I	10.10^{a}±0.27	10.66^{ab}±0.25	11.01^{b}±0.20	11.43^{bc}±0.20	12.06^{c}±0.80	11.05^{A}±0.15
		Group II	10.43^{a}±0.17	11.11^{b}±0.09	11.65^{c}±0.09	12.23^{d}±10.07	12.61^{d}±0.09	11.61^{B}±0.15
		Group III	10.38^{a}±0.14	11.63^{b}±0.08	12.26^{c}+0.11	12.63^{cd}±0.08	12.95^{d}±0.06	11.97^{B}±0.17
2.	PCV (%)	Group I	33.78^{a}±0.36	34.46^{ab}±0.40	35.16^{ab}±0.42	36.10^{bc}±0.54	37.28^{c}±0.70	35.36^{A}±0.31
		Group II	33.71^{a}±0.47	39.23^{b}±0.56	40.35^{b}±0.59	41.20^{b}±0.69	41.58^{b}±0.58	39.21^{B}±0.58
		Group III	34.18^{a}±0.44	39.73^{b}±0.56	42.15^{c}±0.16	42.76^{c}±0.21	43.38^{c}±0.03	40.44^{B}±0.64
3.	TLC (x 10^3/µL)	Group I	18.21^{a}±0.24	16.73^{b}±0.24	15.15^{c}±0.10	14.59^{c}±0.17	12.83^{d}±0.21	15.51^{A}±0.35
		Group II	17.93^{a}±0.20	15.83^{b}±0.25	14.48^{c}±0.19	13.86^{c}±0.16	12.14^{d}±0.26	14.85^{A}±0.37
		Group III	18.06^{a}±0.22	14.95^{b}±0.24	13.93^{c}±0.12	12.90^{d}±0.22	11.58^{c}+0.17	14.29^{A}±0.41
4.	Neutrophil (%)	Group I	81.66^{a}±0.42	80.16^{b}±0.47	78.16^{c}±0.30	76.33^{d}±0.21	74.33^{c}±0.51	78.13^{A}±0.50
		Group II	82.33^{a}±0.42	78.66^{b}±0.33	76.16^{c}±0.30	74.66^{c}±0.33	73.00^{d}±0.44	76.97^{AB}±0.62
		Group III	82.00^{a}±0.57	77.33^{b}±0.21	74.66^{c}±0.33	73.16^{c}±0.03	70.66^{d}±0.33	75.57^{B}±0.73
5.	Lymphocyte (%)	Group I	13.50^{a}±0.22	14.66^{ab}±0.21	15.83^{bc}±0.47	17.50^{cd}±0.76	19.33^{c}±0.42	16.16^{A}±0.42
		Group II	13.50^{a}±0.34	15.83^{b}±0.16	17.00^{b}±0.63	18.83^{c}±0.30	19.83^{c}±0.47	17.00^{A}±0.44
		Group III	13.50^{a}±0.22	16.50^{b}±0.22	17.16^{b}±0.79	19.50^{c}±0.42	21.00^{c}±0.36	17.53^{A}±0.51
6.	Monocyte (%)	Group I	2.17^{a}±0.17	2.00^{a}±0.26	1.83^{a}±0.17	1.83^{a}±0.31	1.50^{a}±0.22	1.86^{A}±0.10
		Group II	2.33^{a}±0.21	2.00^{a}±0.25	1.66^{a}±0.33	1.50^{a}±0.22	1.33^{a}±0.21	1.76^{A}±0.12
		Group III	2.16^{a}±0.16	1.83^{ab}±0.30	1.50^{ab}±0.22	1.33^{ab}±0.21	1.16^{b}±0.16	1.60^{A}±0.11
7.	Eosinophill (%)	Group I	2.33^{a}±0.21	2.00^{a}±0.36	1.83^{a}±0.40	1.67^{a}±0.33	1.50^{a}±0.22	1.86^{A}±0.14
		Group II	2.50^{a}±0.31	1.83^{ab}±0.30	1.50^{ab}±0.34	1.33^{ab}±0.21	1.16^{b}±0.16	1.66^{A}±0.14
		Group III	2.33^{a}±0.21	1.66^{ab}±0.33	1.33^{b}±0.21	1.16^{b}±0.16	1.00^{b}±0.00	1.50^{A}±0.12
8.	Platelets (x10^3/mm^3)	Group I	240.33^{a}±10.89	258.50^{a}±16.39	263.83^{a}±5.64	261.16^{a}±8.60	263.33^{a}±9.18	246.07^{A}±6.73
		Group II	242.00^{a}±11.00	268.00^{a}±5.39	260.66^{a}±8.23	254.00^{a}±7.61	266.83^{a}±6.90	257.77^{A}±5.9
		Group III	249.00^{a}±6.84	269.16^{a}±4.35	257.16^{a}±9.87	266.16^{a}±6.63	260.16^{a}±2.76	258.97^{A}±5.8

Means bearing different superscript (a, b, c, d) within a row differ significantly P<0.05; Means bearing different subscripts (A, B, C, D) within a column differ significantly P<0.05

animals had statistically higher lymphocyte counts on 30th and 60th post operative days compared to pre operative day[1,5], indicating gradual decrease of inflammatory reaction. The higher values of neutrophil counts associated with lower values of lymphocyte counts were noticed in all groups during pre-operative and immediate post-operative days. Cytokines released by macrophages activate the adrenal axis, leading to an increase in glucocorticoid levels[5,6]. This elevation may contribute to the lysis of lymphoid tissues and a reduction in circulating lymphocytes during the initial stage. In the present study, eosinophil and monocyte counts fluctuated within normal physiological limits across all groups, indicating no anaphylactic reactions and confirming the biocompatibility of biomaterials used at the fracture site[1,4,6,13]. Platelet count in the present study fluctuated within the normal range and no significant difference was observed within the groups. The haematological parameters evaluated in the present investigation were summarized in Table 2.

A significant increase in serum calcium levels was observed in all the groups. However, the calcium values differed significantly within the groups and between the groups I & II and I & III. The increase in serum calcium may indicate effective calcium deposition at the fracture site with subsequent formation of new bone with trabeculae[3,14,15,16].

In our study, during the fracture healing there was no significant difference of phosphorus values within the groups or between the groups[14]. The biochemical parameters evaluated in the present investigation are summarized in Table 1.

Serum alkaline phosphatase levels were measured during fracture healing following rigid stabilization. A significant difference of alkaline phosphatase values was recorded within the groups and between the groups I & II and I & III [2,3,12,16]. There were increased alkaline phosphatase levels following fracture immobilization in dogs[17]. Alkaline phosphatase, present in osteoblast membrane, played a role in the synthesis and mineralization of the bone matrix and

its raised levels might be attributed to increased osteoblastic activity to cause bone formation during fractured bone repair and thus formation of new bone matrix[18,19,20].

CONCLUSION

Serial evaluation of haematological and biochemical parameters enabled objective monitoring of inflammatory status and bone metabolic activity during fracture healing in dogs. A significant postoperative decline in leukocyte and neutrophil counts, particularly in mesenchymal stem cell–treated animals, indicated effective immunomodulation and favourable healing dynamics. Alterations in serum calcium and alkaline phosphatase levels corresponded with osteoblastic activity and mineralization at the fracture site. These findings support the utility of haemato-biochemical markers for assessing fracture repair and the biological efficacy of regenerative interventions in canine long-bone fractures. All the animals of IIIrd group exhibited excellent functional limb outcomes with no lameness by the end of 60th post operative day.

ACKNOWLEDGEMENT

The authors acknowledge the Dr. S. Eswari, Professor, Centre for Stem Cell Research and Regenerative Medicine, Madras Veterinary College, Chennai. for her invaluable help in the preparation and timely provision of mesenchymal stem cells for the research study. Also, the authors are thankful to SVVU, Tirupati for providing necessary support for the present research.

Financial support and sponsorship: None

Conflict of interest: None

Use of artificial intelligence for manuscript preparation: The author confirms that there was no use of AI-assisted technology for assisting in the writing of the manuscript and no images were manipulated using AI.

REFERENCES

1. Patil M, Dilipkumar D, Shivaprakash B V, Kasaralikar V R, Tikare V P and Ramesh B K 2017. Physiological and haemato-biochemical changes during repair of femur fracture in dogs. *The Pharma Innovation.* **6(8)**: 381-385
2. Singh C K, Sarma K K, Kalita D, Tamuly S, Hussain J, Deuri B and Nath P J 2017. Haemato-biochemical, radiographic and clinical outcome in healing of femoral fracture with retrograde intramedullary pin in conjunction with demineralized bone matrix in dogs. *Journal of ExperimentalB and Agricultural Science.* **5 (2)**: 201-207.
3. Reddy G A K, Kumar V G, Raghavender K B P and Kumar D P 2020. Evaluation of haemato-biochemical parameters for assessment of fracture healing in dogs. *Pharma Innovation Journal.* **9(9***):* 123-125.
4. Gahlod T R, Dhakate M S, Upadhye S A S and Bawaskar S S 2010. Management of femoral fracture with the use of horn peg in canine. *Veterinary World*. **3(1**): 37-41.
5. Kumar D, Bhargava M K, Singh R, Shahi A, Aparajita J, Swami M and Singh A P 2016. Haematological changes during fracture healing in goats. *International Organization of Scientific Research Journal of Agriculture and Veterinary Science.* **9(09):** 1-3.
6. Chaurasia A, Jawre S, Singh R, Shahi A, Pathak R, Das B and Verma N K 2019. Evaluation of haemato-biochemical parameters using different biomaterials in fracture healing of dogs. *International Journal of Current Microbiology and Applied Sciences.* **8(5):** 2265-2271.
7. Granero-Moltó F, Weis J A, Miga M I, Landis B, Myers T J, O'Rear L and Spagnoli A 2009. Regenerative effects of transplanted mesenchymal stem cells in fracture healing. *Stem Cells.* **27(8):** 1887-1898.
8. Strioga M, Viswanathan S, Darinskas A, Slaby O and Michalek J 2012. Same or not the same? Comparison of adipose tissue-derived versus bone marrow-derived mesenchymal stem and stromal cells. *Stem Cells and Development* **21(14):** 2724-2752.
9. Udehiya R K, Aithal H P, Kinjavdekar P, Pawde A M, Singh R and Sharma G T 2013. Comparison of autogenic and allogenic bone marrow derived mesenchymal stem cells for repair of segmental bone defects in rabbits. *Research in veterinary science.* **94(3):** 743-752.
10. Gibson M A, Brown S G and Brown N O 2017. Semitendinosus myopathy and treatment with adipose-derived stem cells in working German shepherd police dogs. *Canadian Veterinary Journal.* **58(2***):* 241–46.
11. Gugjoo M B, Farooq F, Sakeena Q, Dar E R, Khan S, Amarpal A and Sharma G T 2022. Stem cell therapeutics in veterinary medicine in India. *The Indian Journal of Animal Sciences.* **92(5):** 533-544.
12. Phaneendra M S S V, Lakshmi N, Raghunath M, Raju N K B and Adilaxmamma K 2017. Evaluation of biochemical and haematological parameters for assessment of compound fracture healing in dogs with local antibiotic treatment. *International Journal of Livestock Research.* **8(4):** 138- 143.
13. Pardeshi G D and Ranganath L 2008. Comparison of Type 1a and Type1b external skeletal fixation for tibial fracture repair in dogs. *Indian Journal of Veterinary Surgery.* **29(2):** 93-95.
14. Joshi S, Venugopal S, Nair S S and Sunil Kumar N S 2021. Management of fracture of long bones using string of pearls (SOP) plating technique in dogs. *International of Journal of Science Research.* **10(10):** 1086-1091.
15. Vani G, Veena P, Kumar R V, Lashmi M S, Prameela D R and Kundu B 2021. Evaluation of Serum Biochemical Parameters for Assessment of Long Bone Fracture Healing in Dogs Subjected to Intramedullary Pinning. *International Journal of Current Microbiology and Applied Sciences.* **10(05):** 448-451.
16. Bidari K, Doddamani Jahangirbasha D D and Bhagavantappa B 2023. Biochemical changes during repair of long bone fracture repair using string- of-pearls locking plate in dogs. Matrix. *The Pharma Innovation Journal.* **12 (9):** 1481-1484.
17. Kanwar G, Yadav M, Kumar S, Kirad S and Jain N 2014. Serum alkaline phosphatase a prospective biomarker for assessment of progress of fracture healing. International *Journal Research Applied Natural and Social Sciences.* **3(1):**15-20.
18. Thanoon M, Eesa M J and Abed E R 2019. Effects of platelets rich fibrin and bone marrow on the healing of distal radial fracture in local dogs: Comparative study. *Iraqi Journal of Veterinary Sciences.* **33(2):** 419-425.
19. Das B C, Roy C K, Biswas S, Dey T, Biswas P K and Sutradhar B C 2020. Retrograde Intramedullary pinning for femur fracture management in a Labrador dog-a case report. *Bangladesh Journal of Veterinary and Animal Sciences.* **8(1):** 139-142.
20. Abdulmawjood Y F, Thanoon M G, Ibrahim S M and Alsofy J H 2022. Histopathological study about the effect of nano magnesium oxide and platelets rich fibrin on the healing of induced radial fracture in dogs. *Iraqi Journal of Veterinary Sciences.* **36(I):** 123-130.

Indian J. Vet. Pathol., 50(4) : 339-347, 2026: DOI: https://doi.org/10.56093/248w0v24

RESEARCH ARTICLE

Mitigating effects of *Moringa oleifera* leaf extract on fipronil-induced hematobiochemical alterations in female Wistar albino rats

J. Leela Prasad, K. Sujatha[1*], A. Anand Kumar, Y. Muralidhar[2] and T.V. Chaitanya Kumar[3]
Department of Veterinary Pathology, College of Veterinary Science, Sri Venkateswara Veterinary University, Tirupati-517 502, Andhra Pradesh, India
[1]Centre for Continuing Veterinary Education and Communication, SVVU, Tirupati
[2]Department of Veterinary Pharmacology and Toxicology, CVSc, Tirupati
[3]Department of Veterinary Biochemistry, CVSc, Tirupati

***Address for correspondence**
Dr. K. Sujathal, Professor & Coordinator, CCVEC, E-mail: karamalasujatha@gmail.com
ORCID ID: 0009-0004-4583-2094, 0000-0002-5082-9365

Received: 14.4.26; Accepted: 3.6.26

ABSTRACT

The present study was conducted to evaluate the ameliorative potential of *Moringa oleifera* leaf extract against the fipronil-induced hematobiochemical alterations in female Wistar albino rats. Twenty four female Wistar albino rats were weighed individually and randomly divided into four experimental groups containing 6 rats each group. Fipronil was administered orally at a dose rate of 10 mg.kg^{-1}.bwt dissolved in corn oil to the Group II rats, and *Moringa oleifera* leaf extract at a dose of 250 mg.kg^{-1}.bwt was given orally along with fipronil to the Group IV rats for a period of 45 days. Group I was considered the vehicle control group, whereas Group III served as the *Moringa oleifera* control. Blood was collected at fortnight intervals, and the haematological indices like Hb, TEC, PCV, TLC, lymphocyte count and neutrophil count were estimated; serum was separated, and biochemical indices like ALT, AST, BUN, CRE, TP, and ALB were estimated. A significant decrease in Hb, TEC, PCV, TLC, and *percent* lymphocyte count and a significant increase in *percent* neutrophil count were observed in fipronil-treated rats. A significant increase in ALT, AST, BUN, CRE, and a significant decrease in TP and ALB were observed in fipronil-treated rats. However, a significant improvement was noticed in the *Moringa oleifera*-ameliorated rats, suggesting its protective potential against fipronil-induced toxicity.

Keywords: Fipronil toxicity, hematobiochemical alterations, *Moringa oleifera*, Female Wistar albino rats

INTRODUCTION

Pesticides are chemical agents that are used to protect crops from the organisms that establish a parasitic association with plants. Any organism that derives nutrients from, lives in, or on a plant, thereby damaging the crop yield, is called a pest. Of all the pests, insects account for 18%- 20% of the global crop loss annually and are responsible for a 15%-20% loss of vegetable production[1]. Pest control is one of the effective methods that helps to meet the escalating demand for food production by the growing population. But the irresponsible use of insecticides may eventually harm humans and animals by entering the food chain.

Fipronil is one such chemical having a broad spectrum of insecticidal activity, even in insects that have developed resistance to classical insecticides[2]. This organic compound having a pyrazole ring attached to a phenyl group, acts by blocking the gamma-aminobutyric acid (GABA)-gated chloride channels, resulting in excessive neuronal firing in the insects, leading to prolonged muscular contractions, which eventually cause paralysis and ultimately lead to the death of the insect. Its selective neurotoxic activity against insects over mammals is one of the reasons why it is widely used as an insecticide in agricultural fields and as an ectoparasiticide in veterinary medicine.

In a multi-centre study to determine the pesticide residues in the milk in peri-urban locations[3] reported that the estimated daily intake of fipronil was higher than the acceptable daily intake in children in some areas. Though fipronil shows selectivity towards insects, its chronic intake may impair metabolism even in mammals. Previous studies postulated that prolonged exposure to fipronil may cause neurotoxic, hepatotoxic, nephrotoxic, and reproductive toxic effects in mammals[4].

How to cite this article: Prasad, J.L., Sujatha, K., Kumar, A.A., Muralidhar, Y. and Kumar, T.V.C. 2026. Mitigating effects of *Moringa oleifera* leaf extract on fipronil-induced hematobiochemical alterations in female Wistar albino rats. Indian J. Vet. Pathol., 50(4) : 339-347.

In recent times, there's a shift in attention towards the pharmaceutical value of dietary plants and vegetables, due to the growing awareness among people that vegetables not only have nutritional benefits but also therapeutic properties. *Moringa oleifera* is a plant that has gained widespread attention for its therapeutic significance. Commonly called as Drumstick tree and often termed as miracle tree, as almost every part of the plant has medicinal value. Over the last decade, a consistent

number of studies have demonstrated the antioxidant potential of the plant, attributed to its rich concentrations of phenolic and flavonoid compounds. *Moringa oleifera* leaves are rich in antioxidants such as quercetin, kaempferol, and polyphenols[5], which can neutralize free radicals, decrease lipid peroxidation, and inhibit inflammatory pathways, and have demonstrated protective effects in various organs, such as liver, kidney, and reproductive tissues, and have also been shown to improve haemato-biochemical parameters[6]. Nevertheless, the ameliorating potential of *Moringa oleifera* against fipronil-induced haematological disturbances has not been sufficiently studied.

Therefore, the present study aims to investigate the effect of fipronil on haematological indices and amelioration with *Moringa oleifera* under experimental conditions.

MATERIALS AND METHODS

Procurement of lab animals, fipronil and *Moringa oleifera* leaf extract

A total of 24 female Wistar albino rats of eight to ten weeks old were procured from Kedhar Biolabs, Mahabubnagar, Telangana. Before the experiment, the rats were acclimatized to the laboratory conditions for a period of 14 days. Animals were housed in polypropylene cages and maintained at $25^0C \pm 1^0$ C with a 12-12 hour light/dark cycle throughout the 45-day experimental period. Standard hygienic and animal care protocols were followed based on the Committee for Control and Supervision of Experiments on Animals (CCSEA) guidelines[7] and were given access to *ad libitum* feed and water. The experiment was conducted only after obtaining the Institutional Animal Ethics Committee (IAEC) approval (Approval No. (281/ go/ ReBi/ S/ 2000/ CPCSEA/ CVSC/ TPTY/ 066/ Veterinary Pathology/ 2025 dated: 02.08.2025). The technical grade of fipronil (99% pure; B.no: FIP92B7055) was procured from Gharda Chemicals Ltd., Mumbai. Corn Oil (CAS No.: 8001-30-7) from Central Drug House (P) Ltd., New Delhi, and *Moringa oleifera* leaf extract (Product no: LC25060145) from Chemiloids Life Sciences Pvt Ltd., Vijayawada, Andhra Pradesh.

Study design

A total of 24 female Wistar albino rats of eight to ten weeks old were individually weighed and subsequently arranged into 4 experimental groups, containing six rats each, using a stratified randomization method to minimize variability. Corn oil was used as a vehicle for administering fipronil, as it is having lipophilic nature and a solubility of about >10,000 mg/L[8]. Fipronil and *Moringa oleifera* leaf extract were administered orally for 6 weeks. The dose of fipronil was selected as $1/10^{th}$ of its LD_{50}, that is 10 mg kg^{-1} bwt, while the dose of *Moringa oleifera* was adopted based on previously reported studies[9], where it had shown a protective effect in female rats, that is 250 mg kg^{-1} bwt. Rats in Group I served as vehicle control group, and were offered feed and water *ad libitum*. Rats in Group II were administered fipronil orally at a dose rate of 10 $mg.kg^{-1}$.b.wt for 6 weeks, with corn oil serving as vehicle. Rats in Group III were treated with *Moringa oleifera* leaf extract orally at a dose rate of 250 mg kg^{-1} bwt, and rats in Group IV were treated with fipronil along with *Moringa oleifera* leaf extract at the dose rates of 10 mg kg^{-1} bwt and 250 mg kg^{-1} bwt, respectively. Pooled blood samples were collected at fortnightly intervals from all experimental groups for haematological analysis. The animals were maintained for a period of six weeks and were sacrificed at the end of the experimental period.

Haematology

Pooled blood samples were collected in EDTA-coated vials at fortnightly intervals from all the experimental groups for haematological analysis, including Total Erythrocyte Count (TEC) and Total Leucocyte Count (TLC) estimated by the dilution method[10], haemoglobin estimation by Sahli's method[11] and Packed Cell Volume (PCV) assessed by the Micro haematocrit method[10]. Blood smears were immediately prepared and stained with Field's stain, then analysed for a differential leucocyte count using the Battlement method[10].

Serum biochemistry

At fortnight intervals, blood was collected in clot activator-coated vials and allowed to clot. After clotting, the sample was centrifuged at 4000 rpm for 15 minutes, and the serum was separated. The separated serum was used to estimate Alanine Aminotransferase (ALT), Aspartate Aminotransferase (AST), Total protein (TP), Albumin (ALB), Blood Urea Nitrogen (BUN) and serum creatinine (CRE) levels. All the serum markers were estimated using Biosystems commercial diagnostic kits.

Statistical analysis

The haemato-biochemical parameters were subjected to One-way ANOVA in accordance with[12] using Statistical Package for the Social Sciences (SPSS) version 20 for statistical analysis.

RESULTS

Total erythrocyte count (TEC) (millions/µl)

The mean and S.E values of TEC (millions/µl) in rats of different experimental groups, Group I to IV, were 7.67 ± 0.17^{b}, 6.69 ± 0.89^{a}, 8.49 ± 0.17^{c}, and 8.12 ± 0.99^{bc} respectively, and are shown in Fig.1. A significant ($p<0.05$) decrease in mean TEC was observed in fipronil-treated rats (Group II) when compared to the control rats (Group I). The *Moringa oleifera*-ameliorated rats (Group IV) showed a statistically significant increase in mean TEC compared with the fipronil rats (Group II).

Likewise, there was no significant difference between *Moringa oleifera*-treated rats (Group III) and *Moringa oleifera*-ameliorated rats (Group IV).

Haemoglobin (Hb) (gm%)

The mean and S.E values of haemoglobin (gram%) of rats in different experimental groups, Group I to IV, were 13.94 ± 1.03^{b}, 10.30 ± 0.46^{a}, 15.73 ± 1.17^{b}, and 15.07 ± 0.76^{b}, respectively, and are shown in Fig.2. A significant reduction ($p< 0.05$) in mean haemoglobin levels was observed in fipronil-treated rats (Group II) compared to the control rats (Group I). The *Moringa oleifera* ameliorated rats (Group IV) showed improvement in mean Hb concentration when compared with fipronil-treated rats (Group II), and no significant difference was observed between the control rats (Group I) and *Moringa oleifera*-treated rats (Group III).

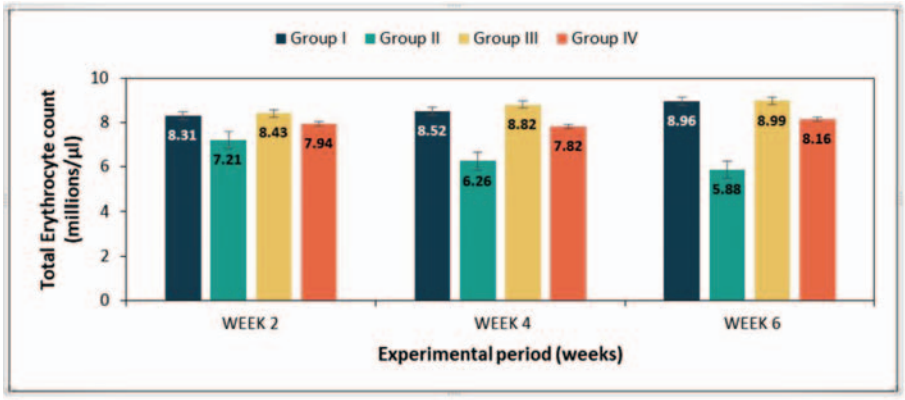

Fig.1. Mean values of TEC (millions/µl) in rats of different experimental groups

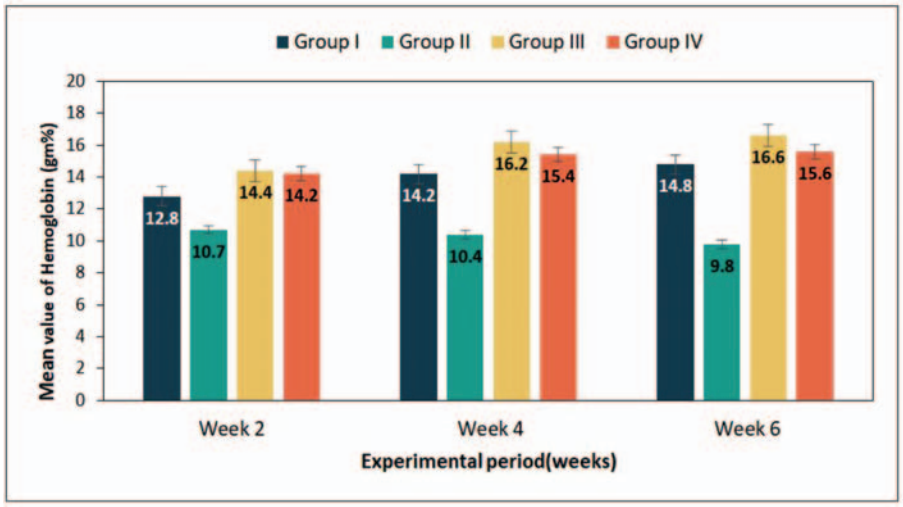

Fig.2. Mean values of haemoglobin (gm%) in rats of different experimental groups

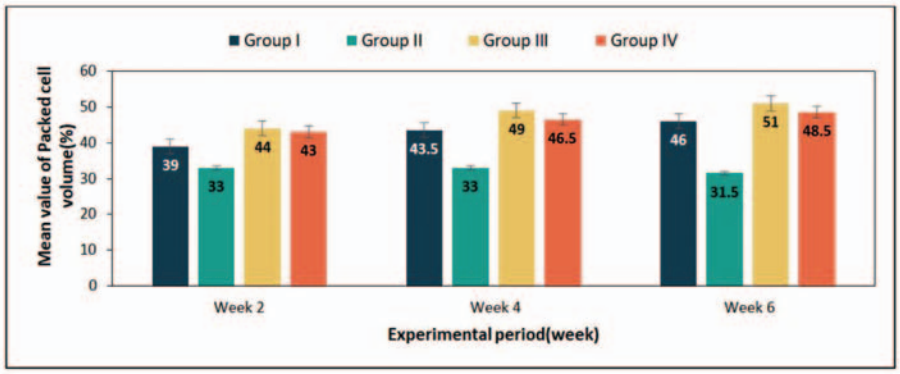

Fig.3. Mean values of PCV (%) in rats of different experimental groups

Packed cell volume (PCV) (%)

The recorded mean and S.E values of PCV (%) of rats in different groups, Group I to IV were 42.83 ± 2.05^{b}, 32.5 ± 0.5^{a}, 48 ± 2.08^{b}, and 46 ± 1.60^{b}, respectively, and are shown in Fig.3. A significant decrease ($P< 0.05$) in the mean PCV values was observed in fipronil-treated rats (Group II) when compared to the control rats (Group I). The rats treated with fipronil and *Moringa oleifera* (Group IV) showed improvement in mean PCV values when compared with fipronil-treated rats (Group II), and no significant difference was observed between the control rats (Group I) and *Moringa oleifera*-treated rats (Group III).

Total leucocyte count (TLC) (Thousands/µl)

The mean and S.E values of Total Leukocyte Count (Thousands/µl) in rats of experimental groups, Group I to IV were 8.08 ± 0.1^{b}, 6.97 ± 0.44^{a}, 8.47 ± 0.04^{b}, and 8.20 ± 0.05^{b}, respectively, and are presented in Fig.4. In fipronil-treated rats (Group II), the TLC values were significantly decreased ($P< 0.05$) than control (Group I). There was a significant ($P<0.05$) increase in TLC values in *Moringa oleifera*-treated rats (Group III) and *Moringa oleifera*-ameliorated rats (Group IV) when compared to the fipronil-treated rats (Group II).

Percent neutrophil count (%)

The mean and S.E values of percent neutrophil count (%) in rats of different experimental groups, Group I to IV, were 16.57 ±

0.82[a], 26.96 ± 0.84[b], 15.14 ± 2.14[a], and 15.76 ± 2.96[a], respectively, and are given in Fig. 5. There was a significant ($p<0.05$) increase in the percent neutrophil count in fipronil-treated rats (Group II) compared to the control rats (Group I). No significant difference was observed between the control and *Moringa oleifera*-treated rats (Group III). A significant ($p<0.05$) reduction in percent neutrophil count was noticed in *Moringa oleifera*-ameliorated rats (Group IV) compared to fipronil-treated rats (Group II).

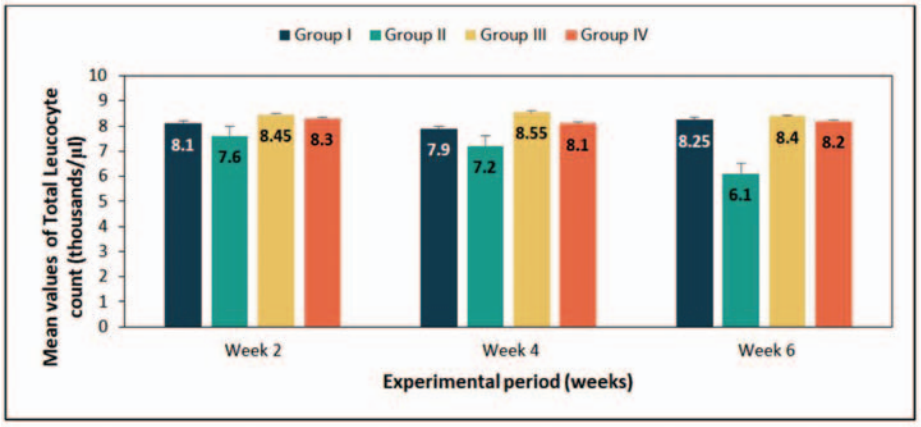

Fig.4. Mean values of TLC (Thousands/µl) in rats of different experimental groups

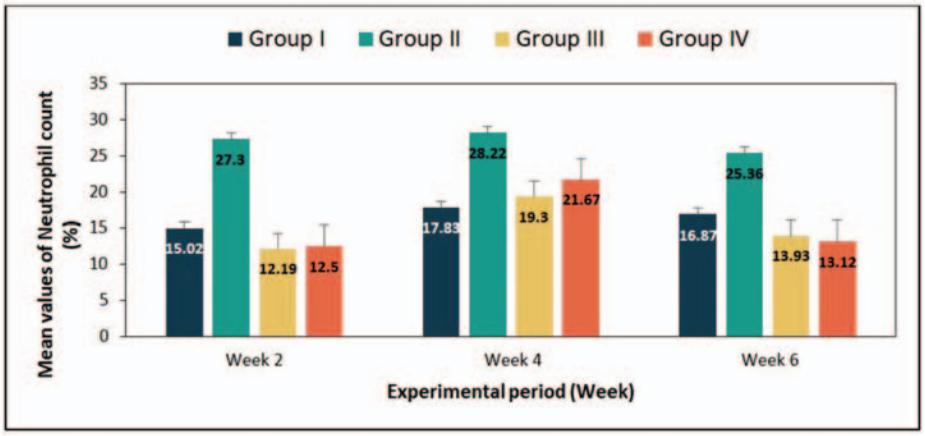

Fig.5. Mean values of Percent neutrophil count (%) in rats of different experimental groups

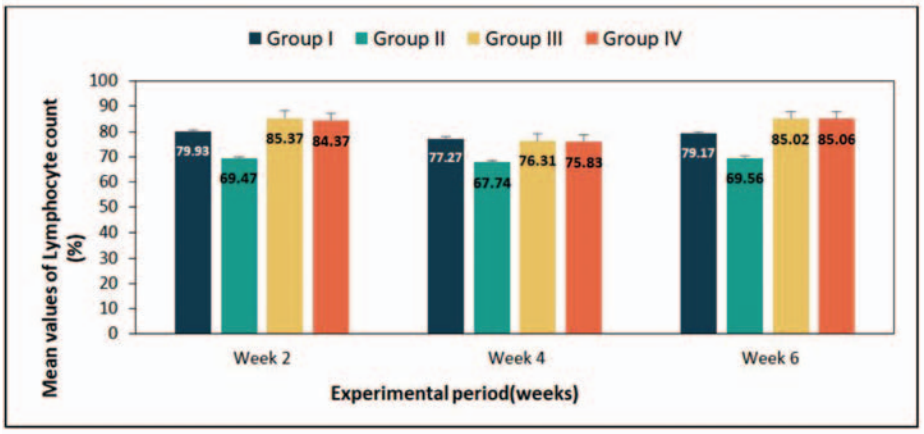

Fig.6. Mean values of percent lymphocyte count (%) in rats of different experimental groups

Percent lymphocyte Count (PLC) (%)

The mean and S.E values of percent lymphocyte count (%) in rats of different experimental groups, Group I to IV were 78.79 ± 0.79[b], 68.92 ± 0.59[a], 82.23 ± 2.96[b], and 81.76 ± 2.97[b], respectively, are given in Fig.6. There was a significant ($p<0.05$) decrease in the percent lymphocyte count in fipronil-treated group (Group II) rats compared to the control rats (Group I). A significant ($p<0.05$) increase in percent lymphocyte count was noticed in *Moringa oleifera*-ameliorated rats (Group IV) compared to fipronil-treated rats (Group II). No significant difference was noticed between the control rats (Group I) and *Moringa oleifera*-treated rats (Group III).

Biochemical profile

Alanine aminotransferase (ALT) (IU/L)

The mean and S.E values of ALT (IU/L) of rats in different groups, Group I to IV, were 44.97 ± 2.02[a], 83.86 ± 6.68[b], 51.75 ± 1.56[a], and 57.67 ± 4.47[a], respectively, and are given in Fig 7. In comparison to control rats (Group I), fipronil-treated rats (Group II) showed a statistically significant ($p < 0.05$) elevation in mean ALT levels. Serum ALT values in *Moringa oleifera* ameliorated rats (Group IV) were significantly ($p < 0.05$) decreased when compared to the fipronil-treated rats (Group II). Meanwhile, no significant difference was noticed in the values of *Moringa oleifera*-treated rats (Group III) compared to control rats (Group I).

Aspartate aminotransferase (AST) (IU/L)

The mean and S.E values of AST (IU/L) of rats in different groups, Group 1 to IV were 105.2±1.63[a], 193.1±14.1[c], 123.57±5.84[ab], and 142.83±4.90[b], respectively, and are given in

Fig.8. There was a significant ($p < 0.05$) increase in mean AST levels in fipronil-treated rats (Group II) when compared to the control rats (Group I). A significant decrease in mean serum AST values was noticed in *Moringa oleifera* ameliorated rats (Group IV) than the fipronil-treated rats (Group II). Although a significant increase ($p < 0.05$) in the mean value was observed in Group IV compared to the control (Group I), this is within the physiological range. No significant difference was noticed in the values of *Moringa oleifera-treated* rats (Group III) compared to control rats (Group I) and the ameliorated rats (Group IV).

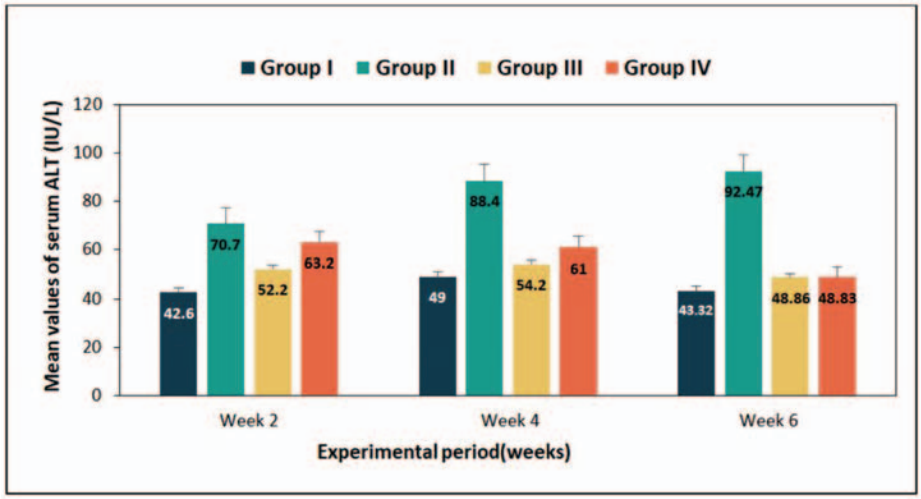

Fig.7. Mean serum ALT(IU/L) values in rats of different experimental groups

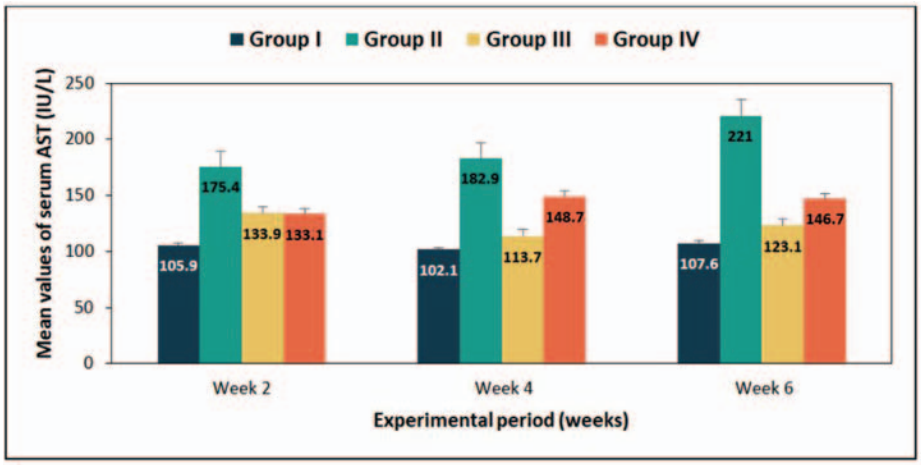

Fig.8. Mean serum AST(IU/L) values in rats of different experimental groups

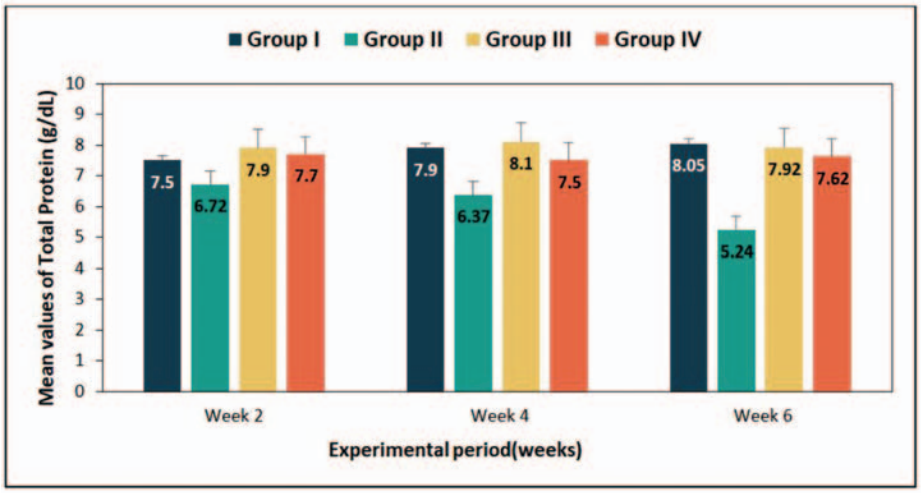

Fig.9. Mean values of serum total protein (g/dL) in rats of different experimental groups

Serum total protein (g/dL)

The mean and S.E serum values of total protein (g/dL) of rats in different groups, Group I, II, III, and IV were 7.81 ± 0.16^{b}, 6.11 ± 0.44^{a}, 7.97 ± 0.62^{b}, and 7.60 ± 0.58^{b}, respectively, and are given in Fig.9. In comparison with the control group of rats, there was a significant decrease ($p<0.05$) in total protein value in fipronil-treated rats (Group II). No significant difference was noticed in the total protein values of *Moringa oleifera*-treated rats (Group III) compared to control rats (Group I). At the same time, these values were restored in *Moringa oleifera*-ameliorated rats (Group IV), when compared to fipronil-treated rats (Group II).

Serum albumin (g/dL)

The mean and S.E serum values of albumin (g/dL) of rats in different groups, Group I to IV were 4.51 ± 0.99^{b}, 3.44 ± 0.28^{a}, 4.67 ± 0.29^{b}, and 4.47 ± 0.90^{b} (g/dL), respectively, and are given in Fig.10. There was a significant decrease ($p<0.05$) in the mean value of albumin in fipronil-treated rats (Group II), when compared to the control rats (Group I). Meanwhile, a significant improvement was noticed in *Moringa oleifera*-ameliorated rats (Group IV) compared to fipronil-treated rats (Group II). No significant difference was noticed in the mean serum albumin values of *Moringa oleifera*-treated rats

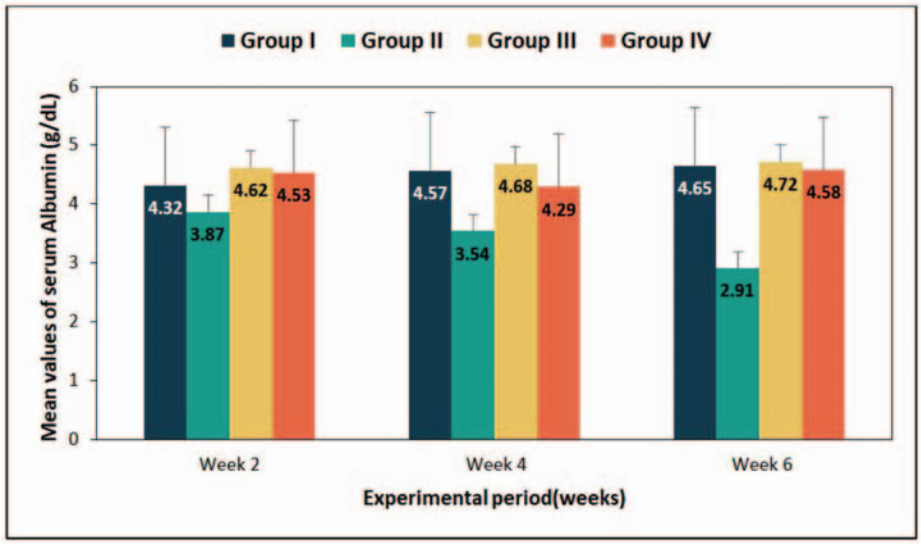

Fig.10. Mean values of serum albumin (g/dL) in rats of different experimental groups

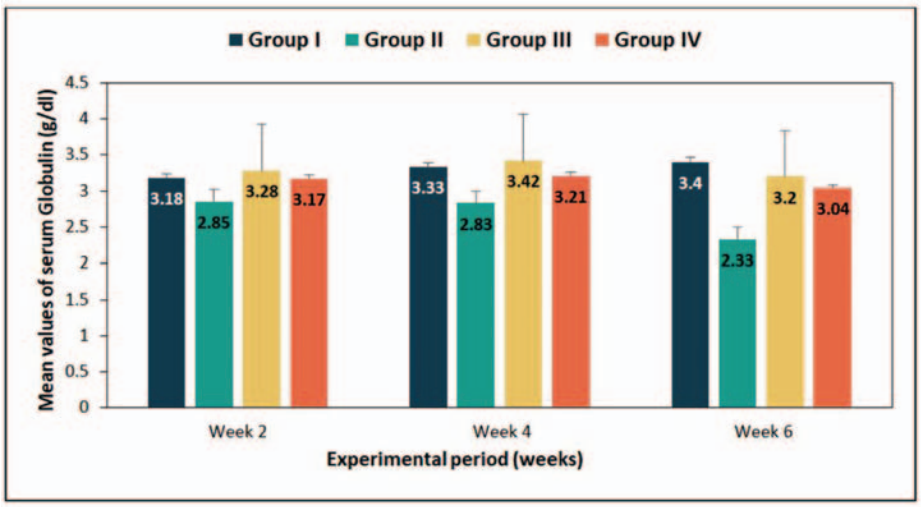

Fig.11. Mean values of serum globulin (g/dL) in rats of different experimental groups

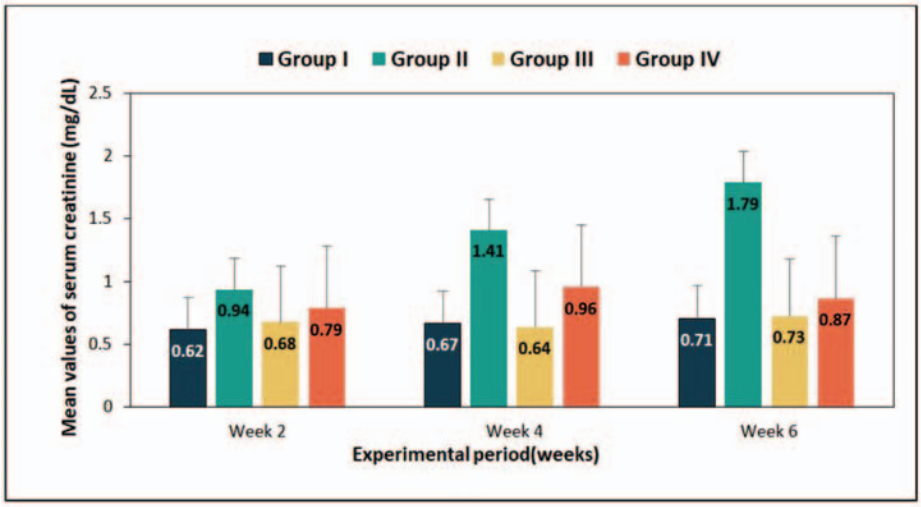

Fig.12. Mean values of serum creatinine (mg/dL) in rats of different experimental groups

(Group III) compared to control rats (Group I).

Serum globulin (g/dL)

The mean and S.E values of serum globulin (g/dL) of rats in different groups, Group I to IV were 3.30 ± 0.06^{b}, 2.67 ± 0.17^{a}, 3.30 ± 0.64^{b}, and 3.14 ± 0.05^{b}, respectively, and are shown in Fig.11. Statistically a significant ($p<0.05$) decrease was observed in mean serum globulin levels in fipronil-treated rats (Group II) when compared to the control rats (Group I). No significant difference was noticed in the *Moringa oleifera*-treated (Group III) and *Moringa oleifera*-ameliorated rats (Group IV) compared to control rats (Group I).

Serum creatinine (mg/dL)

The mean and S.E values of serum creatinine (mg/dL) of rats in different groups, Groups I to IV were 0.67 ± 0.26^{a}, 1.38 ± 0.25^{b}, 0.68 ± 0.45^{a}, and 0.87 ± 0.49^{ab}, respectively, and are presented in Fig.12. A significant ($p<0.05$) increase in the serum creatinine values was observed in fipronil-treated rats (Group II) when compared to control rats (Group I). The rats treated with fipronil and *Moringa oleifera* (Group IV) showed no significant difference in these values when compared with the fipronil-treated rats (Group II), and also with the control rats (Group I). Whereas the *Moringa oleifera*-treated rats (Group III) showed no significant difference in serum creatinine values when compared with control rats (Group I).

Blood urea nitrogen (BUN) (mg/dL)

The mean and S.E values of serum blood urea nitrogen (mg/dL) of rats in different groups, Group I to IV were 25.08 ± 0.90^{b}, 39.24 ± 0.99^{c}, 20.62 ± 0.42^{a}, and 26.69 ± 1.03^{b}, and are given in Fig.13. There was a significant ($p<0.05$) increase in mean serum

BUN values in fipronil-treated rats (Group II) when compared to the control rats (Group I). A significant decrease ($p<0.05$) was observed in the values of *Moringa oleifera*-ameliorated rats (Group IV) compared to fipronil-treated rats (Group II), and a significant decrease ($p<0.05$) was observed in the values of *Moringa oleifera*-treated rats (Group III) compared to the control rats (Group I).

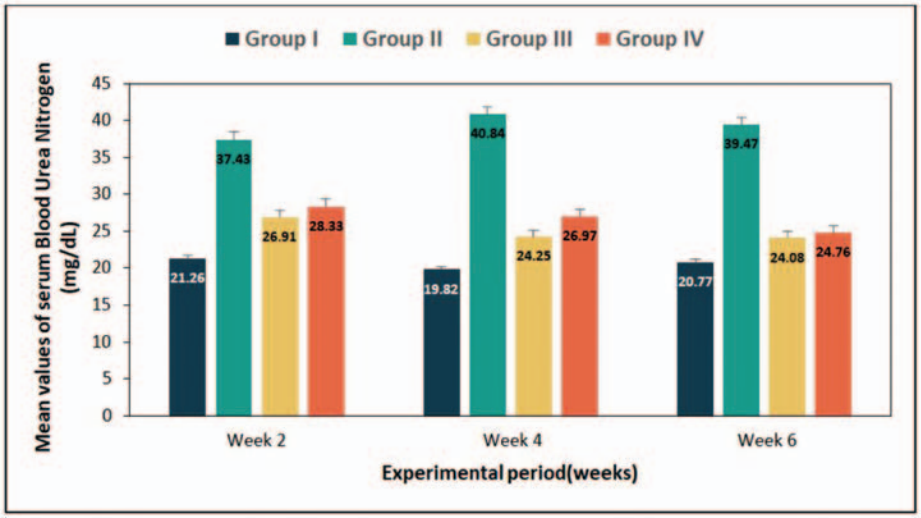

Fig.13. Mean values of serum BUN (mg/dL) in rats of different experimental groups

DISCUSSION

The findings of the present study demonstrated significant alterations in haematological parameters due to exposure to fipronil. The administration of *Moringa oleifera* leaf extract has shown a protective effect, which is evident by improvement in the haematological parameters. There is a remarkable reduction in the TEC, Hb and PCV values in the fipronil-administered rats when compared to the control group. These findings were in accordance with the observations of previous authors[13]. Fipronil, by producing ROS species, causes oxidative damage to the bone marrow and disrupts erythropoiesis[14]. Fipronil disrupts the membrane integrity and stability of erythrocytes through its interaction with membrane phospholipids, resulting in an imbalance in the bilipid layer of the cell membrane. This leads to the production of spherocytes, acanthocytes, and echinocytes, which are prone to hemolysis[15]. The kidneys are the primary source of erythropoietin, which stimulates RBC production in the bone marrow, and the histopathological examination revealed renal damage, supporting the noticeable decrease in the TEC, Hb and PCV values in this study.

A significant reduction in total leucocyte count and lymphocyte count, and an increase in neutrophil count were observed in fipronil-treated rats in comparison to the control rats. These observations are in accordance with[16], where they observed a progressive and steady decrease in the leucocyte count over time. The decrease in lymphocyte count is attributed to the immunotoxic effect of fipronil and oxidative damage to the lymphoid organs. This observation was further supported by the gross pathological findings, wherein the splenic atrophy was observed in the fipronil-treated rats during necropsy. Since lymphocytes constitute the major fraction of leucocytes, their decrease is reflected in the total leucocyte count. The increase in the neutrophil count could be due to the response of the immune system to stressful conditions[14].

Moringa oleifera ameliorated rats (Group IV) exhibited a significant improvement when compared with the fipronil-treated rats in all of the haematological parameters like Hb, PCV, TEC, and also restored lymphocyte and total leucocyte count. These findings are in accordance with[17]. The flavonoids and phenolic compounds in the *Moringa oleifera* act in synergism and aid in improving the haematological parameters through attenuation of oxidative stress, and stimulate the stem cells in producing erythrocytes through erythropoiesis[18]. The *Moringa oleifera* leaves are rich in iron content, which acts as the main nutrient in haematopoiesis, and Vitamin C in *Moringa oleifera* leaves also facilitates iron absorption by forming a chelate with ferric iron that is soluble in the duodenum. The observed increase in leucocyte count is also reported in previous studies[19], where it might be due to its potent antioxidant and immunostimulatory effect which protects the bone marrow from anti-oxidants and stimulates the production of white blood cells and enhances the body's defence mechanism against toxic insult In addition the amelioration of pathological lesions in the kidneys and spleen, where kidneys appeared normal, reduction in splenic atrophy and restoration of the splenic architecture may have contributed to the improvement in the haematological aspects.

The mean values of the liver and kidney function biomarkers ALT, AST, BUN, CRE of the fipronil-treated rats (Group II) were significantly increased compared to the control rats (Group I). These results coincided with the observations of[20]. The liver plays a crucial role in metabolizing insecticides, making it susceptible to the oxidative damage. The elevated serum levels of these enzymes in fipronil treated rats might be due to seepage of enzymes from liver cytosol into the bloodstream, caused by worsened cell membrane permeability or hepatocyte damage, induced by fipronil sulfone, a

metabolite of fipronil that interferes with the electron transport chain, resulting in decreased ATP production, resulting in Ca^{++} influx, eventually compromising membrane integrity and cause the release of AST and ALT[21]. Fipronil enhances NADPH oxidase activity and mitochondrial superoxide production in the kidney, leading to lipid peroxidation and damage renal proteins that results in damage to the glomeruli and tubules, thus impairing filtration and tubular reabsorption. These structural alterations disrupt kidney architecture, reduce filtration efficiency, and hinder the clearance of urea and creatinine[20]. The histopathological examination of the liver revealed atrophied hepatic cords, along with focal necrotic areas in the parenchyma. The kidney revealed degenerated tubules along with moderate vacuolization in the glomeruli. These observations coincided with the elevation of liver and kidney functional biomarkers.

A significant reduction in the serum total protein, albumin, and globulin levels was evident in the fipronil treated rats when compared to the control group. These findings are consistent with previous findings of[22]. Albumin and globulin, synthesized in the liver, acts as carrier proteins, albumin primarily maintains colloid osmotic pressure, whereas globulin plays a key role in immune defence. The decline in these levels in this study might result from decreased protein synthesis in the liver caused by hepatic damage from fipronil exposure. A decrease in serum total protein, albumin, and globulin levels indicates the immunosuppressive effect[23] of fipronil.

These biomarkers were restored to normal in *Moringa oleifera*-ameliorated rats. This recovery towards normal transaminase enzyme and protein levels suggests that *Moringa oleifera* might aid in regenerating parenchymal cells, thus protecting cell membranes from damage and likely reducing the leakage of marker enzymes into the bloodstream[24]. The amended effect on kidney markers could be due to antioxidant activities of *Moringa oleifera* leaves, which are attributable to the presence of polyphenols that increase endogenous antioxidant enzymes, helping to protect tubular cells by upregulating anti-apoptotic proteins and by scavenging ROS. This improvement in functional biomarkers coincided with the amelioration of histopathological lesions and the restoration of histoarchitecture in the liver and the kidney, under microscopic examination.

CONCLUSION

The findings of the present study indicate that fipronil causes alterations in various haematological and biochemical parameters in rats, and co-administration of *Moringa oleifera* along with the fipronil had attenuated these changes and restored them to normal. Therefore, *Moringa oleifera* could be considered as an effective way to mitigate the fipronil-induced haemato-biochemical alterations.

ACKNOWLEDGMENTS

The authors are thankful to the Sri Venkateswara Veterinary University, Tirupati for providing various facilities to carry out the present research work.

Financial support & sponsorship: None

Conflicts of Interest: None

Use of Artificial Intelligence (AI)-Assisted Technology for manuscript preparation: The authors confirm that there was no use of AI-assisted technology for assisting in the writing of the manuscript and no images were manipulated using AI.

REFERENCES

1. Ouaarous M, El Fakhouri K, Taarji N, Baouchi A, Amri M, Ramdani C. 2025. Impact of field insect pests on seed and nutritional quality of some important crops: a comprehensive review. *ACS Omega* **10**: 8779–8792.
2. Aajoud A, Ravanel P, Tissut M. 2003. Fipronil metabolism and dissipation in a simplified aquatic ecosystem. *J Agric Food Chem* **51**: 1347–1352.
3. Gill JPS, Bedi JS, Singh R, Fairoze MN, Hazarika RA, Gaurav A. 2020. Pesticide residues in peri-urban bovine milk from India and risk assessment: a multicenter study. *Sci Rep* **10**: 8054.
4. Singh NS, Sharma R, Singh SK, Singh DK. 2021. A comprehensive review of environmental fate and degradation of fipronil and its toxic metabolites. *Environ Res* **199**: 111316.
5. Chiș A, Noubissi PA, Pop OL, Mureșan CI, Fokam Tagne MA, Kamgang R. 2023. Bioactive compounds in *Moringa oleifera*: mechanisms of action, focus on their anti-inflammatory properties. *Plants (Basel)* **13**(1):20.
6. Kasem TS. 2019 Effect of *Moringa oleifera* on hemato-biochemical and histological alterations in rats after exposure to high voltage electromagnetic field. *J. Res. Fields Specific Educ* **5**(22): 143-166.
7. CCSEA. 2018. Compendium of CPCSEA. *Ministry of Fisheries, Animal Husbandry and Dairying, Government of India*.
8. O'Neil MJ, Heckelman PE, Koch CB, Roman KJ. 2013.The Merck Index - An Encyclopedia of Chemicals, Drugs, and Biologicals. Cambridge: UK: Royal Society of Chemistry; XV edition, 748 pp.
9. Soliman SS, Suliman AA, Fathy K, Sedik AA. 2025. Ovario-protective effect of *Moringa oleifera* leaf extract against cyclophosphamide-induced oxidative ovarian damage and reproductive dysfunction in female rats. *Sci Rep* **15**: 1054.
10. Jain NC. 1986. Schalm's Veterinary Hematology - Lea and Febiger, Philadelphia II edition, pp.1221.
11. Coles EH. 1986. Veterinary clinical pathology. *W.B. Saunders* company, Philadelphia, USA, pp.445-446.
12. Snedecor WG, Cochran GW. 1994. Statistical methods. 8th ed. *Iowa State University Press*, 258–268.
13. Al-Janabi Q, Hamed L, Khaleel Ibraheem A. 2023. Effects of nano-fipronil on male rats' biochemical, liver, and renal functions. *IOP Conf Ser Earth Environ Sci* **1259**: 012033.
14. Ghaffar A, Hussain R, Abbas G, Kalim M, Khan A, Ferrando S. 2018. Fipronil induces hemato-biochemical, histological and genetic damage at low doses in common carp, *Cyprinus carpio*. *Ecotoxicol* **27**: 1261–1271.

15. Yumnam D, Dutta BK, Paul SB, Choudhury S. 2017. Alterations in the erythrocyte membrane and ultrastructural changes in the liver and kidney of albino mice exposed to fipronil. *Nat Environ Pollut Technol* **16**: 273-278.
16. Nakul P, Sujatha K, Kumar A, Vijayalakshmi S. 2024. Fipronil toxicity induced hemato-biochemical alterations in male Wistar albino rats and its alleviation with pomegranate peel extract. *Indian J Vet Pathol* **48**: 159–168.
17. Fachruddin F, Suprayogi A, Manalu W, Hanif N, Darusman HS. 2025. Hematology and reproductive performance of female rats supplemented with kelor (*Moringa oleifera* Lam.) leaf extract during the reproductive period. *Open Veterinary Journal* **15**(6):2651–60.
18. Suzanne DrBBS, Adeline FYS, Theodora K, Dairou H, Pradel KL, Aristide KM. 2020. Hemopoietic effects of some herbal extracts used in treatment of infantile anemia in Cameroon. *World J Pharm Med Res* **6**: 147–155.
19. Nurhayati T, Fathoni MI, Fatimah SN, Tarawan VM, Goenawan H, Dwiwina RG. 2023. Effect of *Moringa oleifera* leaf powder on hematological profile of male Wistar rats. *J Blood Med* **14**: 477–485.
20. Abdel-Daim MM, Abdeen A. 2018. Protective effects of rosuvastatin and vitamin E against fipronil-mediated oxidative damage and apoptosis in rat liver and kidney. *Food Chem. Toxicol* **114**:69–77.
21. Vroon DH, Israili Z. Aminotransferases. 1990. In: Walker HK, Hall WD, Hurst JW, editors. Clinical Methods: The History, Physical, and Laboratory Examinations. 3rd ed. Boston: Butterworths.
22. Behery M, El-Sayed Y, Eldakroury M, Abdelhiee E. 2022. Hepatoprotective Effect of Quercetin Nanoparticles Against Fipronil Toxicity in Adult Male Rats. *Mat. J. Vet. Med* **2**(1):13–7.
23. Nayak AK, Das BK, Kohli MPS, Mukherjee SC. 2004. The immunosuppressive effect of alpha-permethrin on Indian major carp, rohu (*Labeo rohita* Ham.). Fish Shellfish Immunol **16**(1):41–50
24. Singh D, Arya PV, Aggarwal VP, Gupta RS. 2014. Evaluation of antioxidant and hepatoprotective activities of *Moringa oleifera* Lam. Leaves in carbon tetrachloride-intoxicated rats. *Antioxidants* **3**(3):569–591.

Indian J. Vet. Pathol., 50(4) : 348-352, 2026: DOI: https://doi.org/10.56093/6hz5fb92

RESEARCH ARTICLE

Pathological alterations induced by acute oral exposure to Acephate in Wistar rats

C.S. Mishra, R.C. Ghosh, Pramod Kumar and Devesh Kumar Giri*
Department of Veterinary Pathology, College of Veterinary Science and Animal Husbandry, Anjora (DSVCKV) Durg, Chhattisgarh

Address for correspondence
Dr. Devesh Kumar Giri, E-mail: giri.devesh18@gmail.com
ORCID ID: 0009-0005-8000-4697, 0000-0003-3016-5837, 0009-0009-2070-1318, 0000-0001-7555-3337

Received: 8.5.26; Accepted: 3.6.26

ABSTRACT

Acephate is an organophosphate pesticide that has been widely used to control insect pests in agricultural fields for decades. There is increasing concern for public health due to their widespread usage. The current experimental investigation was planned to study the toxicopathological effects of acephate in female Wistar rats following an acute toxic dose. The acute toxic dose of acephate was determined by approximate lethal dose (ALD) method. The ALD for acephate was found to be 1350 mg/kg body weight, orally in female Wistar rats. The rat showed signs of profuse salivation, depression, prostration, piloerection, scant droppings, chromodacryorrhoea, dyspnoea, gasping, clonic convulsion, hunched posture, soiled perineum and loss of reflexes. The rat died at 5 hours and 35 minutes of oral acephate intoxication. The pathomorphological changes observed at necropsy were those of generalised congestion in vital organs i.e. liver, heart, kidneys, lung and brain. Apart from haemorrhages and congestion in liver, lung, kidneys and heart, the histopathological lesions represented tubular necrosis and glomerular degeneration in kidney, degenerative and necrotic changes in cardiac muscles, severe lymphocytolysis in the Malpighian corpuscles in spleen, thickening of interalveolar septa in lung and moderate degenerative and necrotic changes in neurons in brain. It can be concluded that acute toxic dose of acephate causes hepatotoxicity, nephrotoxicity neurotoxicity together with considerable damage to the histoarchitecture of lungs, heart and spleen.

Keywords: Acephate, Organophosphate, Pathomorphology, Toxicopathology

INTRODUCTION

The widespread use of pesticides in public health programme and agriculture has caused severe environmental pollution and potential health hazards. Introduction of new, more toxic and rapidly disseminating pesticides into environment has necessitated accurate identification of their potential hazards to animal and human health. Many pesticides are extremely toxic to mammals and/or other target organisms. The extent of hazard depends on the amount of residue and its toxicity. Today there are some 200 organophosphorus ester insecticides, in the market place formulated into literally thousands of products[1]. Acephate is the International Organization for Standardization (ISO) approved name for the organophosphorus insecticide O, S-dimethyl acetylphosphoramidothioate[2]. It is one of the top ten organophosphate insecticides used in agriculture[3]. Acephate is organophosphorus insecticide with contact and systemic action on sucking and biting insects and has been widely used for the protection of vegetables and fruits due to its wide range activity against Agromyzidae, Lepidopterans', Hymenoptera, Thysanoptera and Aphids[4]. Methamidophos, the primary metabolite of acephate in plants, birds and mammals, has significantly more potent inhibitor of cholinesterase activity than acephate[2].

Acephate can overstimulate the nervous system causing nausea, dizziness, confusion and at very high exposures (accidents or major spills), respiratory paralysis and death. A number of studies showed the toxicity of acephate on different organisms which indicated it as a potent hepatotoxic[5], nephrotoxic[5], neurotoxic, mutagenic, carcinogenic and cytotoxic compound[6,7].

The reports on pathological effects on visceral organs following an acute toxic dose are meager in available literature. The present report puts on record the approximate lethal dose of acephate in Wistar rats along with the clinical signs observed during the study. It also throws light on the pathomorphological alterations in visceral organs associated with acute toxicity of acephate.

How to cite this article: Mishra, C.S., Ghosh, R.C., Kumar, P. and Giri, D.K. 2026. Pathological alterations induced by acute oral exposure to Acephate in Wistar rats. Indian J. Vet. Pathol., 50(4) : 348-352.

MATERIAL AND METHODS

Acute toxicity of acephate in female Wistar rats was determined by approximate lethal dose (ALD) method as described by Hayes[8] after obtaining approval from Institutional Animal Ethics Committee (IAEC). Acephate, 75% SP (TATA ASATAF 75 SP) purity

was obtained from Rallis India Limited Mumbai, India. For this purpose, 6 healthy female rat weighing 110 - 120 g were taken. Based on the reviewed literature, an arbitrary dose of 267 mg acephate/kg body weight dissolved in 1 ml of distilled water was given *per os* to a rat by gastric probe. As the rat survived, second rat was given 1.5 times the initial dose i.e. 400 mg acephate/kg body weight, *per os* and sequentially, several rats were given increasing doses of acephate in the similar manner (600, 900 and 1350 mg acephate/kg body weight, *per os*) until a lowest lethal dose was achieved. One rat was kept as control and given 1 ml distilled water, *per os*. All the rats were critically observed to record the clinical manifestation of toxicity.

The rat died during the acute toxicity study was subjected to detailed post-mortem examination. The representative tissue samples were collected in 10% neutral buffered formalin for histopathological studies. Paraffin embedded tissue sections of 4 - 5 µm were obtained as described by Luna[9] and stained with Haematoxylin and Eosin (H&E) as per the method described by Bancroft and Stevens[10] with slight modifications. The stained sections were examined under light microscope and the lesions were recorded, if any.

RESULTS

ALD and associated clinical manifestations

The approximate lethal dose of acephate was determined as 1350 mg acephate/kg body weight, *per os* in female Wistar rat. The rat intoxicated with an initial arbitrary dose of 267 mg acephate/kg body weight, orally showed mild irritation and hyperactivity just after administration of the dose. However, the rat recovered to normalcy after a short time gap of 25 minutes. Another rat being exposed to 400 mg acephate/kg body weight exhibited the signs of mouth smacking, mild irritation and hyperactivity followed by salivation and depression. The third rat intoxicated with 600 mg acephate /kg body weight showed irritation, hyperactivity and salivation followed by depression, prostration and reduced motor activity. Another rat received 900 mg acephate/kg body weight, orally exhibited the toxic signs instantaneously. The rat exhibited irritation, hyperactivity and tachypnea within 45 minutes, colourless discharge from nostrils, eyes and salivation along with prostration, followed by somnolence 2 hours post exposure. However, the rat recovered after 10 hours from all these signs and assumed normal functions.

Therefore, one more rat was intoxicated orally with a 1.5 times higher dose of 1350 mg acephate /kg body weight. The toxic signs appeared instantaneously following its administration and became more pronounced with passage of time. The toxic signs noticed after 2 hours and 10 minutes comprised of depression, prostration, piloerection, profuse salivation, colourless lacrimation and dyspnoea. Passage of loose droppings with soiled perineum was observed at 3 hours and 45 minutes followed by gasping (deep laboured inspiration, accompanied by a wheezing sound) and clonic convulsions. These signs were accomplished by loss of other reflexes *i.e.* corneal eyelid closure (touching of cornea causes eyelid to close), myotact (ability of animal to retract its hind limb when limb is pulled down over the edge of surface), righting reflex (loss of reflex to maintain normal upright posture when placed on the back), pupillary reflex (constriction of pupil in presence of light) and startle reflex (response to external stimuli such as touch and noise). The toxicity signs were very pronounced at 4 hours and 30 minutes post-intoxication with soiled perineum, severe salivation, exophthalmos, chromodacryorrhoea, hunched posture and prostration (Fig. 1). The rat died at 5 hours and 35 minutes of oral acephate intoxication. As the rat died following intoxication with 1350 mg acephate/kg body weight, the aforesaid dose was considered as approximate lethal dose for Wistar rats.

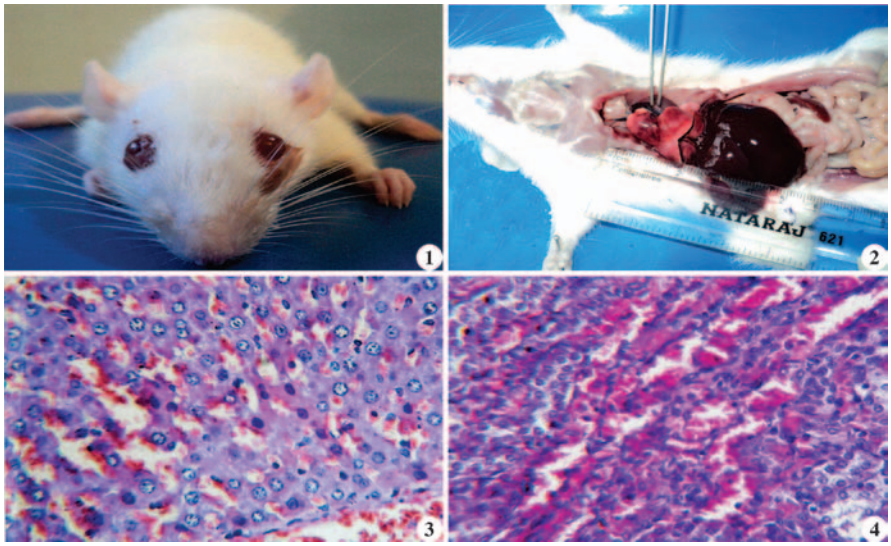

Fig.1. Exophthalmos with chromodacryorrhoea and excessive salivation in female rat exposed to Approximate Lethal Dose of Acephate at 1350 mg/kg body weight, orally; **Fig.2**. Congestion in lung, heart and liver of female rat exposed to Acephate at 1350 mg/kg body weight, orally in acute toxicity study; **Fig.3**. Liver of rat exposed to ALD (Acephate at 1350 mg/kg body weight, orally). Showing haemorrhages in hepatic parenchyma. H&E X400; **Fig.4**. Kidney of rat exposed to ALD (Acephate at 1350 mg/kg body weight, orally). Showing degenerative and necrotic changes of tubular cells and haemorrhages in the intertubular space. H&E X400

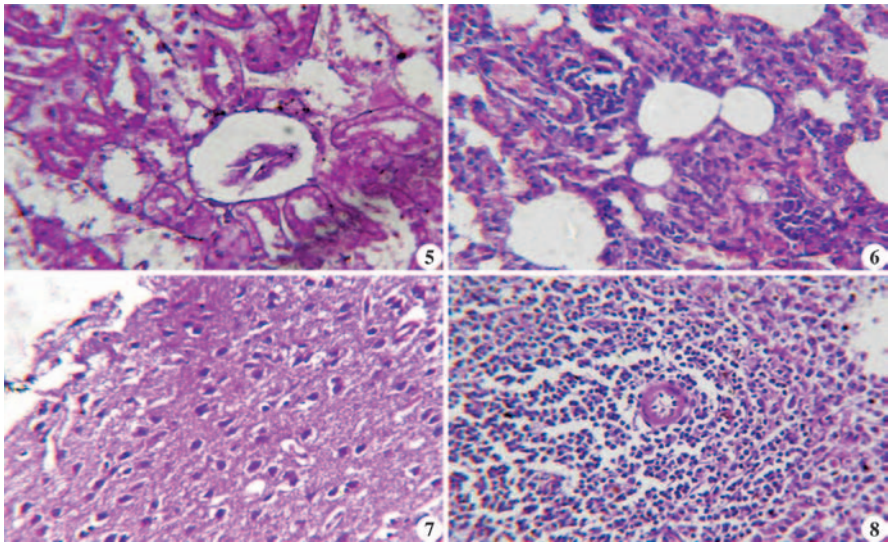

Fig.5. Kidney of rat exposed to ALD (Acephate at 1350 mg/kg body weight, orally). Showing lysis of renal tubular cells and necrosis in the glomerular tuft. H&E X400; **Fig.6**. Lung of rat exposed to ALD (Acephate at 1350 mg/kg body weight, orally). Depicting haemorrhages and thickening of inter alveolar septa. H&E X400; **Fig.7**. Brain of rat exposed to ALD (Acephate at 1350 mg/kg body weight, orally). Showing mild degenerative and necrotic changes in neurons. H&E X400; **Fig.8**. Spleen of rat exposed to ALD (Acephate at 1350 mg/kg body weight, orally). Showing severe depletion in the number of lymphocytes in Malpighian corpuscles. H&E X400.

Pathology of acute acephate toxicity

At necropsy the external examination of the dead female rat showed wet hairs around the mouth, exophthalmos and the soiled perineum region. The pathomorphological changes observed at post-mortem examination of the rat died of acute Acephate toxicity were generalized congestion in the vital organs *i.e.* liver, heart, lungs (Fig. 2), kidneys and brain.

Histopathological screening of the liver sections represented severe degenerative and necrotic changes in hepatocytes along with haemorrhages in the hepatic parenchyma (Fig. 3). There were mild dilatations of sinusoids at places. Histopathology of kidneys revealed pronounced changes in the corticomedullary areas. There were severe haemorrhages in the intertubular spaces (Fig. 4) along with profound degenerative changes in the lining epithelium of proximal convoluted tubules and distal convoluted tubules. In addition to these changes, there was also necrosis in glomerular tuft (Fig. 5).

The representative sections of heart showed mild degenerative and necrotic changes characterized by increased eosinophilia of the cardiac myocytes. Sections of the lung revealed severe congestion and thickening of interalveolar septa with infiltration of erythrocytes (Fig. 6). The histopathological sections of brain showed mild degenerative and necrotic changes in the form of shrunken neurons (Fig. 7). The sections of spleen represented severe depletion of lymphocytes from the Malpighian corpuscles (Fig. 8).

DISCUSSION

The ALD of acephate corroborated closely with the earlier reports[11,12,13]. WHO documented the median oral LD_{50} of acephate in rats as 1000-1400 mg/kg body weight[2]. The other report of the oral LD_{50} of acephate in rats and mice is 360 – 1000 mg/kg body weight[11]. The observed clinical manifestations can be attributed to the inhibition of enzyme acetylcholinesterase in the synapse and neuromuscular junctions. It is moderately toxic to mammals as it gets converted to methamidophos in the body. The common symptoms of acephate poisoning include salivation, nasal discharge, vomiting, diarrhea, nausea, blurred vision, difficulty in breathing, headache, and muscle weakness. Convulsions, coma, and death may occur in cases of severe acute poisoning as reported by earlier coworkers[2,7].

The observations of necropsy in the present investigation were in accordance with the earlier reports[2,5,7,12,13]. The rats exposed to acephate at different dose levels revealed dose dependant pathological changes[12]. Earlier workers[12] further reported that the main target organs affected were found to be liver, kidney, brain and lungs. The pathomorphological changes comprised of varying degrees of congestion, hemorrhages, degeneration, and necrosis in various visceral organs and lysis of lymphoid cells in spleen. Heart, spleen and lung showed congestion and haemorrhages. Prasad and others[13] reported moderate enlargement of liver, pale discoloration and friable consistency. Heart showed petechiae on pericardium and kidneys were swollen and hemorrhagic. Similarly, Londhe and others[14] reported degeneration in liver and kidney of 1/20th of LD50 of acephate treated female rats.

Our findings corroborates well with earlier reports[5,7] who outlined severe damage in hepatic tissue including prominent enlargement of sinusoids, infiltration of mononuclear cell, dilation, hemorrhage and necrosis. They also reported degeneration of glomeruli, Bowman's capsules and associated tubules structure in kidney[5,7]. The histopathological findings in the liver might be due to peroxidation of lipid and tissue damage is the result of induction of oxidative stress due

to excessive generation of free radicals and inhibition of several enzymes involved in ATP generation by the toxicity of pesticides. The mechanism of generation of oxidative stress is related to pesticide biotransformation[15].

Inhalational exposure of acephate in individuals produced pulmonary oedema, haemorrhages, tracheobronchitis and shortness of breath[2]. This clearly indicates direct action of acephate on respiratory tract mucosa and blood vascular system[2]. Moreover, the pathogenesis of tissue damage in acephate toxicity has been attributed to oxidative stress and modification of lipid component of cells as indicated earlier. Cardiac arrest following accidental exposure to high levels of acephate has been attributed to the development of hypocalcaemia and/or hyperkalaemia[15]. The acute lesions in heart might have occurred because of enhanced lipid peroxidation, increased free radical formation and inhibition of various cellular enzymes.

The acute effects of acephate upon the central nervous system could be due to inhibition of enzyme acetylcholinesterase at synaptic junction[13,14,15]. The changes in spleen might be attributed to acute stress imposed by much higher acephate concentration. As reported by earlier workers the main target of organophosphates is central and peripheral nervous system attributed to inactivation of enzyme acetylcholinesterase[16] but acute and subchronic toxicity of organophosphates is also due to disturbance in redox reactions resulting into oxidative stress. The disturbance in the balance between the generation and removal of free radicals within body by organophosphates leads to oxidative stress by production of free radicals such as reactive oxygen species (ROS). The major biomolecules such as proteins, lipids and nucleic acids are attacked by ROS, but lipids are targeted the most and hence lipid peroxidation of cell membranes takes place resulting into pathological lesions.

The results of this study may provide guidelines for selecting doses for subacute and chronic toxicity study of acephate in laboratory rats. Based on the findings of this study, it is concluded that approximate lethal dose of acephate in female Wistar rats is 1350 mg/kg body weight, orally. The important clinical signs included depression, dyspnoea, chromodacryorrhoea, piloerection, hunched posture, profuse salivation, clonic convulsions and loss of various reflexes. Exposure to the acute toxic dose of acephate causes various histopathological alterations in visceral organs indicating its hepatotoxic, nephrotoxic, neurotoxic, pulmonary and cardiotoxic potential. Lack of biochemical evaluation following acephate exposure in Wistar rats is the key limitation of the present investigation. Moreover, continued investigation into the toxicological potential of pesticide residue is vital to deepen our scientific understanding, inform public health strategies, regulatory policies, and sustainable farming practices aimed at protecting both health of human and livestock and also the environment.

ACKNOWLEDGEMENT

The authors are thankful to Dean, College of Veterinary Science and A.H., DSVCKV, Anjora, Durg, C.G for providing necessary facilities to carry out the work.

Financial support & sponsorship: None

Conflicts of Interest: The authors report no conflict of interest.

Use of Artificial Intelligence (AI)- Assisted Technology for manuscript preparation: The authors confirm that there was no use of AI-assisted technology for assisting in the writing of the manuscript and no images were manipulated using AI.

REFERENCES

1. Mulla SI, Ameen F, Talwar MP, Eqani SAMAS, Saxena RNBG, Tallur PN. 2020. Organophosphate pesticides: impact on environment, toxicity, and their degradation, In: Bharagava RN, Saxena S. eds *Bioremediation of Industrial Waste for Environmental Safety* Cham: Springer.
2. World Health Organization. 2005. Pesticide residues in food – 2005, Report of the Joint Meeting of the FAO Panel of Experts on Pesticide Residues in Food and the Environment and the WHO Core Assessment Group on Pesticide Residues Geneva, Switzerland, 20–29 September 2005.
3. Ribeiro TA, Prates KV, Pavanello A, Malta A, Tófolo LP, Martins IP. 2016. Acephate exposure during perinatal life program to type 2 diabetes. *Toxicol*. **372**: 12-21.
4. Spassova D, White T, Singh AK. 2000. Acute effects of acephate and methamidophos on acetylcholinesterase activity, endocrine system and amino acid concentrations in rats. Comparative Biochemistry and Physiology-- Part C: *Pharmacol. Toxicol. Endocrinol*. **126**(1): 79-89.
5. Jain E, Vashishat N. 2003. Toxicity of acephate to liver and kidney of female Wistar rats. *Indian J Entomol* **85**(2): 322-326.
6. Singh AK, Jiang Y. 2002. Immunotoxicity of acute acephate exposure in control or IL-1-challenged rats: correlation between the immune cell composition and corticosteroid concentration in blood. *J. Appl. Toxicol*. **22**: 279–291.
7. Karanth S. 2014. Acephate In: Wexler P. ed. *Encyclopedia of Toxicology* 3rd edn. Academic Press.
8. Hayes AW. 2001. Principles and methods of Toxicology. Philadelphia: Tylor and Francis.
9. Luna LG. 1972. Manual of histological staining methods of the Armed Forces Institute of Pathology. Philadelphia: W. B. Saunders.
10. Bancroft JD, Stevens A. 1990. Theory and Practice of Histological Techniques. Edinburgh: Churchill Livingstone. 113-305.
11. Gupta PK, Moretto A. 2005. A draft on acephate (addendum). Proceedings. Joint meeting on pesticide residues. 3-16.
12. Bhadaniya AR, Kalariya VA, Joshi DV, Patel BJ, Chaudhary S, Patel HB, Patel JM, Patel UD, Patel HB, Ghodasara SN, Savsani HH. 2015 . Toxicopathological evaluation in Wistar rats (*Rattus norvegicus*) following repeated oral exposure to acephate. *Toxicol Indus Health*. **31**(1): 9–17.
13. Prasad MS, Babu KR, Ravikanth SV, Narender P, Jacob DP.

2013. Alterations in the acetylcholinesterase activity in the brain of albino mice exposed to acephate. *The Bioscan* **8**(3): 1039-1041.

14. Londhe SA, Gangane GR, Moregaonkar SD. 2020. Subacute toxicity assessment of acephate and it's amelioration by *Picrorhiza kurroa* in female wistar rats. *Int J Curr Microbiol Appl Sci* **9**(12): 3242-3250.
15. Lin Z, Pang S, Zhang W, Mishra S, Bhatt P, Chen S. 2020. Degradation of acephate and its intermediate methamidophos: mechanisms and biochemical pathways. *Front Microbiol* **11**:2045.
16. Ndonwi EN, Atogho-Tiedeu B, Lontchi-Yimagou E, Shinkafi TS, Nanfa D, Balti EV, Indusmita R, Mahmood A, Katte J, Mbanya A, Matsha T, Mbanya JC, Shakir A, Sobngwi E. 2019. Gestational exposure to pesticides induces oxidative stress and lipid peroxidation in offspring that persist at adult age in an animal model**.** *Toxicol Res* **35**: 241-248.

Indian J. Vet. Pathol., 50(4) : 353-360, 2026: DOI: https://doi.org/10.56093/pmsq3f71

RESEARCH ARTICLE

PET-CT imaging, gross & microscopic features in systemic microsporidial diseases in laboratory rabbits

Yogita Shete*, Abhishek Gupta, Sutapa Rakshit and Sandip Basu
Radiation Medicine Centre, BARC, C/o TMH Annexe, Parel, Mumbai- 400 012

***Address for correspondence**
Dr. Yogita Shete, E-mail: yogeshwarivet@gmail.com
ORCID ID: 0000-0001-8594-9183

Received: 20.5.26; Accepted: 25.6.26

ABSTRACT

Encephalitozoon cuniculi can cause latent disease, especially in lagomorphs, and many wild and domestic animals in various countries. This infection is important for veterinary and public health because it is caused by a potentially zoonotic and opportunistic pathogen. This study investigated subclinical disease pathology in rabbits by comparing findings from Positron Emission Tomography-Computed Tomography imaging with serological titres in rabbit samples. which may be useful in early predicting the disease in clinically healthy rabbits. A total of 4 animals showing higher serological titres had undergone for PET-CT imaging. Rabbits that developed symptoms and had a positive titre were euthanized, and a necropsy was conducted (n=2). Serum creatinine levels were quantified, and histopathological analyses were performed on all vital organs from the affected rabbits. PET-CT imaging showed increased brain, focal liver and kidneys uptake were significantly higher in seropositive animals. Gross lesions showing brain congestion, necrotic kidney with grey cloudy urine were further confirmed of infection by necropsy. Histopathological findings in the kidney, degenerative changes and *Encephalitozoon cuniculi* spores were identified in the tubule and brain. Elevated levels of serum creatinine levels were found to have a significant relationship with the serological status and PET-CT imaging findings in the affected rabbits. This study revealed that PET-CT imaging would be useful for the evaluation of early changes in subclinical infection of the rabbits with *Encephalitozoon cuniculi* in conjunction with the routine ELISA method to increase diagnostic accuracy, & valuable adjunct to clinical interpretation for timely treatment in these laboratory animals.

Keywords: PET-CT Imaging, ELISA, Histopathology, Zoonosis, Laboratory Animals, Encephalitozoonosis, Gross features

INTRODUCTION

Encephalitozoonosis is a zoonotic, microsporidian parasitic disease that affects a wide range of hosts, including humans, dogs, non-human primates, rodents, and birds[1,2,3]. The causative agent, *Encephalitozoon cuniculi* (*E. cuniculi*), is an obligate intracellular spore-forming protozoan parasite (phylum Microsporidia). First identified in a laboratory rabbit in the USA in 1922[4], this infection is now common in domestic and laboratory rabbits worldwide, with clinical signs predominantly have been reported primarily in rabbits.[5&6] Furthermore, the disease has gained increasing attention due to its zoonotic potential[7,8,17].

The form of disease is apparent as chronic and subclinical in nature. In rabbits, *E. cuniculi* mainly affect CNS, renal and ocular system, show neurological signs, chronic renal failure or uveitis.[9] Most common findings reported in the clinical cases are vestibular signs, circling and paresis. However, *E. cuniculi* infective sporont escapes from the immune system, and continues germination progress and reaches at chronic stage in infected animals.[7] Therefore, seropositive cases and clinical signs do not concur.[3,10] Therefore, the confirmatory diagnosis of disease is difficult based on clinical signs.

The grading and distribution of microscopically developed lesion related with *E. cuniculi* infection are partially correlated with clinical signs and in some animals though histologically positive, does not produce any clinical sign of the disease[11]. The previous reports showed many rabbits persevere subclinical form of disease for months together. Post-brain inflammation and infection, infected rabbits exhibit clinical signs, torticollis, paresis and longitudinal rolling the animal is often incapable to cure themselves.

How to cite this article: Shete, Y., Gupta, A., Rakshit, S. and Basu, S. 2026. PET-CT imaging, gross & microscopic features in systemic microsporidial diseases in laboratory rabbits. Indian J. Vet. Pathol., 50(4) : 353-360.

This is unique microsporidia disease once the clinical signs developed, it is very difficult to clinically manage the animals and to restore the normal function. Hence early diagnosis of the disease is very important to provide the appropriate treatment to the animals.

Therapeutic options for *E. cuniculi* infections are scarce. Fenbendazole, an antiparasitic agent, effectively inhibits parasitic replication and curtails disease progression, making it highly valuable for prophylaxis

and early intervention. Nevertheless, it does not repair existing neurological or ocular lesions. Consequently, management during the clinical torticollis stage is strictly supportive, given the absence of a specific curative therapy to reverse the CNS damage inflicted by the parasite. Early diagnosis is critical to stop systemic spread and organ damage[11].

Nuclear medicine imaging with Positron Emission Tomography-Computed Tomography (PET-CT) & Single Photon Emission Computed Tomography is relatively underutilized in laboratory animal diagnostics due to regulatory causes, cost, and expertise limitations, despite its superior capacity for early disease detection. Fluorodeoxyglucose - PET-CT imaging is recognized as an indispensable, high-accuracy tool for diagnosing and staging numerous cancers[12]. Positron-emitting radioisotopes allow for the non-invasive, in vivo, and quantitative mapping of molecular, biochemical, and pathological processes. *E cuniculi* infection also follows the same path, early diagnosis is crucial for planning treatment ahead, leading to improved outcomes.

Diagnosis of *E. cuniculi* infection in rabbits requires a comprehensive approach because of the high prevalence of asymptomatic carriers[13]. Conventional diagnostic methods include physical examination and analysis of blood, urine, and faecal samples in live animals, while definitive diagnosis in deceased animals relies on systematic necropsy, histopathology, and Gram staining of tissues[14]. However, these methods may fail to detect early lesions and subclinical systemic abnormalities *in vivo*. PET-CT is a non-invasive imaging modality that provides anatomical and functional information, enabling sensitive detection of focal and multifocal lesions, even in asymptomatic animals. Therefore, PET-CT may offer comprehensive *in vivo* assessment of disease dissemination. The present study evaluated the prevalence of subclinical disease in a conventional rabbit colony using ELISA and correlated the findings with clinical signs and whole-body PET-CT imaging. In clinically affected rabbits, PET-CT findings were further correlated with histopathological changes to assess the extent of organ involvement.

MATERIALS & METHODS

Animal species selected

Researchers routinely brought different rabbits to the facility for experiments approved under various projects (BAEC/02/22, BAEC/23/24). As routine veterinary care involves monitoring animals for illness, with suspected cases set aside for comprehensive diagnostic evaluation. For this study, the New Zealand White rabbits (n=9; both male and female rabbits) were included under routine health monitoring of the housed animals. All the animals first underwent clinical examination. Blood samples were collected for hematology and ELISA test. Animals suspected clinically (n=1) were segregated and put for imaging and testing to evaluate and diagnose the disease condition.

Sample Analysis

ELISA of rabbit serum samples were tested for the detection of *E. cuniculi* antibodies using a commercial ELISA kit (Medicago AB-18-9001, Sweden). A total of nine (n = 9) serum samples were analysed in duplicate. Indirect ELISA was performed according to the manufacturer's protocol. Briefly, antigen-coated polystyrene microplates were washed with PBS-T, and sample positions were recorded on the ELISA worksheet before sample processing. The plate was sealed and incubated at room temperature (RT) for 60 minutes. It was then washed three times with 350 µL PBS-T per well and tapped upside down on a paper towel. Subsequently, 100 µL of diluted HRP-conjugated antibody was added to each well and incubated at RT for 30 minutes. The plate was washed again three times with 350 µL PBS-T. Conjugate binding was performed by adding 100 µL of diluted HRP-conjugated antibody to each well and incubating the plate in the dark at RT for 30 minutes, followed by three washes with 350 µL PBS-T. Finally, the substrate reaction was initiated by adding 100 µL of TMB substrate to each well, and the plate was incubated at RT for 15 minutes until colour development was observed. The enzymatic colour reaction was stopped by adding 50µl stop solution/well (colour turns yellow) and the optical density was read at 450 nm using a microplate reader. Results were analysed by comparing samples with positive and negative controls. For valid interpretation, the mean negative control absorbance for both control antigen- and EC antigen-coated wells was required to be ≤0.200 OD, while the positive control absorbance for EC antigen-coated wells was required to be >0.800 OD (A450). The sample ratio was calculated as A450 (EC-coated well)/A450 (control antigen-coated well). Samples with a ratio >2 were classified as positive for EC antibodies, whereas samples with a ratio <2 were classified as negative for EC antibodies[15].

Animal PET-CT imaging

PET-CT imaging was performed using a GEMINI TF 16-slice PET-CT scanner. Animals were restrained by intramuscular administration of ketamine (22–80 mg/kg body weight) and xylazine (5 mg/kg body weight). Imaging was acquired using a standard protocol (Serview: 90 kV, 20 mA; CT: 120 kV, 80 mA; PET: 1 min emission/bed). Approximately 1 mCi of 18F-FDG was administered intravenously, and imaging was performed 1 h post-injection. Data were reconstructed using the Row-Action Maximum Likelihood Algorithm (RAMLA), and coronal, sagittal, and transverse images were qualitatively analysed[5,16].

Necropsy findings, and histopathological analysis

Blood samples were collected from rabbits (n = 9) via the ear vein for serological analysis. Animals exhibiting torticollis, neurological signs, and compromised daily activity were euthanized using an overdose of anaesthetics. A complete necropsy was performed to identify pathological lesions in vital organs. The brain, liver, kidneys, and lungs were collected, fixed in 10% neutral buffered formalin, and processed for histopathology. Light microscopic examination was performed to identify and confirm the presence of microsporidia in the tissues[17,18,19].

RESULTS

Clinical diagnosis

In-house screening including serum ELISA testing was performed on all facility-housed New Zealand White rabbits. Subsequently, a physical examination was conducted post-sample collection. All animals appeared clinically healthy, except for one that presented with anorexia and a slight neck tilt, which underwent a whole-body PET-CT scan (Fig.1).



Fig.1. Clinical signs and gross necropsy features. (a) Neck twisting exhibited by the rabbit; **(b)** Necropsy showing abnormally kidney with distended urinary bladder, liver and lung congestions.

Gross and microscopic pathological findings

Central Nervous System (CNS) lesion

Gross examination of the brain revealed diffuse cerebral congestion, multifocal haemorrhages, and focal degenerative lesions. Histopathology showed vascular congestion, perivascular lymphocytic infiltration, glial nodules, astrogliosis, parasitic cysts, neuronal degeneration and necrosis, and vacuolation around cells. Gliosis around pyramidal cells and degeneration of Purkinje cells were also observed. *E. cuniculi* meronts in H&E-stained sections. These findings were consistent with encephalitis (Fig.2).

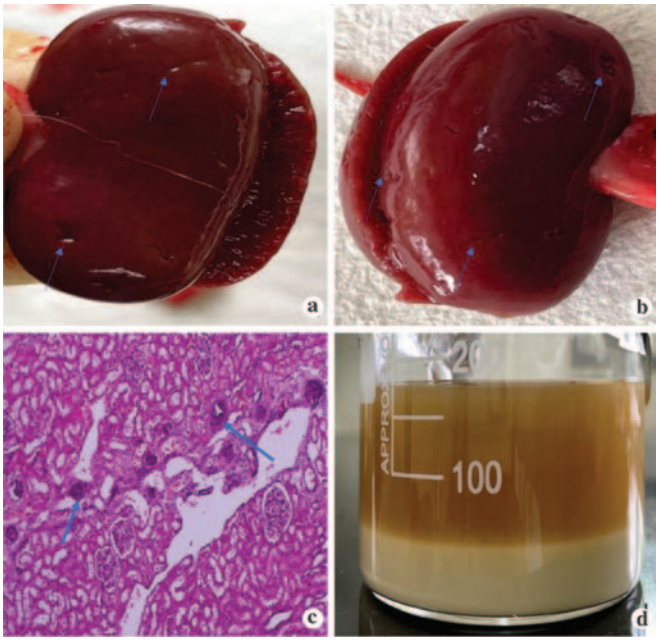

Fig.3. Kidney lesions Grossly multifocal contracted kidneys **(a&b)**; **(c)** Histopathology showed atrophy of glomeruli and tubular swelling and multifocal area inflammatory cell infilteration H&E x100; **(d)** Cloudy yellow dark coloured urine.

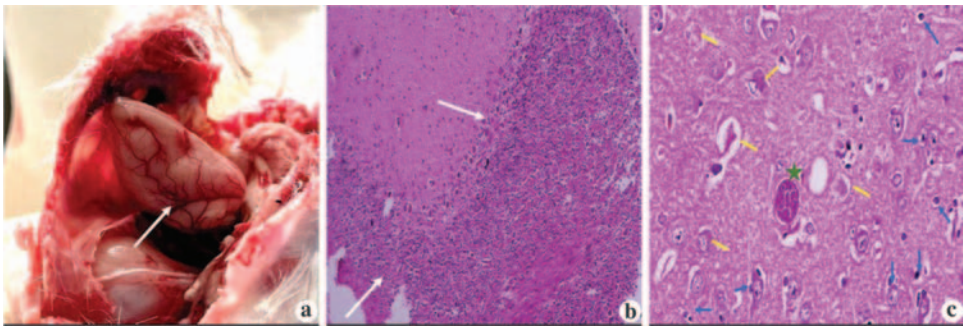

Fig 2: Brain encephalitis: gross & microscopy lesion (a) Grossly showed engorged blood vessels; **(b)** Histopathology showed multifocal area of infiltration of glial cells with neuronal degeneration under 100x stained with H&E stain; **(c)** Rabbit *Encephalitozoon Cuniculi* Brain Lesion charcateristics: Neuron degeneration and necrosis (line), single or multiple large vacuoles visible around cells, multifocal area of gliosis (arrow) around pyramidal cells and degeneration of Purkinje cells. Round parasitophoro vacuoles with *E. Cuniculi* organism (star) H&E x400.

Kidney and liver lesions

Gross examination revealed bilateral renal coloration ranging from dark to pale, with minor adhesion of the capsule to the cortex and multiple superficial, punctate subcapsular pits. The urinary bladder was significantly distended, containing concentrated, foul-smelling, dark yellow urine. Histopathology reveals multifocal tubulointerstitial changes, including tubular degeneration, swelling, and atrophy of the glomeruli,

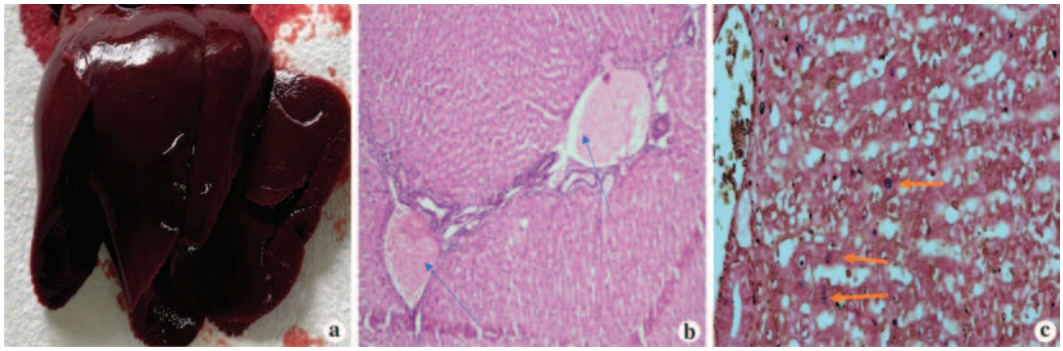

Fig. 4. **Liver lesions. (a)** Grossly liver showed diffuse congesion in all lobes and oosing of blood on cut surface; **(b)** Histopathology presented hepatic degenerative changes with Central and portal vein congestion with multifocal area of infiltration of MNC & PNC infiltration of inflammatory cells under 40x stained with H&E stain.; **(c)** Gram staining of liver section showed Gram positive spores of *E. Cuniculi* in the liver (arrow) H&E x100.

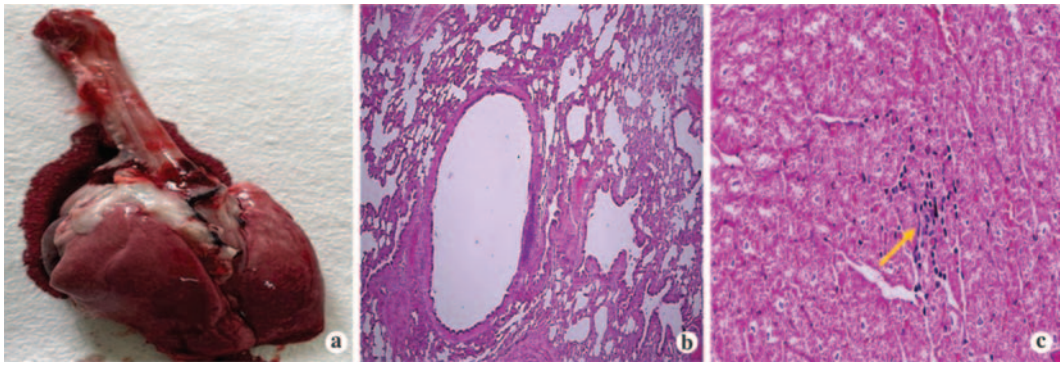

Fig.5. Lung lesions. (a) Lungs grossly showed diffuse congestion of all lobes; **(b)** Histopathology showed interstitial pneumonia and diffuse congestion and infiltration of inflammatory cells. under 40x stained with H&E stain; **(c)** Heart illustrated myofibrillar degeneration, focal necrosis, and mononuclear cell infiltration(yellow arrow) H&E x400.

consistent with nephritis. Serum creatinine level showed 2.8–3.0 mg/dL in clinically positive cases. Microscopic analysis showed few pus cells, epithelial casts, and calcium carbonate crystals, accompanied by high protein levels.

Diffuse congestion of all liver lobes, with profuse oozing of blood from the cut surface, indicative of chronic passive congestion. Hepatic histopathology showed degenerative changes with congestion of the central and portal veins, alongside multifocal MNC (mononuclear cell) and PNC (polynuclear cell) inflammatory infiltration. Encephalitozoon spores were identified

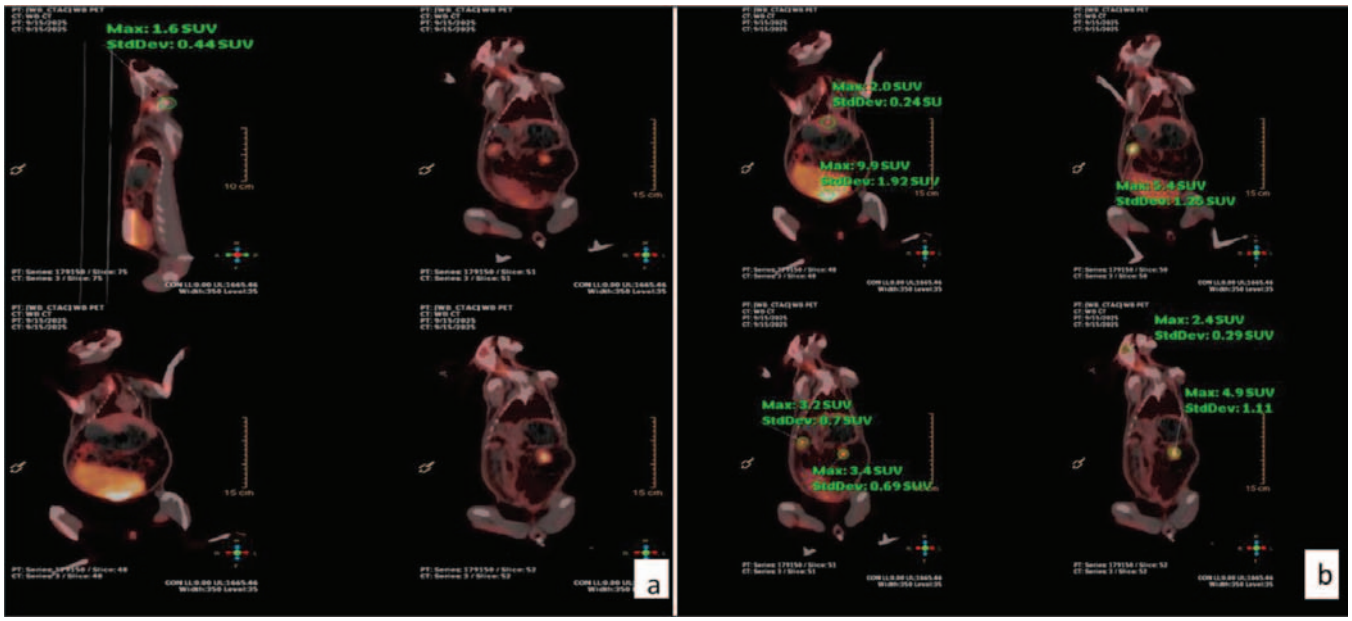

Fig. 6. Whole body PET-CT image in rabbit. (a&b) Quantitative imaging analysis of the PET/CT rabbit images demonstrated variable radiotracer uptake across different organs and anatomical regions. Whole-body PET/CT fused images demonstrated the radiotracer's biodistribution across various anatomical regions in the rabbit, with focal uptake noted in the cervical paraspinal and cervical lymphoid tissues. Prominent uptake and retention were observed in both the liver and kidneys. Quantitative assessment was performed using Standard Uptake Value (SUV) measurements obtained from regions of interest (ROIs) marked on the images.

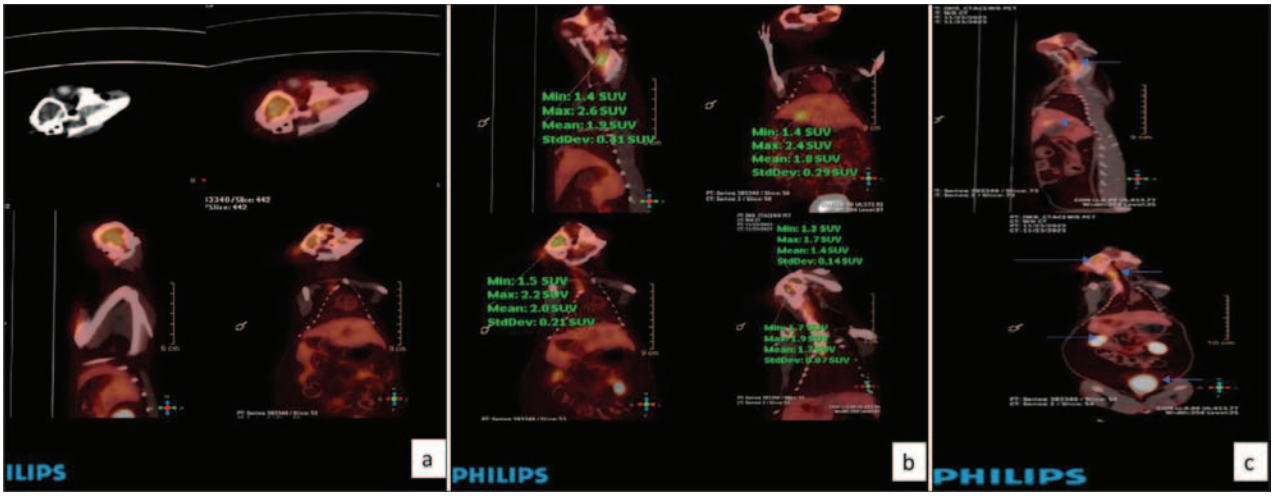

Fig. 7. Whole body PET-CT image in rabbit. Quantitative imaging analysis of the PET/CT rabbit images demonstrated variable radiotracer uptake across different organs and anatomical regions; **(a&b)** Intense brain, liver, kidney and bladder uptake seen in body, **(c)** Multifocal brain, liver, and cervical spinal cord(blue arrow) uptake seen in rabbit PET-CT image rabbit.

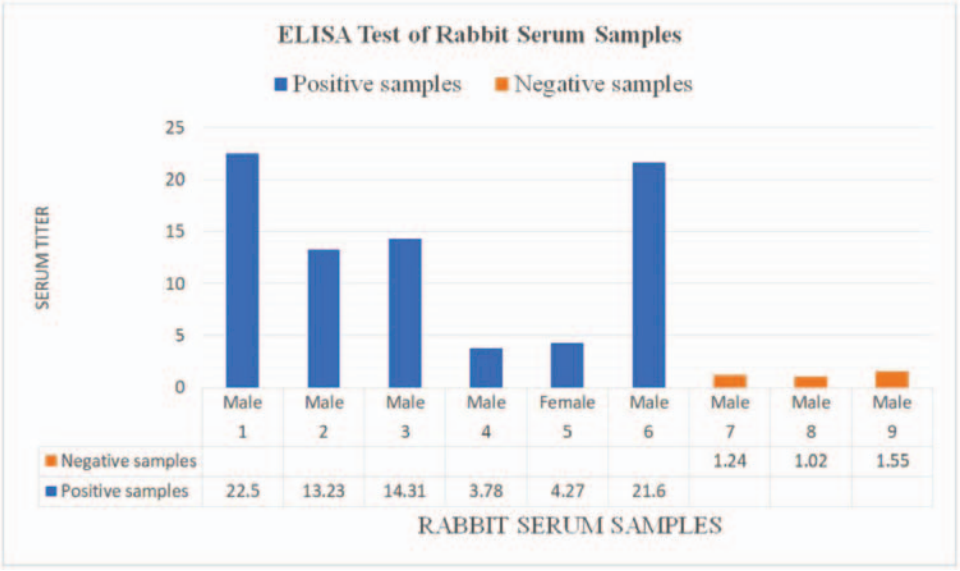

Fig. 8. Rabbit serum sample analysis results by ELISA method showed positive titre and negative titres.

within the liver sections via Gram staining (Fig.3, 4 and 9).

Heart and lung lesions

Grossly, the heart appeared normal; however, microscopic examination revealed patchy myofibrillar degeneration with focal necrosis and mononuclear cell infiltration. The lungs showed diffuse congestion grossly, while histopathology revealed interstitial pneumonia with inflammatory cell infiltration of the alveolar septa (Fig. 5,9).

PET-CT imaging

PET/CT imaging revealed inflammatory changes in the cervical region involving the cervical lymph nodes, paraspinal tissues, and cervical spinal musculature. Both kidneys and an abnormally distended urinary bladder showed increased radiotracer uptake (SUVmax: 9.9 ± 1.92). Focal uptake was also observed in the brain (2.4 ± 0.02 SUVmax), cervical neural structures (2.6 ± 0.41 SUVmax), and liver (2.0 ± 0.24 SUVmax), with mild radiotracer retention in the kidneys (5.4 ± 1.25 and 4.9 ± 1.10 SUVmax) (Figs. 6, 7 and 9). Clinically ill and sub-clinically affected rabbits with high serum titres were treated with fenbendazole, along with anti-inflammatory drugs and fluid therapy according to their clinical condition. However, fenbendazole was ineffective in reversing established neurological lesions, and supportive treatment failed to restore normal posture. Owing to a guarded prognosis, the affected animal was humanely euthanized and subjected to a detailed necropsy.

Serological test result

High levels of specific *E. cuniculi* antibodies were detected in infected rabbits, including seropositive but clinically asymptomatic animals (Fig. 8). ELISA titres differed markedly between positive and negative groups. Positive samples (n = 6) showed titres ranging from 3.78 to 22.50, with a mean of 13.28 ± 8.08, whereas negative samples (n = 3) ranged from 1.02 to 1.55, with a mean of 1.27 ± 0.27 (Table 1). An independent Student's *t*-test demonstrated that the mean

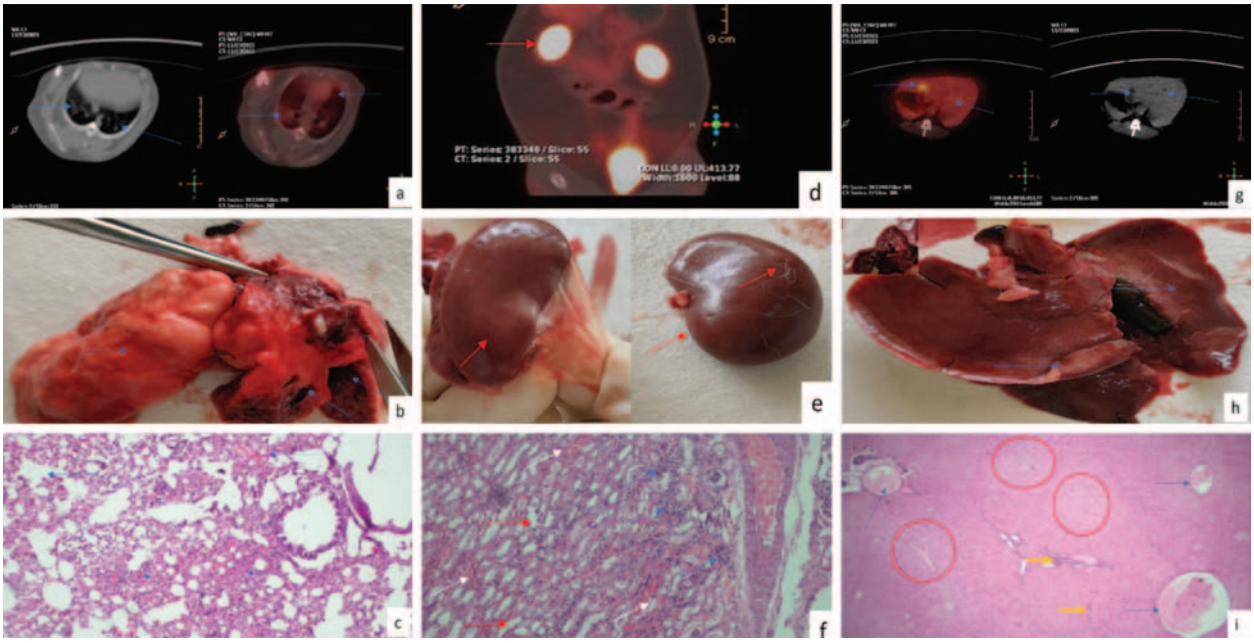

Fig. 9. Rabbit *E. Cuniculi* infection with lesion in lung, kidney and liver with PET-CT imaging. (a) PET-CT showed a prominent bright pink area of high metabolic activity in lung (blue arrow); **(b)** Gross Morphology of lung displays dark red consolidation.; **(c)** Histopathology of lung revealed marked thickening of the alveolar septa and infiltration of inflammatory cells (Hematoxylin and Eosin, 40x); **(d)** PET/CT Scan showed bright areas indicating regions of intense FDG uptake and retention in both the kidneys and bladder**; (e)** Gross morphology of kidney showed multifocal areas of pitting and a contracted kidney**; (f)** Histopathology of kidney showed tubular dilation (red arrow), necrosis, severe interstitial vascular congestion (white arrow), and infiltration of inflammatory cells (blue arrow) (Haematoxylin and Eosin, 40x); **(g)** PET-CT of liver revealed a focal bright yellow spot indicating increased uptake of the radioactive tracer; **(h)** Gross morphology of liver organ presented with hepatomegaly, showing congestion across all lobes and multifocal pale foci on the left lobe (blue arrow); **(i)** Histopathology of Liver exhibited central and portal vein congestion (blue arrow) and panlobular hepatocellular degeneration. Multiple hepatocytes appeared prominently swollen with pale, cleared cytoplasm (circle). Multifocal clusters of inflammatory cells were also present (yellow arrow) (H&E, 40x).

Table 1. ELISA results for sample processed for *E. cuniculi* infection.

Rabbit No	Positive Titre (Mean value : 13.28±3.3)	Negative Titre (Mean value : 1.27±0.15)
Rabbit 1		1.55
Rabbit 2	22.50	
Rabbit 3	13.23	
Rabbit 4	14.31	
Rabbit 5		1.02
Rabbit 6	3.78	
Rabbit 7	4.27	
Rabbit 8		1.24
Rabbit 9	21.60	
Total	N = 6	N = 3

titre of positive samples was significantly higher than that of negative samples (t = 3.64, p = 0.015). These findings confirm a strong serological response and the presence of *E. cuniculi* infection in seropositive rabbits.

DISCUSSION

Diagnosis of *E cuniculi* infection is the challenging for the veterinarian in the field as well as in captive laboratory animals due to their natural propensity of hiding the signs and symptoms[20,21]. A primary goal of recent veterinary research is to improve the accuracy of antemortem diagnosis by exploring advanced techniques, such as PCR and in-vivo imaging to better differentiate between exposure and active infection[22].

Generally, *E. cuniculi* infected rabbits act as asymptomatic carriers for prolonged periods, yet the progression of the parasite can lead to rapid, severe neurological manifestations in otherwise healthy animals[23]. Consequently, thorough clinical history and physical examination are essential for detecting early signs of sickness behavior in laboratory rabbits[24]. Therefore, early diagnosis of *E. cuniculi* relies heavily on attentive clinical evaluation, including monitoring feed intake and weight loss, which are essential for identifying active infections[25-27]. These clinical observations essential for isolating sick rabbits concurred with our findings.

The rabbit exhibited torticollis and longitudinal rolling, characteristic of central vestibular disease and consistent with chronic *E. cuniculi* infection, which commonly manifested with these signs[17,28]. Furthermore,

the observed neurological deficits were often associated with *E. cuniculi* induced renal insufficiency, characterized by elevated serum urea and abnormal phosphorus levels[29,30].

Subclinical *E. cuniculi* infection hindered progressive weight gain, making it a critical indicator for herd managers to detect and isolate affected animals, alongside clinically positive cases.[31] Prompt diagnosis, control measures, and timely treatment of systemic *E. cuniculi* reduce morbidity and mortality in laboratory rabbits. Historically, ELISA has been the established serological method for this diagnosis. Serological analysis in screed rabbits showed that elevated IgG with variable concentration, serves as a marker for recovering or chronic phase of disease. However, published literature showed that both IgM and IgG used in detection of *E. cuniculi* infection. The elevated IgM served as a marker of acute infection, whereas elevated IgG was typical of the convalescent or chronic phase[22,32].

Hybrid nuclear medicine imaging PET-CT, coupled with appropriate radiotracers, delivers superior, integrated anatomic-functional, comprehensive diagnostic information, surpassing the clinical utility of conventional structural or functional imaging techniques. An established in-*vivo* PET-CT imaging method is a very beneficial modality in diagnosis of systemic spread of the infection with help of ^{18}F-FDG radiotracer[33]. This well-established real time imaging methodology was explored in understanding of pathology for *E. cuniculi* disease. The detection of focal hypermetabolism at the junction of the brainstem and upper cervical spine (C1) in PET-CT imaging suggested an underlying lesion, which aligned with the clinical presentation of torticollis in the animals, further higher serological titer and histopathological lesion with parasitic cyst supported confirmatory disease diagnosis of *E. cuniculi.* PET-CT imaging revealed, in addition to cerebral involvement, distinct lesions in the liver, kidneys, and urinary bladder. Kidney associated renal retention and abnormal extended bladder suggestive of nephritis. These findings correlated with the histopathological observations. PET-CT scan findings indicated high metabolic activity in the brain, kidneys, and liver in cases of encephalitozoonosis, which aligned with earlier reported observations of multi-organ dissemination[34]. The intensification of focal radiopharmaceutical uptake was driven by the underlying pathophysiology of inflammation and increased blood supply, enabling the detection of metabolically active tissue areas.[33] Imaging findings suggesting that *E. cuniculi* caused complex, multi-organ disease in rabbits, clinicians must always address this systemic involvement in their treatment protocols.

While conventional serology confirms exposure to *E. cuniculi*, it did not reflect the severity of infection, making clinical diagnosis difficult. Given the long, silent, and often subclinical nature of the infection, ^{18}F-FDG radiotracer imaging represented a valuable step forward in antemortem diagnosis. PET-CT enabled high-accuracy mapping of active granulomatous lesions, allowing practitioners to pinpoint affected organs and determine the true systemic extent of encephalitozoonosis.

Histological findings in the liver, kidney, lung, and heart confirmed the PET-CT imaging results and are in line with earlier reports[17,35]. Furthermore, these observations aligned with established literature indicating that *E. cuniculi* induced lesions were frequently confirmed through histopathology in rats, mice, rabbits, and hamsters.

CONCLUSION

Consequently, PET-CT nuclear imaging techniques represent an advanced method for the diagnosis of diseased conditions in laboratory models. Advanced imaging modalities enable the early detection of pathological changes in preclinical models, facilitating statistically significant data collection throughout the disease process. The combined use of PET-CT or CT imaging with standard monitoring techniques offers much deeper insight and effective diagnostic ways to prevent deterioration conditions of laboratory animals. Further confirmatory diagnosis is supported by histopathology and special gram stain. As a highly sensitive and non-invasive technique, nuclear imaging, when combined with histopathology, serves as a rapid, effective diagnostic tool for identifying fatal, chronic, and challenging disease conditions in animals. However, the need for specialized facilities and specific configurations to handle radioactivity represents a major obstacle for its use in veterinary diagnostics.

ACKNOWLEDGEMENT

The study was conducted at the Animal House Facility, Department of Radiation Medicine Centre, with technical support provided by the facility staff, Bhabha Atomic Research Centre (BARC), Parel, Mumbai.

Financial support and sponsorship: Yes

Conflict of interest: None

Use of artificial intelligence for manuscript preparation: The author confirms that there was no use of AI-assisted technology for assisting in the writing of the manuscript and no images were manipulated using AI.

REFERENCES

1. Magalhaes T, Pinto F, Queiroga F. 2022. A multidisciplinary review about Encephalitozoon cuniculi in a One Health perspective. *Parasitol Res* **121:** 2463-2479.
2. Han B, Weiss L. 2017. Microsporidia: obligate intracellular

pathogens within the fungal kingdom. *Microbiol Spectr* **5:**10-1128.
3. Deplazes P, Mathis A, Baumgartner R, Tanner I, Weber R. 1996. Immunologic and molecular characteristics of Encephalitozoon-like microsporidia isolated from humans and rabbits indicate that Encephalitozoon cuniculi is a zoonotic parasite. *Clin Infect Dis* **223**:557–559.
4. Shadduck J, Pakes S. 1971. Encephalitozoonosis (nosematosis) and toxoplasmosis. *The Am J pathol* **64**: 657-672.
5. Shete Y, Bhatkar P, Bagul S, Rakshit S, Baghel N, Basu S. 2024. Use of nuclear medicine imaging for diagnosis of spontaneous disease conditions in laboratory animals. *Indian J Vet Pathol* **48**: 364-371.
6. Ozkan O, & Alcigir M. 2018. Subacute stage of Encephalitozoon cuniculi infection in eye lesions of rabbit in Turkey. *Iran J Parasitol* **13**: 301-309.
7. Mathis A, Weber R, Deplazes P. 2005. Zoonotic potential of the microsporidia. *Clin Microbiol Rev* **18**:423–425.
8. Al-Sadi H, Al-Mahmood S. 2014. Pathology of experimental Encephalitozoon cuniculi infection in immunocompetent and immunosuppressed mice in Iraq. *Patholog Res Int* **2**: 857036.
9. Jordan CN, Zajac AM, Lindsay DS. 2006. Encephalitozoon cuniculi infection in rabbits. Compendium on continuing education for the practising veterinarian-north American edition **28**:108-116
10. Valencakova A, Halanova M, 2012. Immune response to Encephalitozoon infection review. *Comp Immunol, Microbiol Infect Dis* **35**:1-7.
11. Abu-Akkada SS, Oda SS. 2016. Prevention and treatment of Encephalitozoon cuniculi infection in immunosuppressed rabbits with fenbendazole. *Iran J Vet Res* **17**: 98–105.
12. Hoskinson J, Tucker L. 2001. Diagnostic imaging of lameness in small animals. *Vet clin North Am Small Anim Pract* **31**:165-180.
13. Leblanc A, Peremans K. 2014. PET and SPECT imaging in veterinary medicine. *Semi Nucl Med* **44**: 47-56.
14. Yitbarek D, Dagnaw G. 2022. Application of advanced imaging modalities in veterinary medicine: A review. *Vet Med Res Rep.***13***:* 117-130.
15. Cray C, Arcia G, Schneider R, Kelleher S, Arheart K. 2009. Evaluation of the usefulness of an ELISA and protein electrophoresis in the diagnosis of *Encephalitozoon cuniculi* infection in rabbits. *Am J Vet Res* **70**: 478–482.
16. Phelps M. 2000. Positron emission tomography provides molecular imaging of biological processes. *ProcNatl Acad Sci* **97:** 9226-9233.
17. Gruber A, Pakozdy A, Weissenbock H, Csokai J, Kunzel F, 2009. A retrospective study of neurological disease in 118 rabbits. *J Comp pathol* **140**:31-37.
18. Frohlich J. 2020. Rats and mice. *Ferrets, rabbits, and rodents* 345-367.
19. Brar R, Sandhu H and Singh A. 2002. Veterinary clinical diagnosis by laboratory methods, Kalyani Publisher, India.
20. Calisi, R.M. and Bentley, G.E., 2009. Lab and field experiments: are they the same animal. *Horm Behav* **56**:1-10.
21. Bays TB, 2012. Behaviour of small mammals. In *Ferrets, Rabbits, and Rodents.* WB Saunders 545-556.
22. Doboși AA, Paștiu AI, Bel LV, Pop R, Tabaran AF, Pusta DL. 2024. Antemortem and postmortem diagnosis of encephalitozoon cuniculi in a pet rabbit (Oryctolagus cuniculus)-A case report. *Pathogens* **13**:1122.
23. Doboși AA, Bel LV, Paștiu AI, Pusta DL. 2022. A review of *Encephalitozoon cuniculi* in domestic rabbits (*Oryctolagus cuniculus*)-Biology, clinical signs, diagnostic techniques, treatment, and prevention. *Pathogens* **11**:1486.
24. Weary D, Huzzey J, Von Keyserlingk M. 2009. Board-invited review: Using behavior to predict and identify ill health in animals. *J Anim Sci* **87**:770-777.
25. Robinson N, Brennan M, Cobb M, Dean R. 2015. Clinical examination and weighing of patients in small animal consultations. *Vet Rec* **176**: 387.
26. Langford D, Bailey A, Chanda M, Clarke S, Drummond T, Echols S, Glick S, Ingrao J, Klassen-Ross T, LaCroix-Fralish M, and Matsumiya L. 2010. Coding of facial expressions of pain in the laboratory mouse. *Nat Methods* **7**: 447-449.
27. Fentener van Vlissingen J, Borrens M, Girod A, Lelovas P, Morrison F and Torres Y, 2015. The reporting of clinical signs in laboratory animals: FELASA Working Group Report. *Lab Anim* **49**:267-283.
28. Latney L, Bradley C, Wyre N, 2014. Encephalitozoon cuniculi in pet rabbits: diagnosis and optimal management. *Vet Med Res Rep* **6**:169-180.
29. Melillo A. 2007. Rabbit clinical pathology. *J Exot Pet Med* **16:**135–145.
30. Meredith AL, Richardson J. 2015. Neurological diseases of rabbits and rodents. *J Exot Pet Med* **24:**21–33.
31. Harcourt-Brown F, Holloway H. 2003. Encephalitozoon cuniculi in pet rabbits. *Vet Rec* **152**: 427–431.
32. Sadeghi-Dehkordi Z, Norouzi E, Rezaeian H, Nourian A, Noaman V, Sazmand A. 2019. First insight into Encephalitozoon cuniculi infection in laboratory and pet rabbits in Iran. *Comp Immunol Microbiol Infect Dis* **65:** 37–40.
33. Casali M, Lauri C, Altini C, Bertagna F, Cassarino G, Cistaro A, Erba A, Ferrari C, Mainolfi C, Palucci A, Prandini N. 2021. State of the art of [18F] FDG PET/CT application in inflammation and infection: a guide for image acquisition and interpretation. *Clin Transl Imaging* **9**: 299-339.
34. Toya L, Latney V, Bradley C, Wyre N, Ryan M. **2014.** Encephalitozoon cuniculi in pet rabbits: Diagnosis and optimal management. *Vet Med Res Rep* **5**:169–180.
35. Rodríguez-Tovar L, Nevárez-Garza A, Trejo-Chávez A, Hernández-Martínez C, Hernández-Vidal G, Zarate-Ramos J, Castillo-Velázquez U. 2016. Encephalitozoon cuniculi: grading the histological lesions in brain, kidney, and liver during primoinfection outbreak in rabbits. *J Pathol* **1**: 5768428.

Indian J. Vet. Pathol., 50(4) : 361-369, 2026: DOI: https://doi.org/10.56093/dgn50794

RESEARCH ARTICLE

Integrated anti-oxidant and anti-inflammatory actions of *Saussurea costus* root attenuate severe hepatic pathophysiology in poultry *(Gallus gallus domesticus)* experimentally challenged with *Salmonella enterica* Serovar Typhimurium

Mridul Soni, Rakesh Kumar*, R.K. Asrani, Sahil Choudhary and R.D. Patil
Department of Veterinary Pathology, Dr. G.C. Negi College of Veterinary and Animal Sciences, CSK Himachal Pradesh Agricultural University, Palampur, Himachal Pradesh, 176062, India

***Address for correspondence**
Dr. Rakesh Kumar, E-mail: rkvetpath@gmail.com
ORCID ID: 0000-0002-8481-2094

Received: 15.11.25; Accepted: 28.4.26

ABSTRACT

The present experimental study was designed to investigate the effect of Kuth (*Saussurea costus*) root extract (80% methanolic) dietary supplementation on *Salmonella enterica* serovar Typhimurium (4, 12: i: 1, 2) in Delham-Red birds, aiming to observe the effects on growth response, clinical signs, mortality, and pathological changes. Three hundred day-old Delham-Red chicks were procured and were randomly divided into six groups: Group I - plain control; Group II - *Salmonella* Typhimurium infection only; Group III - *Salmonella* Typhimurium infection + root extract @ 0.5g/l; Group IV - *Salmonella* Typhimurium infection + root extract @ 1g/l; Group V - *Salmonella* Typhimurium infection + root extract @ 2g/l; Group VI - root extract @ 2g/l only. The infections were induced on the 7th day of age, and plant extracts were administered according to group dosage on the 4th day of age. Sacrifice of the birds in different groups was done at regular intervals. The birds were observed for various parameters like clinical signs, mortality, body weight gain, liver and kidney parameters (ALT, AST, total protein, albumin, and creatinine), gross and histopathology of liver, kidney, and spleen post-sacrifice. The groups with plant extract supplementation showed fewer clinical signs, reduced mortality, improved weight gain, liver and kidney parameters, and ameliorative changes in gross and histopathology. Preservation of the liver's normal structure was observed among treatment groups, suggesting the antimicrobial and hepatoprotective effect of *Saussurea costus* against the pathology produced by *Salmonella enterica* serovar Typhimurium in the experimental bird model.

Keywords: Histopathology, Hepatoprotective, Liver damage, *Salmonella enterica* Serovar Typhimurium, *Saussurea costus*

INTRODUCTION

Poultry diseases play an important role in the down growth of this sector. Lack of proper management is one of the predisposing factors for the occurrence of such infectious diseases. Among these infectious diseases, salmonellosis is causing huge losses to the economy of farmers as well as the private poultry sector[3]. *Salmonella* affects a wide range of hosts and is one of the major pathogens of poultry, causing high mortality and economic losses. *Salmonella enterica* serovar Typhimurium is an important intracellular bacterial pathogen that causes food poisoning and gastroenteritis in millions of people worldwide each year[4]. The economic losses due to salmonellosis are a result of mortality, decreased egg production, decrease in body weight gain and reduced feed conversion ratio[5]. *Salmonella* affects the intestinal tract and causes systemic infections in organs involving the liver and spleen in poultry[6].

The antimicrobial activity of medicinal plants against different pathogenic organisms has been well-known for a long. A decreased interest in the use of plant-based medicines and antimicrobials since the discovery of antibiotics has led to concern about the emergence of antibiotic resistance. Since the emergence of antibiotic resistance against bacteria, fungi, viruses and protozoa, there has been a global shift towards plant-based products and by-products to combat antibiotic resistance[7].

The Indian Himalaya region (IHR) is a rich source of medicinal plants and comprises over 1748 plant species with known medicinal properties. *Saussurea costus* (Syn. *Saussurea lappa* or Kuth) is one of the potent medicinal plants that possesses scientific and traditional medicinal properties and is routinely used against several ailments. The plant has been reported to cure various ailments, including bronchitis, jaundice, cough, cold, fever, dysentery, cholera and ulcers.

How to cite this article: Soni, M., Kumar, R., Asrani, R.K., Choudhary, S. and Patil, R.D. 2026. Integrated anti-oxidant and anti-inflammatory actions of *Saussurea costus* root attenuate severe hepatic pathophysiology in poultry *(Gallus gallus domesticus)* experimentally challenged with *Salmonella enterica* Serovar Typhimurium. Indian J. Vet. Pathol., 50(4) : 361-369.

The roots of this plant are known for their therapeutic activities, including anti-inflammatory, anthelminthic, anti-epileptic, anticancerous, antibacterial and anti-larvacidal[8,9]. The activity of *Saussurea costus* is due to the bioactive compounds such as dehydrocostus lactone and costunolide present in the roots[8].Therefore, the present study was planned to study the pathology of experimental salmonellosis with emphasis on the ameliorative effect of *Saussurea costus* root extract in poultry birds.

MATERIALS AND METHODS

Plant material

Freshly collected *Saussurea costus* plant and roots free from dirt and dust were brought from the Lahaul & Spiti (32.6192N, 77.3784E) district of Himachal Pradesh, India. The plant species was identified at the CSIR-Institute of Himalayan Bio-resource Technology (CSIR-IHBT), Palampur, Himachal Pradesh, India. The extract was prepared using a Rotary Evaporator (Model BUCHI Rotavapor R-210) at 45 °C temperature at 175 mbar vacuum pressure and was concentrated until a thick slurry was obtained. Slurry obtained was subjected to lyophilisation till the powdered form was obtained. The percentage yield was recorded and the lyophilised extract was stored at 4°C until further use.

Procurement, serotyping, and assessment of inhibition of bacterial growth

The strain of *salmonella* used was procured from Lala Lajpat Rai University of Veterinary and Animal Sciences (LUVAS), Haryana, India. The bacterial inoculum was sent to the Central Research Institute (CRI), Kasauli on brilliant green agar (BGA) slants for identification and serotyping. The bacteria were found to be *Salmonella enterica* serovar Typhimurium (4,12:i:1,2) as per the identification receipt NSEC/31/22 dated 17.05.2022 received from CRI, Kasauli, Himachal Pradesh, India. The *in vitro* antibacterial activity of *Saussurea costus* root extract was accessed using the disc diffusion method. The discs impregnated with Dimethyl sulfoxide (DMSO) served as a negative control. The isolated organism was tested against various antibiotics like Ceftriaxone (CTR30), Gentamycin (GEN50), Amoxicillin & Clavulanic acid (AMC30), Enrofloxacin (EX10), Levofloxacin (LE5), Oxytetracycline (O30) and Amoxicillin & Salbactum (AMS30/15). Among all the antibiotics used in the *in vitro* trial, Levofloxacin (LE5) appeared to be the most potent, and thus the discs impregnated with Levofloxacin (LE5) served as a positive control. The empty sterile discs were also mounted on petri plates inoculated with bacterial suspension to check for any zone of inhibition.

Viable bacterial count and determination of LD_{50}

The viable bacterial count was determined by making serial dilutions of the *Salmonella enterica* serovar Typhimurium culture, which was incubated in Nutrient broth for 18 hours and then the colonies were counted on BGA plates. The serial dilutions were made in normal saline ranging from 10-1 to 10-7 and from each dilution 0.1 ml was uniformly spread on the BGA petri plates. The plates were inoculated for 24 to 36 hours at 37°C and after incubation the colonies on the plates were counted and the colony forming unit (cfu) per ml was determined.

Day-old chicks (72) were procured from Poultry Farm, COVAS, CSK HPKV, Palampur, Himachal Pradesh, India for the conduction of the pilot experiment and were reared under strict hygienic conditions. The birds were divided into two groups containing 36 birds in each group and each group was further sub-divided into six groups, comprising 6 birds. In one group (36 birds) the infection was given orally, while in another group the infection was given through intra peritoneal route on day 7 of their age. The birds in the first five groups were infected with 1 ml of the normal saline solution (NSS) containing different concentrations of the organism i.e. ($2x10^8$, $2x10^7$, $2x10^6$, $2x10^5$ and $2x10^4$ cfu ml^{-1}, respectively). The duration of the pilot experiment was 10 days. LD50 dose was calculated by using the method of Reed and Muench[10]. The birds were examined for the development of clinical signs and lesions by experimental infection through both routes. There was no presence of clinical signs, mortality and gross lesions in birds infected with the oral route.

Animals, management, and experimentation

Before the arrival of the chicks, the experimental room and cages were fumigated with 10% formalin and potassium dichromate and cleaned with 2.5 % phenol solution. The feeders and water beakers were also washed with 2.5 % phenol solution and later allowed to dry in the sunlight. Cleaning of the cages along with the disposal of the newspaper bedding was done at regular intervals to ensure proper hygiene until the trial was completed. The present study was conducted on day-old Delham Red (DR) birds that weighed around 25 grams and were procured from Poultry Farm, COVAS, CSK HPKV, Palampur, H.P. The birds were procured in two phases and were accordingly divided for pilot as well as final trial. The animals were kept in well-ventilated rooms and were reared under strict hygienic conditions. The birds were provided with chick mash feed obtained from the Department of Animal Nutrition, COVAS, Palampur. The feed given was priorly autoclaved at 15-pound pressure for 15 minutes. The clean and boiled water was provided to the birds throughout the experiment. The 80% methanolic extract of *Saussurea costus* roots at different doses was provided to the birds in drinking water throughout the experimental trial. The experimental cages were labelled containing animals of different groups with the animal number, dose group and dose levels. To conduct the final trial day-old Delham Red

(DR) birds (300 in no.) were also procured from Poultry Farm, COVAS, CSKHPKV, Palampur, Himachal Pradesh, India, and were reared under strict hygienic conditions and were allowed to acclimatize for four days. The experimental trial was conducted as per the guidelines given by the Committee for Control and Supervision of Experiments on Animals (CCSEA), Delhi. The extract was started from day 4 of their age, while the infection was given at day 7 of their age. The birds in the first group, i.e. group I served as controls and were given normal feed and water. The second group (Group II) served as a plain infection group and was given only infection (2×10^6 cfu ml^{-1}) along with *ad libitum* feed and water. The birds in groups III, IV & V were given infection (2×10^6 cfu ml^{-1}) along with the 80% methanolic extract of *Saussurea costus* roots @ 0.5g, 1g & 2g per litre of water, respectively. Group VI was only provided with 80% methanolic extract of *Saussurea costus* roots @ 2g per litre of water. The birds were closely monitored throughout the experiment, and the trial was continued till 21 DPI (28 days of age).

Clinical symptoms, mortality and body weight

Regular monitoring of the birds was done throughout the experiment, and were observed at least thrice a day to check for any clinical signs and mortality. The clinical signs to be monitored included huddling near the light source, dullness, loss of appetite, soiling of the vent and drooping of the head and wings. The mortality throughout the experiment was properly recorded. To assess the response of the 80% methanolic root extract of *Saussurea costus* on body weight 3 birds from each group were weighed on the days of sacrifice, i.e. 1, 3, 5, 7, 10, 14 & 21 DPI. The data obtained was properly recorded.

Serum biochemical estimation

Three birds from each group were selected on the day of the sacrifice i.e. 1, 3,5,7,10,14 & 21 DPI and approximately 2-3 ml of blood from the heart was collected. The blood sample was allowed to stand and remain undisturbed to obtain the serum. The serum collected was stored at -20°C until further use. The serum obtained was used for the estimation of serum biochemicals, which included alanine aminotransferase (ALT), aspartate aminotransferase (AST), total protein (TP), total creatinine (CRT) & albumin (ALB). Estimation of biochemical parameters was carried out using the diagnostic kits (Agappe diagnostics Ltd, India) and semi-automatic biochemical analyser (AGAPPE MISPA-NEO, India).

Gross pathological examination

The birds were sacrificed throughout the experiment, and those who died during the experiment were subjected to detailed necropsy examination. After the detailed necropsy examination, approximately 0.5 cm thick representative tissue sections of the liver were collected in 10 % neutral buffered formalin (NBF) for histopathological examination from three birds in each group on 1, 3, 5, 7, 10, 14 &21 DPI. After 24 hours 10 % formalin solution was discarded, and freshly prepared 10 % neutral buffered formalin was used for proper fixation of tissue samples.

Histopathological examination

Liver tissue sections were subjected to processing after proper fixation. Tissues were washed overnight in running tap water, dehydrated in ascending grades of alcohol, cleared in benzene and embedded in paraffin as per the standard protocol[11]. Around 3-5 µ thick sections were obtained using a microtome (MICROM, Germany). The sections obtained were stained using routine Haematoxylin and Eosin stain (H&E).

Re-isolation of *Salmonella enterica* serovar Typhimurium

The re-isolation of the *Salmonella* Typhimurium was done by taking swabs from the liver of the birds sacrificed at different intervals. The swabs were taken under aseptic conditions and were later streaked on BGA plates. The streaked plates were incubated for 24 to 48 hours at 370C and bacterial growth was examined.

Statistical analysis

The data related to the body weight, biochemical values, gross and microscopic lesions scoring was subjected to one-way and two-way ANOVA by the GraphPad Prism version 9. Data was presented by mean ± S.E.M. level of significance at $p^* \leq 0.05\%$, $p^{**} \leq 0.01\%$, $p^{***} \leq 0.001\%$ and $p^{****} \leq 0.0001\%$ (One-way ANOVA and two-way-ANOVA followed by Tukey's multiple comparison test).

RESULTS

***In vitro* experimental study**

The percent recovery of *Saussurea costus* roots was found to be 6%. The methanolic extract of *Saussurea costus* roots exhibited the most potent antibacterial potential with a zone of inhibition of 10.0 mm (Fig.1). S*almonella enterica* serovar Typhimurium expressed maximum sensitivity for Levofloxacin, followed by Enrofloxacin & Ceftriaxone. It was found to be resistant to Oxytetracycline.

Clinical symptoms, mortality pattern, and body weight gain

The birds in groups I (plain control) and group VI (plant extract only) were completely healthy and didn't express any clinical signs of illness throughout the experiment. The clinical signs were mainly observed in the birds of groups II, III, IV, and V. On day 1 post-infection, there was a slight reduction in the feed and water intake of the birds in group II which were given *Salmonella enterica* serovar Typhimurium infection alone. The clinical signs were seen progressing with

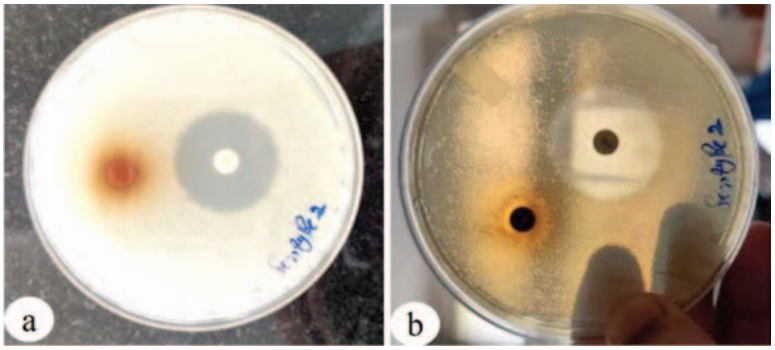

Fig. 1. (a) Photograph depicting the zone of inhibition exhibited by the methanolic extract of roots of *Saussurea costus* against *Salmonella enterica* serovar Typhimurium; **(b)** Photograph depicting the zone of inhibition by the standard antibiotic Levofloxacin.

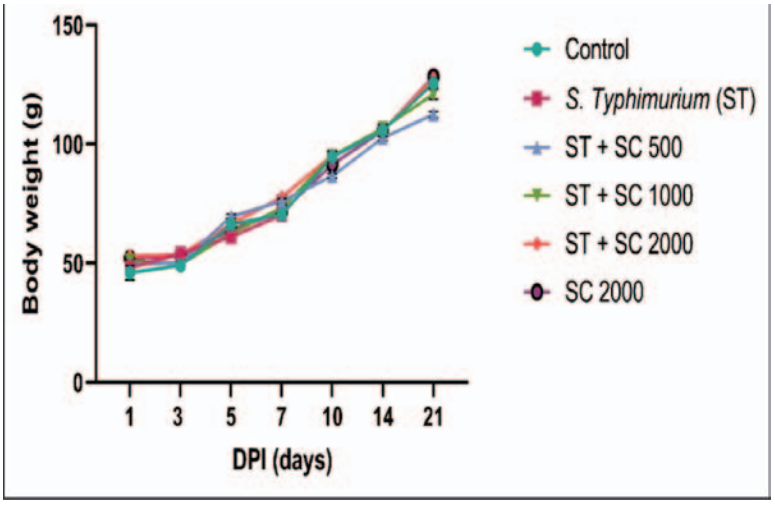

Fig. 2. Effect of different treatments on the body weight of chickens in various treatment groups. Data represent mean ± S.E.M. (n=50) level of significance at p* ≤ 0.05%, p** ≤ 0.01%, p*** ≤ 0.001% and p**** ≤ 0.0001%.

the subsequent days post-infection in group II given infection alone. On day 3 post-infection, the birds in group II showed signs of huddling near the source of light, somnolence, ruffled feathers, greenish-yellow diarrhoea, and reduced feed and water intake. In the present experimental trial, the clinical signs were seen at peak from day 3 to 10 DPI and then gradually tended to decrease but were observed upto 14 DPI with varying intensity. The onset of the clinical signs is attributed to toxaemia produced by the *Salmonella* when it reaches the systemic circulation. The severity of the clinical signs was decreased in the groups treated with the methanolic extracts of *Saussurea costus* roots i.e. groups III, IV, and V. The majority of the clinical signs like ruffled feathers, huddling near the source of light, somnolence, and reduced feed and water intake with soiling of the vent were observed on 3 DPI. The clinical signs were observed upto 10 DPI, but the severity of the signs was significantly decreased in these groups and were seen occasionally at 10 DPI. From 10 DPI onwards, the birds in the groups treated with methanolic extract of *Saussurea costus* roots appeared normal.

In the present experimental study, no mortality was observed in the birds of groups I (plain control) and VI (plant extract only). Mortality was observed and recorded in the birds of groups II, III, IV and V. The peak mortality was observed in infection groups from 1DPI to 3DPI; thereafter, there was a decline in the mortality pattern, though it continued up to 14 DPI. Mortality in the treated groups (III, IV, and V) was lower as compared to the group given infection alone (group II). No mortality was observed in various infected groups after 10 DPI.

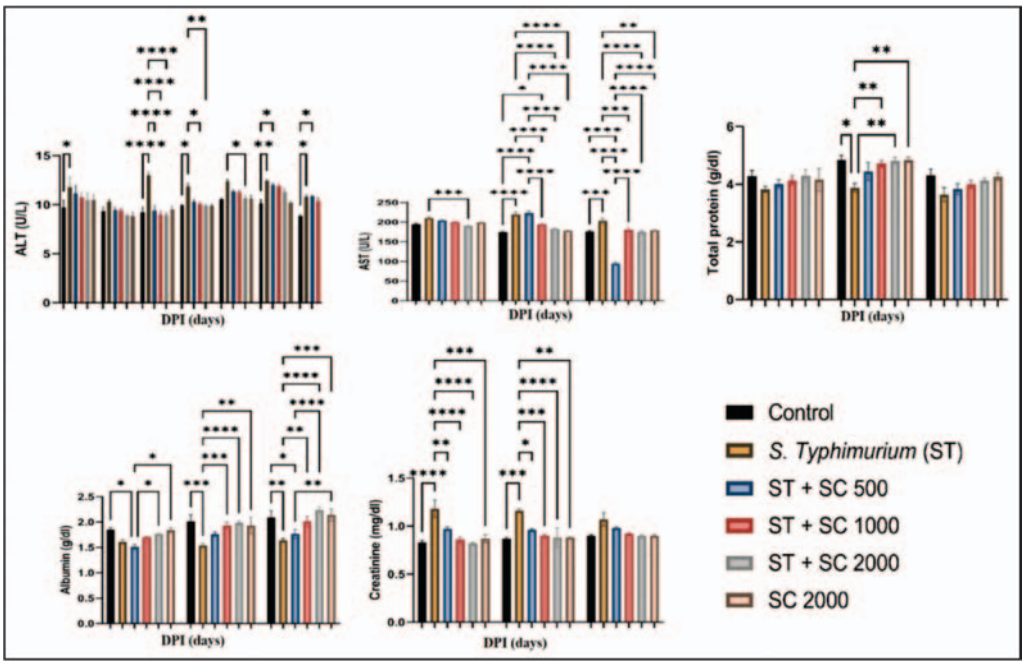

Fig. 3. Effect of different treatments on the serum biochemical parameters of chickens in various treatment groups. Data represent mean ± S.E.M. (n=50) level of significance at p* ≤ 0.05%, p** ≤ 0.01%, p*** ≤ 0.001% and p**** ≤ 0.0001%.

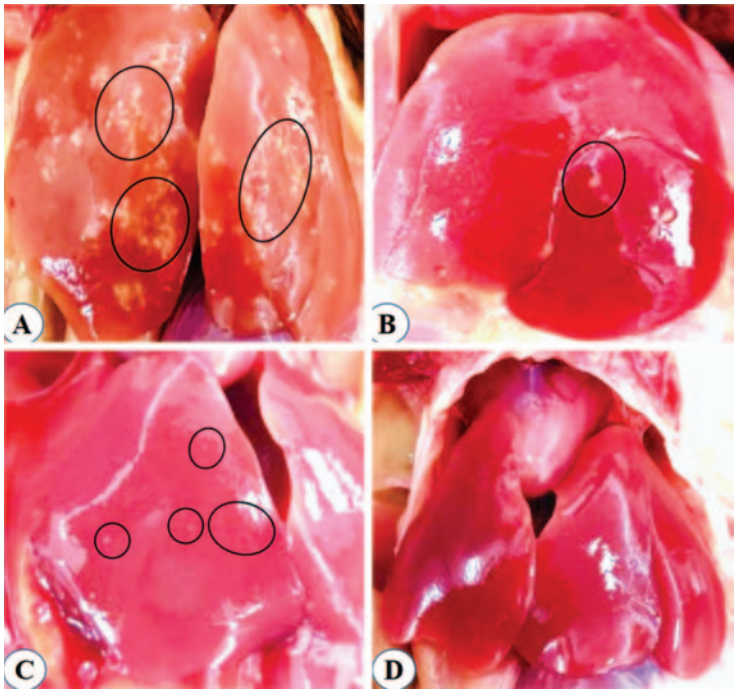

Fig. 4. Gross pathology depicting the effect of different treatments on the liver of poultry birds. **(A)** Positive control group II with severe areas of coagulative necrosis; **(B)** Group III treated with *Saussurea costus* exhibiting multifocal necrotic lesions; **(C)** Group IV treated with *Saussurea costus* reflecting few necrotic foci; **(D)** Group V treated with *Saussurea costus* showing almost normal hepatic parenchyma.

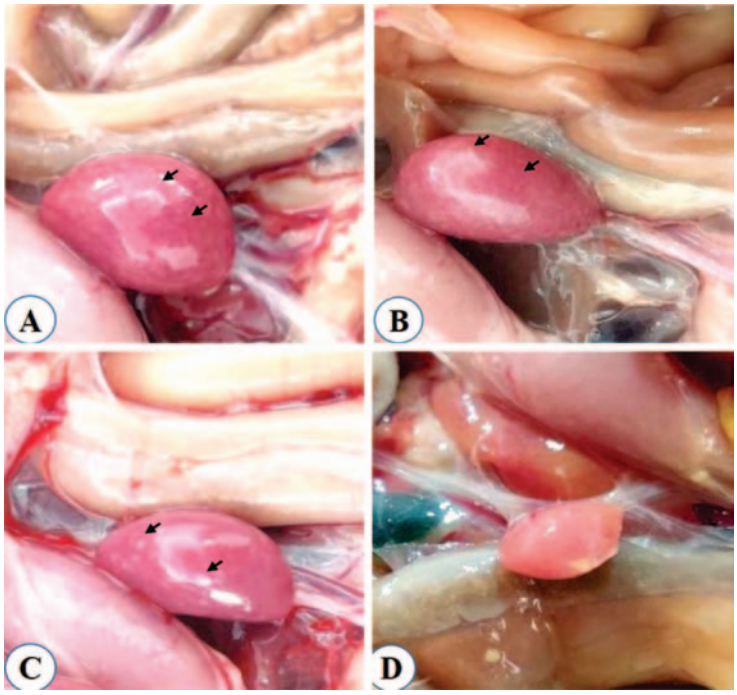

Fig. 5. Gross pathology depicting the effect of different treatments on the spleen of poultry birds. **A.** Positive control group II with multifocal areas of necrosis. **B.** Group III treated with *Saussurea costus* exhibiting multifocal necrotic lesions. **C.** Group IV treated with *Saussurea costus,* reflecting the presence of a few necrotic foci. **D.** Group V treated with *Saussurea costus* showing almost normal spleen.

Overall, there was a rational increase in the body weight of birds with the progression of the experimental trial in all the groups. The mean body weight values were higher in groups IV, & V in comparison to group II throughout the trial period. At 5, 7 and 21 DPI, a significant ($P \leq 0.05$) increase in the body weight of birds in group V was observed in comparison to birds in group II (Fig. 2).

Biochemical changes

The mean serum ALT activity in group II (plain infection) was highest in comparison to the other infected groups (III, IV, and V) at different time intervals. The serum ALT values were highest in infected groups as compared to the control groups I (plain control) and VI (plant extract only). At 5, 10 and 21 DPI, there was a significant ($P \leq 0.05$) difference in the value of ALT in the plain infected group (II) from those of various treated groups. The ALT values of both the groups I and VI were in similar ranges depicting no adverse effect of methanolic root extract of *Saussurea costus* on the liver.

The mean serum AST activity in group II (plain infection) was highest in comparison to the other infected groups (III, IV, and V) at different time intervals. The lowest serum AST activity was observed in groups IV, and V as compared to group II. A significant ($P \leq 0.05$) difference in the values of the AST in different treatment and infection groups was observed at 1, 5, 7, 10 and 21DPI. The AST values in the group SD were more or less close to that of group I depicting no adverse effect of methanolic extract of *Saussurea costus* roots.

The mean value of serum creatinine at 1, 3, 5, 7, 10 and 14 DPI was found to be significantly ($P \leq 0.05$) slightly elevated in group II than in other groups. No significant changes in the creatinine values were recorded in groups III, IV, & V representing the protective effect of the methanolic extract of *Saussurea costus* roots on the kidneys. A significant ($P \leq 0.05$) increase in the value of serum total protein in group V was observed on 3, 7 and 14 DPI in comparison to group II. The value of total protein in groups (IV, & V) was found to be in similar ranges when compared to those in groups (I, & VI). The total protein values were lowest in group II in comparison to the various treatment groups (Fig. 3).

Gross pathology

No visible gross pathology was observed in groups I and VI. Hepatomegaly accompanied

by necrotic foci was the most consistent gross finding in group II throughout the experimental trial. At 1 DPI, hepatomegaly was characterised by rounding of the edges of the liver along with the sinusoidal dilation. These lesions were seen to increase in intensity with the progression of the experimental trial. At 3 DPI, necrotic foci on the liver parenchyma were evident which tend to increase in severity upto 10 DPI. At 3, 5, 7 & 10 DPI multifocal to coalescing, variable-sized, creamish to off-white-coloured necrotic foci were recognisable on the caudodorsal surface of the liver. From 14 & 21 DPI, onwards there was a significant decline in the intensity of visible lesions, especially necrotic foci.The positive control group II showed severe necrosis of liver and spleen at different time intervals and the gravity of necrotic lesions was redued in the groups treated with *Saussurea costus* root extract (Figs. 4 & 5).

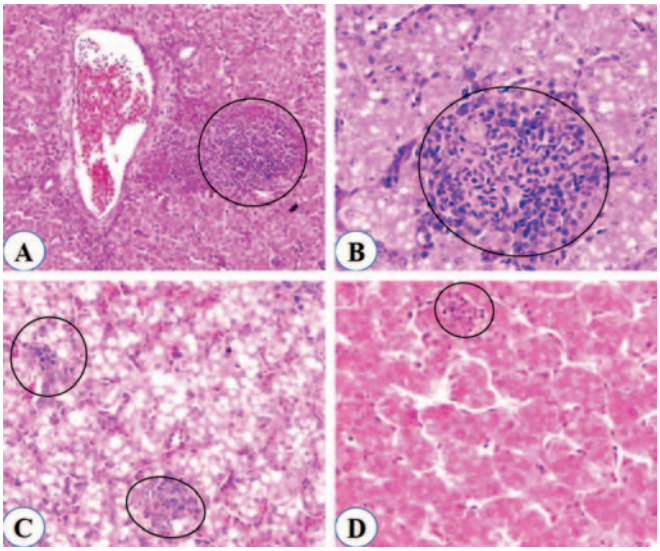

Fig. 6. Histopathology depicting the effect of different treatments on the liver of poultry birds. **(A)** Positive control group II with moderate perivascular infiltration of inflammatory cells in the necrotic area (encircled) (H&E x10); **(B)** Group III treated with *Saussurea costus* exhibiting necrotic foci with lymphocytes (encircled) and increased Kupffer cell activity (H&E x20); **(C)** Group IV treated with *Saussurea costus,* reflecting the presence of multifocal areas of necrosis (encircled) with sinusoidal congestion and fatty degeneration (H&E x20); **(D)** Group V treated with *Saussurea costus* showing mild necrosis. (H&E x20).

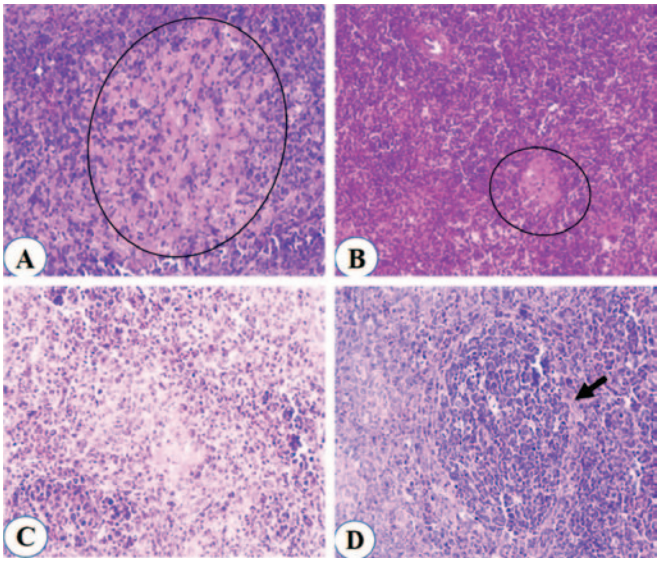

Fig. 7. Histopathology depicting the effect of different treatments on the spleen of poultry birds. **(A)** Positive control group II with focal necrotic foci (encircled) with moderate white pulp hyperplasia (H&E x20); **(B)** Group III treated with *Saussurea costus* exhibiting a focal necrotic area (encircled) (H&E x10); **(C)** Group IV treated with *Saussurea costus,* reflecting the presence of near to normal intact follicle in association with surrounding reticuloendothelial cell hyperplasia (H&E x20); **(D)** Group V treated with *Saussurea costus* with near to normal lymphoid follicle (arrow) (H&E x40).

The histopathological examination of the liver in group II (*Salmonella* Typhimurium infection only) comprised of severe multifocal areas of necrosis, infiltration of heterophils and lymphocytes, sinusoidal dilation, degenerative changes and increased cellular granularity. The microscopic lesion score intensity was highest in group II on 5, 7 & 10 DPI. In groups IV, & V on 10, 14 & 21 DPI, the liver was found to be normal and there was a dose-dependent decline in the severity of occurrence of lesions. The liver was devoid of areas of necrosis, and infiltration of inflammatory cells and few degenerative changes were observed along with sinusoidal congestion (Fig. 6). Severe homogenous eosinophilic areas of necrosis, reticuloendothelial cell hyperplasia, depletion of lymphoid follicles and blood-filled sinuses were present in the spleen in group II as compared with other treatment groups (Fig. 7). In the heart from 3 to 7 DPI severe fibrinous pericarditis and

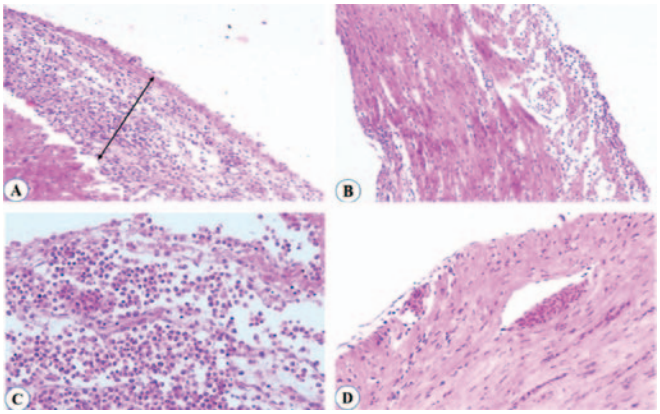

Fig. 8. Histopathology depicting the effect of different treatments on the heart of poultry birds. **(A)** Positive control group II showing severely thickened pericardium with infiltration of heterophils (arrow) (H&E x10); **(B)** Group III treated with *Saussurea costus* exhibiting mild fibrinous pericarditis along with heterophils population (H&E x10); **(C)** Group IV treated with *Saussurea costus* showing thickened pericardium, fibrin and infiltration of heterophils (H&E x20); **(D)** Group V treated with *Saussurea costus* showing near to normal cardiac parenchyma (H&E x10)

infiltration of heterophils and lymphocytes was found. In group III similar lesions were recorded but the intensity of the lesions was reduced in comparison to group II on 5, 7 & 10 DPI. The severity and intensity of lesions in groups IV, & V were reduced and the maximum intensity of lesions was observed upto 7 DPI (Fig. 8).

DISCUSSION

Salmonella is a facultative intracellular pathogen and causes both systemic and acute localized infections whereas chronic infections appear as an asymptomatic carrier state[12]. Fowl typhoid and pullorum disease are septicaemic diseases which are caused by *Salmonella* Gallinarum and *Salmonella* Pullorum, respectively in poultry. *Salmonella enterica* serovar Typhimurium is a bacterial pathogen that causes food poisoning and gastroenteritis in millions of people worldwide each year[4]. *Salmonella enterica* serovar Typhimurium causes food poisoning in humans, and infection also leads to bacteraemia causing cardiovascular, bone and joint infections in humans[13,14]. Eggs are the major vehicle of *Salmonella* transmission and there are mainly two ways through which eggs get infected. Either *Salmonella* infects the ovaries of healthy hens and contaminates the eggs or droppings from the infected birds contaminate the outer shells of eggs and penetrate when shells are cracked[15].

Abdalkareem et al.[16] have shown the antibacterial effect of the methanolic extract of *Saussurea costus* against human bacterial pathogens (*Bacillus cereus, Staphylococcus aureus, Escherichia coli* and *Pseudomonas aeruginosa*) at different concentrations ranging from 6.25 mg/ml to 100 mg/ml. The maximum activity was observed at a concentration of 100 mg/ml against *Bacillus cereus* and *Staphylococcus aureus,* with zones of inhibition of 26 mm and 25 mm, respectively. Khalid et al.[17] demonstrated the antimicrobial activity of three different extracts (methanolic, cold water and hot water) of costus roots against *Staphylococcus aureus, Pseudomonas Aeruginosa, Bacillus subtalis, Salmonella typhi* and *Enterococcus faecalis*. There were no clinical signs in the plain control group, and the intensity of signs among infected groups was least in the group V as compared to other groups. The mortality rate was found to be highest in group II in comparison to other groups III, IV, & V, and no mortality was recorded in groups I & VI. Body weight was minimal in group II and highest in group V treated with the highest dose of plant extract. In the previous studies, the birds have also been shown to exhibit signs of reduced feed and water intake, huddling near the source of light, ruffled feathers and greenish-yellow diarrhoea when infected with *Salmonella* organism[18]. The onset of the clinical signs is attributed to toxaemia produced by the *Salmonella* when it reaches the systemic circulation. The bacterium-mediated phagocytosis, recruitment of neutrophils, cytokine secretion and imbalance in electrolytes are some of the mechanisms of pathogenesis[19]. *Salmonella* can produce both endotoxins as well as exotoxins and the endotoxins are known to produce a variety of biological responses. In contrast, exotoxins consisting of cytotoxins and enterotoxins can kill host cells[20].

The serum biochemical examination revealed that ALT & AST values were significantly elevated while total protein and albumin were lower in concentration in the plain infection group (II) as compared to the control group (I). The values of biochemicals (ALT, AST, total protein, albumin and creatinine) among different treatment groups SA, SB & SC were generally significantly lowered as compared to the group II (*Salmonella* Typhimurium infection only) suggesting an *in vivo* protective effect of 80 % methanolic root extract of *Saussurea costus* against the pathology of infection. The findings are per the results of Shah et al.[21]; Chiroma et al.[18]; and Abou Zeid et al.[22] who found that the ALT values were elevated in *Salmonella*-infected groups during their experimental studies. The elevated values in different infected groups could be attributed to the hepatocellular damage done by the organism. Alnahdi et al.[23] studied the hepatoprotective effect of methanolic extract of *Saussurea costus* against deltamethrin-induced liver toxicity in albino rats. Kadhem[24] performed a study on rabbits to investigate the effect of aqua-ethanolic extract of *Saussurea costus* against hepatic and renal toxic effects of paracetamol toxicity. The paracetamol was administered @ 300 mg/Kg body weight for 14 days and the effect of *Saussurea costus* was studied with a dose of 300 mg/Kg bw.

The gross pathology comprised of hepatomegaly, necrotic foci, liver paleness, splenomegaly and fibrinous pericarditis were reduced in *Saussurea costus* treated groups as compared with group II. No visible gross pathology was observed in groups I, and VI. In the present study based on the gross pathology and lesions intensity score a dose-dependent effect of the 80% methanolic root extract of *Saussurea costus* was evident. The group treated with the highest dose of the extract expressed a significant reduction in gross pathology which was more or less comparable with the control group I.

The histopathological examination of the liver in group II (*Salmonella* Typhimurium infection only) comprised severe multifocal areas of necrosis, infiltration of heterophils and lymphocytes, sinusoidal dilation, degenerative changes and increased cellular granularity. In groups IV, & V , the liver was found to be normal and there was a dose-dependent decline in the severity of occurrence of lesions. Kumar et al.[25] conducted an experimental trial in Japanese quail to study the pathology of *Salmonella* Typhimurium infection. Grossly, they recorded splenomegaly, hepatomegaly, granular appearance of the liver and fibrinous pericarditis.

Histopathological changes recorded were fatty degeneration and heterophils accumulation in the liver, reticuloendothelial hyperplasia in the spleen, catarrhal enteritis and hyalinization of lymphoid follicles.

The present study has evaluated the hepatoprotective effect of *Saussurea costus* root extract against *Salmonella* Typhimurium infection, although a definitive mechanistic confirmation would require targeted evaluation of antioxidant defence systems, xenobiotic-metabolising enzymes, and inflammatory signalling pathways such as NF-Kb.

CONCLUSION

In conclusion, the methanolic root extract of *Saussurea costus* exhibited maximum antibacterial activity against *Salmonella enterica* serovar Typhimurium at a 100 mg/ml concentration in an *in vitro* experimental study. *Saussurea costus* root extract has shown a significant reduction in the serum biochemical parameters (ALT, AST, TP, and Albumin) in the treatment groups indicating its hepatoprotective activity. The 80% methanolic *Saussurea costus* root extract exhibited anti-bacterial activity against pathogenic *Salmonella enterica* serovar Typhimurium indicated by the reduction in the gravity of gross and microscopic pathological lesions such as necrosis, inflammatory cells infiltration & fibrinous pericarditis in different organs. In a nutshell, the present study suggests that *Saussurea costus* root extract is a potential plant to combat bacterial organisms and express a good antibacterial activity and create a scope to explore its active principles further for the treatment/prevention of various bacterial infections along with its exact mechanism of action.

ACKNOWLEDGEMENTS

Authors thank the administration of CSK HPKV, Palampur, Himachal Pradesh, India, and the Director, CSIR-Institute of Himalayan Bioresource Technology, Palampur, Himachal Pradesh, 176061, India for infrastructural support.

Financial support & sponsorship*:* None

Conflict of interest : None

Use of artificial intelligence (AI)-assisted technology for manuscript preparation: The authors confirm that there was no use of AI-assisted technology for assisting in the writing of the manuscript and no images were manipulated using AI.

REFERENCES

1. BAHS (Basic Animal Husbandry Statistics). 2019. Department of Animal Husbandry, Dairying and Fisheries, Government of India. pp. 10.
2. Rajkumar U, SV Rama Rao and RP Sharma. 2010. "Backyard Poultry Farming changing the face of rural and tribal livelihoods." *Ind Farming* **60 (2).**
3. Geetha M and KM Palanivel. 2018. "A Brief Review on Salmonellosis in Poultry". *Internatl J of Current Microbiol and Appl Sci* **7 (5):** 1269-1274. DOI: https://doi.org/10.20546/ijcmas.2018.705.153
4. Grassl GA, Y Valdez, KSB Bergstrom, BA Vallance and BB Finlay. 2008. "Chronic enteric *Salmonella* infection in mice leads to severe and persistent intestinal fibrosis". *Gastroenterol* **134 (3**): 768–780.
5. Ayesha K, MS Mehmood, I Hussain F, Siddique A Rafique and ZR Abbas. 2014. "Bacteriological and epidemiological investigation of pullorum disease in selected poultry farms of Faisalabad, Pakistan". *Global Veterinaria* **12 (4)**: 455-460.
6. Coburn B, GA Grassl and BB Finlay. 2007. "*Salmonella* the host and disease: a brief review*," Immunol and Cell Biol* **85 (2)**: 112–118.
7. Gupta PD and TJ Birdi. 2017. "Development of botanicals to combat antibiotic resistance". *J of Ayurv and Integrat Med* **8 (4):** 266–275
8. Liu ZL, Q He, SS Chu, CF Wang, SS Du and ZW Deng. 2012. "Essential oil composition and larvicidal activity of *Saussurea lappa* roots against the mosquito *Aedes albopictus* (Diptera: Culicidae)". *Parasitol Res* **110(6)**: 2125–2130
9. Negi JS, VK Bisht, AK Bhandari, CP Kuniyal, VP Bhatt and R Bisht. 2014. "Chemical fingerprinting and antibacterial activity of *Saussurea lappa* Clarke". *Appl Biochem and Microbiol* **50 (6)**: 588–593
10. Reed LJ and H Muench. 1938. "A simple method of estimating fifty percent endpoints". *The Am J of Hyg* **27**: 493–497
11. Luna LG. 1968. "Manual of Histological Staining Methods". Armed Forces Institute of Pathology. New York, NY: McGraw Hill Book Company.
12. Shivaprashad HL. 1997. "Pullorum disease and fowl typhoid. In: *Diseases of Poultry*, 10th ed. (BW Calnek *et al*., eds.)", lowa State University press, Ames, IA, USA. 82-9.
13. Bohez L, R Ducatelle, F Pasmans, N Botteldoorn, F Haesebrouck and F Van Immerseel. 2006. "*Salmonella enterica* serovar Enteritidis colonization of the chicken caecum requires the HilA regulatory protein". *Vet Microbiol* **116**: 202–210.
14. Lan R, G Stevenson, K Donohoe, L Ward and PR Reeves. 2007. "Molecular markers with potential to replace phage typing for *Salmonella enterica* serovar Typ himurium. *J of Microbiol Meth* **68**: 145–156.
15. Deryck D and Pattron. 2004. "Scientific status summary on bacteria associated with foodborne diseases and also related to public health significance of Salmonella in institute of food technologists", Chicago.
16. Abdalkareem M, M Aldaw, E Ismail, A Alyaa Abu and K Eitha. 2017. "Evaluation of antimicrobial activity of different solvent extracts of *Saussurea lappa". World Journal of Pharmacy and Pharmaceut Sci* **6 (9)**.
17. Khalid A, U Rehman, A Sethi, S Khilji, U Fatima, MI Khan, MK Waqas, QN Saqib, MHHB Asad, K Farzana, S Mahmood, A Waseem, T Ismail and G Murtaza. 2011. "Antimicrobial activity analysis of extracts of *Acacia modesta, Artimisia absinthium, Nigella sativa* and *Saussurea lappa* against Gram positive and Gram negative microorganisms". *African J of Biotech* **10 (22)**: 4574-4580.
18. Chiroma MA, S Adamu, JJ Gadzama, KAN Esievo, H Abdulsalam, AG Balami, JE Samson, Y Muhammad and AJ Atata. 2017. "Some plasma biochemical changes in layers experimentally infected with *Salmonella* Gallinarum". *African J of Cellu Pathol* **9 (2)**: 66-72.
19. Berhanu G and F Abdisa. 2020. "Pullorum disease and fowl typhoid in poultry: a review." *British J of Poul Sci* **9**: 48-56.
20. Foley SL, TJ Johnson, SC Ricke, R Nayak and J Danzeisen.

2013. "*Salmonella* Pathogenicity and Host Adaptation in Chicken-Associated Serovars". *Microbiology and Mol Biol Rev* **77 (4)**: 582–607

21. Shah NS, KA Shayaib, DM Mohammed, MS Masood and BA Shakoor. 2013. "Haematological and some biochemical changes in experimental fowl typhoid infection in broiler chickens". *Comp Clin Pathol* **22 (1):** 83-91
22. Abou Zeid MAM, SA Nasef, IEA Gehan and AM Hegazy. 2020. "A Field Study on Biochemical Changes Associated with *Salmonella* Infection in Ducklings". *J of World's Poult Res* **10 (2S)**: 250-262.
23. Alnahdi HS, NO Ayaz and ME Elhalwagy. 2016. "Prophylactic effect of cousts *saussurea lappa* against liver injury induced by deltamethrin intoxication". *International Journal of Clinical and Experimen Pathol* **9 (1)**: 387-394.
24. Kadhem M. 2019. "Protective of ethanolic extract of *Saussurea lappa* against paracetamol-induced hepatic and renal damage in male rabbits". *Asian J of Pharmaceu and Clin Res* **12**: 68-73.
25. Kumar S, JR Sadana and SK Mishra. 2001. "Studies on clinical signs, growth response and haematological changes of Japanese quail, (*Coturnix coturnix japonica)* infected with *Salmonella* Typhimurium". *Ind J of Poult Sci* **36 (3)**: 335-337

Indian J. Vet. Pathol., 50(4) : 370-377, 2026: DOI: https://doi.org/10.56093/35b4gy92

RESEARCH ARTICLE

Molecular epidemiology and pathobiology of Newcastle disease virus in chickens in and around Hyderabad

Pavan Kumar Sangamoni, Swathi Bora*, Ravi Kumar Yadala, L. Gopala[2], B. Raju[3] and D. Madhuri
Department of Veterinary Pathology, P.V. Narsimha Rao Telangana Veterinary University, Rajendranagar-500030, Telangana, India
[1]Department of Veterinary Microbiology,
[2]Research scientist, IgY Immunologix India Pvt Ltd, Narsingi village, Rajendranagar-500089

***Address of correspondence**
Dr. Swathi Bora, Associate Professor; E-mail: drswathibora@gmail.com
ORCID ID: 0000-0003-4141-4026

Received: 23.3.26; Accepted: 3.5.26

ABSTRACT

Newcastle disease (ND) is a highly contagious respiratory viral disease affecting various avian species caused by *avian paramyxovirus-1* (APMV-1). The present study aimed to determine the incidence, seasonal distribution, pathological alterations, and molecular prevalence of Newcastle disease virus (NDV) in chickens from different locations in and around Hyderabad. During June to November, 2025, a total of 439 dead birds from 32 poultry flocks were subjected to detailed postmortem examination. Of these, 262 birds showed respiratory lesions, among these 104 were confirmed as viral respiratory infections. The present study recorded an overall incidence of 65 cases (62.50 %) for Newcastle disease virus using RT-PCR targeting F gene. Grossly, affected birds showed pulmonary oedema and congestion of lungs. Trachea showed severe congestion with areas of haemorrhages and air sacs were thickened and cloudy. Microscopically, lesions include tracheal epithelial hyperplasia, deciliation, necrosis, degeneration, vascular congestion and mononuclear infiltration within the lamina propria, mucosa and submucosa. Lung exhibited edema, congestion, bronchial deciliation, heterophilic plugs and epithelial thickening of parabronchi. Viral isolation was carried out in embryonated chicken eggs through the Allantoic cavity route for isolation of the virus and confirmed using RT-PCR. Flock wise analysis revealed that, out of 32 flocks screened, 13 (40.63%) flocks were found positive for NDV. Seasonal wise incidence showed that NDV predominant throughout the study period with higher winter occurrence than the rainy season. Bidirectional sanger sequencing of the 304 bp F gene amplicon revealed >95% nucleotide identity confirming the isolates as Avian paramyxovirus-1 (NDV).

Key words: Egg inoculation, Histopathology, Incidence, Newcastle disease, RT-PCR

INTRODUCTION

New castle disease, also termed as fowl plague is a highly contagious viral disease affecting various avian species[1]. The disease caused by *avian paramyxovirus-1* (APMV-1), a negative sense RNA virus of the genus *Orthoavulavirus*, infecting numerous domestic and wild birds. The virus targets respiratory, nervous, digestive and lymphoid system[2]. It was first documented in 1926 with outbreak noticed in Java, Indonesia and later in Newcastle, England[3]. In India, initial outbreak of NDV occurred in 1927 at Ranikhet in Uttarakhand[4]. The genome of virus consists of nucleocapsid, phosphoprotein, matrix, fusion, haemagglutinin-neuraminidase, and RNA polymerase genes which are essential for virus application, with the fusion (F-protein) cleavage site serving as a key marker of virulence and tissue tropism[5]. The pathogenicity of NDV is determined by the amino acid sequence at the unprocessed F protein cleavage site[6]. Based on F gene nucleotide sequences, NDVs are grouped into class I and class II. Class I NDVs mainly occur in wild birds with low virulence, while class II strains predominate in domestic poultry and typically more pathogenic[4]. NDV categorized into viscerotropic velogenic (Doyle), neurotropic velogenic (Beach), mesogenic (Beaudette), lentogenic (Hitchner), and asymptomatic enteric pathotypes based on virulence and clinical presentation[7].

The virus infects more than 240 bird species, notably domestic poultry-chickens, ducks, turkeys, guinea fowl, quail and pigeons[8]. Waterfowl and wild birds serve as natural reservoirs of NDV[9]. The disease transmission is through oral or aerosol inhalation with a incubation period of 1–3 days[10, 11]. Definitive diagnosis is based on detecting viral antigens, either through virus isolation from swabs or organs using hemagglutination inhibition or molecular methods. The virus can be cultured in cell lines such as African green monkey kidney cells, hepatocytes and chicken embryo fibroblasts[1].

How to cite this article : Sangamoni, P.K., Bora, S., Yadala, R.K., Gopala, L., Raju, B. and Madhuri, D. 2026. Molecular epidemiology and pathobiology of Newcastle disease virus in chickens in and around Hyderabad. Indian J. Vet. Pathol., 50(4) : 370-377.

MATERIALS AND METHODS

Location and duration of the work

The research work has performed at Department of Pathology, College of Veterinary Science, Rajendranagar and IgY Immunologix India Pvt Ltd, located in Narsingi, Hyderabad. Sample collection, processing and interpretation of research work was conducted for a period of six months from June 2025 to November 2025.

Collection of samples

In the present investigation, a total of 439 dead birds were submitted for necropsy from various poultry flocks located in and around Hyderabad and were subjected to a detailed postmortem examination. Birds that exhibited gross respiratory lesions during necropsy were selected for subsequent pathological and molecular investigation. The collected samples were then divided into two sets – one portion of tissue was fixed in 10% neutral buffered formalin for histopathological examination, while the other portion of tissue was collected in Viral Transport Medium (VTM) was prepared using Dulbecco's Modified Eagle Medium (DMEM) as the base, and fetal bovine serum (FBS) was added to a final concentration 5% (v/v) to stabilize viral particles during transport and storage. To prevent bacterial and fungal contamination, the medium was supplemented with gentamicin (50 µg/mL), ciprofloxacin (10 µg/mL), and amphotericin B (10 µg/mL). The final VTM was filter-sterilized (0.22 µm) and stored at 4°C until use for molecular analysis. All collected specimens were properly labelled, documented, and transported to the Department of Veterinary Pathology under refrigerated conditions to prevent decomposition and preserve diagnostic quality.

Gross pathology

Submitted dead birds were subjected for detailed necropsy examination as per standard procedure. Gross lesions were recorded in larynx, trachea and lungs along with other organs for diagnostic correlation.

Histopathology

Based on gross examination of the respiratory lesions and in correlation with lesions on other organs, relevant sample were collected in 10% neutral buffered formalin, washed with PBS, and dehydrated through graded ethanol (70-100%). Tissues were then cleared in xylene and embedded in paraffin at 55-65°C. Thin sections of 5µ thick were cut, placed on clean slides coated with Mayer`s egg albumin, stained by H&E and viewed microscopically[12]. Histopathological scoring of tracheal and pulmonary lesions of ND was performed following the criteria described[13].

Egg inoculation

Tissue samples were finely minced and triturated with sterile sand in a mortar pestle under aseptic conditions in the virology laboratory. A 10% (w/v) organ suspension was prepared in viral transport medium. The homogenate was transferred to sterile tubes and centrifuged at 3000 rpm for 20 minutes at 4°C. The resulting supernatant was collected and passed through a 0.45 µm filter. Fertile eggs were incubated at 37.5°C for nine days prior to inoculation. Viability of embryos was confirmed by candling in a dark room, and the boundaries of the air cell were marked to identify the inoculation site. Eggs showing no embryonic growth were included. Shell surface was disinfected with ethanol, after which a small opening was made at the marked region using a sterile drill, without damaging the underlying membranes. Using a sterile 1mL syringe with a fine gauge needle, 0.1 mL of the virus suspension was injected through the shell and chorioallantoic membrane into the allantoic cavity. The perforation was sealed with sterile wax or adhesive tape, and the eggs were incubated at 37.5°C for 2-4 days and examined every 24 hours by candling to monitor embryo viability. Subsequently, allantoic fluid was collected and embryos were examined in sterile petri dishes for cytopathic changes.

Molecular detection of different viral respiratory agents by PCR

Total RNA was extracted from tissues stored at −20 °C in viral transport medium. Briefly, approximately 50 mg of tissue was aseptically placed in a DNase- and RNase-free 1.5 mL microcentrifuge tube containing 1 mL of TRI Reagent® (Sigma-Aldrich, Cat. No. T9424) and 1 unit of RNase Inhibitor (SRL Chemicals, Sisco Research Laboratories, Cat. No. 62030). The tissue was homogenized using a sterile motorized homogenizer until a uniform suspension was obtained. The homogenate was incubated at room temperature for 15 min to facilitate complete lysis and dissociation of nucleoprotein complexes. Subsequently, 200 µL of chloroform was added, and the mixture was vortexed thoroughly for 15–30 s. The mixture was incubated at room temperature for 15 min and then centrifuged at 12,000 g for 15 min at 4°C.

The aqueous phase containing RNA was carefully recovered and precipitated by adding 500 µL of isopropanol, followed by incubation at room temperature for 15 min. The mixture was centrifuged at 12,000 g for 15 min at 4 °C to pellet the RNA. The RNA pellet was washed once with 75% ethanol prepared in DEPC-treated water and centrifuged at 7,500 g for 5 min. After removing the ethanol, the pellet was air-dried and resuspended in 50 µL of nuclease-free water, followed by incubation at 60 °C for 5 min. The extracted RNA and DNA concentration and purity (A260/280) were measured using a FLUO star Omega filter-based multi-mode microplate reader.

Complementary DNA was prepared by reverse transcription using the First Strand cDNA Synthesis Kit

(Quick Protocol, NEB #M0277). The reaction mixture was incubated at 25 °C for 5 min to allow primer annealing, followed by 42 °C for 1 hour for cDNA synthesis. The enzyme was inactivated by incubating at 85 °C for 5 min. The synthesized cDNA was then used for downstream PCR applications.

PCR amplification was performed using a thermal cycler (Heal Force Touch) using PowerPol 2X PCR Mix with Dye V2 (Cat. No. RK20729). For amplification of NDV-F gene, RT-PCR began with initial denaturation at 98°C for 1minute, followed by 30 cycles consisting of denaturation at 98°C for 10 sec, annealing at 55°C for 30 sec, and extension at 72°C for 1 min, with a final extension step at 72°C for 5 minutes and hold for indefinite time at 4°C. Primers targeting the Fusion (F) gene of Newcastle Disease Virus (NDV; *Avian paramyxovirus-1*) were used. The forward primer (NDV-F) sequence was TACACCTCATCCCAGACAGG and the reverse primer (NDV-R) was AGTCGGAGGATGTTGGCAGC, yielding an expected amplicon of approximately 304 bp[14]. These primers specifically amplify the negative-sense single-stranded RNA (ssRNA) genome region corresponding to the F gene.

RESULTS

Incidence

During the study period, postmortem examinations were performed on a total of 439 dead birds presented to Department of Veterinary Pathology from various farms in and around Hyderabad. Among these, 262 birds exhibited gross lesions suggestive of respiratory diseases, 104 were confirmed to have viral respiratory infections. Among the 104 positive cases of viral respiratory infections in chickens, NDV was the major important pathogen detected in the present investigation, accounting for nearly two-thirds of the positive (65) cases with an incidence rate of 62.5%.

The investigation included sampling from 32 poultry flocks. The flocks varied in scale, each flock comprised between approximately 5,000 and 20,000 birds, reflecting considerable variation in flock size. During the study period approximately 5 tissue samples (trachea or lungs) from each flock were collected, pooled together and considered as a single sample for molecular detection. Out of 32 flocks screened, 13 (40.63%) flocks were found positive for NDV.

The season wise NDV infections in chickens showed marked variation between the winter and rainy months. Detailed seasonal wise incidence was presented in Table 1. In rainy season (June - September), a total of 280 birds were subjected to necropsy. Out of these, 31 birds were positive for ND with an incidence rate of 11.07%. In contrast, during the winter months (October and November), 159 birds were subjected to detailed postmortem examination. Among these, 34 birds tested positive for ND, corresponding to a higher incidence rate of 21.38% in comparison to rainy season. NDV was identified consistently throughout the study period and remained as a predominant respiratory pathogen showing a higher occurrence in the winter season than during the rainy season.

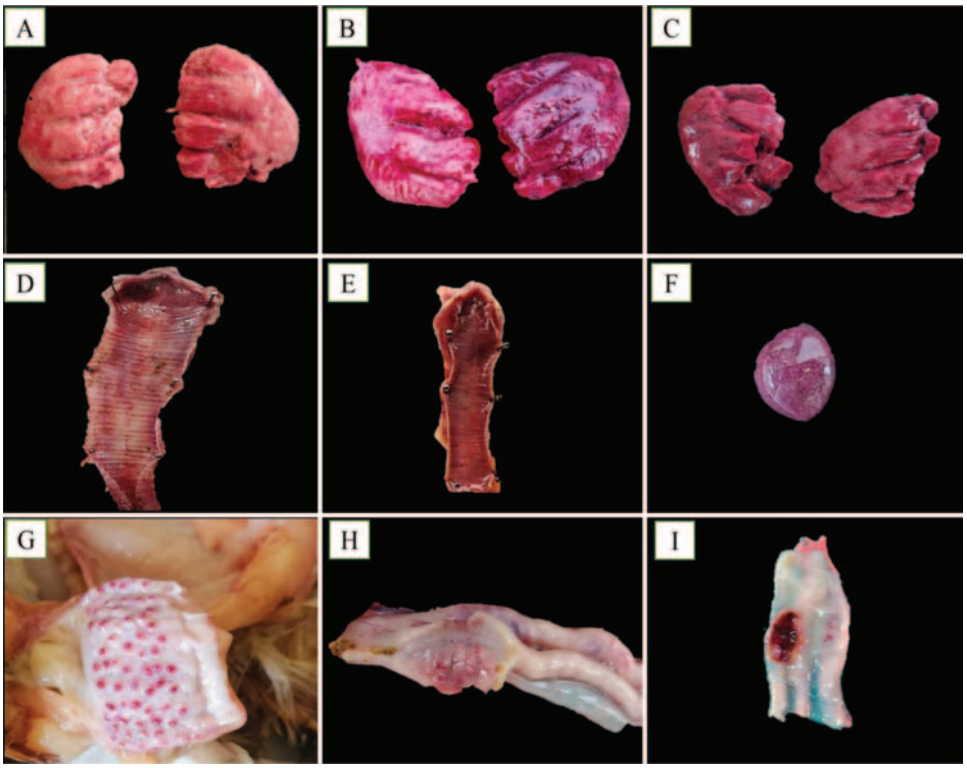

Fig. 1. Gross pathology of different organs in chicken in NDV infection. **A.** Lungs showing moderate to severe congestion. **B.** Lungs showing severe congestion appearing dark red in colour. **C.** Lungs showing moderate congestion along with edema. **D.** Trachea revealed congestion around the tracheal rings along with areas of hemorrhages. **E.** Trachea mucosa showing severe congestion and hemorrhages throughout the entire trachea. **F.** Spleen shows multiple necrotic whitish foci on its surface. **G.** Presence of pin point hemorrhages on proventricular glands. **H.** Enlarged caecal tonsils showing areas of hemorrhages. **I.** Intestinal mucosa showing circular, well demarcated, button like hemorrhagic ulcers.

Table 1. Distribution of lesion scores of tracheas and lungs for NDV

Disease	Organs	Score-1	Score-2	Score-3	Score-4	Total cases
NDV	Trachea	5	8	10	13	**36**
	Lungs	3	6	9	11	**29**

Table 2. Season wise summary of respiratory viral infections in chickens.

Season	Months covered	Total number of dead birds examined	Total number of positive birds	Incidence (%)
Rainy	June to September	280	31	11.07
Winter	October & November	159	34	21.38

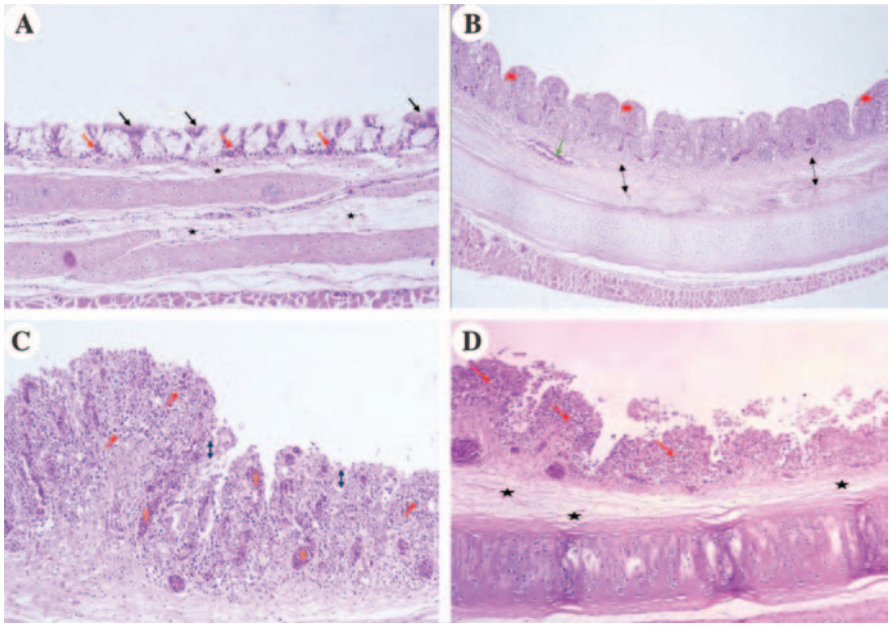

Fig 2. Microscopic alterations of trachea in NDV infection. **A.** Mild- Clumping of cilia (black arrow), Submucosal edema (black asterisk), Mild mononuclear infiltration (red arrow); **B.** Moderate- Epithelial hyperplasia (red asterisk), Mucosal thickening (double headed black arrow), vascular congestion (green arrow); **C.** Severe- mononuclear infiltration (red arrow), haemorrhage (orange asterisk), Necrosis of the epithelial cells (black double-sided arrow); **D.** Very severe- Submucosal edema (black asterisk), Multifocal loss of epithelium, mononuclear infiltration (red arrow).

Gross pathology

On gross examination, birds affected with ND exhibited pulmonary oedema and mild to severe congestion of lungs (Fig. 1, A-C). The trachea revealed severe congestion around the tracheal rings along with areas of hemorrhages (Fig. 1, D, E) and thoracic air sacs were thickened and cloudy. The spleen shows multiple necrotic whitish foci on its surface (Fig.1 F). The majority of cases showed petechial

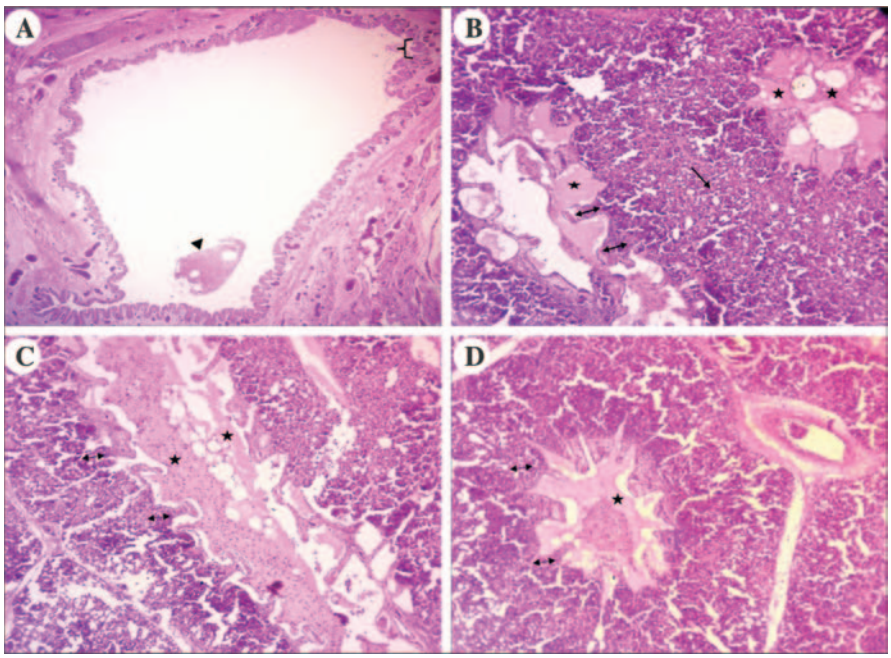

Fig 3. Microscopic alterations of lungs in NDV infection. **A.** Mild- loss of cilia (bracket), necrotic plug in the lumen of bronchi (arrow head); **B.** Moderate- Epithelial thickening (double headed black arrow), parabronchial edema (black asterik), mononuclear infiltration (black arrow); **C.** Severe epithelial thickening (double headed black arrow), parabronchial edema admixed with inflammatory cells partly obstructed lumen (black asterik); **D.** Very severe epithelial thickening (double headed black arrow), parabronchial edema admixed with inflammatory cells completely obstructed lumen (black asterik).

hemorrhages located at the tip of the proventricular glands (Fig. 1, G). The caecal tonsils were enlarged and exhibited serosal hemorrhages with a congested, haemorrhagic mucosa (Fig.1 H). The intestinal mucosa showed oval, well demarcated, button like hemorrhagic ulcers (Fig.1, I).

Histopathology

In the present study, histopathological lesions of the trachea and lungs in ND were assessed using a lesion-scoring system, wherein score-1 denoted mild lesions, score-2 for moderate lesions, socre-3 severe lesions and score-4 very severe lesions. The detailed distribution of lesion scores is presented in Table 2.

In NDV infected birds, the tracheal mucosal epithelium showed changes ranging from mild to marked hyperplasia, deciliation and infiltration of mononuclear cells within the lamina propria, mucosa and submucosa (Fig. 2 A) In several cases, the trachea exhibited multifocal to diffuse necrosis of epithelial lining, accompanied by vascular congestion, submucosal edema and mild to moderate mononuclear infiltration (Fig. 2 B). In few birds, tracheal epithelial lining showed degenerative and necrotic changes accompanied by hemorrhage, congestion of blood vessels, mononuclear cell infiltrations and submucosal edema (Fig. 2 C-D).

The primary and secondary bronchi revealed denudation of cilia along with heterophil plug formation and mononuclear inflammatory cell infiltration around the bronchi (Fig. 3, A). In most of the cases, the parabronchi showed changes ranging from mild to severe epithelial thickening and mild to severe edema of parabronchi and atria were also observed (Fig. 3, B-D)

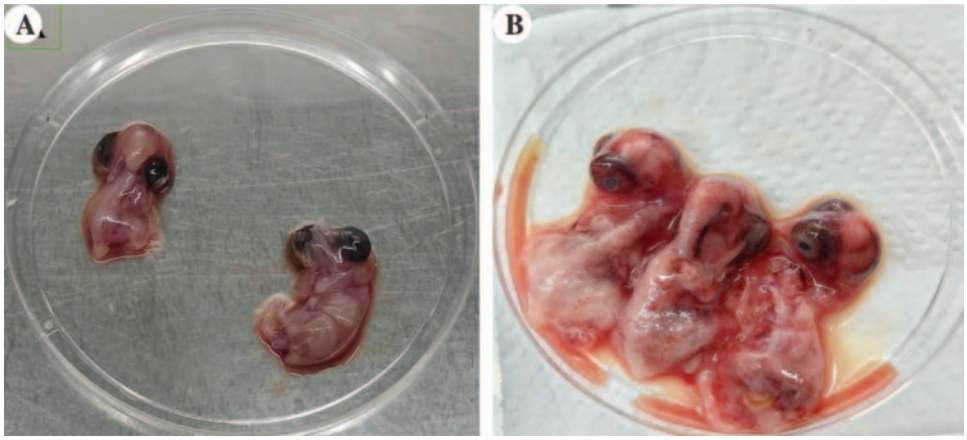

Fig 4. Gross pathological changes in NDV infected chicken embryos. A- Apparently normal embryos. B- Infected embryos showing petechial hemorrhages over the head, neck and limbs along with generalized edema

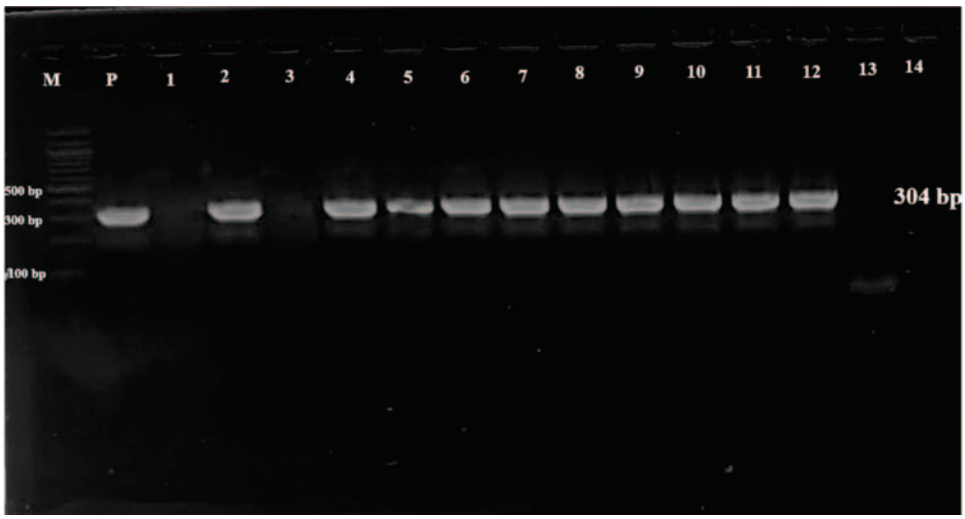

Fig. 5: Agarose gel profile illustrating F-gene- specific PCR amplicons of Newcastle disease virus. Lane M: 100 bp ladder, Lane P: Positive control; Lane 1-14: Field samples, Lane 2,4,5,6,7,8,9,10,11,12-Positive for ND

Egg inoculation

A 9-day old chicken embryo inoculated with the field strain of NDV showed marked pathological changes, including petechial hemorrhages over the head, neck and limbs along with generalized edema of the embryo (Fig.4 A, B).

Molecular detection of NDV

Among the various viral pathogens associated with respiratory infections, NDV was identified in 65 samples, accounting for an incidence of 62.5% of the 104 positive cases. To confirm the presence of NDV in the collected samples, RT-PCR was carried out using primers specific for the Fusion(F) gene. The PCR product was run on a 1.5% agarose gel along with a 100-bp DNA ladder. A distinct band around 304 bp, which matches the expected size for the targeted region of F gene, was visible in the positive samples (Fig. 5).

Nucleotide sequencing of NDV

Sanger Sequencing and Bioinformatic Analysis Bidirectional Sanger sequencing was performed

by Eurofins Genomics India Pvt. Ltd. (Hyderabad) using the same PCR primers (10 pmol/µL). The consensus nucleotide sequence was analyzed using BLASTn against the NCBI non-redundant (nr) database. Results PCR amplification yielded a clear 304-bp amplicon consistent with the expected size of the NDV F gene fragment. Sequencing confirmed the identity of the isolate, with >95% nucleotide identity to reference NDV strains (e.g., GenBank accessions PX409119.1and LC885048.1). Based on molecular evidence, the isolate was conclusively identified as Newcastle disease virus (Avian paramyxovirus 1).

DISCUSSION

In the current investigation, the study aimed for detection NDV. Among the birds examined, 104 birds were found to be positive for viral respiratory. The present study recorded an overall incidence of 65 cases (62.50 %) for Newcastle disease virus as a single infection. It was emerged as the predominant etiological agent responsible for respiratory disease outbreaks. These results corroborate with previous studies that identified the presence of NDV [13, 15-17]. The incidence of ND observed in the present study was marginally higher than that reported in some earlier investigations, which may be related to methodological variations among studies, including variations in number of pathogens targeted, longer study durations, difference in flock size and the number of samples analyzed by other researchers.

Flock wise analysis of viral respiratory infections in the present study showed that, out of 32 flocks screened, 13 (40.63%) flocks were found positive for NDV. The flock wise incidence observed in the present study has been previously reported[18].

In the present study, overall seasonal wise analysis showed a higher incidence of viral respiratory infections during the winter months compared to rainy season. NDV was identified consistently throughout the study period and remained as a predominant respiratory pathogen with an increased occurrence during winter season compared to rainy season. Comparable seasonal patterns have also been documented in previous studies, who also reported higher incidence of NDV in winter months[19,20, 21].

In the present study, chickens that succumbed to Newcastle disease exhibited gross respiratory lesions marked by various degree of congestion and edema of the lungs. In the present report lungs exhibited edema, congestion and areas of hemorrhage. The present investigation shows a close correlation with previously reported studies[22, 23]. Similar lesions were also reported in sonali chickens[24]. Trachea revealed mild to moderate congestion particularly around the cartilaginous rings, hemorrhages and mucosal congestion, as reported in earlier studies [3, 23, 25]. Air sacs were thickened[26] and cloudy or opaque and showed increased vascularity [3, 27].

Intestinal mucosa showed well demarcated, raised, circular button like ulcers which are hemorrhagic and these lesions were accompanied by mucoid to catarrhal enteritis[28]. Similar splenic lesions, characterized by enlargement and multiple discrete small necrotic foci on spleen[29]. In the present study, the caecal tonsils were enlarged and exhibited serosal hemorrhages with a congested, haemorrhagic mucosa. Our findings align with the comparable lesions documented[28]. The most frequent gross lesion observed in our study was pinpoint or petechial hemorrhages located at the tip of the proventricular glands[16].

In the current study, tracheal tissues from birds that died of NDV infection birds exhibited varied degrees of epithelial hyperplasia, loss of cilia and infiltration of lymphocytes in lamina propria and presence of submucosal lymphoid nodule. Comparable tracheal histopathological findings were also reported previously[13]. The trachea exhibited patchy necrosis of epithelium, congestion and edema in submucosa and infiltration. Similar lesions were also observed [23]. In few birds tracheal epithelial lining showed degenerative and necrotic changes accompanied by hemorrhage, congestion of blood vessels and mononuclear cell infiltrations. Comparable findings have also been documented earlier[24].

Pulmonary congestion, edema and mononuclear cell infiltration involving both alveolar septa and air spaces in NDV infection[24]. Comparable lung lesions were also evident in the present study. The bronchi exhibited ciliary loss with heterophilic plug formation and peribronchial mononuclear infiltration and parabronchial edema was consistent with earlier reports[13].

In the present study, embryos infected with NDV exhibited prominent lesions such as petechial hemorrhages over the head, neck and limbs along with generalized edema. These observatons are in agreement with the earlier findings reported[30].

RT-PCR was performed to detect the fusion (F) gene of new castle disease virus. A distinct band around 304 bp, which matches the expected size for the targeted region of F gene, was visible in the positive samples by using specific primers. Similar trends were documented in the present work[31] . These results are consistent with earlier reports[32, 33]. The PCR results confirm that NDV was circulating in the sampled population in Telangana.

ACKNOWLEDGMENTS

We would like to express our gratitude to P.V.

Narsimha Rao Telangana Veterinary University for providing necessary facilities and funds to carry out the research work.

Conflict of Interest : None

Financial Support & Sponsorship*:* None

Use of Artificial Intelligence (AI)-Assisted Technology for Manuscript Preparation: The authors confirm that there was no use of AI-assisted technology for assisting in the writing of the manuscript and no images were manipulated using AI.

REFERENCES

1. Moustapha A, Talaki E, Akourki A and Ousseini M. 2023. Newcastle disease virus in poultry: current status and control prospects. *World's Vet J* **13**(2):240-9.
2. Suarez D L, Miller P J, Koch G, Mundt E and Rautenschlein S. 2020. Newcastle disease, other avian paramyxoviruses, and avian metapneumovirus infections. *Dis Poultry* **13**: 109-66.
3. Gopal P A, Narayanaswamy H D, Sathyanarayana M L, Rao S, Rathnamma D and Hemadri D. 2023. Studies on respiratory tract pathology and molecular diagnosis of Newcastle disease in chickens in Karnataka. *Pharma Innovation* **12**:772-9.
4. Ravishankar C, Ravindran R, John A A, Divakar N, Chandy G, Joshi V, Chaudhary D, Bansal N, Singh R, Sahoo N and Mor S K. 2022. Detection of Newcastle disease virus and assessment of associated relative risk in backyard and commercial poultry in Kerala, India. *Vet Med Sci* **8**(3):1146-56.
5. Wang Y, Jiang Z, Jin Z, Tan H and Xu B. 2013. Risk factors for infectious diseases in backyard poultry farms in the Poyang Lake area, China. *Public Lib Sci One* **8**(6): e67366.
6. Jindal N, Chander Y, Chockalingam A K, De Abin M, Redig P T and Goyal S M. 2009. Phylogenetic analysis of Newcastle disease viruses isolated from waterfowl in the upper midwest region of the United States. *Virol J* **6**(1):191.
7. Dimitrov K M, Afonso C L, Yu Q and Miller P J. 2017. Newcastle disease vaccines— A solved problem or a continuous challenge. *Vet Microbiol* **206**:126 36.
8. Puro K and Sen A. 2022. Newcastle disease in backyard poultry rearing in the northeastern states of India: Challenges and control strategies. *Frontiers in Vet Sci* **9**: 799813
9. Getabalew M, Alemneh T, Akeberegn D, Getahun D, and Zewdie D. 2019. Epidemiology, diagnosis & prevention of Newcastle disease in poultry. *American J Biomedical Sci Res* **3**(1): 50-59.
10. Brown V R and Bevins S N. 2017. A review of virulent Newcastle disease viruses in the United States and the role of wild birds in viral persistence and spread. *Vet Res* **48**(1):68
11. Naz D, Rahman S, Aslam M A and Muhammad F. 2022. Newcastle disease virus in poultry with an interface as a human vector. *Vet Vac* **1**(1):100003.
12. Luna G L H T. 1968. *Manual of histological and special staining techniques*. 2nd ed., The Blakistone Divison McGraw-Hill Book Company, Inc. NewYork, Toronto London: 1-5 and 9-34.
13. Kaore M, Singh K P, Palanivelu M, Kumar, Ashok Kumar M, Reddy M R and Kurkure N V. 2018. Patho-epidemiology of respiratory disease complex pathogens (RDCPs) in commercial chicken. *Indian J Vet Pathol* **42**(4): 231-238.
14. Aldous E W and Alexander D J. 2001. Detection and differentiation of Newcastle disease virus (avian paramyxovirus type 1). *Avian pathology* **30**(2):117-28.
15. Broomand Z, Jafari R A and Mayahi M. 2018. Detection of Newcastle disease, H9N2 avian influenza, and infectious bronchitis viruses in respiratory diseases in backyard chickens in Ahvaz, Iran, in 2014-2015. *Archives of Razi Institute* **73**(1):19-25.
16. Momin A G and Singh D. 2018. Pathology and molecular diagnosis of Newcastle disease in chickens in and around Shillong, Meghalaya. *International J Curr Res* **10**:66251-4.
17. Deka P, Das S, Deka P, Nath M K, Hazarika R, Das G and Sarma M. 2022. Molecular Detection of Newcastle Disease Virus from Field Outbreaks in Assam, India. *Indian J Vet Sci Biotech* **18**(3), 97-99.
18. El-Shall N A, Sedeik M E, El-Nahas A F, Abdel-salam R A and Awad A M. 2019. Epidemiological Surveillance of Some Avian Respiratory Viral Diseases in Broiler Chickens. *Alexandria J Vet Sci* **61**(1).
19. Nwanta J A, Egege S C, Alli- Balogun J K and Ezema W S. 2008. Evaluation of prevalence and seasonality of Newcastle disease in chicken in Kaduna, Nigeria. *World Poultry Sci J* **64**(03): 416-423.
20. Olabode H O K, Damina M S, Ahmed A S, Moses G D and Wun gak Y S. 2012. Retrospective study of Newcastle disease in commercial poultry farms in Ilorin, Kwara State-Nigeria. *Vom J Vet Sci* **9**: 66 -70.
21. Bhutia L D and Singh Y D. 2016. Pathological studies on viral diseases of poultry in Mizoram, India. *Indian J Applied Res* **6**(9):606-10.
22. Bhutia L D, Rajkhowa T K, Ravindran R, Arya R S. Roychoudhury P, Mandakini, R K and Singh Y D. 2017. Occurrence of Newcastle disease in poultry population of Mizoram, India. *Indian J Vet Pathol* **41**(2): 151-154.
23. Dhaygude V S, Sawale G K, Chawak M M, Bulbule N R, Moregaonkar S D and Gavhane D S. 2017. Molecular characterization of velogenic viscerotropic Ranikhet (Newcastle) disease virus from different outbreaks in desi chickens. *Vet World* **10**(3):319.
24. Sajal S S, Rani S, Rahman M M, Mondal A and Alam K J. 2024. Sero-pathological Investigation of Newcastle Disease in Sonali Chicken in Narsingdi District in Bangladesh. *J Patuakhali Sci Tech Univ* **14**(1&2).
25. Regmi S, Bhatta R, Pal P, Shrestha A, Mató T, Puri B and Paudel S. 2024. Clinicopathological and Molecular Investigation of Newcastle Disease Outbreaks in Vaccinated and Non-Vaccinated Broiler Chicken Flocks in Nepal. *Animals* **14**(16):2423.
26. Shafi M, Jan S, Basher A, Shah S A, Shabir S, Mir M S, Kamil S A, Shah F and Mudasir S. 2023. Clinico-pathological assessment of naturally occurring Newcastle disease in broiler chicken reared in northern Himalayas. *Pharma Innovation J* **12**(8): 1436-1449
27. Gowthaman V, Singh S D, Dhama K, Barathidasan R, Anjaneya and Ramakrishnan M A. 2011. Pathology and molecular diagnosis of Newcastle disease virus infection in broiler breeders. *Indian J Vet Pathol* **35**(2):168 170.
28. Ali M, Khan M, Aslam A, Rehman H, Anjum A, Waheed S, Usman S, Masood S, Ullah A and Masood A. 2021. Molecular characterization and pathology of virulent newcastle disease virus isolated from broiler chickens in District Lahore, Pakistan. *Indian J Anim Res* 1420:1-8.
29. Maqbool B and Darzi M M. 2017. Comparative Pathology of Lymphoid Organs of Broiler Chicken in Commonly Encountered Disease Outbreaks. *Vet Res* **10**(2):6-14.
30. Bordoloi S, Nayak A, Singh A P, Singh R V, Jadav K, Dubey A, Jogi J, Shakya P and Himani K. 2021. Isolation and molecular characterization of Newcastle disease virus in layers. *Indian J Anim Res* **1**:9.

31. Collins M S, Bashiruddin J B and Alexander D J. 1993. Deduced amino acid sequences at the fusion protein cleavage site of Newcastle disease viruses showing variation in antigenicity and pathogenicity. *Archives virol* **128**(3-4):363 70.
32. Mihreteab B, Kgotlele T, Neguse F, Petros Y, Habtemariam H, Berhane Y, Wehab M, Cattoli G, Meki I K and Dundon W G. 2023. Phylogenetic analysis of Newcastle disease virus detected in Eritrea between 2017 and 2021. *Avian Pathol* **52**(6):426-31.
33. Molla G, Bitew M, Alemayehu D H, Mohammed A A, Ayele A, Tuki K and Guadie D. 2025. Molecular characterization and genotyping of Newcastle disease viruses using whole-genome sequencing from poultry farms in parts of Amhara Regions, and central Ethiopia. *Virol J* **22**(1):353.

Indian J. Vet. Pathol., 50(4) : 378-380, 2026: DOI: https://doi.org/10.56093/0zh5gx62

CASE REPORT

Pathological effects of immature amphistomosis in a goat – A case report

K. Thilagavathi* and J. Selvaraj
Department of Veterinary Pathology, Veterinary College and Research Institute, TANUVAS, Orathanadu, Thanjavur District, Tamil Nadu - 614 625

***Address for correspondence**
Dr. K. Thilagavathi, E-mail: thilagapatho@gmail.com
ORCID ID: 0000-0002-1624-251X

Received: 12.5.26; Accepted: 7.7.26

ABSTRACT

Immature amphistomosis is yet a very poorly understood disease of ruminants and falls under the category of neglected disease and often remains undiagnosed. An adult female goat carcass was submitted to the Department of Veterinary Pathology, Veterinary College and Research Institute, Orathanadu for necropsy. On necropsy examination, duodenal and proximal jejunal mucosa showed patchy areas of severe haemorrhage with thickened wall. Mucosa also showed multiple grey fleshy spots of 1-2 mm in diameter which were tightly attached to the mucosa. Intestinal scraping on microscopic examination, showed numerous motile immature amphistome flukes of various sizes with oral and ventral suckers. Histopathologically, intestine revealed the presence of cut section of immature amphistome flukes on the mucosa, submucosa and muscularis layer of intestine. The present case reported the pathological effects due to immature amphistomosis infection in a goat.

Key words: Immature amphistomes, Goat, Pathological effect

Livestock plays an important role in the economy of poor people in India. Domesticated small ruminants, especially sheep and goat are important sources of protein for many countries. Due to improper care, unhygienic environmental conditions, extreme climatic variations and close contact with infected animals, livestock get infected with a variety of parasites[1]. Paramphistomosis, a trematode infectious disease in ruminants, has been neglected but has recently emerged as an important cause of productivity loss[2]. Paramphistomosis (Amphistomosis) is a disease caused by digenean trematodes belonging to the family *Paramphistomatidae*. Adult paramphistomes are the main parasites in the rumen and reticulum of sheep, goats, cattle and buffaloes. Their early stages are in the small intestine and then migrate through the abomasum towards the rumen[1]. Immature paramphistomiosis is yet a very poorly understood disease of ruminants and falls under the category of neglected disease and often remains undiagnosed. It results in high death rates, reduced weight gain and milk production. Immature paramphistomiosis is a major problem in Indian subcontinent. The fluke causes havoc mortality in small domestic ruminants. Mortality rate may reach up to 75-88%. Prevalence and outbreak of immature amphistomiasis have been reported from Northern and also from Southern part of India[3]. The present communication reports about the pathological effects due to immature amphistomes infection in a goat.

An adult female goat carcass was submitted to the Department of Veterinary Pathology, Veterinary College and Research Institute, Orathanadu for necropsy. Duodenum and jejunum were collected in 10 % formalin for histopathological examination. Intestinal scrapping was taken for parasite identification. Intestinal tissues were processed in ascending grades of alcohol and cleared in xylene which was impregnated with melted paraffin to made tissue block. The 4µm tissue section was cut in a microtome which was deparaffinise in xylene, rehydrated in alcohol, stained with staining by haematoxylin and Eosin[4].

How to cite this article: Thilagavathi, K. and Selvaraj, J. 2026. Pathological effects of immature amphistomosis in a goat – A case report. Indian J. Vet. Pathol., 50(4) : 378-380.

On necropsy examination, both conjunctival mucous membranes were blanched indicating that the animal had anaemia which was supported by previous report[5] who stated that the clinical signs noticed in immature paramphistomosis, were because of helminthic parasites which adversely affect the absorption and utilization of proteins, minerals and vitamins as well as upset the general metabolism of the host by causing diarrhoea, anaemia and liver disorders.

Peritoneal, thoracic and pericardial cavities contained straw coloured fluid. It was in accordance with previous reports[4,6]. Duodenal and proximal jejunal mucosa showed patchy areas of severe haemorrhage,

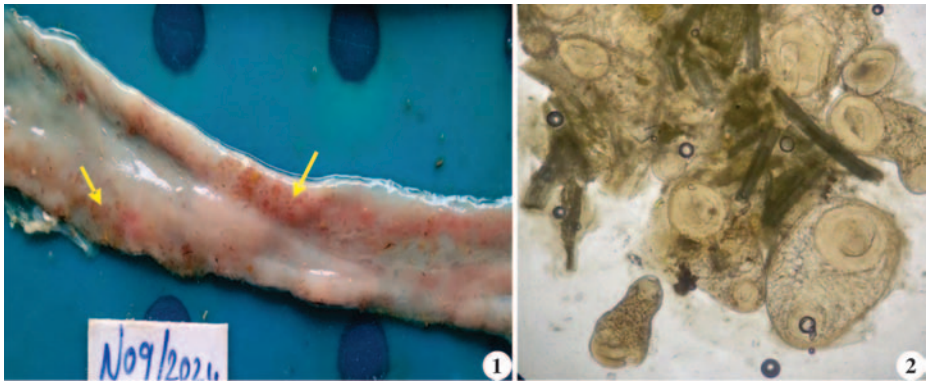

Fig. 1. Intestinal mucosa showing multiple grey fleshy spots of 1-2 mm in diameter (arrow) attached to the mucosa; **Fig. 2.** Intestinal scraping showing immature amphistome flukes with oral and ventral sucker.

petechiae in few areas and thickened wall. Mucosa also showed multiple grey fleshy spots of 1-2 mm in diameter which were tightly attached to the mucosa (Fig. 1). Intestinal scraping on microscopic examination, showed numerous motile immature amphistome flukes of various sizes with oral and ventral suckers (Fig. 2). These lesions were similar to earlier reports[7,8]. Histopathologically, intestine revealed the presence of cut section of immature

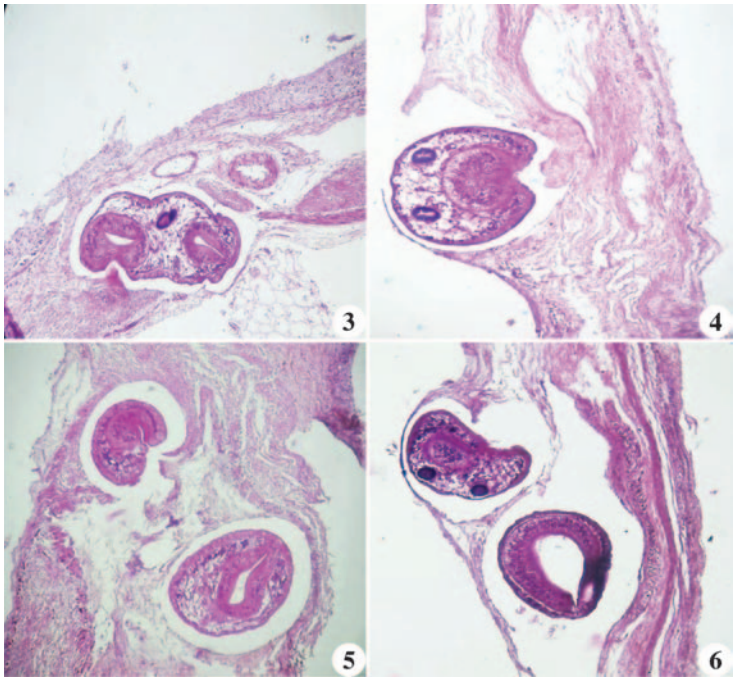

Fig. 3. Intestine showing cut section of amphistome fluke in muscularis layer with oral and ventral sucker (H&E x40); **Fig. 4.** Intestine showing cut section of amphistome fluke with plugging of sub-mucosal layer (H&E x40); **Fig. 5.** Intestine showing cut section of amphistome fluke with plugging of sub-mucosal layer (H&E x40); **Fig. 6.** Intestine showing cut section of amphistome fluke causing compression of inner circular muscle fibres (H&E x40).

amphistomes flukes on the mucosa, submucosa and muscularis layer of intestine. Flukes were attached to the surface of intestine or embedded in the mucosa to the level of muscularis mucosa layer (Fig. 3). Plugging of flukes through suckers into sub-mucosal layer (Figs. 4 and 5) were also observed. The pathological lesions due immature amphistome fluke infection were in strong agreement with previous report[6] who observed similar lesions, in addition with flattened villi and desquamated epithelium were reported. The high number of immature stages of the paramphistomes in the duodenum and upper ileum

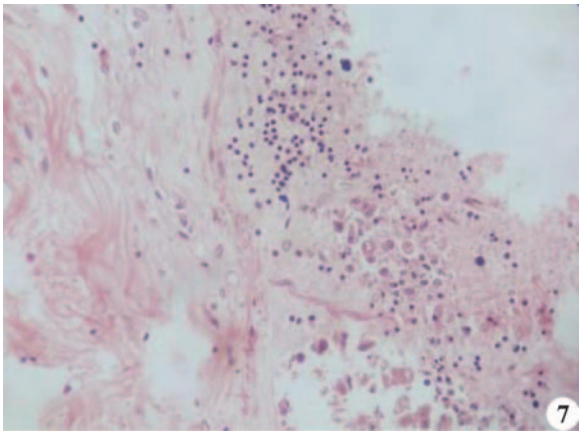

Fig. 7. Intestine showing focal infiltration of mononuclear cells and eosinophils in submucosal layer (H&E x400).

are responsible for severe pathological changes. These are embedded in the mucosa and are plug feeders, drawing pieces of the mucosa into the suckers which pinch them off causing necrosis and haemorrhage[9]. In the present case, fluke invaded into intestinal wall causing displacement as well as compression of inner circular muscle fibres (Fig. 6). There was focal infiltration of mononuclear cells and eosinophils were observed in submucosal layer (Fig. 7) which was supported by previous report[10]. The present case reported the pathological effects due to immature amphistomes infection in a goat.

Financial support & sponsorship*:* None

Conflict of interest : None

Use of artificial intelligence (AI)-assisted technology for manuscript preparation: The authors confirm that there was no use of AI-assisted technology for assisting in the writing of the manuscript and no images were manipulated using AI.

REFERENCES

1. Sivajothi S and Reddy BS. 2014. Immature paramphistomosis in a sheep herd. *Int J Biol Res* **2 (2):** 140-142.
2. Tehrani A, Javanbakht J, Khani F, Hassan MA, Khadivar F, Dadashi F Alimohammadi S and Amani A. 2015. Prevalence and pathological study of paramphistomum infection in the small intestine of slaughtered ovine. *J Parasit Dis* **39(1):** 100-106.
3. Sujatha T, Monda S, De AK, Perumal P, Sawhney S, Bala PA, Sunder J, Praveenraj J, Bhattacharya D and Chakurkar EB. 2023. First recorded outbreak of *Paramphistomum cervi* in Andaman local goats (*Capra aegagrus hircus*) from Bay Island of India: A brief communication. *Indian J Anim Sci* **93 (1):** 29–32.
4. Suvarna SK, Layton C and Bancroft JD. 2018. Bancroft's Theory and Practice of Histological Techniques, 8th Edn. Elsevier, Churchill Livingstone, USA.
5. Anand L, Dhanachand C, Mohilal N and Sharatkumar S. 2000. Prevalence of intestinal helminths in dairy cattle of Manipur, Uttar Pradesh. *J Zool* **20:** 93-95.
6. Balachandran C, Raman A and Pazhanivel N. 2010. An outbreak of amphistomosis in an organized sheep farm. *Tamil Nadu J Vet Anim Sci* **6:** 286-288.
7. Mondal MMH, Alim MA, Shahiduzzaman M, Farjana T, Islam MK, Das PM and Islam MZ. 2002. Pathology of Amphistomiasis in ruminants in Bangladesh. *Bangladesh Vet J* **36(3-4):** 103-108.
8. Kumar PC, Sundar SN and Prasad DV. 2016. Outbreak of immature paramphistomosis in Nellore Jodipi sheep. *J Parasit Dis* **40(2):** 533-35.
9. Soulsby EJL. 2006. Helminths, arthropods and protozoa of domesticated animals, 7th Edn. Bailliere Tindall, London, pp. 69-71.
10. Singh RP, Sahai BN and Jha GJ. 1984. Histopathology of the duodenum and rumen during experimental infections with *Paramphistomum cervi*. *Vet Parasitol* **15:** 39-46.

Indian J. Vet. Pathol., 50(4) : 381-383, 2026: DOI: https://doi.org/10.56093/78agjk39

CASE REPORT

Pathomorphology of ulcerated cutaneous eosinophilic granuloma in a horse

M. Karthick, M. Thangapandiyan, K. Gopal*, D.C. Monisha, P. Srinivasan and K. Balamurugan[1]
Department of Veterinary Pathology, Veterinary College and Research Institute, Namakkal, Tamil Nadu Veterinary and Animal Sciences University, Tamil Nadu
[1]Veterinary Assistant Surgeon

***Address for correspondence**
Dr. K. Gopal, E-mail: drvetpal@gmail.com
ORCID ID: 0000-0002-8747-9776

Received: 12.5.26; Accepted: 3.6.26

ABSTRACT

Eosinophilic granuloma is a non-neoplastic inflammatory dermatopathy of horses, characterized typically by nodular or occasionally ulcerative lesions associated with marked eosinophilic infiltration and collagen degeneration. A 5-year-old stallion was presented with a solitary, gradually enlarging mass on the right mandibular region. The lesion was firm, ulcerated, non-pedunculated and had irregular margins. Histopathological examination revealed a well-defined granulomatous lesion with dense infiltration of eosinophils admixed with macrophages and lymphocytes. The dermis showed marked collagen degeneration with formation of characteristic "flame figures," representing degenerated collagen fibres coated with eosinophilic granule proteins. Fibroplasia, neovascularization and perivascular inflammatory cell infiltration were also observed. No evidence of cellular atypia, mitotic activity or parasitic structures was observed. Based on the histopathological findings, the lesion was diagnosed as eosinophilic granuloma.

Keywords: Eosinophilic granuloma, Histopathology, Horse, Skin

How to cite this article: Karthick, M., Thangapandiyan, M., Gopal, K., Monisha, D.C., Srinivasan, P. and Balamurugan, K.2026. Pathomorphology of ulcerated cutaneous eosinophilic granuloma in a horse. Indian J. Vet. Pathol., 50(4) : 381-383.

Cutaneous nodular lesions are commonly encountered in equines and may arise from neoplastic, inflammatory or parasitic causes. Among the non-neoplastic conditions, eosinophilic granuloma is a frequently observed dermatopathy, typically presenting as firm dermal nodules that may occasionally undergo ulceration[1]. In certain cases, eosinophilic dermatoses may represent a component of a broader multisystemic eosinophilic disorder involving epithelial tissues[2]. Although the exact etiopathogenesis remains unclear, the condition is generally considered to be associated with hypersensitivity reactions to insect bites, trauma, allergens or foreign materials[3]. Similar lesions have also been reported in other equids, including mules[4].

Parasitic infections, particularly those caused by *Habronema* spp., have also been implicated in the development of eosinophilic granulomatous lesions[5]. Pathologically, the lesion is characterized by collagen degeneration (collagenolysis) accompanied by marked eosinophilic infiltration and granulomatous inflammation[6]. Histologically, a distinctive feature is the presence of "flame figures," which consist of degenerated collagen fibres coated with eosinophilic granule proteins and are considered a hallmark of this condition[7]. Clinically, such lesions may resemble neoplastic conditions, including equine sarcoids and squamous cell carcinoma, thereby necessitating confirmation through cytological and histopathological examination. The present report describes a case of eosinophilic granuloma affecting the mandibular region of a horse.

A 5-year-old stallion was presented with a solitary, progressively enlarging mass on the right side of the mandible. The lesion was ulcerated, firm and non-pedunculated with irregular margins. No systemic abnormalities were observed. A biopsy sample was collected and fixed in 10% neutral buffered formalin. Routine paraffin embedding was carried out and sections of 4 µm thickness were stained with haematoxylin and eosin (H&E) for microscopic examination.

Grossly, a solitary, firm, raised, non-pedunculated mass was observed on the right mandibular region, showing surface ulceration, irregular margins and moderate adherence to the underlying tissues (Fig 1). The cut surface appeared grey to yellowish. Histopathological examination revealed a large area of necrosis on the overlying epidermis with clumps of bacteria, severe infiltration of neutrophils and dermis showing severe inflammatory changes with dense inflammatory infiltration. The infiltrate predominantly

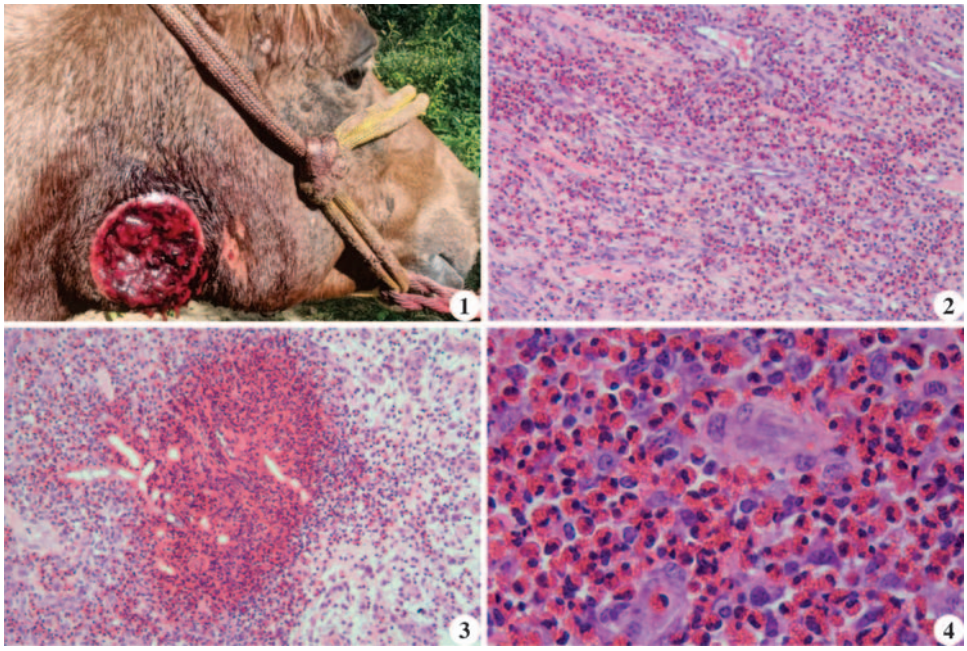

Fig. 1. Ulcerated solitary mass on the right mandibular region of the horse; **Fig. 2.** Dense eosinophilic infiltration in the dermis with collagen degeneration and early flame figure formation (H&E x100); **Fig. 3.** Collagenolysis with characteristic flame figures surrounded by numerous eosinophils (H&E x100); **Fig. 4.** Higher magnification showing eosinophil-rich granulomatous inflammation with multinucleated giant cells (H&E x400).

minor trauma[1,3] and may occasionally be associated with parasitic infections such as habronemiasis[5]. In the present case, although the exact aetiology could not be established due to lack of clinical history, the lesion is most likely attributable to a localized hypersensitivity reaction, possibly triggered by insect bite or minor trauma, in the absence of parasitic involvement or systemic disease. The lesion, located in the mandibular region, represents an uncommon site, as most reported cases involve the neck, back or withers[1,4]. The ulcerated appearance of the mass necessitated differentiation from neoplastic conditions such as equine sarcoid and squamous cell carcinoma. However, the absence of cellular atypia and invasive behaviour supported a non-neoplastic inflammatory origin.

Microscopic examination revealed features such as dense eosinophilic infiltration, collagenolysis, granuloma formation and perivascular cuffing, which are consistent with earlier reports[1,2]. The identification of flame figures, along with associated fibroplasia and vascular changes, further substantiates the diagnosis and aligns with previously described eosinophilic collagenolytic granulomas in horses[1,3,6,7]. Although eosinophilic dermatoses may be associated with systemic involvement, the lack of such findings in this case indicates a localized condition[2]. Differential diagnoses, including parasitic granulomas and neoplastic lesions[5], were excluded in the present case based on the absence of parasitic structures and neoplastic features. From a therapeutic standpoint, eosinophilic granulomas may respond to corticosteroid treatment; however, surgical excision is often recommended for large or solitary lesions[1,5]. The well-defined nature of the lesion in the present case supports surgical management, which is generally associated with a good prognosis.

composed of eosinophils admixed with macrophages and lymphocytes, resulting in disruption and separation of collagen bundles (Fig. 2). Marked collagen degeneration (collagenolysis) with formation of characteristic flame figures was observed, surrounded by numerous eosinophils and occasional multinucleated giant cells (Fig. 3). Additionally, areas of eosinophil-rich granulomatous inflammation characterized by the presence of multinucleated giant cells were evident (Fig. 4). No evidence of neoplastic proliferation or parasitic structures was observed.

Eosinophilic granuloma is considered to arise from a hypersensitivity reaction to insect bites, allergens or

ACKNOWLEDGEMENT

The authors are thankful to the Department of Veterinary Pathology, Veterinary College and Research Institute, Namakkal for providing the laboratory facility.

Financial support and sponsorship: None

Conflict of interest: None

Use of artificial intelligence for manuscript preparation: The author confirms that there was no use of AI-assisted technology for assisting in the writing of the manuscript and no images were manipulated using AI.

REFERENCES

1. Abbasi MF, Azizi S, Kheirandish R, Paidar A and Oloumi MM. 2015. Surgical treatment of too large eosinophilic granuloma in an Arabian horse. *Iran J Vet Surg*. **10**(2):73–76.
2. Wilkie JSN, Yager JA, Nation PN, Clark EG, Townsend HGG and Baird JD. 1985. Chronic eosinophilic dermatitis: a manifestation of a multisystemic eosinophilic epitheliotropic disease in five horses. *Vet Pathol*. **22**:297–305.

3. Slovis NM, Watson JL, Affolter VK and Stannard AA. 1999. Injection site eosinophilic granulomas and collagenolysis in horses. *J Vet Intern Med*. **13**(6):606–612.
4. Grigoletto R, Fantinato-Neto P, Strefezzi RF and Dória RGS. 2015. Eosinophilic granuloma in a mule. *J Cytol Histol*. **S3**:016.
5. Tyrnenopoulou P, Diakakis N, Psalla D, Traversa D, Papadopoulos E and Antonakakis M. 2018. Surgical management of eosinophilic granuloma associated with *Habronema* spp. infection. *Equine Vet Educ*. **30**(4):194–198.
6. Caston SS and Fales-Williams AJ. 2016. Eosinophilic granuloma in the forelimb of an Arabian mare. *J Equine Vet Sci*. **39**:78–81.
7. Devi VR, Hewicker-Trautwein M and Rohlmann B. 2006. Eosinophilic collagenolytic granuloma in a horse. *Indian J Vet Pathol.* **30(2):** 54

Indian J. Vet. Pathol., 50(4) : 384-385, 2026: DOI: https://doi.org/10.56093/v41vkr83

CASE REPORT

Fibrosarcoma in a labrador retriever dog

K. Kalai, B. Debroy* and S.W. Monsang[1]
Department of Veterinary Pathology, College of Veterinary Sciences and A.H., R.K. Nagar, Tripura (West) -799008, India
[1]Department of Veterinary Surgery

***Address for correspondence**
Dr. B. Debroy, E-mail: biplabvets@yahoo.co.in
ORCID ID: 0000-0002-8013-6498

Received: 2.5.26; Accepted: 3.7.26

ABSTRACT

Fibrosarcoma is an aggressive malignant tumour originating from fibrous connective tissue. The present case report describes a 7-year-old female Labrador Retriever dog presented with a prominent, firm, tennis ball–sized mass on the right side of the face. The lesion was extending into the oral cavity and causing marked discomfort and difficulty in feeding. Microscopic examination revealed densely packed spindle-shaped fibroblastic cells arranged in an interwoven and herringbone pattern, exhibiting marked cellular atypia, pleomorphism and increased mitotic activity. Areas of inflammation, angiogenesis and necrosis were also evident within the tumour mass. Based on these characteristic histopathological features, the lesion was diagnosed as fibrosarcoma. This report emphasizes the importance of early recognition, histopathological confirmation and timely intervention to improve clinical management and prognosis in affected animals.

Keywords: Dog, Fibrosarcoma, Labrador Retriever, Tumour

How to cite this article: Kalai, K., Debroy, B. and Monsang, S.W. 2026. Fibrosarcoma in a labrador retriever dog. Indian J. Vet. Pathol., 50(4) : 384-385.

Fibrosarcoma is a highly aggressive malignant neoplasm arising from fibroblasts of fibrous connective tissue and is characterized by infiltrative growth and a tendency for local recurrence[1]. In dogs, fibrosarcoma is reported in the skin and subcutaneous tissues; however, they may also occur in various anatomical locations including the oral cavity, extremities and facial region[2]. Canine oral fibrosarcoma is the third most frequently encountered malignant mesenchymal tumour affecting the oral cavity of dogs[3]. Tumours involving the facial area are of particular clinical concern because of discomfort, facial deformity, feeding difficulties and impairment of normal oral functions. The diagnosis of fibrosarcoma generally relies on a combination of clinical findings, cytological and histopathological examination. Early recognition and accurate diagnosis are essential for timely therapeutic or surgical intervention and improved clinical outcomes. The present case report describes the clinical presentation and diagnosis of facial fibrosarcoma in a Labrador retriever dog.

A 7-year-old female Labrador Retriever was presented with a history of a progressively enlarging swelling on the right side of the face. According to the history, the mass had gradually increased in size over time and was associated with noticeable discomfort during feeding. On physical examination, a firm, well-demarcated multilobulated mass approximately the size of a tennis ball was observed on the right facial region (Fig. 1). The swelling extended internally into the oral cavity, causing distortion of the adjacent tissues. The mass was non-ulcerated externally but appeared to exert pressure on surrounding structures, contributing to the feeding difficulties. No other significant systemic abnormalities were detected during the general clinical examination.

For confirmatory diagnosis, biopsy samples from the mass were aseptically collected and fixed immediately in 10% neutral buffered formalin. The samples were processed by routine paraffin embedding technique. Sections of 4-5 µm thickness were cut using rotary microtome and stained with routine haematoxylin and eosin (H&E) following standard protocol[6]. Microscopic examination revealed a highly cellular neoplasm composed predominantly of densely packed spindle-shaped cells arranged in interwoven fascicles (Fig.2). The neoplastic cells exhibited elongated nuclei, moderate cytoplasm and indistinct cell borders. Marked cellular atypia and pleomorphism were evident, along with increased mitotic figures in several fields (Fig.3). In addition, multifocal areas of inflammatory cell infiltration, prominent angiogenesis and focal necrosis were observed within the tumour mass (Figs. 4, 5).

Based on the clinical presentation and characteristic microscopic findings, the tumour was diagnosed as fibrosarcoma. Surgical excision of the tumour mass with wide margins was performed based on the biopsy report. The histopathological examination of the excised tumour mass also revealed similar features of fibrosarcoma. The oral gross lesions observed in the present case are similar with earlier report[3].The microscopic

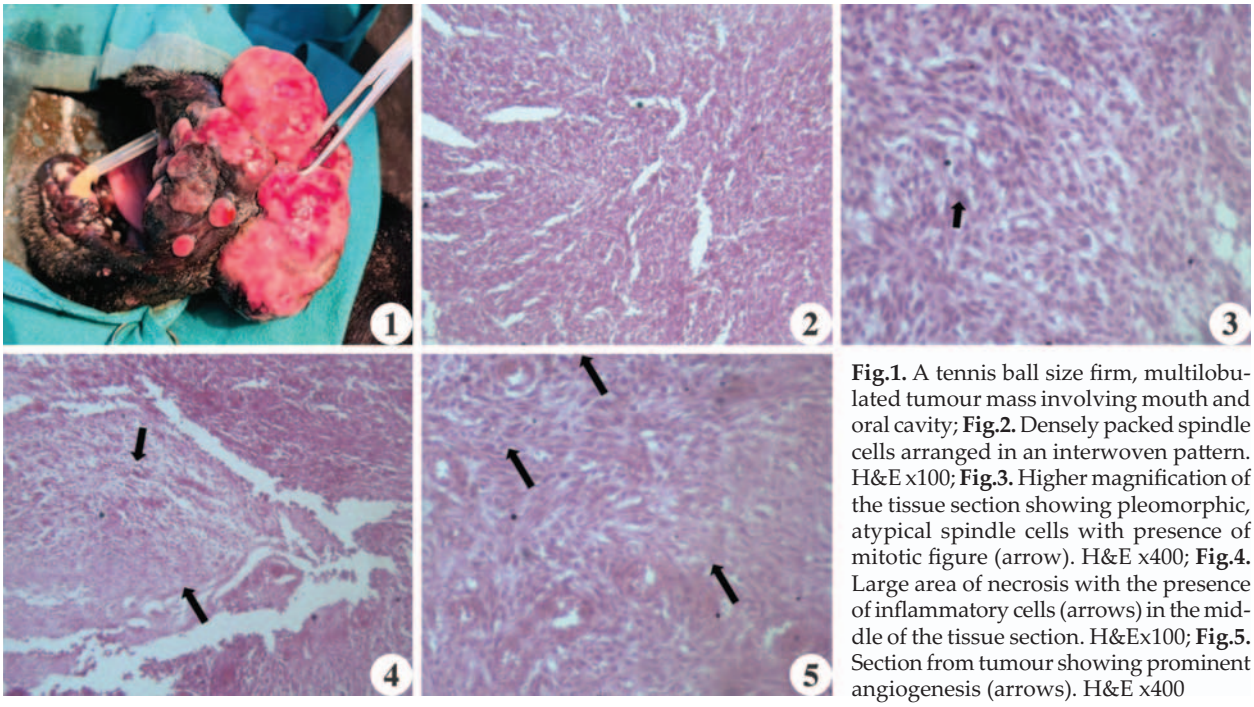

Fig.1. A tennis ball size firm, multilobulated tumour mass involving mouth and oral cavity; **Fig.2.** Densely packed spindle cells arranged in an interwoven pattern. H&E x100; **Fig.3.** Higher magnification of the tissue section showing pleomorphic, atypical spindle cells with presence of mitotic figure (arrow). H&E x400; **Fig.4.** Large area of necrosis with the presence of inflammatory cells (arrows) in the middle of the tissue section. H&Ex100; **Fig.5.** Section from tumour showing prominent angiogenesis (arrows). H&E x400

features observed in the present case were consistent with the classical morphology of fibrosarcoma reported in dogs and similar histopathological findings, including proliferation of spindle-shaped fibroblastic cells with cellular atypia and focal necrosis were also documented in canine fibrosarcoma cases [4,5]. Anaplasia and angiogenesis also reported earlier in a case of vaginal fibrosarcoma in dog[7]. Recognition of these characteristic features is crucial for differentiating fibrosarcoma from other soft tissue sarcomas and for guiding suitable therapeutic strategies. Early recognition of such aggressive neoplasms is essential for timely therapeutic intervention. Complete surgical excision of the tumour at an early stage plays a crucial role in prolonging life span and reducing the chances of recurrence.

ACKNOWLEDGEMENT

The authors thank the Principal, C.V.Sc. & A.H. R.K. Nagar, Tripura (W) for providing necessary facilities to carry out the research.

REFERENCES

1. Augsburger D, Nelson P, Kalinski T, Udelnow A, Knosel T. 2017. Current diagnostics and treatment of fibrosarcoma -perspectives for future therapeutic targets and strategies, *Oncotarget* **8** (61): 638–653.
2. Goldschmidt MH and Hendrick MJ. 2002 Tumors of the Skin and Soft Tissues. In: Meuten, D.J., Ed., Tumors in Domestic Animals, 4th Edition, Wiley, USA.
3. Verma A, Madhu Swamy Y, Shobha J, Dubey A, Rajput N. 2024. Oral fibrosarcoma in dog: Cytological, histopathological and immunohistochemical diagnosis. *Indian J Anim Res* **58**(3): 422-428.
4. Begum S, Deka A, Tamuli SM, Dutta B, Buragohain M. 2022. Fibrosarcoma in a dog: Case report. *Pharm Innov J* **11**(11): 1098-1100.
5. Soujanya S and Madhuri D. 2019. Cutaneous fibrosarcoma in dog. *J Entomol Zool Stud* **7**(1):861-863.
6. Luna LG. 1968. Manual of histological staining methods of the Armed Forces Institute of Pathology, 3rd edn., McGraw-Hill Book Company, New York, USA.
7. Mumba C, Pandeyl GS, Chijikwa J, Munjita S. 2013. Multiple Vaginal fibrosarcoma in a dog. *Indian Vet J* **90**(2):108-109.

Indian J. Vet. Pathol., 50(4) : 386-387, 2026: DOI: https://doi.org/10.56093/nqct3w45

CASE REPORT

An unusual case of fibroma in a Japanese quail

D.C. Monisha*, K. Gopal, P. Srinivasan, M. Karthick and P. Thirunavukkarasu[1]
Department of Veterinary Pathology, [1]Department of Poultry Science, Veterinary College and Research Institute, Namakkal
TANUVAS, Tamil Nadu, India

***Address for correpondence**
Dr. D.C. Monisha, Ph.D., Scholar, E-mail: dcmonishadpi@gmail.com
ORCID ID: 009-0003-1360-054X , 0000-0002-8747-9776

Received: 29.4.26; Accepted: 2.6.26

ABSTRACT

The incidence of fibroma is commonly reported in domestic animals. In chicken so far fibrosarcoma has been reported. The present case describes about the unusual case of cutaneous fibroma in a quail. A 6-months old Japanese quail was presented to Department of Veterinary Pathology, Namakkal for postmortem examination. The mass was located on 3rd toe of left leg of about 1.5 cm in diameter. On cut section it was greyish white in colour and rubbery in consistency. Histopathological examination revealed wavy bundles of spindle shaped fibroblasts. The cells are oval, elongated and indistinct nucleoli with abundant collagen. The collagenous fibres were in the form of whorls and they stain blue with Masson's trichrome staining. Immunohistochemistry showed strong expression for vimentin. Based on histopathology, histochemistry and immunohistochemistry this case was diagnosed as fibroma.

Keywords: Cutaneous fibroma, Masson's trichrome, Quail and Vimentin

How to cite this article: Monisha, D.C., Gopal, K., Srinivasan, P., Karthick, M. and Thirunavukkarasu, P. 2026. An unusual case of fibroma in a Japanese quail. Indian J. Vet. Pathol., 50(4) : 386-387.

Fibromas are non-malignant tumors of mesenchymal origin and consists of fibrous connective tissue arising from the fibroblasts. These growths tend to enlarge slowly and are well-defined[1]. These tumors are commonly located in eyelids, wings, between the toes and beak commissure[2]. The incidence has been reported in 24-week-old layer pullet while multifocal visceral fibrosarcoma has been reported in 2 years old hen[2] and petbirds[3]. The development of tumorous growth like fibroma is due to several factors such as hereditary influences, persistent stress, exposure to radiation, viral agents, endocrine imbalances and prolonged contact with various chemical and physical irritants[4]. The cutaneous fibromas are classified into two types as hard (dermato fibromas) and soft fibromas. Hard fibromas are predominantly composed of dense collagen fibres with a little cellular component, whereas soft fibromas (fibroma molle) are made up of loose arrangement of cells with minimal fibrous connective tissue[5]. These tumors are well defined, white to gray, elevated or rounded masses usually firm in consistency, measuring about 0.5×2 cm in diameter. The fibroma and fibrosarcoma are similar in appearance on gross examination, the only distinguishing feature of fibrosarcoma is that these tumors have irregular margins and often ulcerated[6].

A 6 months old Japanese quail was brought to Department of Veterinary Pathology, Veterinary College and Research Institute, Namakkal for postmortem examination. Detailed postmortem examination was carried out. On gross examination, the mass was located on the left leg – 3rd toe. The respective sample was collected in 10 % formalin. Paraffin embedded tissue sections were cut into 4µm thickness and stained with Haematoxylin and Eosin (H&E). Further, Masson trichrome staining was done as per the procedure[7] and immunohistochemistry for Vimentin was done as per the protocol of earlier author[8].

The mass was located on 3rd toe of left leg measuring about 1.5 cm in diameter (Fig. 1). On gross examination, the mass was white to grey in colour, firm and rubbery in consistency. The histological examination of the mass revealed numerous oval to spindle shaped fibroblasts with interlacing bundles of collagenous fibre and had elongated to oval nuclei and indistinct nucleoli (Fig. 2). Special staining was done to confirm the collagen in the neoplastic mass and it was positive for Masson's trichrome. The collagenous fibres were in the form of whorls and appeared blue in colour (Fig. 3). The immunohistochemical staining showed strong positive expression for vimentin with abundant interlacing bundles of collagen fibres (Fig. 4).

Fibromas are benign mesenchymal tumors of the skin and soft tissues which originates from the fibrocytes with predominance of collagen fibres. These tumors are most commonly observed in adult animals with no significant influence on sex or species[9]. Actually, collagen determines the type of tumor to

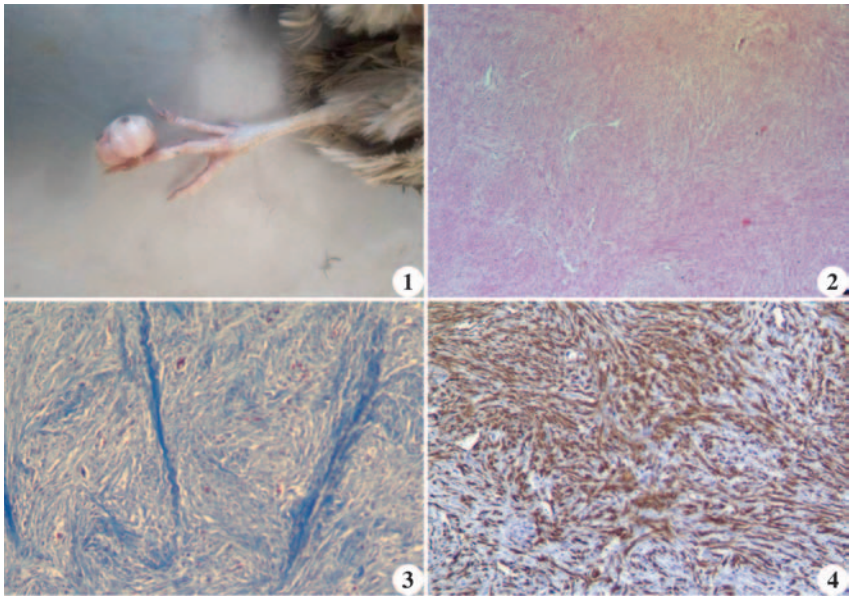

Fig. 1. The pedunculated oval mass in the third toe; **Fig. 2.** The histopathological examination revealed abundant collagen with oval to spindle shaped fibroblast and interlacing bundles of collagen fibres (H&E x40); **Fig. 3.** Masson trichome stain revealed numerous collagenous fibres which were arranged in the whorls and appeared blue in colour (Masson trichome stain x100); **Fig. 4.** The immunohistochemical staining for vimentin showed strong positive expression in interlacing bundles of fibroblast (IHC x100)

Masson's trichrome staining which showed positive for collagen fibres by a characteristics blue staining of stromal fibres. This finding further supports the fibroblastic origin of the tumor and is well correlated with the dense collagenous stroma observed in the histopathological sections. These observations are in agreement with previous reports, where fibromas were similarly confirmed using special stains such as Masson's trichrome[12].

The immunohistochemical staining in the present case showed strong positive expression of vimentin which further confirms the mesenchymal origin. This finding correlates well with the histopathological observation of spindle shaped fibroblastic cells arranged in interlacing bundles[9]. Absence of marked cellular atypia and low mitotic figures confirms the benign nature of the tumor. Hence, IHC plays a important role in substantiating the diagnosis of fibroma in this case.

Financial support and sponsorship: None

Conflict of Interest: None

Use of Artificial Intelligence for manuscript preparation: The author confirms that there was no use of AI-assisted technology for assisting in the writing of the manuscript and no images were manipulated using AI.

REFERENCES

1. Goldschmidt MH, Hendrick MJ. 2002. Tumors of the skin and soft tissues. In: Tumors of Domestic Animals, 4th ed., Iowa State Press, Iowa. Pp. 78-81.
2. Reece RL. 1996. Some observations on naturally occurring neoplasms of domestic fowls in the State of Victoria, Australia (1977–87). *Avian Pathol* **25**(3): 407-447.
3. Sanchez Godoy F, Ledesma Ramirez I and Morales Salinas E. 2020. A retrospective study of neoplasms in ornamental and pet birds diagnosed at the Hospital de Aves of the Universidad Nacional Autonoma de Mexico (2007-2014). *Braz J Vet Pathol* **13**(1): 1-11.
4. Jubb KVF and Kennedy PC. 1963. The Skin and Appendages. In: Jubb KVF, P.C. Kennedy PC and Palmer N, Pathology of Domestic Animals, 4th ed. 2:565.
5. Kumar KM, Rao CM, Veena P, Amrita V, Reddy KS, Kumari DV and Baba MS. 2014. Surgical management of fibroma in a bullock: A case report. *Int J Sci Environ Technol* **3**: 2284-2286.
6. Schmidt RE, Reavill DR, Phalen D. 2003. Pathology of pet and aviary birds. Ames (IA): Iowa State Press. pp. 153–92.
7. Bancroft JD and Gamble M. 2012. Theory and practice of histological techniques. 7th ed. Edinburgh. Churchill Livingstone, London. Pp.105-125.
8. Gopal K, Vijayakumar M, Kokila S, Thilagavathi K, Arulmozhi A and Balachandran P. 2024. Gingival haemangioma in a Jersey cross bred calf. *Indian J Vet Pathol* **48**(4): 372-374.
9. Meuten DJ. 2002. Tumors in domestic animals. 4th ed. Iowa: Iowa State Press, pp. 84-86.
10. Mana HP, Haruna AA, Mohzo DL and Abba A. 2021. Fibroma Molle (Acrochordon) in a Caucasian female Dog: case report. *Int J Vet Sci Anim Husb* **6**(6): 11-15.
11. Subapriya S, Vairamuthu S, Pazhanivel N, Ali M and Sumathi D. 2020. Pathology of cutaneous fibroma in a German Shepherd Dog. *Pharma Innov* **9**(4): 176-177.
12. Chonat A, Sharma A, Santha Devi A, Narayane R, Sanguida A and Raja R. 2026. The rare occurrence of a solitary collagenous fibroma in the gingiva of a 2-year-old child: A case report. *Case Rep Dent* **2026**(1): 5566658-5566673.

Title of Thesis	:	Pathology of porcine parvovirus infection in pig and expression of recombinant NS1 protein to evaluate the immunodiagnostic potential
Name of the Student	:	**Deepti Singh**
Name of the Guide	:	Dr Chandrakanta Jana
Degree/Year	:	PhD/2026
Name of the University	:	ICAR-Indian Veterinary Research Institute, Izatnagar, Bareilly, Uttar Pradesh

Porcine parvovirus type 1 (PPV1) is a non-enveloped, single-stranded DNA virus recognized as one of the most significant infectious agents responsible for reproductive failure in swine worldwide. It is the primary etiological agent of SMEDI syndrome (stillbirth, mummification, embryonic death and infertility), affecting pregnant sows following transplacental infection. The present study was undertaken to investigate the occurrence, molecular epidemiology, pathological consequences and immunodiagnostic characterization of PPV1-associated reproductive failure in swine populations across commercial farrow-to-finish farms. Clinically affected herds exhibited classical signs of reproductive failure, including reduced litter size, stillbirths, mummified fetuses, infertility and repeat breeding in otherwise healthy sows. Among live-born piglets, weakness, stunted growth and transient diarrhea were frequently observed. Molecular screening revealed PPV1 positivity in 60.2% of stillborn/mummified foetuses (109/181). Co-infections of PPV1 and PCV2 occurred in 23.7% of fetuses and 9% of necropsy samples. Mixed viral-bacterial infections involving *Streptococcus suis* and *Haemophilus parasuis* were observed in 2.6% of necropsy cases. All samples were found to be negative for PRRSV, PCV3 and *Brucella suis*. Gross pathological examination revealed severely mummified foetuses with variable degrees of congestion and haemorrhages in stillborn fetal tissues. Histopathology demonstrated multisystemic lesions including pulmonary oedema, myocardial and hepatic degeneration, renal tubular damage, lymphoid depletion and intestinal crypt necrosis with inflammation. Quantitative PCR (qPCR) showed highest PPV1 load in placenta followed by liver, intestine, stomach, heart and uterus, with consistently high levels in mummified foetuses, indicating active replication. PMWS cases with PPV1, PCV2 and bacterial co-infection showed serous effusions, lymphoid depletion and widespread inflammatory and degenerative changes in tissues. The PPV1 isolate was successfully adapted in the Embryonic Swine Kidney-4 cell line (ESK-4), producing cytopathic effects from the sixth passage onward and confirmed viral propagation across passages by qPCR. Phylogenetic analysis of NS1 gene showed close genetic similarity (97.7-99.8%) to global PPV1 strains, particularly Danish and Indian isolates. The phylogenetic analysis of VP2 gene placed the isolate within the Asiatic lineage. The NS1 gene (truncated) was cloned and expressed in *E. coli* BL21 (DE3), yielding a ~45 kDa recombinant protein confirmed by SDS-PAGE and Western blotting. Immunization of rabbits with rNS1 induced strong humoral responses at 42 days post inoculation. The sera showed immunoreactivity comparable to commercial antibodies across multiple porcine tissues, validating its diagnostic potential. Overall, the study provides comprehensive evidence of PPV1-associated reproductive failure with widespread pathological lesions in foetal tissues and establishes a reliable immunodiagnostic platform in swine health management.

Book Review by Megha Sharma, Scientist, ICAR-IVRI, Izatnagar

on

Textbook on Pathology of Diseases of Laboratory Animals authored by Somvanshi, R

1st edition (2026), soft bound, published by DKMA (ICAR), Pusa Campus, New Delhi

Laboratory animals constitute an indispensable component of contemporary biomedical and veterinary research and are extensively used in investigations involving infectious diseases, vaccine development, toxicology, immunology, oncology, experimental therapeutics and translational medicine. However, information on diseases of laboratory animals is frequently dispersed across general veterinary pathology texts, laboratory animal medicine references and individual scientific publications, creating a need for a focused resource dedicated specifically to their pathology. Dr. R. Somvanshi has addressed this need through his *Textbook on Pathology of Diseases of Laboratory Animals*, published by the Directorate of Knowledge Management in Agriculture, Indian Council of Agricultural Research (ICAR), New Delhi. The book is particularly noteworthy because it represents the contribution of an author with more than four decades of experience in Veterinary Pathology and laboratory animal disease research, bringing considerable practical and diagnostic experience to this specialized subject.

This 150-page textbook provides a dedicated reference on the pathology of diseases affecting laboratory animals and occupies an important position at the interface of Veterinary Pathology, laboratory animal (mice, rat, guinea pig and rabbit) medicine and experimental biomedical research. Its focused approach distinguishes it from conventional Veterinary Pathology textbooks, in which diseases of laboratory animals are generally covered only briefly or dispersed across different sections. In this respect, the book can be considered one of its kind in the Indian veterinary literature, particularly as a specialized text devoted to the pathological understanding of laboratory animal diseases. The subject is of considerable practical importance because spontaneous diseases, subclinical infections and background lesions may occur in laboratory animals and can influence experimental observations. Recognition of these changes is essential for differentiating naturally occurring pathology from experimental or treatment-related lesions and, consequently, for the appropriate interpretation of research findings.

The book has substantial educational value across different levels of veterinary training. For B.V.Sc. & A.H. students, it provides a focused resource for developing an understanding of diseases and pathological changes occurring in laboratory animal species and serves as a useful complement to conventional veterinary pathology textbooks. For post graduate students specializing in Veterinary Pathology, the book can serve as an important reference for advanced learning, practical training, dissertation work and research planning. Its utility extends further to research scientists working in experimental pathology, infectious diseases, toxicology, immunology, oncology, vaccine development and other disciplines involving laboratory animal models. Another useful feature is its potential application in competitive examination preparation, including the Agricultural Research Service (ARS) and other examinations in veterinary and agricultural sciences. The focused treatment of laboratory animal pathology provides students with a consolidated source of information that can complement standard Veterinary Pathology textbooks and examination-oriented material. The book therefore has relevance beyond academic instruction and can contribute to the broader understanding of pathology as an essential component of laboratory animal health assessment and experimental research.

The rapidly evolving nature of laboratory animal science provides scope for further expansion in subsequent editions. Future editions could incorporate emerging areas such as molecular pathology, advanced diagnostic techniques, genetically modified laboratory animals, and contemporary developments in toxicologic and translational pathology. Greater integration of these emerging approaches with conventional morphological pathology would further enhance the book's utility for researchers and diagnostic pathologists.

Overall, *Textbook on Pathology of Diseases of Laboratory Animals* is a timely and valuable contribution to Veterinary Pathology and laboratory animal science, addressing a specialized area for which dedicated resources are relatively limited in the Indian context. The author's extensive professional experience, together with the focused scope of the book, gives it particular practical and academic relevance. By bringing the pathology of laboratory animal diseases together in a dedicated volume, the book makes a meaningful contribution to veterinary literature and reinforces the importance of laboratory animal pathology in the interpretation and advancement of modern experimental biomedical research.

SUPERANNUATION

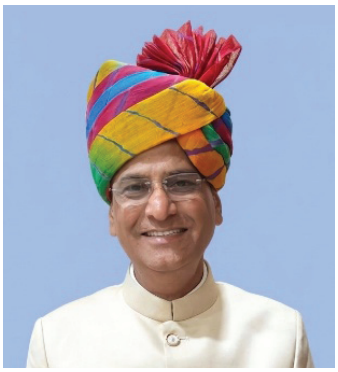

Prof. (Dr.) Rohitash Dadhich, FIAVP

Prof. (Dr.) Rohitash Dadhich, a distinguished academician, scientist, teacher, and administrator in the field of Veterinary Pathology, was born on 20 August 1966 in Bikaner to the respected educationist Shri Shabd Sharan Ji Sharma and Smt. Champa Devi Sharma. He completed his B.V.Sc. & A.H. in 1994, M.V.Sc. in 1996, and Ph.D. in 2004 from the College of Veterinary and Animal Science, Bikaner, exemplifying academic excellence and lifelong dedication to education and veterinary science. His professional journey began on 30 October 1995 as a Veterinary Assistant Surgeon in the Department of Animal Husbandry, Government of Rajasthan, and after serving at the grassroots level for livestock conservation, he entered the field of higher education in 2014. He rendered his valuable services as Professor and Head at the College of Veterinary and Animal Science, Navania (Udaipur), and later at the Post Graduate Institute of Veterinary Education and Research, Jaipur, besides successfully shouldering important administrative responsibilities as Dean, College of Dairy and Food Technology, Bassi, Faculty Dean, and Dean Students' Welfare (DSW) at Rajasthan University of Veterinary and Animal Sciences, (Jobner) Jaipur. As an inspiring teacher and accomplished scientist, he guided 6 Ph.D. and 9 M.V.Sc. scholars, published more than 60 research papers in reputed journals, and presented 63 research papers at various conferences. He also represented Rajasthan as an expert member of the prestigious ICAR, BSMA Committee and contribute in the revision of the veterinary curriculum. His valuable contribution to establishing modern pathology museums and state-of-the-art laboratories at Navania, Udaipur and Jaipur is highly commendable. In recognition of his outstanding and long-standing contributions to Veterinary Pathology, he was honoured by the Indian Association of Veterinary Pathologists (IAVP) with the **Best Veterinary Pathology Teacher Award–2022** and the prestigious **IAVP Fellowship Award–2024**. Beyond his academic and administrative excellence, his simple, humble, creative, and warm personality, along with his deep passion for music and singing, has made him truly special and widely admired. His nearly three decades of dedicated and illustrious service will remain a lasting source of inspiration for generations of veterinarians, teachers, and researchers.

He superannuated from his active service on 31.08.2026. The Indian Association of Veterinary Pathologists wishes him a healthy, peaceful and fulfilling post-retirement life.

OBITUARY



Dr S.C. Mukherjee

Dr Subhas Chandra Mukherjee, an eminent Veterinary Scientist, distinguished teacher and pioneering leader in the field of Fish Pathology and Aquatic Animal Health, who passed away at Pune on 05.9.2026.

Dr Mukherjee was a highly respected teacher, mentor and scientist whose contributions significantly advanced Fish Pathology, aquaculture and aquatic animal health management in India. Dr Mukherjee has an outstanding career, a pleasing personality, a good sportsman and a veteran tennis player, who went on to become an effective and distinguished leader in Fish Pathology.

His pioneering work on fish diseases and innovative disease-management strategies, including his contribution to the development of CIFAX for the management of Epizootic Ulcerative Syndrome (EUS), will remain an important part of his scientific legacy and his contributions to Veterinary Science and aquatic animal pathology will continue to inspire future generations. He will also be remembered for his leadership, academic excellence and inspiring personality.

The Indian Association of Veterinary Pathologists (IAVP) conveys its heartfelt condolences to his bereaved family, colleagues, students and admirers.

LIST OF REVIEWERS FOR 2026 ISSUES (VOLUME 50) OF IJVP

1. Dr Nagarajan K, MVC, TANUVAS
2. Dr Munish Batra, Panthnagar, GB Panth UAT
3. Dr G. Gangane, Parbhani, MAFSU
4. Dr N. Jayanthi, Udamalpet, TANUVAS
5. Dr P. Amaravathi, Tirupati, SVVU
6. Dr Neeraj Gangwar, Mathura, DUVASU
7. Dr Sudharani CH, Gannavaram, SVVU
8. Dr K. Gopal, Namakkal, TANUVAS
9. Dr Susitha Rajkumar, ICAR-CCARI, Goa
10. Dr Nithya P, Chennai, TANUVAS
11. Dr Rinku Sharma, ICAR-IVRI, Palampur
12. Dr Babu Prasath, Orathnadu, TANUVAS
13. Dr I. Hemanth, Garividi, SVVU
14. Dr Geeta Devi Leishangthem, Ludhiana, GADVASU
15. Dr Arul Mozhi A, Namakkal, TANUVAS
16. Dr Chandrakant Jana, ICAR-IVRI, Izatnagar
17. Dr B.J. Trangadia, Junagarh, Kamadhenu University
18. Dr K. Krithiga, Pookode, KVASU
19. Dr Aditya Acharya, Bhubaneswar, OUAT
20. V. Ravikanth, Korutla, PVNRTVU
21. Dr Pravin R Rathod, Parbhani, MAFSU
22. Dr Deepak Kumar, Patna, BASU
23. Dr Anita Rathore, Bikaner, RAJUVAS
24. Dr Tareni Das, ICAR-DFMD, Bhubaneswar
25. Dr V. Samatha, Gannavaram, SVVU
26. Dr M. Asok Kumar, ICAR-IVRI, Bareilly
27. Dr Pradeep M, Pookode, KVASU
28. Dr Manoranjan Rout, ICAR-DFMD, Bhubaneswar
29. Dr B.C. Girish, Hassan, KVAFSU
30. Dr V. Ramadevi, Gannavaram, SVVU
31. Dr M. Thangapandiyan, Udumalpet, TANUVAS
32. Dr K. Sateesh, Gannavaram, SVVU
33. Dr Nawab Nashiruddllah, Jammu, SKUAST
34. Dr Shesh Asopa, Bikaneer, RAJUVAS
35. C. Divya, Manuthy, Thrissur, KVASU
36. Dr Mamta Kumari, Udaipur, RAJUVAS
37. Dr D. Basheer Ahmad, Theiny, TANUVAS
38. Dr B.L. Jangir, LUVAS, Hissar
39. Dr Chandratre Gauri, LUVAS, Hissar
40. Dr Kamal Purohit, Bikaner, RAJUVAS
41. Dr K. Sushma, LUVAS, Hissar
42. Dr J.G. Patel, Himmatnagar, Kamadhenu University
43. Dr A. Nasrren, Tirupati, SVVU
44. Dr Rakesh Kumar, Palampur, CSKHPKV
45. Dr Mohan Settar, MB Veterinary College, Rajasthan
46. Dr Tridib Kumar Rajkhowa, CAU, Mizoram
47. Dr Shrirang Jamadagni, AYUSH, GOI, New Delhi
48. Dr R. Madheswaran, Udumalpet, TANUVAS
49. Dr Pawan Kumar, ICAR-IVRI, Izatnagar
50. Dr Ranjeet Ingole, Akola, MAFSU
51. Dr Sanjiv Kumar, Patna, BASU
52. Dr S. Ramesh, Chennai, TANUVAS
53. Dr S.S. Devi, Trissur, KVASU
54. Dr Monalisa Sahoo, ICAR-DFMD, Bhubaneswar
55. Dr Manoj Kumar, ICAR-NIHAD, Bhopal
56. Dr Jeetendra K. Rawal, Bhuj, Kamadhenu University
57. Dr Kanika Kalai, Agartala
58. Dr Sarjana Meena, RAJUVAS
59. Dr Debasish Behera, Agartala
60. Dr Jasmine Pamia, OUAT, Bhubaneswar
61. Dr Poornima Gumasta, Patna, BASU
62. Dr Shailendra Singh, Mohw, NDVSU
63. Dr Avantika Srivastav, Banda, BUAT
64. Dr P. Suvaneeth, Thrissur, KVASU
65. Dr R. Ananda Raja, ICAR-CIBA, Chennai
66. Dr Senthil Kumar, ICAR-NIHAD, Bhopal
67. Dr R.V. Ramana Murty, Garividi, SVVU
68. Dr Shameem Ara Begum, Guwahati, AVFU
69. Dr Megha Sharma, ICAR-IVRI, Bareilly
70. Dr N. Sailaja, Tirupathi, SVVU
71. Dr Shilpa Sood, Jammu, SKUAST
72. Dr R. Kumar, RIVER, Puduchery
73. Dr J. Selvaraj, Orathanad, TANUVAS
74. Dr Rabindra Nath Hansda, Kolkatta, WBVFSU
75. Dr Thangaturai R, Tirunelveli, TANUVAS
76. Dr M. Saminathan, ICAR-IVRI, Mukteswar

A. Anand Kumar
Chief Editor